5-2015

dLipin-A Link between Lipid Metabolism, Glucose Homeostasis and Growth in Drosophila melanogaster

Sandra Schmitt
University of Arkansas, Fayetteville

dLipin- A Link Between Lipid Metabolism, Glucose Homeostasis and Growth in *Drosophila melanogaster*

dLipin- A Link Between Lipid Metabolism, Glucose Homeostasis and Growth in *Drosophila melanogaster*

A dissertation submitted in partial fulfillment
of the requirements for the degree of
Doctor of Philosophy in Biology

by

Sandra Schmitt
Free University of Berlin, Germany
Diploma in Biological Sciences, 2007

May 2015
University of Arkansas, Fayetteville

This dissertation is approved for recommendation to the Graduate Council.

_____
Dr. Michael H. Lehmann
Thesis Director

_____ _____

Dr. Yuchun Du
Committee Member

Dr. Gisela F. Erf
Committee Member

_____
Dr. David S. McNabb
Committee Member

Abstract

Lipins are a family of highly conserved proteins found from yeasts to humans. Lipins have dual functions, serving as phosphatidate phosphatase enzymes (PAP) in the synthesis of neutral fats (triacylglycerols, TAG) and as transcriptional co-regulators that affect the expression of genes involved in lipid and fatty acid metabolism. Thus, they play central roles in metabolic control. Disruption of Lipin function has been implicated in lipodystrophy, obesity and insulin resistance. Using dLipin, the *Drosophila* homolog of Lipin, as a model, I aimed to elucidate the relationship between the two biochemical functions of Lipin and metabolic homeostasis. I discovered there is a strong interconnection between TAG synthesis and insulin pathway activity. Reduced activity of dLipin and other enzymes involved in TAG synthesis disrupted insulin pathway activity by interfereing with phosphatidylinositol (3,4,5)-trisphosphate (PIP3) synthesis. Mosaic analysis revealed that cell-autonomous loss of dLipin activity in fat the body negatively affects cell growth. Genetic interaction experiments indicated that *dLipin* and the insulin pathway regulate adipogenesis in an interdependent fashion. Furthermore, I found that the nutrient sensing complex TORC1 regulates dLipin activity in lipid metabolism by controlling dLipin's subcellular localization. Hence, the insulin pathway as well as the TORC1 pathway each appears to be a central regulator of dLipin activity and its functions in lipid metabolism. Nuclear functions of dLipin did not seem to have an effect on insulin pathway activity. Thus, metabolic disturbances observed after *dLipin* knockdown seem to be primarily caused by reduced PAP activity provided by dLipin. Taken together, the results position dLipin as a central target to further study the link between TAG synthesis and insulin and TORC1 pathway activity.

Acknowledgements

I wish to thank all of the members of my academic committee and especially my advisor, Michael Lehmann, for their support of this project.

Without the support and encouragement of my family and friends I would have not been able to finish this difficult journey. Special thanks goes to Jeff, Lucy, my parents as well as my sister Andrea and my life-long friend Nicki who did the best they could to keep me sane. In addition to emotional support, Jeff's scientific input was immensely helpful. Last but not least, I want to thank Elizabeth Ruck for her moral support.

Table of contents

I. Introduction

II. Materials and Methods

III. Results

A. Linking dLipin and insulin pathway activity in *D. melanogaster*

I. Introduction

With obesity constituting a rising epidemic in the USA and worldwide, research into fat metabolism has become a hot topic. As of 2013, more than 2/3 of the adult population in the USA were overweight (Body Mass Index (BMI) > 25) and of these, about 1/3 were obese (BMI> 30). Being overweight or obese poses numerous health hazards and current healthcare costs attributed to obesity are estimated to be 254 billion US$ (Go et al., 2013). Health risks associated with obesity include the metabolic syndrome, hypertension, coronary artery disease and stroke, respiratory defects, cancers, infertility and impotence, osteoarthritis, liver and gall bladder disease and diabetes (Kopelman; 2007). 90 Ninety % per cent of people with type 2 diabetes have a BMI> 23 suggesting that even being only slightly overweight puts individuals at an immediate risk of developing type 2 diabetes (Kopelman, 2007). Prevalence of childhood obesity and associated type 2 diabetes is rising steadily (Deckelbaum and Williams, 2001). As of 2012, 9.3% of the US population has diabetes and 33% of the adult population over the age of 20 shows signs of prediabetes (National Diabetes Statistics Report, 2014). With obesity and diabetes representing the 2nd and 7th leading cause of death in the USA research into how fat metabolism and insulin sensitivity are connected and controlled is more important than ever.

1. Characterization of Lipin

During times of excess nutrient uptake energy can be stored either as triacylglycerol (TAG) or glycogen and saved for times of nutrient deprivation. In animals, TAG is stored in lipid droplets within adipocytes, specialized fat storage cells, but virtually all cells have the capacity to synthesize and store TAG in lipid droplets. Lipid droplets consist of a core of neutral lipids

(TAGs), which is enclosed by a layer of phospholipids and associated proteins (Thiele and Spandl, 2008).

A mutant mouse strain, the *fatty liver dystrophy* mouse (*fld*), displays significant loss of fat tissue (lipodystrophy) in concert with ectopic fat accumulation in the liver and other imbalances in lipid metabolism (Langner et al., 1991). The *fld* mouse was later shown to carry a mutation in a novel gene, named *lipin1*. Two additional mouse *lipin* genes were identified by sequence similarity, *lipin2* and *lipin3* (Peterfy et al., 2001). Homologs of mouse *lipin* genes were also discovered in *Homo sapiens* and many genetic model organisms like *Saccaromcyes cerevisae*, *Arabidopsis thaliana*, *Caenorhabditis elegans*, *Drosophila melanogaster* as well as *Shizosaccharomyces pombe, Plasmodium falsiparum* and *Trypanosoma brucei*, indicating that the lipin gene family is evolutionary conserved (Pelletier et al., 2013; Peterfy et al., 2001). Inadequate adipose tissue in the *fld* mice was associated with glucose intolerance and increased atherosclerosis (Reue et al., 2000). Studies with mammalian *lipin1* revealed that *lipin1* is not only a lipodystrophy gene, but also an obesity gene, as overexpression of *lipin1* in adipose tissue and skeletal muscle of transgenic mice caused excess fat accumulation (Phan and Reue, 2005). All three Lipins were identified as Mg^{2+}-dependent phosphatidate phosphatase enzymes (PAP) (Donkor et al., 2007). PAP activity is required for the conversion of phosphatidic acid (PA) into diacylglycerol (DAG), an important step of the glycerol-3-phosphate pathway pictured below (Fig. 1).

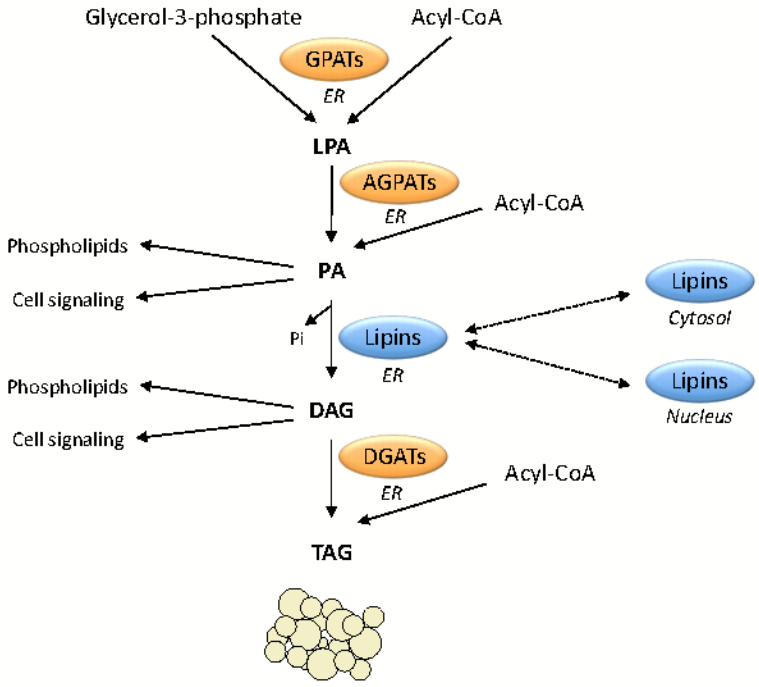

Fig. 1: Canonical glycerol-3-phosphate pathway that leads to the synthesis of TAG. Gycerol-3-phosphate (G-3-P) is converted into lysophosphatidic acid (LPA) by glycerol-3-phosphate 2-O-acyltransferase (GPAT). 1-acylglycerol-3-phosphate O-acyltransferase (AGPAT) subsequently transforms LPA into phosphatidic acid (PA). Lipin then catalyzes the conversion of PA into diacylglycerol (DAG), followed by the conversion of DAG into triacylglycerol (TAG) by diglyceride acyltransferase (DGAT). The final product, TAG, is then stored in fat droplets. Figure modified from Csaki et al, 2013.

In their role as essential glycerolipd synthesis enzymes, Lipins emerged as attractive targets for research that aims to elucidate the correlation between fat and glucose metabolism.

1.2. lipin gene family

As mentioned above, lipin genes are present in organisms ranging from *Homo sapiens* to yeast. I will shortly summarize the major findings concerning molecular Lipin function(s). Lipin proteins possess dual cellular roles, serving as PAP enzymes for TAG and phospholipid synthesis and as transcriptional co-regulators in the regulation of lipid metabolism and

adipogenesis genes (Finck et al., 2006; Reue and Zhang, 2008). All mammalian lipin homologs possess PAP activity (Donkor et al., 2007).

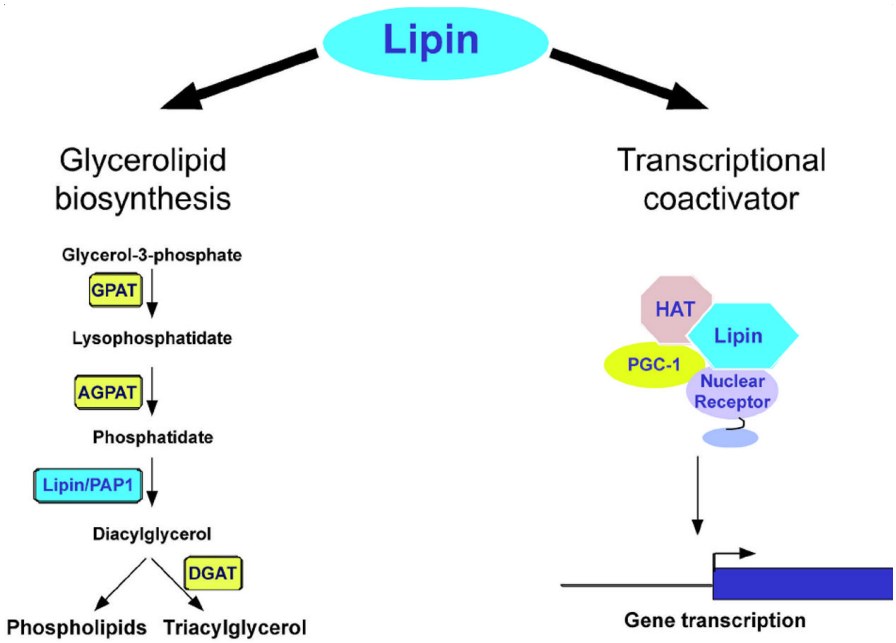

Fig. 2: Lipin proteins possess dual function as PAP enzymes and transcriptional co-regulators. Lipin functions as a PAP enzyme in the glycerolipid synthesis pathway, thus contributing to TAG and phospholipid production. Lipin can also participate in the control of fat metabolism by altering gene transcription in concert with nuclear receptors and other transcription factors. Image modified from Reue and Zhang, 2008.

1.2.1. Mammalian Lipins

Mammalian Lipin functions have so far been most extensively studied and this is especially true for *lipin1*, the gene disrupted in the *fld* mouse. Disruption of *lipin1* results in lipodystrophy accompanied by insulin resistance, neuropathy, atherosclerosis, abnormal triglyceride levels and neonatal fatty liver in mice (Langner et al., 1989; Peterfy et al., 2001; Reue et al., 2000).

Lipin1 accounts for virtually all PAP activity in white and brown adipose tissue and in skeletal muscle, and for most of of the PAP activity in liver and brain (Donkor et al., 2007). Overexpression of *lipin1* in adipose tissue led to increased fat accumulation, as did overexpression of lipin1 in muscle (Phan and Reue, 2005). Hence, Lipin1 is required for cellular lipid accumulation through its role as a PAP enzyme. Furthermore, secretion of very low density lipoproteins (VLDL) was negatively affected after loss of Lipin1 activity, which implicates Lipin1 in processes involved in VLDL sequestration (Khalil et al., 2009).

Lipin1 was also identified as a transcriptional co-regulator that influences expression of genes involved in fatty acid oxidation (Finck et al., 2006). Fatty acid oxidation takes place in hepatic mitochondria and represents a catabolic pathway that produces energy.

During times of starvation, hepatic fatty acid oxidation is upregulated. *Peroxisome proliferator-activated receptor* (*PPAR*) *α* is a gene encoding a nuclear receptor that regulates numerous genes involved in fatty acid oxidation. Accordingly, *PPARα* expression is induced upon starvation. It was shown that starvation-induced *PPARα* expression is dependent on Lipin1 activity and mediated in concert by Lipin1 and peroxisome proliferator activated receptor γ coactivator-1 α (PGC-1α). To regulate gene expression, Lipin1 and PGC-1α interact directly (Finck et al., 2006). The nuclear receptor hepatocyte nuclear factor 4 α (HNF4α) was identified as an interaction partner of nuclear Lipin1. The interaction between HNF4a and Lipin1 positively regulates expression of genes involved in fatty acid catabolism (Chen et al., 2012). Thus, Lipin1 affects transcription of genes involved in hepatic fatty acid oxidation via modulation of *PPARα* expression and interaction with HNF4a.

Lipin1 also influences adipogenic gene expression by regulating transcriptional activity of peroxisome proliferator-activated receptor γ (PPARγ) and CAAT/enhancer binding protein α (C/EBPα) in preadipocytes (Peterfy et al., 2005; Phan et al., 2004). During the process of adipogenesis cells differentiate from preadipocytes to adipocytes and final cell number of adipose tissue is determined. *PPARγ* and *C/EBPα* are master regulator genes of adipogenesis and together, control the terminal differentiation process (Farmer, 2006). It was later shown that Lipin1's PAP activity is required for PPARγ transcriptional activity and it was furthermore suggested that Lipin1 affects PPARγ activity by adjusting PA levels (Zhang et al., 2012). New data points to the possibility that Lipin1 might also directly bind to PPARγ and thereby induce a conformational change in PPARγ. This conformational change in PPARγ is proposed to cause a release of co-repressors and in turn enhance recruitment of PPARγ co-activators (Kim et al., 2013). This would then allow PPARγ to activate gene expression. Lipin1 is thus involved in controlling transcriptional activity of PPARγ and C/EBPα by mechanisms that require further investigation, but that might rely on Lipin1's PAP activity.

Lipin1 also controls lipogenic and cholesterogenic gene expression in hepatocytes by directly affecting sterol regulatory element binding protein (SREBP) protein levels (Peterson et al., 2011). SREBPs are transcription factors that control biosynthesis of cholesterol and fatty acids. In the presence of low cellular sterol levels, SREBPs are activated and partake in transcription of lipogenesis and cholesterogenesis genes. Peterson et al. (2011) identified Lipin1 as a negative regulator of nuclear SREBP function.

In addition, Lipin1 negatively regulates transcriptional activity of the nuclear factor of activated T cells c4 (NFATc4) in adipocytes. NFATc4 activity is repressed by direct protein-

protein interaction with Lipin1. These data suggest a possible role for Lipin1 in mediating inflammatory response in adipose tissue (Kim et al., 2010).

In summary, Lipin1 functions as a PAP enzyme and a transcriptional co-regulator. Lipin1's PAP activity is indispensable for TAG synthesis and is possibly also involved in the control of adipogenic gene expression. Lipin1's transcriptional co-regulator activity contributes to fatty acid metabolism by directly controlling *PPARα* expression and HNF4a activity and influences inflammatory gene transcription via interaction with NFATc4. SREBP-mediated lipid biogenesis is also affected by Lipin1 activity but the exact mechanisms underlying this interaction remain elusive.

Lipin2 and Lipin3 were identified based on amino acid similarity to Lipin1 (Peterfy et al., 2001). Lipin2 and 3 also exhibit PAP activity, but so far these two members of the *lipin* family have been much less well characterized. *lipin1*, *lipin2* and *lipin3* display distinct tissue expression levels, suggesting that the different *lipin* genes have independent physiological roles (Donkor et al., 2007). *lipin2* is predominantly expressed in liver, kidney and brain (Donkor et al., 2007). A possible involvement of Lipin2 in adipogenesis has been postulated (Donkor et al., 2009; Grimsey et al., 2008). Even less is known about Lipin3. *lipin3* is expressed in the gastrointestinal tract and, to a much smaller degree, in the liver (Donkor et al., 2007).

The three human Lipins display 44-48% amino acid identity to the corresponding mouse paralogs. The human Lipin proteins are encoded by *LPIN1*, *LPIN2* and *LPIN3*. Human *lipin* homologs are less well studied than their mouse counterparts. In contrast to studies in mouse, *LPIN1* expression in human adipose tissue is not always positively correlated with adiposity (Chang et al., 2010, Miranda et al., 2007; Mlinar et al., 2008). Expression levels of *PPARγ* in

adipose tissue were positively correlated with *LPIN1* expression, as were *ADIPOQ* (adiponectin) expression levels. This suggests that higher LPIN1 levels promote maturation of adipocytes with increased TAG content (Chang et al., 2010). *LPIN1* expression in adipose tissue is furthermore positively correlated with insulin sensitivity and with expression of genes involved in fatty acid oxidation and lipolysis. An especially strong correlation was found between *LPIN1* expression and *PPARα*. Thus, *LPIN1* might play a critical role in human fatty acid oxidation comparable to mouse *lipin1* (Donkor et al., 2008). *Glucose transporter 4* (*GLUT4*) gene expression was also positively correlated with *LPIN1* mRNA levels (van Harmelen et al., 2007). Thus, *LPIN1* expression correlates positively with insulin sensitivity and increased fatty oxidation in humans. Studies of human populations found that certain *LPIN1* and *LPIN2* polymorphisms are associated with type 2 diabetes and other metabolic traits (Aulchenko et al., 2007; Chang et al., 2010).

Deficiency in *LPIN1* has been implicated in recurrent acute myoglobinuria during childhood and statin-induced myopathy (Zeharia et al., 2008). *LPIN2* deficiency can lead to Majeed Syndrome (Ferguson et al., 2005) and psoriasis (Milhavet et al., 2008).

It thus appears that human *LPIN* genes overall seem to affect metabolic processes involved in glucose and lipid homeostasis in a similar way as mouse *lipin* homologs.

1.2.2. Lipin homologs in yeast, *C. elegans* and *A. thaliana*

In 2009 the *C. elegans lipin1* homolog was identified (Golden et al., 2009; Gorjanacz and Mattaj, 2009), *lpin-1*. Loss of LPIN-1 activity in *C. elegans* resulted in defects in fat storage, ER organization and nuclear membrane breakdown, irregular nuclear morphology and abnormal

chromosome segregation. Worms with *lpin-1* knockdown were reduced in size (Golden et al., 2009).

Mutations of *PAH1*, the *lipin* homolog in *S. cerevisae* resulted in lower TAG content in mutant cells along with elevated PA levels (Han et al., 2006). PAH1 function was also required for fat droplet formation (Adeyo et al., 2011). PAH1 was further implicated in the transcriptional control of phospholipid biosynthesis genes (Santos-Rosa et al., 2005). Cells with *PAH1* deficiency exhibited excess nuclear expansion, possibly caused by transcriptional changes of phospholipid synthesis genes induced by elevated PA levels (Han et al., 2007). Thus, PAH1 may influence phospholipid synthesis directly as a transcriptional co-regulator by repressing expression of phospholipid synthesis genes and additionally by modulating PA levels via its PAP activity (Siniossoglou, 2009). The lipin homolog of the fission yeast (*ned1*$^{+}$) affects chromosomal segregation and ER expansion (Tange et al., 2002). Thus, both *PAH1* and *C. elegans lpin-1* appear to contribute to nuclear envelope dynamics.

lipin homologs in *A. thaliana* (*AtPAH1* and *AtPAH2*) contribute to galactolipid synthesis and phosphate starvation resistance (Nakamura et al., 2009).

1.2.3. Lipin homolog in *D. melanogaster*

Mutations in the *Drosophila* lipin homolog *dLipin* resulted in animals with decreased TAG content, which suggests that dLipin also functions as a PAP enzyme (Ugrankar et al., 2011; Valente et al., 2010). Expression of dLipin was found to be strongest in the fat body, ring gland, ovaries, Malphigian tubules, midgut and ceca. dLipin showed both cytoplasmic and nuclear staining, which indicates that dLipin might also possess nuclear function in *Drosophila* (Ugrankar et al., 2011). Like mice deficient in *lipin1*, *Drosophila* larvae deficient for *dLipin*

displayed severe lipodystrophy. Lipodystrophy was accompanied by changes in fat body cell shape and size and a reduction in fat droplet size (Ugrankar et al., 2011). Cells were rounded in appearance and exhibited a wide variability in cell size. Ketone body formation was increased in animals deficient for dLipin. Thus, it appears that fatty acid metabolism was altered. Larval development was delayed, larval lethality increased, and the few animals reaching the pupal stage died as pharate adults. This suggests that dLipin is required for the formation of energy stores in developing larvae. Ultrastructure analysis showed that dLipin is required for proper assembly and function of mitochondria, autophagosomes and cell nuclei. It was also shown that dLipin is required for starvation resistance (Ugrankar et al., 2011). These data on dLipin indicate that Lipin's function in TAG synthesis is conserved between mammalian species and *Drosophila*, as defects observed in flies lacking *dLipin* resemble the mammalian *lipin* phenotype.

2. Lipin protein structure

Lipin PAP activity depends on a short amino acid motif that is conserved among species (DXDXT motif) and a conserved serine (S734) residue (Donkor et al., 2009). The PAP motif is located in the conserved CLIP domain of the protein and it is present in Lipin homologs from mammals to protists (Donkor et al., 2006, Pelletier et al., 2013) (Fig. 3). In addition to the PAP motif, Lipin homologs of mammals and *Drosophila* contain a co-regulator motif (LXXIL motif) that is evolutionarily conserved and also located in the CLIP domain (Finck et al., 2006; Peterfy et al., 2001). The LXXIL motif is required for Lipin's transcriptional co-regulator activity (Finck et al., 2006). Mutations in the PAP motif have no effect on transcriptional activity, whereas changes in the co-regulator motif not only reduce transcriptional, but also PAP activity (Reue and Brindley, 2008). In addition to the PAP and co-regulator motifs, Lipin also has a nuclear localization signal (NLS). The NLS is required for nuclear localization, but might also affect

membrane association and physiological functions of Lipin (Khalil et al., 2009). The conservation of CLIP and NLIP domains is summarized in Fig. 3.

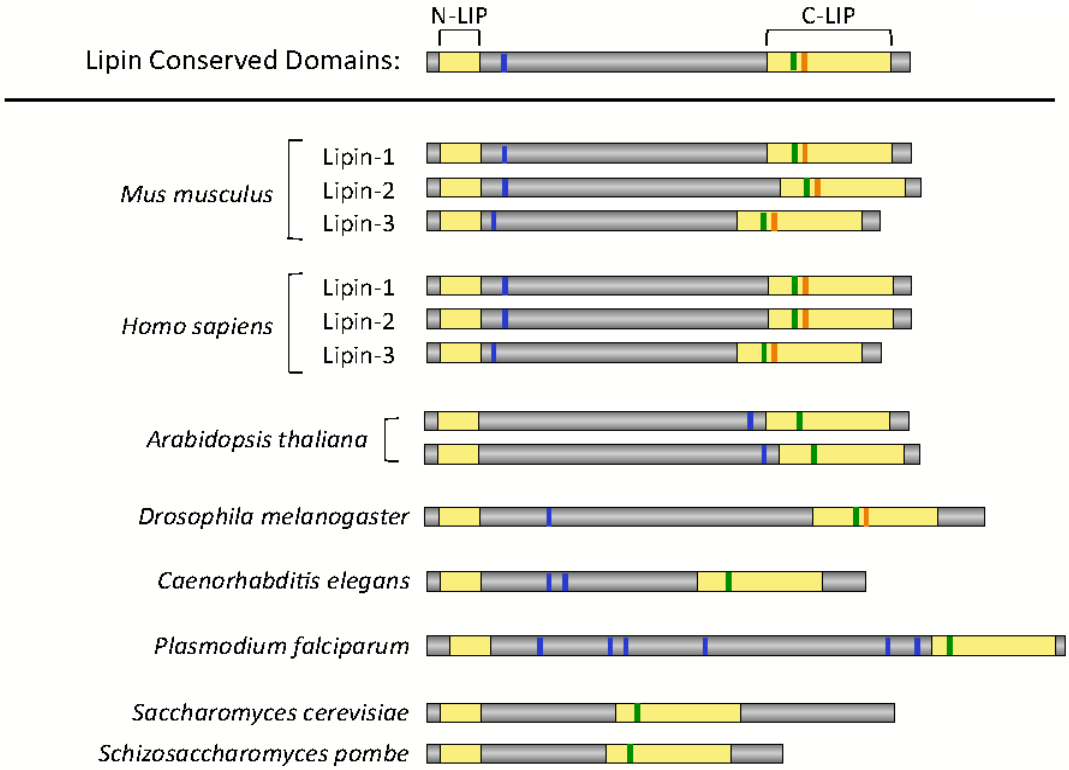

Fig. 3: A comparison of the structure of Lipin proteins across species shows that protein domains are evolutionarily conserved. Lipin homologs from the indicated species are schematically depicted. Lipin possesses two highly conserved domains, the NLIP domain and the CLIP domain (yellow bars). Presence of nuclear localization signals (blue) is shown. The PAP motif (green) and the transcriptional co-regulator motif (orange) are both located in the CLIP domain. The PAP motif is conserved among all species, whereas the transcriptional co-activator motif is only present in mammals and *Drosophila*. Image modified from Csaki et al., 2013.

Regulation of Lipin activity

In 2008, it was found that *lipin1* expression is positively regulated by glucocorticoids and cAMP. The stimulatory effect of glucocorticoids was antagonized by insulin (Manmontri et al., 2008; Zhang et al., 2008). A glucocorticoid-response element was identified in the promoter

region of *lipin1*. Increased glucocorticoid levels during adipogenesis induced expression of *lipin1* in preadipocytes and thus promoted cell differentiation (Zhang et al., 2008). Glucocorticoid levels are also elevated during times of physiological stress, like starvation, diabetes, hypoxia and obesity (Manmontri et al., 2008).

In addition, SREBP-1 activates *LPIN1* expression (Ishimoto et al., 2009). SREBPs are transcription factors that control biosynthesis of cholesterol and fatty acids. In the presence of low cellular sterol levels, SREBPs are activated and partake in transcription of lipogenesis and cholesterogenesis genes. Thus, cellular sterol levels also regulate LPIN1 expression.

In adipose tissue, *lipin1* expression is also triggered by thiazolidinediones and harmine; both of which promote insulin sensitivity (Park et al., 2010; Yao-Borengasser et al., 2006). *lipin1* expression is further influenced by estrogen levels, as high estrogen levels negatively correlate with *lipin1* expression in the uterus and liver (Gowri et al., 2007). Cytokines, tumor necrosis factor α and interleukin-1 negatively regulate *Lipin1* expression, which leads to an increase in lipolysis in adipose tissue and hence a reduction in fat stores during infection (Reue and Brindley, 2008).

In addition to control at the transcriptional level, Lipin1 activity can be modulated at the protein level. It was shown that PAP activity is primarily cytosolic and translocates to the ER in response to fatty acids (Gomez-Munoz et al., 1992). The ER represents the major site of TAG biosynthesis and fat droplet formation (Wilfling et al., 2013). Thus, subcellular localization of Lipin corresponds with molecular Lipin function. The change in Lipin1's subcellular localization has been attributed to a change in Lipin's phosphorylation status (Gomez-Munoz et al., 1992; Harris et al., 2007; Huffmann et al., 2002). High cellular concentrations of fatty acids, as well as

the presence of epinephrine and oleic acid, induce dephosphorylation of Lipin1 and recruitment of Lipin1 to the ER (Harris et al., 2007). Multiple rapamycin-sensitive phosphorylation sites have been identified in Lipin1 (Harris et al., 2007; Peterson et al., 2011). Rapamycin-sensitivity of the phosphorylation sites indicates that phosphorylation at these residues is dependent on the Ser/Thr kinase target of rapamycin (TOR). Rapamycin acts as an inhibitor of TOR action. TOR is part of a nutrient sensing protein complex (TOR complex 1, TORC1) and integrates both nutrient and growth factor/insulin signaling (Dibble and Manning, 2013). Mammalian TORC1-mediated (mTORC1) phosphorylation of Lipin1 promotes cytoplasmic Lipin1 retention and loss of mTORC1 activity has been shown to promote nuclear translocation of Lipin1 (Peterson et al., 2011). Thus, dephosphorylation of Lipin1 seems to be required for nuclear translocation and ER association of Lipin1.

Insulin signaling promotes cytoplasmic retention of Lipin1 by stimulating an interaction between Lipin1 and 14-3-3 proteins (Peterfy et al., 2009). Furthermore, Lipin1's serine106 residue has been identified as being specifically phosphorylated upon insulin signaling in a rapamycin-sensitive manner (Harris et al., 2007), which indicates that TOR and insulin pathway might control Lipin localization in concert. The PAP activity of Lipin1 itself was not modified by phosphorylation events, suggesting that Lipin1's phosphorylation status does not affect its enzymatic activity (Harris et al., 2007), but rather that TOR and insulin influence Lipin1's activity by modulating its subcellular localization.

Lipin1's serine106 residue was later identified to be the target site for the phosphatase Dullard (Wu et al., 2011). This is consistent with the observation that yeast PAH1 is dephosphorylated by Nem1, the yeast homolog of Dullard (Santos-Rosa et al., 2005). In neuronal cells, it was found that sumoylation of Lipin1 resulted in its nuclear localization (Liu and Gerace,

2009). Furthermore, recent work by Eaton et al. (2013) suggests that Lipin1's membrane association, and hence its catalytic activity, may be regulated by pH levels and membrane phospholipid composition (Eaton et al., 2013).

In summary, Lipin activity is regulated on a transcriptional level by glucocorticoids and metabolic status as well as on a posttranslational level via phosphorylation and sumoylation. Intracellular pH and membrane composition may also influence Lipin activity. The effects of posttranslational modifications on Lipin activity still require more investigation and are not well understood at this point. It also appears that Lipin activity is closely associated with TOR and insulin pathway activity. In the next section, I will outline general aspects of TOR and insulin pathway activity and the influence of TOR and insulin pathway activity on lipid metabolism.

4. Roles of TOR and insulin signaling in metabolic homeostasis

Animals need to balance nutritional status with growth while maintaining overall energy homeostasis. Thus, pathways evolved that coordinate metabolic demands with dietary input. From yeast to mammals, favorable nutritional conditions promote cell growth by activation of the TOR pathway (Dann and Thomas, 2006). TOR is an effector of cell growth by integrating signals from growth factors/insulin and nutrients, especially amino acids and cellular energy status (AMP/ATP ratio). TOR activity is reduced in response to certain physiological cues. These cues include hypoxia, reducing conditions, DNA damage and starvation (Wullschleger et al., 2006). TOR functions in two distinct complexes, TOR Complex 1 (TORC1) and TOR Complex 2 (TORC2). Mammalian TORC1 (mTORC1) consists of mTOR, raptor and mLST8. mTORC2 is made up of mTOR, rictor, SIN1, mLST8 and Protor.

4.1. General functions of mTORC1

mTORC1 is activated by nutrients and by growth factor signaling/insulin signaling. Insulin pathway input is communicated to mTORC1 via protein kinase B (AKT). AKT phosphorylates the mTORC1 inhibitor complex tuberous sclerosis complex 1/2 (Tsc1/2) and thus allows ras homolog enriched in brain (Rheb), an mTORC1 activator, to phosphorylate mTORC1 (Manning and Cantley, 2003). AKT also phosphorylates and thus inhibits proline-rich AKT substrate 40 (PRAS-40), which is an mTORC1 inhibitor (Sancak et al., 2007).

How exactly amino acids activate mTORC1 is still subject to research, but it is proposed, that the ragulator-rag complex recruits mTORC1 to lysomes, the site of Rheb activity (Dibble and Manning, 2013; Sancak et al., 2010). Activated mTORC1 then phosphorylates downstream targets, S6 kinase (S6K) and eukaryotic initiation factor 4E-binding protein 1 (4EBP1), and consequently promotes cell growth (Magnuson et al., 2012). S6K positively regulates protein synthesis in numerous ways, including translation initiation, translational elongation and mRNA processing, and thus promotes cell growth (Magnuson et al., 2012). S6K activation also increases nucleotide synthesis required for DNA and RNA synthesis (Ben-Sahra et al., 2013). 4EBP1 is an inhibitor of cap-dependent translation as it binds to the eukaryotic translation initiation factor 4F (eIF4F) (Gingras et al., 1999). mTORC1-mediated phosphorylation of 4EBP1 releases eIF4F from 4EBP1 and in turn activates translation (Gingras et al., 1999). Furthermore, ribosome biogenesis is also mediated by mTORC1 (Iadevaia et al., 2014).

Autophagic processes are negatively regulated by mTORC1 as mTORC1 was identified to directly phosphorylate and consequently inactivate Unc-51-like autophagy activating kinase-1 (ULK1) and death-associated protein 1 (DAP1) (Kim et al, 2011; Koren et al., 2010). Thus,

mTORC1 mediates cell growth by coordinating protein synthesis, nucleotide synthesis and autophagy (Betz and Hall, 2013).

4.2. General functions of mTORC2

The mechanisms leading to mTORC2 activation are still unknown, but believed to be initiated by growth factors (Kim and Guan, 2011). Once activated, mTORC2 affects AKT activity by phosphorylation of the hydrophobic motif in AKT (serine473) (Sarbassov et al., 2005). mTORC2 also phosphorylates and activates protein kinase C ζ (PKCζ) and, thus, regulates cell migration and cytoskeleton formation (Li and Gao, 2014). mTORC2-mediated phosphorylation of serum- and glucocorticoid-induced protein kinase 1 (SGK1) implicates mTORC2 activity in the mediation of cell proliferation/survival (Garcia-Martinez and Alessi, 2008). SGK1 is a kinase that positively influences cell proliferation and inhibits apoptosis (Lang et al., 2006). A possible negative feedback loop exists between mTORC1 and mTORC2 activity that is speculated to lead to changes in mTORC2 protein interactions (Treins et al., 2010). In summary, mTORC2 mediates cell growth by coordinating cytoskeleton formation, cell migration and cell proliferation.

A)

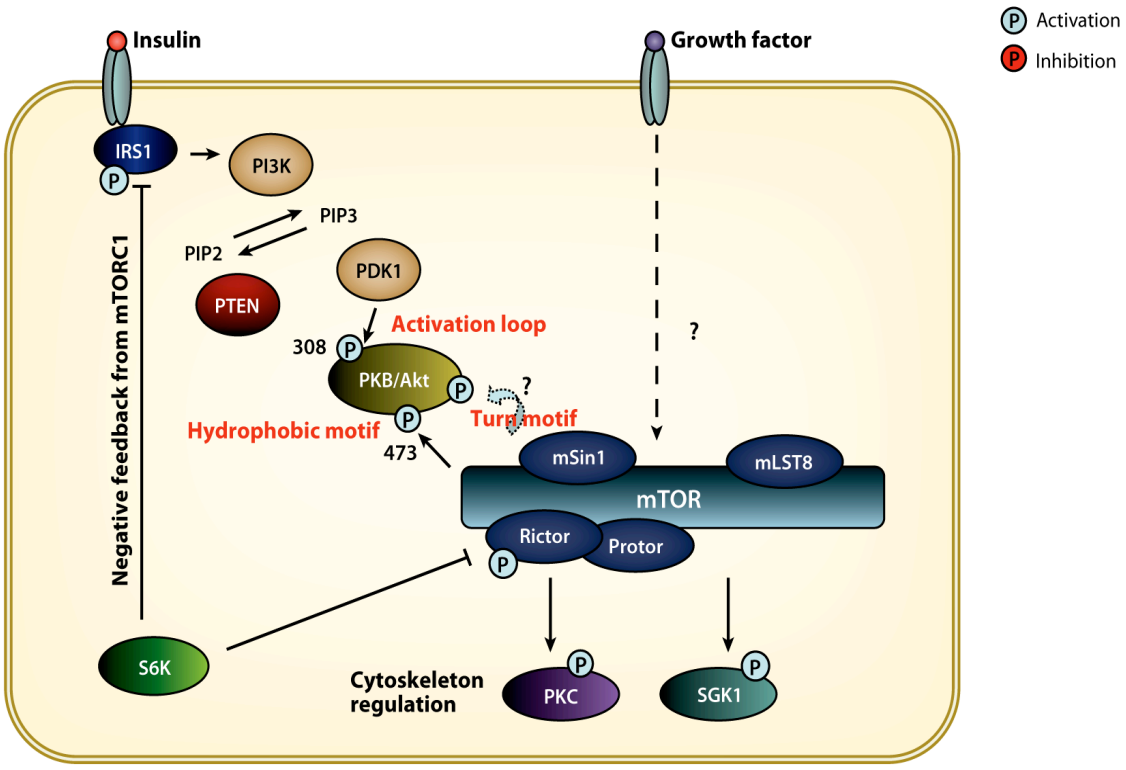
Activation
Inhibition
Insulin
Growth factor
IRS1
PI3K
PIP3
PIP2
PDK1
PTEN
Activation loop
308
PKB/Akt
Hydrophobic motif
473
Turn motif
?
Negative feedback from mTORC1
mSin1
mLST8
mTOR
Rictor
Protor
S6K
Cytoskeleton regulation
PKC
SGK1

B)

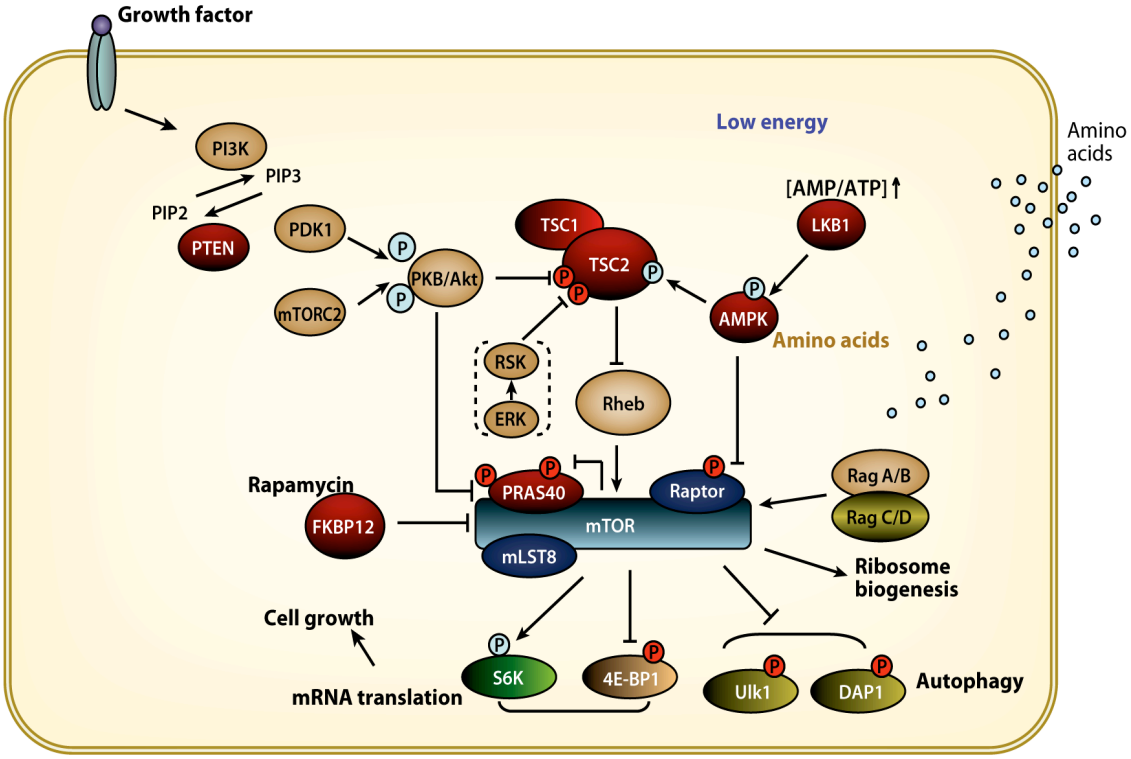
Growth factor
Low energy
Amino acids
PI3K
PIP3
PIP2
PTEN
PDK1
PKB/Akt
mTORC2
TSC1
TSC2
[AMP/ATP]↑
LKB1
AMPK
Amino acids
RSK
ERK
Rheb
Rapamycin
FKBP12
PRAS40
Raptor
mTOR
mLST8
Rag A/B
Rag C/D
Ribosome biogenesis
Cell growth
mRNA translation
S6K
4E-BP1
Ulk1
DAP1
Autophagy

Fig. 3: Overview of mTORC1 and mTORC2 signaling pathways. These images summarize the mTORC1 (A) and TORC2 (B) pathways. For further explanation, please refer to main text. Image modified from Kim and Guan, 2011.

4.3. Functions of mTORC1 and mTORC2 in lipid metabolism

The above figure displays effects of mTORC1/mTORC2 activity on general metabolism, cell survival and cytoskeleton dynamics (Fig. 3). TOR-induced cell growth has been mostly studied by measuring protein synthesis as a biological output but it is becoming clear that other anabolic pathways are also affected by TOR activity, likely also lipid synthesis (Birse et al., 2010; Laplante and Sabatini, 2009 and 2012). Research shows that mTORC1 and mTORC2 directly affect lipid biogenesis.

Adipogenesis is promoted by both mTORC1 and mTORC2 activity. Inhibition of 4EBP1 by TORC1 is believed to allow for PPARγ translation and thus activates adipogenic gene expression (Zhang et al., 2009). Activation of S6K is also implicated in adipogensis, as S6K knock out mice show a lack of fat accumulation due to a defect in adipocyte formation (Carnevalli et al., 2010). Recently it has been discovered that mTORC2 plays a role in adipogenesis as well. It was demonstrated that mTORC2 positively affects adipogenesis by phosphorylation of AKT (Yao et al., 2013).

In addition to adipogenesis, mTORC1 also has a role in hepatic lipid biogenesis. mTORC1 appears to modulate hepatic lipogenesis mainly by regulation of SREBP activity. The regulation of SREBP might be mediated by mTORC1 activation of S6K (Duevel et al., 2010). Additionally, SREBP regulation by mTORC1 may be communicated through Lipin1 (Peterson et

al., 2011). As mentioned previously, Lipin1 is a target of mTORC1-dependent phosphorylation, which in turn affects Lipin1's subcellular localization. Upon loss of mTORC1 activity, dephosphorylated Lipin1 enters the nucleus and represses SREBP activity and thus lipid biogenesis (Peterson et al., 2011). Hence, mTORC1 regulates lipid biogenesis via S6K and Lipin1, although the exact molecular mechanisms still remain elusive.

mTORC2 also influences lipogenesis, although substrates and pathways involved remain largely unknown. It has been proposed that part of the influence of mTORC2 on lipogenesis results from its effects on SGK1 and AKT activity (Laplante and Sabatini, 2012). mTORC2 was identified as a suppressor of lipolysis in adipose tissue (Kumar et al., 2010). In addition, hepatic lipogenesis appears to be subject to mTORC2 regulation as mice with a reduction in mTORC2 activity display reduced expression of key lipid synthesis genes in the liver (Yuan et al., 2012).

These data implicate both mTOR complexes as central regulators of lipid metabolism and also suggest that aspects of mTOR-mediated regulation of lipid homeostasis might be brought about by changes in Lipin1 activity.

4.4. General functions of the insulin pathway

As mentioned previously, Lipin activity appears to be regulated by the insulin pathway. The insulin pathway integrates growth factor/insulin signaling with anabolic cellular processes. In mammals, circulating insulin-like growth factors (IGFs) promote cell and tissue growth, and circulating insulin regulates carbohydrate and lipid metabolism (Siddle, 2012). Dimerization of insulin or insulin-like growth factor receptors (IR/IGRF) triggers autophosphorylation of the receptors, which in turn promotes recruitment and phosphorylation of insulin receptor substrate 1 and 2 (IRS1, IRS2) proteins (Manning and Cantley, 2007). IRS1/2 phosphorylation activates

phosphatidylinositol-4,5-bisphosphate 3-kinase (PI3K) (Hemmings and Restuccia, 2012). PI3K consists of a regulatory p85 subunit and a catalytic p110 subunit (Vogt et al., 2010). The catalytic p110 subunit phosphorylates phosphatidylinositol (4,5) bisphosphate (PIP2) to produce phosphatidylinositol (3,4,5) trisphosphate (PIP3) (Vogt et al., 2010). This phosphorylation step is antagonized by phosphatidylinositol 3, 4, 5 trisphosphate 3-phosphatase (PTEN) (Kishimoto et al., 2003). PIP3 at the plasmamembrane recruits phosphoinositide-dependent kinase-1 (PDK1) and AKT. At the plasma membrane, PDK1 activates AKT through phosphorylation. In addition, mTORC2-mediated phosphorylation of AKT is required for maximal AKT activation (Hemmings and Restuccia, 2012). AKT then phosphorylates many downstream substrates and promotes cell survival by blocking proapoptotic proteins and processes (Manning and Cantley, 2007). Forkhead box protein O (FOXO) transcription factors are phosphorylated by AKT, which leads to FOXO's removal from the nucleus. By removing FOXO transcription factors from the nucleus, AKT inhibits expression of proapoptotic and cell cycle arrest genes (Burgering and Kops, 2002). AKT positively affects cell growth by activation of mTORC1 via Tsc1/2 and PRAS-40 phosphorylation (Manning and Cantley, 2007). Metabolic processes are also targeted by AKT. AKT promotes glucose transporter 4 (GLUT4) membrane translocation and thus promotes glucose uptake (Cong et al., 1997). In addition, glycogen synthesis is stimulated by AKT through inhibition of glycogen synthase kinase 3 (GSK3) (Manning and Cantley, 2007). Cell proliferation is regulated by AKT in part by interfering with p27 function (Manning and Cantley, 2007; Taguchi and White, 2008). Thus, insulin pathway activity is involved in upregulation of many cellular anabolic pathways.

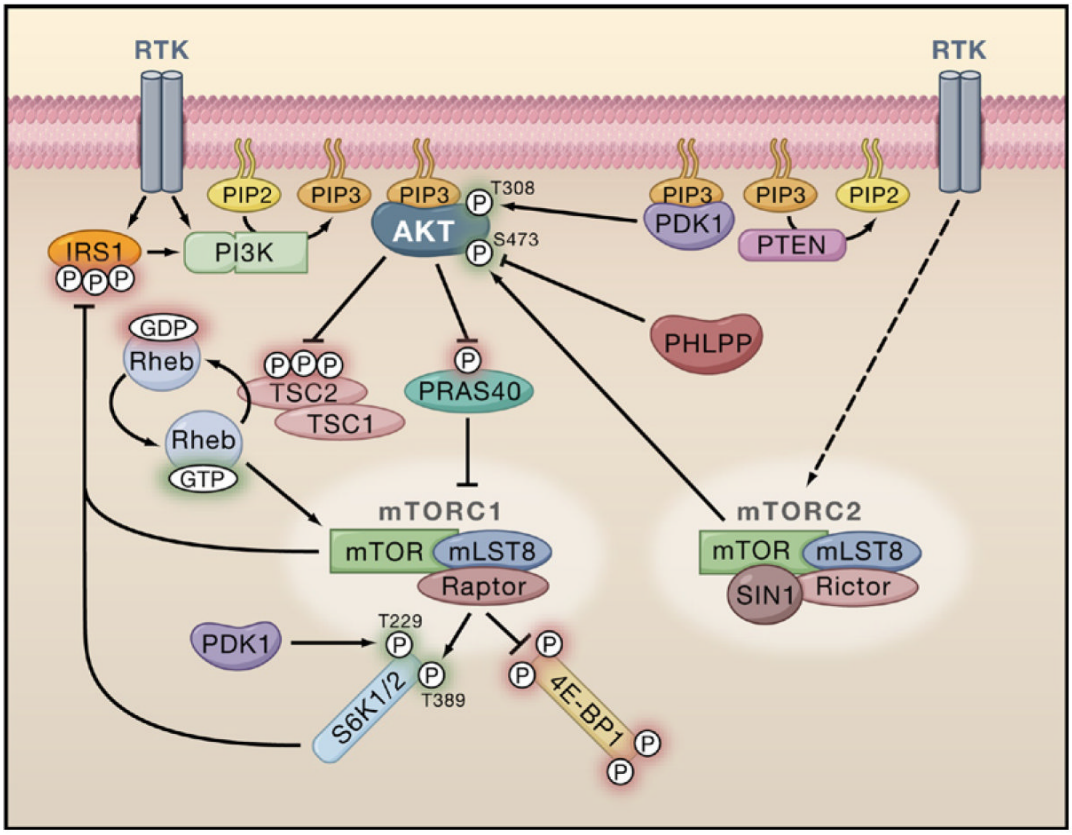

Fig. 4: Overview of the insulin pathway. The insulin pathway activity modulates glucose and lipid metabolism and cell survival, proliferation and growth. For further explanation, please refer to the main text. Image modified from Manning and Cantley, 2007.

4.5. Functions of the insulin pathway in lipid metabolism

Insulin pathway activity also influences lipid metabolism. In the next section I will elaborate on the relationship between insulin and lipid metabolism. Insulin pathway activity is closely associated to lipid homeostasis, as evidenced by the development of insulin signaling imbalances induced by either lipodystrophy or obesity. Impaired insulin pathway activity is strongly associated with an increase in circulating free fatty acids and TAGs (Frayn et al., 2001). Also, ectopic lipid accumulation is a common side effect of reduced insulin sensitivity (Frayn et al., 2001).

In adipocytes, insulin signaling enhances TAG production and downregulates lipolysis (Czech et al., 2013). Two lipolytic pathways exist; one mediated by protein kinase A (PKA) and the other by protein kinase G (PKG) (Czech et al., 2013; Miyoshi et al., 2007; Sengenes et al., 2003). Insulin signaling reduces activity of both lipolysis pathways (Czech et al., 2013). AKT also inhibits hydrolysis of TAG through upregulation of mTORC1 activity, which results in a reduction of adipose triglyceride lipase (ATGL) mRNA (Chakrabarti et al., 2010). Therefore, adipocyte lipolysis is attenuated in response to insulin pathway activation. At the same time, lipogenic mechanisms in adipocytes are upregulated; in particular fatty acid uptake and de-novo fatty acid synthesis (Czech et al., 2013; Stahl et al., 2002).

In the liver, insulin pathway activity increases de-novo fatty acid synthesis via activation of acetyl-CoA carboxylase (ACC), a key enzyme in fatty acid synthesis (Berggreen et al., 2009). In addition, insulin pathway activity also modifies lipogenic gene transcription (Assimacopoulos-Jeannet et al., 1995; Sul et al., 2000). In hepatocytes, this is mediated by insulin/mTOR-stimulated processing of SREBPs (Ferre and Foufelle, 2007; Shimomura et al., 1998). The exact mechanism of how SREBP control is communicated remains elusive, but as mentioned before, Lipin1 activity appears to play an important role as a negative regulator of nuclear SREBP activity (Peterson et al., 2011).

In conclusion, both the TOR and the insulin pathway contribute to lipid metabolism control, in some instances in concert. Lipin activity appears to be targeted by both pathways with regard to SREBP control. Thus, Lipin could represent an important mediator between TOR/insulin pathway and lipid homeostasis. The exact mechanisms of the TOR/insulin pathway-induced and Lipin-communicated effects on lipid metabolism still warrant further investigation. *Drosophila melanogaster* has been used as a model system to investigate fat metabolism as well

as TOR/Insulin signaling (Baker and Thummel, 2007; Grewal, 2008; Teleman, 2009). *Drosophila* only has one *lipin* homolog, *dLipin*, which simplifies genetic studies. In the next section, I will summarize insulin and TOR pathways of the fly and point to shared and distinct characteristics between mammalian and *Drosophila* insulin/TOR signaling. I will summarize the most important aspects of lipid and glucose metabolism in the fly.

5. Lipid and glucose metabolism in *D. melanogaster*

Drosophila shares most of the basic metabolic functions found in mammals. Flies have a gastrointestinal tract that is similarly functionally segregated as the mammalian counterpart, fat body that functions as mammalian liver and white adipose tissue, oenocytes that perform basic hepatocyte-like functions in lipid-processing and specific neurosecretory cells in the brain that maintain insect metabolic homoeostasis in a way comparable to mammalian pancreatic β cells (Canavoso et al., 2001; Gutierrez et al, 2007; Rulifson et al., 2002). Organismal growth in *Drosophila* is restricted to the larval stages. After metamorphosis the adult fly no longer increases in size. Like mammals, *Drosophila* stores energy as TAG and glycogen. Lipid stores are the primary energy source for insects during diapause, embryonic development and prolonged flight (Arrese and Soulages, 2010). Both TAG and glycogen are stored in the fat body, though TAG represents the major energy reserve. TAG is synthesized via the glycerol-3 phosphate pathway involving dLipin and stored in intracellular lipid droplets. Mobilization of TAG reserves is mediated by triglyceride lipases. In *Drosophila* the *Brummer* gene encodes a lipid droplet associated TAG lipase homologous to the mammalian adipocyte triglyceride lipase (ATGL) (Groenke et al., 2005). Glycogen is mobilized mostly in the form of the dissacharide trehalose (Thompson, 2003). TAG and glycogen stores can be mobilized by adipokinetic hormone (AKH) released from the corpora cardiaca (Arrese and Soulages, 2010). TAG and

glycogen from fat body stores are mobilized during times of energy depletion like starvation, flight and during embryogenesis.

Both, the insulin and TOR pathways can activate TAG production in the fat body of *Drosophila* (Birse et al., 2010; DiAngelo and Birnbaum, 2009, Teleman et al., 2005). This suggests that in *Drosophila*, lipid metabolism is regulated by the insulin and TOR pathways, similarly compared to mammalian systems.

6. Functions of TOR in *D. melanogaster*

The *Drosophila* homolog of mammalian TOR, dTOR functions in many ways comparable to mammalian TOR in processes controlling cell growth and metabolism (Oldham et al., 2000). Amino acid input is the major trigger for dTOR-induced cell growth, and cellular amino acid status is most likely communicated to dTOR via the amino acid transporter, *slimfast* (Colombani et al., 2003). dTOR activates metabolic gene expression in an amino acid sensitive fashion and controls cell cycle progression (Li et al, 2010; Patel et al., 2003). Furthermore, dTOR is known to coordinate endocytotic and nutrient uptake processes to control cell growth in the fat body (Hennig et al., 2006). Cell growth was strongly targeted by dTOR in endoreplicative tissue (Britton and Edgar, 1998). dTOR, like mammalian TOR, inhibits autophagy (Scott et al., 2004).

dTOR also influences lipid metabolism (Birse et al., 2010; Teleman et al., 2005). Birse et al. (2010) demonstrated that systemic reduction of TOR activity resulted in decreased overall TAG stores in animals fed a high-fat or normal diet. This was caused by a decrease in lipogenesis in combination with increased lipolysis (Birse et al., 2010). Teleman et al. (2005)

observed that animals with reduced TOR activity displayed significantly reduced fat stores. Thus, it appears that dTOR is an important regulator of systemic lipid metabolism.

Drosophila has two TOR complexes, TORC1 and TORC2. As in mammalian systems, *Drosophila* TORC2 phosphorylates AKT at the hydrophobic motif while the rapamycin-sensitive TORC1 is believed to primarily control cell growth and overall metabolism of the fly (Sarbassov et al., 2005, Teleman, 2009). The signaling pathway leading to TORC1 activation in *Drosophila* is basically identical to the pathway in mammalian systems, and is summarized in Fig. 5. Like its mammalian counterpart, dTOR appears to be involved in the insulin pathway cascade. However, the crosstalk between the dTOR and insulin pathways seems to be complicated and dTOR and insulin pathway activity are not always directly connected but can also be uncoupled (Colombani et al., 2003; Oldham et al., 2000; Pallares-Cartes et al., 2012).

7. Functions of the insulin pathway in *D. melanogaster*

The insulin pathway in *Drosophila* strongly resembles the mammalian insulin signaling systems. Not only are molecular components of the pathway conserved, but also physiological output. *Drosophila* has eight insulin-like peptides (dILPs), which are homologous to mammalian insulin in action and protein sequence (Kannan and Fridell, 2013). Each dILP has a distinct expression pattern, which implies that each dILP possesses a unique physiological function. dILPs 1, 2, 3 and 5 are expressed in neurosecretory brain cells, whereas dILPs 4 and 5 are expressed in the midgut. dILP 6 is mainly produced in the fat body, dILP 7 in the ventral nerve cord of the brain and the newly discovered dILP 8 in imaginal discs (Kannan and Fridell, 2013). Larval ablation of the neurosecretory cells that are responsible for releasing dILPs 2, 3 and 5 resulted in a phenotype that mirrors the physiological effects of insulin resistance in mammals

(Rulifson et al., 2002; Broughton et al., 2005). dILP binding activates the *Drosophila* homolog of the mammalian insulin receptor, InR. Two insulin receptor substrate proteins exist in *Drosophila*, namely Chico and Lnk. As in the mammalian insulin pathway, phosphorylation of IRS recruits PI3K (p60 and p110 subunits) to the plasma membrane where it catalyzes the generation of PIP3. PIP3 accumulation activates PDK1 and AKT. These protein interactions are all highly conserved between flies and mammals (Teleman, 2009). The interaction between AKT and FOXO has been especially well studied in flies (Teleman, 2009). It was found that overexpression of FOXO led to growth arrest and food avoidance as well as reduced cell size, cell number and reduced lipid stores (Kramer et al., 2003; Puig et al., 2003; Teleman et al., 2005). By modulating FOXO activity, AKT affects growth, cell proliferation and metabolism in *Drosophila*. As is the case in mammals, lipid metabolism might be controlled by dTOR and insulin pathway through SREBP regulation in *Drosophila* (Porstmann et al., 2008).

Thus, the insulin pathway output of *Drosophila* is comparable to that in mammals, with effects on overall metabolism and growth; although the exact mechanisms involved still require further elucidation. Overall, the high degree of functional conservation of TOR/insulin signaling and the physiological similarities regarding lipid and glucose metabolism between mammals and flies predispose *Drosophila* as a prime candidate to elucidate the interconnection and crosstalk amongst TOR/insulin pathway activity and lipid/glucose homeostasis. Figure 5 summarizes the TOR/insulin pathway in *Drosophila*.

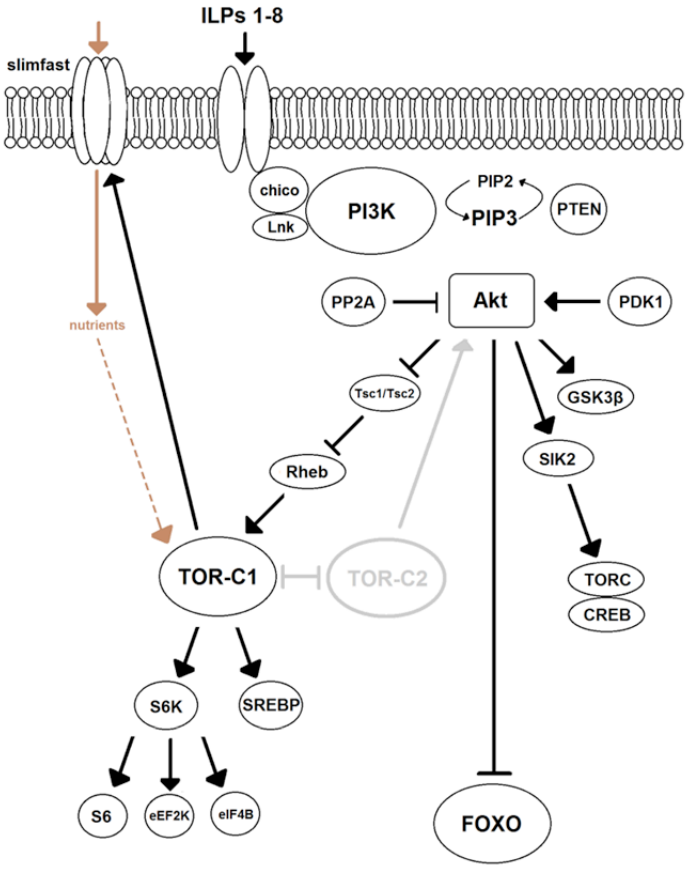

Fig. 5: TOR/insulin pathway in *Drosophila*. dILPs are secreted by insulin-producing cells throughout the body and bind to the insulin receptor homolog, InR. This leads to dimerization and subsequent autophosphorylation of InR, followed by binding of the fly IRSs, Chico and Lnk. Phosphorylation of the IRSs recruits PI3K to the plasma membrane where it catalyzes the generation of PIP3. PIP3 located at the plasma membrane triggers the activation of PDK1 and AKT. Thereby PDK1 phosphorylates and thus activates AKT. AKT is further phosphorylated by TORC2. Activated AKT then targets downstream components to adjust metabolic and growth related cellular responses. Amongst the targets are TORC1, FOXO and GSK3β. Image modified from Teleman, 2009.

There are also differences in insulin pathway dynamics between *Drosophila* and mammals. One important difference is that in *Drosophila* glucocorticoids do not play a role in insulin signaling because flies do not synthesize glucocorticoids (Teleman, 2009). Another difference is that in *Drosophila* the complexity of the insulin cascade is reduced. *Drosophila* possesses homologs for all components of the insulin pathway present in mammals, but a single

fly homolog often represents multiple mammalian signaling components. This means that mutations in fly insulin signaling cascade components may give more direct and clear effects, but it also implies that direct comparisons of fly and mammalian protein function is sometimes not straightforward, as mammalian proteins might exhibit specialized functions (Teleman, 2009).

8. Goals of PhD research

Drosophila represents an ideal model for genetic manipulation and interaction experiments. As described earlier, the insulin and TOR pathways are highly conserved on both the physiological and molecular level between flies and mammals. In addition, Lipin function appears to be conserved between flies and mammals. Thus, I conducted experiments aimed to further elucidate the relationship between dLipin's dual activity in fat metabolism and TOR/insulin signaling using *Drosophila* as a model system. With the fat body representing the major site for TAG and glycogen storage, I focused my research on the fly fat body. In my research I addressed the following questions:

1. How are dLipin and insulin pathway activities linked in *Drosophila*? I investigated the relationship between dLipin and insulin signaling by exploring the effects of dLipin activity on cell growth and by measuring insulin pathway activity in flies with reduced dLipin expression. Genetic interaction studies were carried out to shed light on the epistatic relationship between dLipin and the insulin cascade and to investigate the effects of insulin pathway activity on dLipin function. To investigate the role of insulin pathway activity in dLipin regulation, I examined the effect(s) of insulin pathway modifications on dLipin localization.

2. How is insulin resistance induced in animals that lack Lipin activity? As previously mentioned, *lipin1* deficiency results in insulin resistance but it is not known whether the lack of

PAP or transcriptional co-regulator activity is responsible for this effect. Therefore, I aimed to address how the loss of either of these activities affects insulin pathway activity in *Drosophila*. To this end, I expressed dLipin lacking the PAP motif and dLipin lacking its NLS in animals with RNAi-mediated *dLipin* knockdown and examined insulin pathway activity in the larval fat body.

3. How are Lipin and TOR activities linked in *Drosophila*? To address the question of whether dLipin activity is also subject to regulation by TOR in *Drosophila*, I examined cellular localization and abundance of dLipin in the larval fat body upon reducing TOR activity. The epistatic relationship between TOR and dLipin was investigated with genetic interaction experiments.

II. Materials and Methods

1. Fly stocks

Simplified genotype	Genotype	Description	Source
w1118	w^{1118}	*white* mutant used as a recipient strain for P element transformations and as control fly line for experiments.	Bloomington Drosophila Stock Center (BDSC)
dLipin			
dLipinRNAi	w^{1118}; *P{GD14004}v36007*	Gal4-driven expression of double-stranded *dLipin* RNA.	Vienna Drosophila Research Center (VDRC) #36007
Df7095	w^{1118}; *Df(2R)Exel7095/CyO*	Deficiency removing chromosomal regions 44B3-44C2, including the entire *dLipin* gene at 44B4-44B5.	BDSC #7860
$dLipin^{e00680}$	w^{1118}; *PBac{RB}CG8709e00680/CyO*	*dLipin* containing piggyBac element in 5' UTR of the *dLipin* gene.	Harvard Exelixis Collection #e00680
LipinWT6M	w^{1118}; *UASdLipinWT*	GAL4 driven expression of wildtype *dLipin*.	Lehmann Laboratory
lipin1	w^{1118}; *UASlipin1*	Gal4 driven expression of homo sapiens *lipin1*.	Sandra Schmitt

lipin2	*w^{1118}; UASlipin2*	Gal4 driven expression of homo sapiens *lipin2*.	Sandra Schmitt
lipin3	*w^{1118}; UASlipin3*	Gal4 driven expression of homo sapiens *lipin3*.	Sandra Schmitt
WTdLipin	*w^{1118}; UASWTdLipin*	GAL4 driven expression of *WTdLipin*.	Sandra Schmitt
ΔNLSdLipin	*w^{1118}; UASΔNLSdLipin*	GAL4 driven expression of *dLipin* lacking the nuclear localization signal (NLS).	Sandra Schmitt Peter Du
ΔPAPdLipin	*w^{1118}; UASΔPAPdLipin*	GAL4 driven expression of *dLipin* with mutation in the PAP catalytic site.	Sandra Schmitt Peter Du
TOR signaling pathway			
raptorRNAi	*y^1 sc^* v^1; P{TRiP.HMS00124}attP2*	Gal4-driven expression of double-stranded *raptor* RNA.	BDSC #41912
rictorRNAi	*y^1 sc^* v^1; P{TRiP.HMS01588}attP2*	Gal4-driven expression of double-stranded *rictor* RNA.	BDSC #36699
Tsc1RNAi	*y^1 sc^* v^1; P{TRiP.GL00012}attP2*	Gal4-driven expression of double-stranded *Tsc1* RNA.	BDSC #35144
Tsc2RNAi	*y[1] sc[*] v[1]; P{y[+t7.7]*	Gal4-driven expression of double-	BDSC #35401

	v[+t1.8]=TRiP.GL00321}attP2	stranded *Tsc2* RNA.	
TORRNAi	*y^1 sc* v^1; P{TRiP.HMS00904}attP2*	Gal4-driven expression of double-stranded *TOR* RNA.	BDSC #33951
Rheb	*w[*]; P{w[+mC]=UAS-Rheb.Pa}3*	Activation of TOR	Lehmann Laboratory
Insulin signaling pathway			
PI3K92EWT	*y[1] w[1118]; P{w[+mC]=UAS-Pi3K92E.Exel}3*	GAL4 driven expression of wild type PI3K92E.	BDSC #8287
PI3K92E^{domneg}	*y[1] w[1118]; P{w[+mC]=UAS-Pi3K92E.A2860C}1*	GAL4 driven expression of a dominant negative version on PI3K92E.	BDSC #8288
PI3K21BHA	*y[1] w[*]; P{w[+mC]=UAS-Pi3K21B.HA}2*	GAL4 driven expression of dominant negative version of PI3K21B.	BDSC #25899
Dp110CAAX	*P{Dp110-CAAX}1, y^1 w^**	Gal4 driven expression of constitutively active Pi3K92E.	BDSC #25908
InRWT	*y[1] w[1118];P{w[+mC]=UAS-InR.Exel}2*	GAL4 driven expression of wild-type InR.	BDSC #8262
InR$^{const.active}$	*y[1] w[1118]; P{w[+mC]=UAS-InR.del}2*	GAL4 driven expression of a constitutive active	BDSC #8248

		version of InR.	
InRDN	*y^1 w^{1118};P{UAS-InR.K1409A}3*	Gal4 driven expression of a dominant negative version of InR.	BDRC #8253
AKT^{myr}		GAL4 driven expression of myristoylated, active form of *Akt*.	Lehmann Laboratory
$AKT^{myrlacZ}$		GAL4 driven expression of myristoylated, active form of *Akt*.	Lehmann Laboratory
chico	*UASchico*	Gal4 driven expression of *chico*.	Saitoe laboratory, Tokyo Metropolitan Institute of Medical Science
Reporter lines			
ubiPLC	*P{Ubi-PH-PLCδ-GFP}*	Ubiquitous expression of *GFP* fused to PIP2 specific PH domain.	Pichaud Laboratory, University College London
tGPH	*w^{1118}; P{tGPH}4*	Ubiquitous expression of *GFP* fused to PIP3 specific PH domain.	BDSC #8164
DcgGFP	*Gal4Dcg; DcgGFP*	Fat body GFP marker.	Graff Laboratory, UT Southwestern Medical Center
Gal4 driver lines			
TubGAL4	*y^1 w^*; P{tubP-GAL4}LL7/TM3, Sb^1*	Ubiquitous expression of GAL4.	BDSC #5138

FB(cg)	*w^{1118}; P{CgGAL4.A}2*	Expression of GAL4 in fat body, hemocytes and lymph gland.	BDSC #7011
FB(r4)	*y[1] w[*]; P{w[+mC]=r4-GAL4}3*	Expression of Gal4 in fat body and salivary glands.	BDSC #33832
DJ761	*w[1118]; P{w[+mW.hs]=GawB}DJ761*	GAL4 expression in all larval tissues except CNS and imaginal discs.	BDSC #8185
hsGAL4	*w; P(GAL4-hsp70)*	Heat-shock induced GAL4 expression.	Lehmann Laboratory
daGal4	*w[1118]; P{daGAL4.w[-]}3*	Weak, ubiquitous Gal4 expression.	BDSC #8641
TubCD2GAL4	*TubCD2GAL4*	Inducible driver used in FLIP-out technique to generate mosaic animals.	Campbell Laboratory, University of Pittsburgh
hsflp; UASGFP/CyO	*hsflp;UASGFP/CyO*	Expression of heat shock induced Flip recombinase and Gal4 driven GFP.	Campbell Laboratory, University of Pittsburgh
Fat synthesis enzymes			
AGPAT3RNAi	*w^{1118}; P{GD16262}v48593*	GAL4 driven expression of double stranded *AGPAT3* RNA.	VDRC #48593
DGAT2RNAi	*w^{1118}; P{GD16204}v48584*	GAL4 driven expression of double stranded *DGAT2*	VDRC #48584

		RNA.	
GPAT4RNAi	*w^{1118}; P{GD3566}v10281/TM3*	GAL4 driven expression of double stranded *GPAT4* RNA.	VDRC #10281
Experimental animals			
***dLipin* knockdown**			
Df7095/ $dLipin^{e00680}$	*Df(2R)Exel7095/ PBac{RB}CG8709e00680*	Transheterozygous for *dLipin* hypomorphic allele and *Df7095*.	Sandra Schmitt
dLipinRNAi/TubGAL4	*P{GD14004}v36007/ P{tubP-Gal4}LL7/TM3, Sb^1*	Ubiquitous knockdown of *dLipin*.	Sandra Schmitt
dLipinRNAi/Fb(cg)	*P{GD14004}v36007/ P{Cg-GAL4.A}2*	Knockdown of *dLipin* in fat body cells.	Sandra Schmitt
hsflp; dLipinRNAi/UASGF;TubCD2GAL4		Mosaic animals	Sandra Schmitt
Insulin pathway and *dLipin* interaction			
Dp110CAAX; dLipinRNAi/FB(cg); tGPH	*P{Dp110-CAAX}1, y^1 w^*;P{GD14004}v36007/ P{Cg-GAL4.A}2; P{tGPH}4*	Test genetic interaction between *PI3K92E* and *dLipin* with regard to PIP3 levels.	Sandra Schmitt
dLipinRNAi/FB(cg); tGPH	*P{GD14004}v36007/ P{Cg-GAL4.A}2; P{tGPH}4*	Localize PIP3 fat body cells with active dLipin knockdown.	Sandra Schmitt

Df7095/ dLipin^{e00680}; tGPH	*Df(2R)Exel7095/ PBac{RB}CG8709e00680; P{tGPH}4*	PIP3 labelled in transheterozygous animals.	Sandra Schmitt
dLipinRNAi/FB(cg); InRDN/DcgGFP	*P{GD14004}v36007/ P{CgGAL4.A}2;P{UAS-InR.K1409A}3/ DcgGFP*	Fat body labelled with GFP in animals carrying *dLipin* and *InRDN* transgenes.	Sandra Schmitt
dLipinRNAi/FB(cg); InRDN	*P{GD14004}v36007/ P{CgGAL4.A}2;P{UAS-InR.K1409A}3*	Test genetic interaction between *dLipin* and *InRDN* in fat body cells.	Sandra Schmitt
dLipinRNAi/FB(cg); tGPH/WTdLipin	*P{GD14004}v36007/ P{Cg-GAL4.A}2; P{tGPH}4/ UASdLipinWT*	PIP3 labelled in cells with *dLipin* knockdown and *WTdLipin* expression.	Sandra Schmitt
dLipinRNAi/FB(cg); tGPH/ΔNLS dLipin	*P{GD14004}v36007/ P{Cg-GAL4.A}2; P{tGPH}4/ UASdLipinΔNLS*	PIP3 labelled in cells with *dLipin* knockdown and *ΔNLSdLipin* expression.	Sandra Schmitt
dLipinRNAi/FB(cg); tGPH /ΔPAP dLipin	*P{GD14004}v36007/ P{Cg-GAL4.A}2; P{tGPH}4/ UASdLipinΔPAP*	PIP3 labelled in cells with *dLipin* knockdown and *ΔPAPdLipin* expression.	Sandra Schmitt
TOR pathway and *dLipin* interaction			
FB(cg); TORRNAi	*P{CgGAL4.A}2;P{TRiP.HMS00904}attP2*	Knockdown of *TOR* in fat body cells.	Sandra Schmitt
FB(cg); raptorRNAi	*P{Cg-GAL4.A}2;*	Knockdown of *raptor*	Sandra Schmitt

	P{TRiP.HMS00124}attP2	in fat body cells.	
FB(cg); rictorRNAi	*P{Cg-GAL4.A}2; P{TRiP.HMS01588}attP2*	Knockdown of *rictor* in fat body cells.	Sandra Schmitt
FB(cg); Tsc1RNAi	*P{Cg-GAL4.A}2; P{TRiP.GL00012}attP2*	Knockdown of *Tsc1* in fat body cells.	Sandra Schmitt
FB(cg); Tsc2RNAi	*P{Cg-GAL4.A}2; v[+t1.8]=TRiP.GL00321}attP2*	Knockdown of *Tsc2* in fat body cells.	Sandra Schmitt
dLipinRNAi/FB(cg); raptorRNAi/tGPH	*P{GD14004}v36007/ P{Cg-GAL4.A}2; P{TRiP.HMS00124}attP/P{tGPH}4*	PIP3 localization after *dLipin* and *raptor* knockdown.	Sandra Schmitt
dLipinRNAi/FB(cg); raptorRNAi/ WTdLipin	*P{GD14004}v36007/ P{Cg-GAL4.A}2; P{TRiP.HMS00124}attP/UASdLipinWT*	Concomitant *dLipin* and *raptor* knockdown in the fat body with simultaneous expression of *WTdLipin*.	Sandra Schmitt
dLipinRNAi/FB(cg); raptorRNAi/ ΔNLSdLipin	*P{GD14004}v36007/ P{Cg-GAL4.A}2; P{TRiP.HMS00124}attP/UASdLipinΔNLS*	Concomitant *dLipin* and *raptor* knockdown in the fat body with simultaneous expression of *ΔNLSdLipin.*	Sandra Schmitt
dLipinRNAi/FB(cg); raptorRNAi/ ΔPAPdLipin	*P{GD14004}v36007/ P{Cg-GAL4.A}2; P{TRiP.HMS00124}at*	Concomitant *dLipin* and *raptor* knockdown in the fat body with simultaneous	Sandra Schmitt

	tP/UASdLipinΔPAP	expression of *ΔPAPdLipin*.	
dLipin chromosome staining			
hsGal4; dLipinWT6M	*w; P(GAL4-hsp70); P{GD14004}v36007*	Expression of *dLipin* in salivary gland for chromosome staining.	Sandra Schmitt
FB(cg); TORRNAi	*P{Cg-GAL4.A}2; P{TRiP.HMS00904}attP2*	*TOR* knockdown in fat body tissue.	Sandra Schmitt
Rescue experiments			
Df7095/ dLipin^{e00680}; WT dLipin/FBr4	*Df(2R)Exel7095/ PBac{RB}CG8709e00680;UASWTdLipin/r4-GAL4*	Expression of *WTdLipin* in fat body of *dLipin* mutants.	Sandra Schmitt
Df7095/ dLipin^{e00680}; ΔNLSdLipin /FBr4	*Df(2R)Exel7095/ PBac{RB}CG8709e00680;UASΔNLSdLipin/r4-GAL4*	Expression of *dLipin* lacking NLS in fat body of *dLipin* mutants.	Sandra Schmitt
Df7095/ dLipin^{e00680}; ΔPAPdLipin/FBr4	*Df(2R)Exel7095/ PBac{RB}CG8709e00680;UASΔPAPdLipin/r4-GAL4*	Expression of *dLipin* lacking PAP motif in fat body of *dLipin* mutants.	Sandra Schmitt
Df7095/ dLipin^{e00680}; ΔPAP dLipin/TubGal4	*Df(2R)Exel7095/ PBac{RB}CG8709e00680;UASΔPAPdLipin/tubP-Gal4*	Strong ubiquitous expression of *dLipin* lacking PAP motif in *dLipin* mutants.	Sandra Schmitt
Df7095/ dLipin^{e00680}; lipin1/ TubGal4	*Df(2R)Exel7095/ PBac{RB}CG8709e00*	Strong ubiquitous expression of human	Sandra Schmitt

	680;UASlipin1/tubP-Gal4	*lipin1* in *dLipin* mutants.	
Df7095/ dLipin^{e00680}; lipin2/ TubGal4	*Df(2R)Exel7095/ PBac{RB}CG8709e00680;UASlipin2/tubP-Gal4*	Strong ubiquitous expression of human *lipin2* in *dLipin* mutants.	Sandra Schmitt
Df7095/ dLipin^{e00680}; lipin3/ TubGal4	*Df(2R)Exel7095/ PBac{RB}CG8709e00680;UASlipin3/tubP-Gal4*	Strong ubiquitous expression of human *lipin3* in *dLipin* mutants.	Sandra Schmitt
Df7095/ dLipin^{e00680}; lipin1/ FBr4	*Df(2R)Exel7095/ PBac{RB}CG8709e00680; lipin1/r4-GAL4*	Expression of human *lipin1* in fat body of *dLipin* mutants.	Sandra Schmitt
Df7095/ dLipin^{e00680}; lipin2/ FBr4	*Df(2R)Exel7095/ PBac{RB}CG8709e00680; lipin2/r4-GAL4*	Expression of human *lipin2* in fat body of *dLipin* mutants.	Sandra Schmitt
Df7095/ dLipin^{e00680}; lipin3/ FBr4	*Df(2R)Exel7095/ PBac{RB}CG8709e00680; lipin3/r4-GAL4*	Expression of human *lipin3* in fat body of *dLipin* mutants.	Sandra Schmitt
Df7095/ dLipin^{e00680}; lipin1/ DJ761	*Df(2R)Exel7095/ PBac{RB}CG8709e00680; lipin1/ GawB}DJ761*	Expression of human *lipin1* in nearly all larval tissues of *dLipin* mutants.	Sandra Schmitt
Df7095/ dLipin^{e00680}; lipin2/ DJ761	*Df(2R)Exel7095/ PBac{RB}CG8709e00680; lipin2/ GawB}DJ761*	Expression of human *lipin2* in nearly all larval tissues of *dLipin* mutants.	Sandra Schmitt
Df7095/ dLipin^{e00680}; lipin3/ DJ761	*Df(2R)Exel7095/ PBac{RB}CG8709e00680; lipin3/ GawB}DJ761*	Expression of human *lipin3* in nearly all larval tissues of *dLipin* mutants.	Sandra Schmitt

ΔNLSdLipin/TubGal 4	*UASΔNLSdLipin/ tubP-Gal4*	Strong ubiquitous expression of *ΔNLSdLipin* for ecdysone rescue experiment.	Sandra Schmitt

Table 1: List of all fly lines used in experiments described in this thesis. Fly lines are listed with genotype, a short description of the experiment(s) they were used in and the source they were obtained from.

2. Plasmids

Name	Description	Source
pUASTattB	Fly transformation vector containing attB site.	Basler Laboratory, University of Zurich
pBluescriptKSII	Cloning vector	Stratagene
pCMV-SPORT6 lipin1	Vector containing human *lipin1* cDNA	Mammalian Gene Collection
pENTR223.1-Sfi lipin2	Vector containing human *lipin2* cDNA	Mammalian Gene Collection
pCR-XI-TOPO lipin3	Vector containing human *lipin3* cDNA	Mammalian Gene Collection
GH19076	*dLipin* cDNA in POT2 vector	Berkley Drosophila Genome Project (BDGP)
pTV2	Fly transfomation vector; Ends-in-Mutagenesis	Sekelsky Laboratory, University of North Carolina
pTarget	Fly transformation vector; Ends-in-Mutagenesis	Sekelsky Laboratory, University of North Carolina

Table 2: List of all plasmids used. A short description of each plasmid is given and the source of the plasmid listed.

3. Antibodies

Primary Antibodies

Name	Host	Dilution	Source
anti-dLipin	rabbit	Western Blot: 1:1000 Immunohistochemistry: 1:400 Chomosome staining: 1:200 to 1:2000	Lehmann Laboratory
anti-phosphoAKT	rabbit	Western Blot: 1:1000	Cell Signaling Technology #4060
anti-panAKT	rabbit	Western Blot: 1:1000	Cell Signaling Technology #2125
anti-4EBP1	rabbit	Western Blot: 1:2000	Nahum Sonenberg Laboratory, Goodman Cancer Center
anti-phospho 4EBP1	rabbit	Western Blot: 1:1000	Cell Signaling Technology #2855
anti-actin	rabbit	Western Blot: 1:500	Sigma Aldrich #A2066
anti-tubulin	rabbit	Western Blot: 1:1000	Cell Signaling Technology #2125
anti-p110	goat	Immunohistochemistry: 1:400 to 1:50	Santa Cruz Biotechnology #sc-7248

Secondary Antibodies

Name	Conjugate	Host	Source
anti-rabbit	Alexa Fluor 647	Goat	Life Technologies

anti-rabbit	Rhodamine	Donkey	Jackson ImmunoResearch
anti-rabbit	Alkaline Phosphatase	Donkey	Jackson ImmunoResearch
anti-goat	Alexa Fluor 647	Donkey	Jackson ImmunoResearch

Table 3: List of all primary and secondary antibodies used. For primary antibodies host species and dilution as well as source are listed. For secondary antibodies host species, conjugate and source are listed.

4. Primers

Name	Sequence	Description
NLSmutafwd	5'GGTGTCCAAGAGCAAAACCTCGCAAATGAAGAAGA3'	Site-directed mutagenesis: Introduced deletion of nuclear localization signal (NLS) into *dLipin* cDNA.
G-Cmutafwd	5'GGTGGTGATCTCGGAGATTGACGGCACCATCA3'	Site-directed mutagenesis: Introduced point mutation changing GAC codon into GAG within phosphatidic phosphatase catalytic motif.
nonmutarev	5'GCCATTCAGCCGTACGACTAGGTTAGGC3'	Site-directed mutagenesis: non-mutagenic reverse primer.
lipinfwdnew	5'GCTGCGGCCGCGTTGCTATGGCTGTGGCCAC3'	Site-directed mutagenesis: Used to amplify 6kb of *dLipin* gene. Introduced NotI restriction site at 5' end.
NLSREV	5'GACTGGGTACCCACCAGCGCCGTCTCCAGCTC3'	Site-directed mutagenesis: Used to amplify 6kb of *dLipin* gene. Introduced KpnI restriction site at 3' end.

GCISceIrevnew	5’CATCGAACCAGGTATTACCCAGTTATCCCTAGGCGGTCGAACTCCTCGTCCGAGGGTGGT3’	Site-directed mutagenesis: Introduction of ISceI site and SexA1 restriction site.
NLSseqfwd	5’CTTCAAACGAAGCTGAGACGA3’	Site-directed mutagenesis: Verification of NLS deletion after site directed mutagenesis.
GCseqfwd	5’GCACCAATGCAAGCTTCAATGC3’	Site-directed mutagenesis: Verification of base exchange after site directed mutagenesis.
ISceseqfwd	5’CCCAGGTGCAGCAAAGCGAGC3’	Site-directed mutagenesis: Verification of presence of ISceI site.
lipin2fwdNot	5’GTCAGGCGGCCGCCCGTCAAGGCCCACCATGAAT3’	Amplification of human *Lipin2* cDNA. Introduces NotI cutting site.
lipin2Kpnrev	5’CTGAGGTAGCGCCCTAAGACAGGTCATCCA3’	Amplification of human *Lipin2* cDNA. Introduces KpnI cutting site.
lipin3fwd	5’GACTGCGGCCGCAGCACCAGCCATGAACTACGT3’	Amplification of human *Lipin3* cDNA. Introduces NotI cutting site.
lipin3rev	5’CTGATCTAGAGGCTGGTTCAGTCCAGGGTATC3’	Amplification of human *Lipin3* cDNA. Introduces XbaI cutting site.
rp49rev	5’ GCGCTTGTTCGATCCGTA 3’	Amplification of *rp49* transcript for qRT PCR analysis.
rp49fwd	5’ CGGATCGATATGCTAAGCTGT 3’	Amplification of *rp49* transcript for qRT PCR
Fruit Fly PI3k92E	Sequence not published; Qiagen RT^2 qPCR primer set for amplification of PI3K92E fragment (#330001)	Amplification of *Dp110* transcript for qRT PCR analysis.

Table 4: List of all primers used in experiments. Primer name, sequence as well as a short description of how they were used in given.

5. Fly maintenance

Flies were grown and maintained on standard fly food prepared with 1.8% yeast, 6.1% cornmeal, 1.3% corn syrup, 1.1% agar and 8.2% malt extract in tap water. The food contained 0.75% propionic acid and 1% tegosept to suppress bacterial and fungal growth. Flies were kept at 25 °C.

6. Molasses agar plates

500ml of distilled H_2O containing 3.5% agar and 14% molasses. The mixture was autoclaved for 20minutes at 15 psi on liquid cycle, and then after cooling to about 60°C, poured into small petri dishes. The molasses plates were stored at 4°C.

7. Media

Liquid Broth (LB) was used to grow bacterial cultures. For 1 liter of LB 950ml distilled H_2O was mixed with 10g tryptone, 5g yeast extract and 10g NaCl. The pH was adjusted to 7.0 with 10N NaOH. The volume was then adjusted to 1Liter with distilled H_2O. The medium was sterilized by autoclaving for 20 minutes at 15 psi on liquid cycle. For LB media plates, 15g/L of Bacto Agar was added to the medium before autoclaving. Antibiotics were added to media at the following concentrations: Ampicillin (50mg/ml): 150μg/ml; Chloramphenicol (34mg/ml): 170μg/ml; Kanamycin (10mg/ml): 50μg/ml.

8. Preparation of competent *E.coli* cells

5ml of LB were inoculated with a single colony of *Escherichia coli* (*E. coli*). The bacterial culture was grown overnight at 37°C with constant shaking. 1ml of the overnight culture was transferred into 100ml of preheated (37°C) LB and grown at 37°C and 240 rpm for 2 hours or until final OD_{600} of 0.3-0.6. The cells were then placed on ice, divided into two pre-chilled 50 ml polypropylene tubes and pelleted by centrifugation in a tabletop centrifuge at 1,600 x g and 4°C for 7 minutes. The supernatant was discarded and the bacterial pellet re-suspended in 10 ml ice cold 0.1M $CaCl_2$ followed by centrifugation at 1,100 x g and 4°C for 5 minutes. The cells were kept overnight at 4°C. The next day, 480µl 80% glycerol was added to the cells. Aliquots of 100µl were pipetted into pre chilled Eppendorf tubes and immediately stored at -80°C.

9. Transformation of competent cells

Competent cells were defrosted on ice and 100µl 0.1M $CaCl_2$ added. DNA was added to the cells in a volume not exceeding 5% of the volume of the competent cells. Contents of the tube were gently mixed followed by a 30 minute incubation period on ice. Cells were heat shocked at 42°C for 2 minutes in a water bath, and immediately transferred back to ice. 800µl of LB broth were added and the cells grown at 37°C and 220 rpm for 90 minutes. Cells were plated onto LB media plates, containing a selective antibiotic if needed.

10. Ligation

All ligations were carried out using T4 DNA Ligase (New England BioLabs # M0202S) according to the manufacturer's recommendations. The ligation reactions were kept at 16°C in a water bath overnight and transformed into competent *E. coli* cells the following day.

11. Generation of *pUASTattBlipin1*, *pUASTattBlipin2* and *pUASTattBlipin3* constructs

The human genome encodes three lipin paralogs. To test whether Lipin function is conserved between *Drosophila melanogaster* and *Homo sapiens*, and in order to determine whether any human lipin paralog can replace the single *Drosophila melanogaster* lipin gene (*dLipin*), UAS responder lines for all three human *lipin* paralogs were created. These responder lines were then expressed in *dLipin* mutant animals (*Df7095/ dLipin*^{e00680}). To this end, each human *lipin* paralog was cloned into the *Drosophila pUASTaTTB* transformation vector.

The plasmid *pCMV-SPORT6 lipin1* (Table 2) was grown in LB media containing ampicillin overnight at 37°C with shaking. Plasmid DNA was prepared from the overnight culture using the GenScript QuickCleanII Plasmid Miniprep Kit (# L004320). *lipin1* cDNA was cut from the vector backbone using KpnI and AvrII and the *lipin1* fragment separated from the plasmid DNA by agarose gel electrophoresis. The *lipin1* fragment was cut out from the gel, and the DNA purified using the QuickCleanII Gel Extraction Kit from Genscript (# L00418). The final destination vector, *pUASTattB*, was prepared by cutting with KpnI and and XbaI (XbaI and AvrII have compatible ends for ligation), and a ligation reaction with both components was set up.

pENTR223.1-Sfi lipin2 plasmid (Table 2) was grown in LB overnight at 37°C with shaking and chloramphenicol added as the selective antibiotic. Plasmid DNA was isolated the

following day using the GenScript QuickCleanII Plasmid Miniprep Kit (# L004320). *lipin2* cDNA was amplified using PCR (forward primer: lipin2fwdNot; reverse primer: lipin2Kpnrev; Table 4). Phusion High-Fidelity DNA Polymerase (New England BioLabs #F-S30S) was used to amplify the fragment. The *lipin2* fragment was then digested with NotI and KpnI as was the destination vector *pUASTattB*. A ligation reaction with both components was set up.

pCR-XI-TOPO lipin3 plasmid (Table 2) was grown in LB overnight at 37°C with shaking and kanamycin added as the selective antibiotic. Plasmid DNA was purified the following day using the GenScript QuickCleanII Plasmid Miniprep Kit (# L004320). *lipin3* cDNA was amplified in a PCR reaction (forward primer: lipin3fwd; reverse primer: lipin3rev; Table 4). Phusion High-Fidelity DNA Polymerase (New England BioLabs #F-S30S) was used to amplify the fragment according to manufacturer's recommendations. *lipin3* cDNA and the destination vector *pUASTattB* were cut with NotI and XbaI, and ligated.

All three ligation reactions were transformed into *E.coli* cells and plated on LB plates with ampicillin as the selective antibiotic. Colonies were picked the next day and DNA prepared using GenScript QuickCleanII Plasmid Miniprep Kit (# L004320). Analytical restriction digestions were conducted to verify the presence of *lipin* inserts in the clones picked. . To screen for presence of *lipin1* fragment the construct was digested with KpnI and XmaI, *lipin2* presence was detected by cutting with NotI and KpnI whereas *lipin3* presence was verified by restriction digest with NotI and XbaI. Positive clones were grown up in 50ml ampicillin containing LB medium overnight at 37°C with shaking and plasmid was DNA purified using Qiagen HiSpeed Plasmid Midi Kit (# 12643). The DNA was sent off to BestGene Inc for injection into fly embryos. For the sake of simplicity, these constructs are being referred to as *lipin1*, *lipin2* and *lipin3* in the remainder of the text.

12. Site-directed mutagenesis and generation of *pUASTattBWTdLipin*, *pUASTattBΔPAPdLipin* and *pUASTattBΔNLSdLipin* constructs

dLipin cDNA (plasmid GH19076) was used to create three different UAS responder lines. *WTdLipin* is a construct used to express wild type *dLipin*. *ΔPAPdLipin* encodes dLipin with a point mutation at position 2886 of the nucleotide sequence. This point mutation leads to an encoded protein with a glutamate (Glu or E) residue at position 812 of the protein instead of an aspartate (Asp or D) residue (D812E). This change in the amino acid sequence results in a loss of phosphatidic acid phosphatase activity (PAP activity) (Finck *et al*.; 2006). *ΔNLSdLipin* encodes a mutant dLipin lacking the nuclear localization signal (NLS; amino acid positions 276-281), thus this protein is not able to translocate to the nucleus and affect gene regulation. I targeted the NLS instead of the co-regulator motif because previous research showed that deletion of the co-regulator motif not only affects nuclear activity, but also PAP activity of Lipin1 (Reue and Brindley; 2008). To identify the putative NLS in dLipin I used the openly accessible PredictNLS software from the Rost laboratory (https://rostlab.org/owiki/index.php/PredictNLS).

MNSLARVFSNFRDFYNDINAATLTGAIDVIVVEQRDGEFQCSPFHVRFGKLGVLRSREK
VVDIEINGVPVDIQMKLGDSGEAFFVEECLEDEDEELPANLATSPIPNSFLASRDKANDT
MEDISGVVTDKNASEELLLPLPLPRRNSIDFSKEEPKEAVVEGSKFENQVSDYTQRRHTD
NTLERRNLSEKLKEFTTQKIRQEWAEHEELFQGEKKPADSDSLDNQSKASNEAETEKAIP
AVIEDTEKEKDQIKPDVNLTTVTTSEATKEVSKSKT**KKRRKK**SQMKKNAQRKNSSSSSL
GSAGGGDLPSAETPSLGVSNIDEGDAPISSATNNNNTSSSNDEQLSAPLVTARTGDDSPLS
EIPHTPTSNPRLDLDIHFFSDTEITTPVGGGGAGSGRAAGGRPSTPIQSDSELETTMRDNR
HVVTEESTASWKWGELPTPEQAKNEAMSAAQVQQSEHQSMLSNMFSFMKRANRLRKE
KGVGEVGDIYLSDLDAGSMDPEMAALYFPSPLSKAASPPEEDGESGNGTSLPHSPSSLEE
GQKSIDSDFDETKQQRDNNRYLDFVAMSMCGMSEQGAPPSDEEFDRHLVNYPDVCKSP
SIFSSPNLVVRLNGKYYTWMAACPIVMTMITFQKPLTHDAIEQLMSQTVDGKCLPGDEK
QEAVAQADNGGQTKRYWWSWRRSQDAAPNHLNNTHGMPLGKDEKDGDQAAVATQT
SRPTSPDITDPTLSKSDSLVNAENTSALVDNLEELTMASNKSDEPKERYKKSLRLSSAAIK

KLNLKEGMNEIEFSVTTAYQGTTRCKCYLFRWKHNDKVVIS**DIDGT**ITKSDV**LGHIL**PM
VGKDWAQLGVAQLFSKIEQNGYKLLYLSARAIGQSRVTREYLRSIRQGNVMLPDGPLLL
NPTSLISAFHREVIEKKPEQFKIACLSDIRDLFPDKEPFYAGYGNRINDVWAYRAVGIPIM
RIFTINTKGELKHELTQTFQSSGYINQSLEVDEYFPLLTNQDEFDYRTDIFDDEESEEELQF
SDDYDVDVEHGSSEESSGDEDDDEALYNDDFANDDNGIQAVVASGDERTADVGLIMRV
RRVSTKNEVIMASPPKWINS

Putative NLS; **PAP active site**; **Co-activator motif**

Fig 6: Protein (CG8709-PA) sequence of dLipin isoform A with nuclear localization signal (NLS), PAP active site and co-activator motive. The NLS is deleted in *ΔNLSdLipin* construct and the PAP site changed from DIDGT to EIDGT in the *ΔPAPdLipin* construct via site-directed mutagenesis.

Plasmid GH19076 was grown in LB with chloramphenicol acting as the selective antibiotic. Site-directed mutagenesis was carried out using the Change-IT Multiple Mutation Site Directed Mutagenesis Kit by USB (# 78480) to create *ΔPAPdLipin* cDNA (forward primer: G-Cmutafwd; reverse primer: nonmutarev; Table 4) and *ΔNLSdLipin* (forward primer: NLSmutafwd; reverse primer: monmutarev; Table 4). Successful mutagenesis was confirmed by sequencing (primers: GCseqfwd and NLSseqfwd; Table 4). The mutated and wild- type *dLipin* cDNAs were isolated from the *pOT2* vector using XhoI and EcoICRI and the cDNA fragment separated from the vector backbone by agarose gel electrophoresis. The cDNA fragments were cut out from the gel and the DNA was purified using the QuickCleanII Gel Extraction Kit from Genscript (# L00418). *pUASTattB* served as the final transformation vector. The vector was cut with XbaI and the 5' overhang filled in with Klenow enzyme. This was followed by digestion with XhoI. To reduce religation of potentially partially digested plasmid, the vector was treated with Shrimp Alkaline Phosphatase (Promega # M9910) according to the manufacturer's recommendations. The prepared *pUASTattB* vector was then used for ligation with the cDNA fragments. Transformed cells were plated onto LB agar plates with ampicillin as the selective

antibiotic and incubated at 37°C overnight. Clones were picked and grown in LB with ampicillin at 37°C overnight. DNA was purified from bacterial cultures using GenScript QuickCleanII Plasmid Miniprep Kit (# L004320). Identification of positive bacterial transformants was achieved by analytical digestion of extracted DNA with EcoRI and XhoI. Positive clones were grown up in 50ml ampicillin containing LB medium overnight at 37°C with shaking and DNA was then purified using Qiagen HiSpeed Plasmid Midi Kit (# 12643). The DNA was sent to BestGene Inc for injection into fly embryos. From this point onwards, for the sake of simplicity, I will refer to these lines as *WTdLipin*, *ΔNLS dLipin* and *ΔPAPdLipin*.

13. Site-directed mutagenesis and cloning of *pTV2ΔPAPdLipin* and *pTargetΔNLSdLipin* donor constructs for ends-in-targeting gene replacement

Bac-Clone #RP98-9N11 (BACPAC Resources Center) served as a template to amplify 6kb of the *dLipin* gene. The clone was grown in LB with chloramphenicol as the selective antibiotic. Phusion High-Fidelity DNA Polymerase (New England BioLabs #F-S30S) was used to amplify the fragment (forward primer: lipinfwdnew; reverse primer: NLSREV; Table 4). The 6kb fragment was cloned into *pBluescriptKSII* via KpnI and NotI restriction sites. T4 DNA Ligase (New England BioLabs # M0202S) was used to ligate vector DNA with the 6kb fragment, colonies were picked and DNA extracted with GenScript QuickCleanII Plasmid Miniprep Kit (# L004320). Presence of the 6kb *dLipin* insert was verified in an analytical digestion with KpnI and NotI. Site-directed mutagenesis was then carried out with positive clones using the Change-IT Multiple Mutation Site Directed Mutagenesis Kit by USB (# 78480). To knock out the PAP activity (ΔPAP) of dLipin, D812 was converted into E (D812E, forward primer: G-Cmutafwd; reverse primer: nonmutarev; Table 4). In order to eliminate the nuclear co-

regulator function of dLipin, the Nuclear Localization Signal was deleted (ΔNLS) (NLS; AA 276-281; forward primer: NLSmutafwd; reverse primer: monmutarev; Table 4). For a more detailed description please refer to Materials and Methods 12. Clones were screened for successful mutagenesis/deletion by sequencing (primers: GCseqfwd and NLSseqfwd; Table 4).

An I-SceI site was inserted into these sequences using PCR (forward primer: lipinfwdnew; reverse primer: GCISceIrevnew; Table 4). Thereby, 3kb of the mutated *dLipin* gene were amplified via PCR and an I-SceI recognition sequence attached to the generated fragment's 3'end. The I-SceI sequence was added to the reverse primer. Additionally, a NotI cutting site was introduced at the 5' and of the PCR fragment, and a SexAI site at the very 3' end. Using SexAI and NotI restriction sites in the plasmid containing the original mutated DNA, 3kb were cut out and replaced with the 3kb PCR that now contain the I-SceI site. The 3kb I-SceI fragment and the plasmid containing the remainder 3kb of *dLipin* were ligated. The Ligation reaction was transformed into methylation negative cells (*dam*$^-$/*dcm*$^-$ Competent cells; New England Biolabs # 29521) as SexA1 cuts only unmethylated DNA. Cells were plated on to LB plates containing ampicillin as the selective antibiotic and incubated at 37°C overnight. Plasmid DNA was extracted from colonies using the GenScript QuickCleanII Plasmid Miniprep Kit (# L004320) and presence of the I-SceI site confirmed via sequencing (primer: ISceseqfwd; Table). Using KpnI and NotI restriction sites, the entire 6kb fragment containing the D812E mutation was cut out and ligated into the *pTV2* plasmid that had been cut with the same restriction enzymes to generate *pTV2ΔPAPdLipin*. The *ΔNLSdLipin* fragment was cut with KpnI and NotI and ligated into the *pTarget* plasmid that had been digested with the same restriction enzymes to create *pTargetΔNLSdLipin*. Analytical digest with KpnI and NotI was used to verify the presence of the 6kb fragments in the final constructs. Positive clones were grown in 50ml ampicillin

containing LB medium overnight at 37°C with shaking and DNA purified using Qiagen HiSpeed Plasmid Midi Kit (# 12643). DNA for both constructs was sent off to BestGene Inc for injection into fly embryos.

14. Genetic interaction experiments between *dLipin* and members of the TOR and Insulin pathways

To test whether *dLipin* and Insulin/TOR signaling affect each other, genetic interaction experiments were conducted. Therefore, *dLipin* was knocked down or overexpressed in concert with members of the Insulin and TOR signaling pathways. Offspring with both genetic modifications, should exhibit either an enhancement or rescue of the *dLipin* or Insulin/TOR phenotype if there are any interactions. To this end, fly lines expressing *dLipinRNAi* or *dLipinWT6M* or hypomorphic *dLipin* mutants were crossed with lines expressing RNAi against genes involved in the TOR and insulin pathways gene, hypomorphic TOR and insulin pathway mutants or TOR and insulin pathway overexpression lines.

The following is a list of genotypes created to study possible genetic interactions between *dLipin* and genes of the TOR and insulin pathways.

Simplified genotype	Description
dLipinRNAi/InR$^{cont.active}$;FB(r4)	Expression of constitutive active form of InR in concert with *dLipinRNAi* using fat body-specific driver.
dLipinRNAi/InR$^{cont.active}$; DJ761	Weak ubiquitous expression of constitutively active form of InR in concert with *dLipinRNAi*.
dLipinRNAi/PI3K21BHA; FB(r4)	Expression of dominant negative form of PI3K21B in concert with *dLipin* knockdown using fat body-

	specific driver.
dLipinRNAi/PI3K21BHA; DJ761	Weak ubiquitous expression of constitutive active form of InR in concert with *dLipinRNAi*.
PI3K21BHA; LipinWT6M/FB(r4)	Expression of dominant negative form of PI3K21B in concert with *WTdLipin* using fat body specific driver.
dLipinRNAi/FB(cg); PI3K92E$^{dom.neg.}$	Expression of dominant negative form of PI3K92E with concomitant *dLipin* knockdown using fat body specific driver.
dLipinRNAi/FB(cg); PI3K92E	Expression of wild-type *PI3K92E* in concert with *dLipin* knockdown using fat body specific driver.
dLipin^{e00680}/ dLipin^{e00680}; AKT^{myr}/ FB(r4)	Expression of activated AKT in fat body in hypomorphic *dLipin* mutant background.
Df7095/ dLipin^{e00680}; AKT^{myrlacZ}/ FB(r4)	Expression of activated AKT in fat body in transheterozygous *dLipin* mutant background.
Dp110CAAX; dLipinRNAi/ FB(cg)	Expression of constitutively active form of Dp110 in concert with *dLipinRNAi* using fatbody specific driver.
dLipinRNAi/FB(cg); InR$^{dom.neg.}$	Expression of dominant negative form of InR in concert with *dLipinRNAi* using fat body specific driver.
dLipin^{e00680}/ dLipin^{e00680};Rheb/hsGal4	Expression of *Rheb* with fatbody specific driver in hypomorphic *dLipin* mutant background.
dLipinRNAi/FB(cg); Rheb/InR$^{dom.neg.}$	Simultaneous expression of *Rheb*, *dLipinRNAi* and *InR$^{dom.neg.}$* using fat body specific driver.
dLipinRNAi/FB(cg); TORRNAi	Simultaneous RNAi-mediated knockdown of *TOR* and *dLipin* using fat body specific driver.
dLipinRNAi/FB(cg); raptorRNAi	Simultaneous RNAi-mediated knockdown of *raptor* and *dLipin* using fat body specific driver.
dLipinRNAi/FB(cg); rictorRNAi	Simultaneous RNAi-mediated knockdown of *rictor*

	and *dLipin* using fat body specific driver.
dLipinRNAi/FB(cg); Tsc1RNAi	Simultaneous RNAi-mediated knockdown of *Tsc1* and *dLipin* using fat body specific driver.
dLipinRNAi/FB(cg); Tsc2RNAi	Simultaneous RNAi-mediated knockdown of *Tsc2* and *dLipin* using fat body specific driver.

Table 5: List of genetic interaction experiments conducted to investigate the relationship between dLipin and Insulin/TOR pathway.

To detect potential interaction between *dLipin* and genes of the TOR/insulin pathways, offspring was examined for different parameters, depending on the genetic makeup of the animals. The parameters included: effects on larval development and fat body morphology (fat droplet size, cell size, cell shape).

15. Analyses of genetic interaction between *dLipin* and insulin receptor (*InR*)

To investigate larval viability in animals with concomitant *dLipin* and $InR^{dom.neg.}$ expression, flies with the following genotype were generated: *dLipinRNAi/FB(cg);* $InR^{dom.neg.}$.

To this end the following cross was set up:

Parental cross: *FB(cg)/FB(cg)* X *dLipinRNAi/CyOGFP;* $InR^{dom.neg.}$*/Tb,TM6B*

→ *FB(cg)/CyOGFP; Tb,TM6B:* Control animals; 25% genotype frequency expected.

FB(cg)/CyOGFP; $InR^{dom.neg.}$: Experimental animals expressing $InR^{dom.neg.}$; 25 % genotype frequency expected.

FB(cg)/dLipinRNAi; Tb,TM6B: Experimental animals expressing dLipinRNAi; 25 % genotype frequency expected.

FB(cg)/dLipinRNAi; InR$^{dom.neg.}$: Experimental animals expressing both transgenes; 25% genotype frequency expected.

As a measure for larval lethality, I counted pupae formed for each genotype. As genotype frequencies for each genotype were known, it was possible to directly compare the number of pupae formed by control animals with any of the three experimental genotypes. I analyzed the numbers using Chi-square statistical analyses.

16. Rescue of *dLipin* mutants by expression of human *lipin* transgenes

To investigate functional conservation between *dLipin* and the three human *lipin* paralogs (*lipin1, lipin2 and lipin3*) transgenic fly lines were generated for expression of each of the homologs in *Drosophila* (11).

Crosses were set up to analyze rescue effects for each of the three homologous genes. Flies of the two following genotypes were analyzed:

Df7095/ dLipin^{e00680}; lipin1/2/3 / DJ761

Df7095/ dLipin^{e00680}; lipin1/2/3 / TubGAL4

Df7095/ dLipin^{e00680}; lipin1/2/3 / FBGAL4.

Animals transheterozygous for *dLipin* mutations and carrying both human *lipin* transgene and driver were analyzed with regard to fat body development and larval lethality. To compare larval lethality between different genotypes, I examined the number of pupae formed by animals of the different genotypes. I set up individual crosses for each human *lipin* transgene. The genotype frequency for resulting genotypes was known, thus I was able to compare the number of pupae formed with the control genotype (*Df7095/ dLipin^{e00680}; lipin1/2/3*) to the number of

pupae formed with experimental genotype (*Df7095/ dLipin^{e00680}; lipin1/2/3 / Gal4*)., Chi-Square analyses were conducted to assess statistical significance.

Parental cross exemplified for *lipin1*:

Df7095/ CyOGFP; lipin1/lipin1 X *dLipin^{e00680}/CyOGFP; Gal4/ Tb,TM6B*

➔ Genotypes that were compared: *Df7095/ dLipin^{e00680}; lipin1/ Gal4:* experimental animals

Df7095/ dLipin^{e00680}; lipin1/Tb,TM6B: control animals

Genotype frequencies for both genotypes were 50% compared to each other. I compared the number of pupae formed with control genotype to the number of pupae formed with experimental genotype using Chi-Square analysis. The number of pupae formed with control genotype was set to 100% and % for the number of pupae formed with experimental genotype was calculated.

17. Rescue of *dLipin* mutants or animals with RNAi mediated *dLipin* knockdown by expression of *ΔPAPdLipin*, *ΔNLSdLipin* and *WTdLipin* constructs

To determine the rescue effects of dLipin lacking either catalytic or transcriptional co-regulator activity, *ΔPAPdLipin*, *ΔNLSdLipin* and *WTdLipin* transgenes were expressed in a *dLipin* transheterozygous mutant background, or concomitant with *dLipinRNAi*. Animals of the following genotypes were generated:

Df7095/ dLipin^{e00680}; ΔPAPdLipin, ΔNLSdLipin or *WTdLipin / daGAL4*

Df7095/ dLipin^{e00680}; ΔPAPdLipin, ΔNLSdLipin or *WTdLipin / TubGAL4*

Df7095/ dLipin^{e00680}; ΔPAPdLipin, ΔNLSdLipin or *WTdLipin / FBGAL4*

dLipinRNAi / FBGal4; ΔPAPdLipin, ΔNLSdLipin or *WTdLipin / tGPH.*

These fly strains were observed with regard to fat body development, fat body morphology, larval lethality and PIP3 localization. Animals of the genotypes *dLipinRNAi/FBGal4; ΔPAPdLipin/tGPH, dLipinRNAi/FBGal4; ΔNLSdLipin/tGPH* and *dLipinRNAi/FBGal4; WTdLipin/tGPH* were examined for PIP3 localization. Transheterozygous *dLipin* mutants with concomitant expression of *ΔPAPdLipin, ΔNLSdLipin* or *WTdLipin* were examined with regard to fat body morphology and larval lethality. I set up individual crosses for each dLipin construct. To compare larval lethality between control (*Df7095/ dLipin^{e00680}; Gal4*) and experimental genotypes (*Df7095/dLipin^{e00680}; ΔPAPdLipin, ΔNLSdLipin* or *WTdLipin/GAL4*), I examined the number of pupae formed for the specific genotypes. The genotype frequency for resulting genotypes was known thus, I was able to compare the number of pupae formed with control genotype (*Df7095/dLipin^{e00680}; ΔPAPdLipin, ΔNLSdLipin* or *WTdLipin*) to the number of pupae formed with experimental genotype (*Df7095/dLipin^{e00680}; ΔPAPdLipin, ΔNLSdLipin* or *WTdLipin/Gal4*). To assess statistical significance, Chi-Square analysis was conducted.

Parental cross exemplified for *WTLipin*:

Df7095/ CyOGFP; Gal4/Tb X *dLipin^{e00680}/CyOGFP; WTdLipin/WTdLipin*

➔ Genotypes that were compared: *Df7095/ dLipin^{e00680}; WTdLipin/Gal4:* experimental animals

Df7095/ dLipin^{e00680}; WTdLipin/Tb: control animals

Genotype frequencies for both genotypes were 50% compared to each other. I compared the number of pupae formed with control genotype to the number of pupae formed with

experimental genotype using Chi-Square analysis. The number of pupae formed with control genotype was set to 100% and % for the number of pupae formed with experimental genotype was calculated.

18. Generation of mosaic animals for *dLipinRNAi*

The goal of this experiment was to generate larval fat body tissue with single cells that lack dLipin activity in an otherwise wild type dLipin background. These mosaic animals were generated using the flip-out technique (Blair, 2003). Animals were kept at 25 °C on standard food. At this temperature basal expression of a heat-shock induced FLP (flippase) recombinase led to the activation of the *TubGAL4* driver in only a small number of cells. This is possible because the FLP recombinase targets the FRT (flippase recognition target) sites flanking a CD2 cassette that was introduced to prohibit the expression of *Gal4* from the driver promoter (*Tubulin α* promoter). The CD2 cassette was subsequently removed via site-specific recombination by the FLP recombinase, which allowed for the expression of *Gal4* from the *Tubulin* promoter. Presence of Gal4 then triggered *dLipinRNAi* expression in these cells. Mosaic cells were further marked with *UASGFP* (*Green fluorescent Protein*). Hence, only very few cells expressed both *dLipinRNAi* as well as the marker *GFP*.

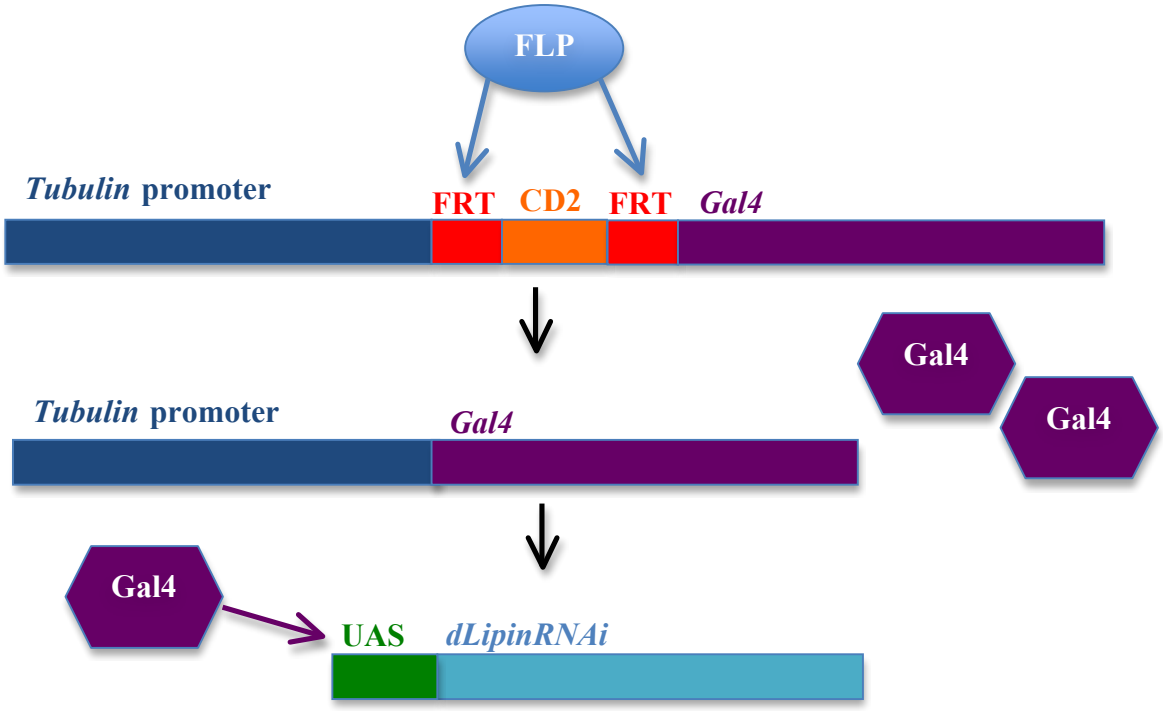

Fig. 7: Depiction of the FLP-out process in mosaic cells. In single cells, expression of *FLP* recombinase was triggered. FLP recombinase subsequently targets the FRT sites flanking a CD2 cassette and removes it. This allows expression of *Gal4* form the *Tubulin* promoter. The transcription factor Gal4 then binds to its target sequence UAS (upstream activating sequence) and activates expression of *dLipinRNAi*. In addition to *dLipinRNAi*, Gal4 also triggers expression of *GFP*.

Final cross:

hsflp/hsflp; UASGFP X dLipinRNAi; Tub-CD2-Gal4

=> Mosaic animals: *hsflp; UASGFP/dLipinRNAi; Tub-CD2-Gal4*

Fat body from mosaic animals was dissected in PBS pH7.4 (137mM NaCl, 2.7mM KCl, 10mM Na_2HPO_4, 1.8mM KH_2PO_4; pH adjusted with HCl) and fixed in 4% formaldehyde for 30 minutes. To verify successful *dLipin* knockdown the tissue was stained with anti-Lipin antibody. Visualization of lipid droplets was achieved by staining with HCS LipidTOX Deep Red neutral lipid stain (Invitrogen # H34477). After staining was completed the tissue was mounted in

Slowfade Gold antifade reagent with DAPI (Invitrogen # P36931) and examined under a Carl Zeiss AxioVision microscope.

19. Fat droplet staining

Fat droplets were stained with Bodipy 493/503 (Invitrogen # D2191) or HCS LipidTOX Deep Red neutral lipid stain. Fat body was dissected in PBS, pH7.4 followed by fixation in 4% formaldehyde for 30 minutes. The stains were diluted in PBS, pH 7.4. BODIPY was diluted to a final concentration of 1 μg/ml, whereas HCS LipidTOX Deep Red was used at a 1:400 dilution. Fixed tissue was stained for 30-60 minutes at room temperature. Tissue was protected from light during this step to prohibit photo bleaching. After staining was completed, tissue was mounted in Slowfade Gold antifade reagent with DAPI (Invitrogen # P36931). Images were taken using a Carl Zeiss AxioVision microscope. Bodipy stained fat droplets were viewed with a GFP filter, and HCS LipidTOX Deep Red stained fat droplets with a Cy5 filter. DNA was viewed using the DAPI filter setting.

20. dLipin antibody staining

Tissue was dissected on ice in PBS, pH 7.4 and fixed in 4% formaldehyde for 30 minutes. After fixation, tissue was washed 4 times in PBST (PBS plus 0.2% Tween20) for 10 minutes and then blocked in PBST with 1% Normal Donkey serum (NDS) or Normal Goat Serum (NGS), depending on the secondary antibody used. Blocking lasted for at least 2 hours at room temperature accompanied by gentle shaking. Affinity purified anti-dLipin antibody was added at 1:400 dilution in PBST with 1% NDS or NGS, and tissue was stained overnight at 4°C with gentle shaking. Tissue was then washed four times in PBST for 10 minutes each and the secondary antibody was added. Secondary antibodies used were Rhodamine conjugated donkey

anti-rabbit IgG (Jackson ImmunoResearch #69532; Table 3) and Alexa Fluor 647 conjugated goat anti-rabbit IgG (Life Technologies #A21244; Table 3), both used at a 1:1000 dilution (in PBST with 1% NDS or NGS). The incubation period lasted 2 hours during which samples were wrapped in aluminium foil to prohibit photo bleaching. Tissue was then washed 4 times in PBST for 10 minutes each, and mounted in Slowfade Gold antifade reagent with DAPI (Invitrogen # P36931). Images were captured with a Carl Zeiss AxioVision microscope.

21. Measurement of hemolymph sugar levels

The Glucose Assay Kit by Cayman Chemical Company (#10009582) was used to measure the hemolymph sugar levels of feeding third instar larvae. Hemolymph of five *Df(2R)Exel7095*/ *dLipin*^{e00680} feeding third instar larvae and five heterozygous larvae was collected. Triplicate samples were analyzed for each genotype (total n for each genotype: 15). 0.5µl of hemolymph were mixed with 19 µl PBS, pH7.4. After centrifugation at 13,000 x g for 10 min, 10µl of supernatant were added to 100 µl Assay Buffer (100mM PBS at pH 6.5). 0.05 units/ml trehalase (Sigma #T8778) were added to samples and standards and the tubes incubated at 37°C overnight. 50 µl of samples and standards were then transferred to 500 µl Enzyme Mix and incubated for 10 min at 37°C. 150 µl of the reactions were pipetted to a cuvette and absorption measured at 514nm in a UV-spectrophotometer. A linear regression graph for standards was created and glucose concentrations in samples calculated.

22. SDS-Polyacrylamide Gel Electrophoresis (SDS-PAGE)

A BioRAD Mini-PROTEAN® System was used for SDS Gel electrophoresis. First, the components of the resolving gel were mixed in a flask and poured between the glass slides. The resolving gel consisted of Acrylamide-bis (30%-0.8%), Lower Buffer (3M Tris Base, 0.8% SDS,

pH 8.8 adjusted with concentrated HCl), 75% Sucrose, TEMED, 5% Ammoniumpersulfate and distilled H_2O. The pipetting scheme for the resolving gel depended on the desired thickness of the gel.

The gel was covered with layering Buffer (1:8 dilution of Lower Buffer) and left to polymerize. After completion of the polymerization process, the layering buffer was removed with Whatman filter paper, and the stacking gel added. The stacking gel was made up of the following components: Acrylamide-bis (30%-0.8%), Upper Buffer (0.5M Tris Base, 0.4% SDS, pH 6.8 adjusted with concentrated HCl), 75% Sucrose, TEMED, 5% Ammoniumpersulfate and distilled H_2O. The comb was inserted quickly after addition of the resolving gel mix, and the gel left to polymerize. Upon completion of this polymerization process, the comb was removed and the gel inserted into the electrophoresis chamber. Gel Running Buffer (0.025 M Tris Base, 0.192 M Glycine, 1% SDS) was poured into the tank. The samples and Protein Marker (Prestained Protein Marker, New England Biolabs # P7708S or PAGE RULER Prestained Plus, Thermo Scientific # 26619) were loaded. Prior to loading, samples were dissolved in Sample Buffer (4% SDS, 20% glycerol, 10% 2-mercaptoethanol, 0.004% bromphenol blue, 0.125 M Tris HCl) and heat denatured for 5 minutes at 95°C. After marker and samples were loaded, the gel was run at 250V until clear separation of the marker bands was achieved (~30min). The BioRad PowerPac™ HC Power Supply served as the power source for the electrophoresis process.

23. Western Blot Analysis

Protein Transfer

The Mini Trans-Blotcell from BioRad was used for Western-Blotting. After completion of gel electrophoresis, the gel was placed onto a PVDF membrane, which had been pre-wetted in

100% methanol for 5minutes. Whatman filter paper sheets and a layer of fiber pads held the gel and PVDF membrane together. It is important to prevent the formation of air bubbles between the gel and the PVDF membrane when setting up this sandwich. This can be achieved by running a pasteur pipette gently across the sandwich. The sandwich was placed into the buffer tank in a gel holder cassette and the buffer tank was filled with transfer buffer (25 mM Tris, 192 mM Glycine, 20% (v/v) methanol (pH 8.3)). After addition of a magnetic stirrer and the BioIce Cooling unit, the cables were connected with the electrodes of the power source (BioRad PowerPac™ HC Power Supply) and the proteins transferred onto the membrane at 100V for 65minutes. After the protein transfer was completed the membrane was soaked in 5% powdered milk in TBST (50 mM Tris, 150mM NaCl, 0.05% Tween 20) for 1 hour. The membrane was then washed in TBST for a short time, and 5ml 5% powdered milk in TBST was added. The primary antibody was added to the TBST and the membrane incubated in the primary antibody at 4°C with light shaking overnight. Alternatively, the primary antibody was diluted in 5% Bovine Serum Albumin in TBST. For dilution ratios of primary antibodies please refer to Table 3. Three washing steps in TBST followed this incubation period, with every washing step lasting 10 minutes. 5ml TBST plus secondary antibody (dilution 1:2000, Table 3) was added to the membrane and the membrane incubated for at least 2 hours at room temperature. Excess antibody was washed away in TBS-T for 10 minutes. This washing step was repeated 3 times.

Detection

Proteins were detected in a colorimetric reaction using alkaline phosphatase conjugated to the secondary antibody. After antibody treatment the membrane was prepared for detection by soaking in TBS-$MgCl_2$ (50mM Tris, 150mM NaCl, 5mM $MgCl_2$) for 5minutes. During this incubation step the substrate solution was prepared (15ml TBS-$MgCl_2$, 0.10ml NBT (50mg/ml),

0.05ml BCIP (50mg/ml); BCIP/NBT Color Development Substrate from Promega #S3771). A combination of NBT and BCIP was used, as combining the two substrates yields an intense, black-purple precipitate that provides much greater sensitivity than either substrate alone. The pretreated membrane was put into the substrate solution and developed until protein bands were visible. To stop the colorimetric reaction, the membrane was transferred into 10% acetic acid.

24. Salivary gland chromosome staining

Before the staining procedure, Buffer A was freshly prepared (10X: 150mM Tris-HCl pH 7.4, 600mM KCl, 150mM NaCl, 5mM Spermidin, 1.5mM Spermin). Salivary glands of wandering third instar larvae were dissected in physiological solution A (0.7% NaCl in distilled H_2O). These animals expressed *hsGal4; dLipinWT6M*. Wandering third instar larvae were subjected to an hour-long heat shock at 37°C. . Dissection of larval salivary glands was conducted immediately after heat shock, 2hs after heat shock and 24hs after heat shock. Dissected glands were placed into solution B for 25 sec. for fixation (for 1ml: 10% of 37% formaldehyde, 70% distilled H_2O, 10% Triton X100, 10% Buffer A). After fixation, glands were quickly rinsed in solution C (for 1ml: 10% of 37% formaldehyde, 40% distilled H_2O, 50% glacial acetic acid), and placed on a cover slip containing a drop of solution C for 3-4 minutes. The coverslip with salivary glands was picked up with a microscopic slide and pressure was applied by pressing down with a finger or the handle of the forceps. The slide was then turned around and the coverslip/slide sandwich pressed tightly between two sheets of blotting paper. The slide was flash frozen in liquid N_2 and the coverslip removed with a razorblade. The area of the chromosome squash was labeled with a pencil and the slide immersed into 100% ethanol for at least 10 min. Slides were then washed in KP-Buffer (10X: 1.4M NaCl, 0.1M Potassiumphosphate ph 7.4) twice for 10 min. Any residual KP-Buffer was removed by shaking

the slide quickly and 20µl primary antibody solution added (dLipin: 1:200 to 1:2000). Slides were incubated in moist chamber overnight at 4°C. The primary antibody and the cover slip were removed by two washes in KP-Buffer, with each wash lasting 10 min. 40µl of secondary antibody solution (Rhodamine conjugated anti-rabbit 1: 1000) was pipetted onto a coverslip and the coverslip placed upon the slide. Incubation in the secondary antibody solution lasted for 2 hrs at room temperature. The cover slip was removed by swirling it through KP-Buffer, and the slide washed twice in KP-Buffer for 10 min. The slides were mounted in Slowfade Gold antifade reagent with DAPI (Invitrogen # P36931), and images taken with a Carl Zeiss AxioVision microscope.

25. Fat body chromosome staining

Fat body tissue of third instar larvae was dissected in physiological solution (0.7% NaCl in distilled H_2O), and the fat body tissue transferred to 6µl fixative solution (40% acetic acid. 30% lactic acid, 30% distilled H_2O) that had been pipetted onto a coverslip. After 3-5 minutes a slide was lowered onto the coverslip and pressure was applied by pressing down with a finger. The slide was then turned around and the coverslip/slide sandwich pressed tightly between two sheets of blotting paper. The slide was then immersed into liquid N_2 and the coverslip removed with a razorblade. The slide was immediately transferred into PBS at room temperature. This was followed by an immersion into PBST (PBS plus 1% Triton X-100) for 20minutes at room temperature. For blocking, slides were immersed into blocking solution (PBS plus 1% non fat dry milk) and left there for a 30 minute incubation period. Slides were then treated with the primary antibody (dLipin: 1:200 to: 2000), diluted in PBS, 1% BSA for 60 minutes at RT or overnight at 4°C in humid chamber. Excess antibody was removed by washing 3 consecutive

times in PBS, 0.5% nonfat dry milk for 5 minutes. The secondary antibody (Rhodamine conjugated anti-rabbit 1: 1000) was added diluted in PBS, 1% BSA and the slides incubated for 60 min at room temperature. Excess antibody was washed away in 3 washing steps, each lasting 5 min, in PBS at 4°C. Slides were mounted in Slowfade Gold antifade reagent with DAPI (Invitrogen # P36931), and images taken with a Carl Zeiss AxioVision microscope.

26. Quantitative RT-PCR

To measure transcript levels of *dp110* following *dLipin* knockdown, quantitative RT-PCR was utilized. Fat body tissue from 100 w^{1118} larvae and 140 *dLipinRNAi/FBcg* larvae (feeding stage) was collected and RNA extracted using TRIzol Reagent (Invitrogen #15596-018). The extracted RNA was then treated with DNaseI (New England Biolabs #M0303S) to remove traces of genomic DNA and further purified using Direct-zol RNA MiniPrep (Zymo Research #R2050S). To determine changes in expression levels of *dp110* following *dLipin* knockdown *dp110* transcripts were amplified using specific primers (Fruit Fly PI3k92E). *rp49* (ribosomal protein 49) a housekeeping gene ubiquitously expressed in *D. melanogaster* was selected as the normalizer gene or endogenous control. *rp49* was amplified using the rp49fwd and rp49rev primerset (Table 4). HotStart-IT SYBR Green One-Step qRT-PCR Master Mix Kit (Affymetrix # 75770) was used for qPCR reactions. To determine the reaction efficiencies of *dp110* and *rp49*, a standard curve was generated for each gene by plotting the log of known template concentrations against the Ct (threshold cycle) values for those concentrations. Relative *dp110* expression levels were quantified using the standard curve method (REAL-TIME PCR from Theory to Practice, Invitrogen).

Fold difference: $(E_{Dp110})^{\Delta CtDp110}/(E_{rp49})^{\Delta Ctrp49}$

E= efficiency from standard curve $E=10^{(-1/slope)}$

$\Delta C_{tdp110} = C_{tdp110}w^{1118} - C_{tdp110}$dLipinRNAi

$\Delta C_{trp49} = C_{trp49}w^{1118} - C_{trp49}$dLipinRNAi

RNA samples were analyzed in triplicates.

27. PIP2 and PIP3 visualization

Phosphatidylinositol 4,5-bisphosphate (PIP2) and Phosphatidylinositol (3,4,5)-triphosphate (PIP3) can be visualized taking advantage of the fact that specific Pleckstrin homoly domains (PH domain) show a specific binding affinity for either of these phospholipids. To visualize PIP3, the PIP3 specific PH domain of general receptor for phosphoinositides-1 (GRP1) was fused to green fluorescent protein (GFP), which generates a fusion protein called GPH. Expression of the *GPH* construct was under control of the *Tubulin* promoter, hence the whole construct is called *tGPH* (Britton et al., 2002).

Fig. 8: Schematic representation of the tGPH construct. Image modified from Britton et al., 2002.

As the GPH protein exhibits a specific affinity for binding to PIP3, PIP3 present in the cell will be labeled green upon GPH binding. PIP2 was tracked by a PIP2 specific PH reporter. To this end the PIP2-specific PH domain of phospholipase Cδ (PCLδ) was fused to a GFP

reporter to generate the fusion protein PLCδPH-GFP (Gervais et al., 2008). Expression of the *PLCδPH-GFP* construct was under control of a *Tubulin* promoter. PLCδPH-GFP binds specifically to PIP2, thus PIP2 presence in the cell will be represented by green fluorescence.

As PIP2 and PIP3 are both generated at the plasma membrane, presence of these phospholipids will be reflected in GFP signaling that concentrates at the plasma membrane. Fat body tissue from third instar feeding larvae was dissected in PBS and the tissue fixed for 10 minutes in 4% formaldehyde. After fixation, tissue and cell staining was documented using a Carl Zeiss AxioVision microscope.

28. dLipin localization following alterations of TOR/Insulin signaling

dLipin localization was analyzed after knockdown of TOR signaling in third instar wandering larvae. Genotypes investigated were the following: *FB(cg); TORRNAi* and *FB(cg); raptorRNAi*. Additionally, insulin pathway activity was reduced and any effects on dLipin localization documented. The observed genotypes analyzed were: *FB(cg); InR*$^{dom.neg.}$ and *FB(cg) / PI3K21BHA*. Fat body tissue from larvae of these genotypes was stained with dLipin antibody and samples mounted in Slowfade Gold antifade reagent with DAPI (Invitrogen # P36931). To determine any change in dLipin localization, images were taken with a Carl Zeiss AxioVision microscope.

29. Cell measurements

Cell area was measured using the AxioVision software (available on Carl Zeiss AxioVision microscope) or ImageJ software (http://rsb.info.nih.gov/ij/download.html). To determine the cell size of cells that did not show clear cell boundaries, the distance between neighboring nuclei was measured. In cells where the nucleocytoplasmic ratio was analyzed,

nuclear area was measured in addition to cell area, and the ratio between the two calculated. Data was analyzed statistically using unpaired two-tailed Student's t-Test.

30. Embryo collection and timing of larvae for *dLipin/raptor* genetic interaction studies

To ensure that larval development was as homogenous as possible, parental adult flies were allowed to lay eggs on molasses plates for a period of 4 hours only. To prohibit the deposition of retained eggs, flies were put on food for two hours beforehand so they could lay any retained egg. The eggs laid within the 4 hour time period were transferred with a wet brush onto standard fly food, and kept at 25°C. Larvae were allowed to develop for 5 or more days before larval size and fat body development was compared. Larval and fat body tissue morphology was examined using a Carl Zeiss Stereomicroscope and a Carl Zeiss AxioVision microscope, respectively.

31. Ecdysone rescue experiments

Standard fly food containing 120µg/ml 20-Hydroxyecdysone (20 HE) was prepared. 20 HE was diluted in 100% ethanol and added to the food after it had cooled down to approximately 50°C. Ethanol was also added to the food of control flies, to ensure that there were no differences between the 20 HE food and the normal food, except for the addition of 20 HE. Adult flies were kept on food at 25°C and transferred daily onto new food. Number of pupae formed and developmental timing of control and experimental offspring was compared and data were analyzed with the Chi-Square test. The following cross was set up:

Parental cross: *TubGal4/Tb* X *ΔNLSdLipin/ΔNLSdLipin* either on food with or without 20-HE

→ *TubGal4; ΔNLSdLipin*: Experimental animals 50% genotype frequency expected.

Tb,TM6B; ΔNLSdLipin: Control animals 50% genotype frequency expected.

III. Results

A. Linking dLipin and insulin pathway activity in *D. melanogaster*

Studies with mice and humans have established a strong connection between the mammalian homologs of *dLipin* and insulin signaling. Mice with the *fld* (*fatty liver dystrophy*) mutation display reduced glucose tolerance and decreased sensitivity to insulin stimulation (Reue et al., 2000). The *fld* mutation was subsequently identified as a mutation within the *lipin1* gene (Peterfy et al., 2001). Similar findings were described for human adipose tissue, where low *lipin1* transcript levels correlate with increased insulin resistance (Suviolahti et al., 2006). Furthermore, insulin signaling influences subcellular localization and phosphorylation of Lipin1 in human adipocyte cell lines (Harris et al., 2007). All these results were collected in either mice or humans, both of which possess multiple lipin paralogs in their genomes, a fact that complicates research in these organisms due to redundancy among the different lipin paralogs. *Drosophila melanogaster* on the other hand has one lipin gene (*dLipin*) (Peterfy et al., 2001) making this model organism a prime candidate to examine effects of Lipin on insulin signaling.

1. dLipin is necessary for cell growth

The fat body has emerged as the main tissue of dLipin activity in *Drosophila* (Ugrankar et al., 2011). Diacylglycerol (DAG) produced by dLipin is the immediate precursor for triacylglycerol (TAG) synthesis. The larval fat body functions as the storage organ for TAG and is the major metabolic organ of the developing larvae. As TAG synthesis is dependent on proper dLipin function, any effect of dLipin loss should be especially prominent within the tissue of TAG production. It is for this reason, that I concentrated my work on the fat body.

1.1. Cell-autonomous loss of dLipin activity in the fat body affects cell growth and fat content

One telltale sign of disrupted insulin signaling is a reduction in cell growth (Lehner, 1999; Johnston and Gallant, 2002). To test whether dLipin deficiency leads to a cell size defect, mosaic animals were generated. These mosaic animals had single cells within the fat body that exhibited diminished *dLipin* levels. By knocking down *dLipin* in single cells only, it is possible to observe the cell-autonomous effects of dLipin loss. Knockdown of dLipin activity was achieved by downregulation of *dLipin* mRNA via RNAi in single cells. A *TubulinGal4* driver was used to express a RNAi transgene in single cells, which resulted in a cell specific reduction of *dLipin* mRNA and, consequently, dLipin protein.

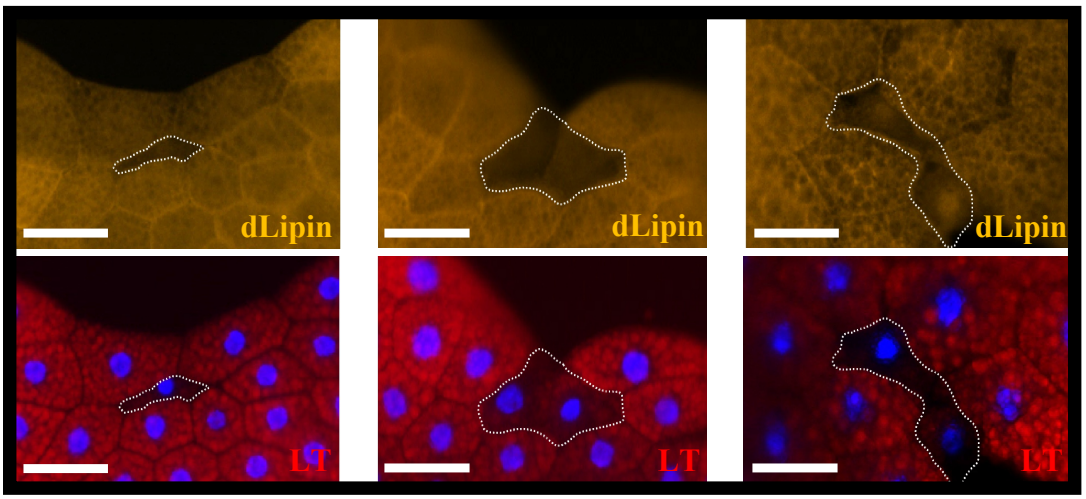

Fig. 9: dLipin is required cell-autonomously in the fat body for normal fat droplet formation and cell growth. Fat body cells in mosaic animals that were deficient in dLipin protein contained few fat droplets and were reduced in size. Fat droplets were stained with LipidTOX Deep Red (LT) and dLipin protein was detected using an affinity-purified dLipin antibody (dLipin). Note that although strongly reduced in some knockdown cells, residual dLipin can still be detected in the cell nucleus. Depicted are cells of feeding third instar larvae. Scale bar: 100µm.

A reduction of *dLipin* affected cell size in a cell-autonomous fashion (Fig. 9). Cells with successful *dLipin* knockdown are outlined. Antibody staining indicated that dLipin protein was

strongly reduced in these cells. The dLipin deficient cells were not only reduced in size, but also exhibited reduced fat content. Thus, not only cell size, but also fat synthesis is controlled by *dLipin* cell-autonomously.

1.2. Ubiquitous knockdown of *dLipin* results in cell size variability

Ugrankar et al. (2011) described a *dLipin* mutant phenotype that was characterized by a wide variability of cell sizes in the fat body, including many hypertrophic cells. It was hypothesized that this phenotype constituted a secondary compensatory effect caused by the reduced total fat mass in these animals. I reproduced these data by knocking down *dLipin* ubiquitously in third instar larvae using a strong *TubulinGal4* driver and a *dLipinRNAi* construct. Cells size following *dLipin* knockdown was highly variable, a phenotype mirroring the *dLipin* mutant phenotype (Fig. 10).

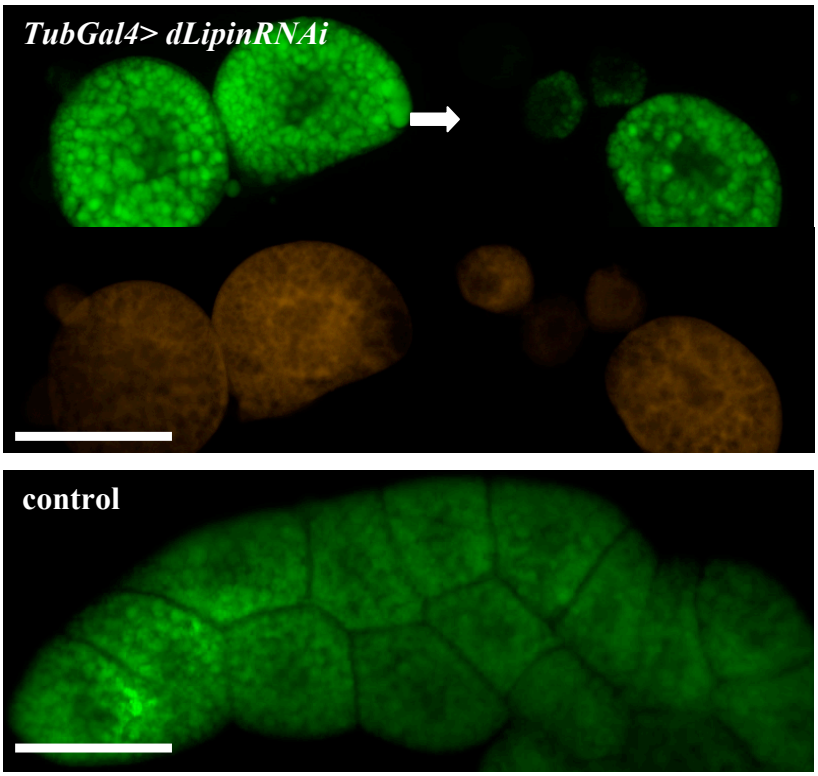

Fig. 10: Systemic knockdown of *dLipin* results in cell size heterogeneity and cells with reduced fat content. *TubulinGal4>dLipinRNAi* fat body cells displayed a change in cell morphology, cell size and fat content. Cells were rounded, of very variable size and often contained smaller fat droplets, or lacked fat droplets. This phenotype closely resembled the *dLipin* mutant phenotype (Ugrankar *et al.*, 2011). Fat droplets were stained with Bodipy (green) and cell membranes with with CellMask Plasma stain (orange). Some very small cells, visualized by plasma membrane staining, lacked fat droplets (arrow). Fat body cells from wild-type dLipin control flies (w^{1118}) were polygonal with normal fat content and fat droplets of normal size. Depicted are fat body cells of feeding third instar larvae. Scale bar: 100µm.

Data concerning cell growth collected by mosaic analysis and ubiquitous *dLipin* knockdown differed drastically. Cell-autonomous *dLipin* knockdown resulted in a cell growth deficit, whereas systemic *dLipin* knockdown resulted in extreme cell size variability. This discrepancy in cell growth defects emphasizes the importance of investigating not only system wide but also cell-specific gene knockdown to grasp the full extent of effects caused by the gene knockdown.

1.3. Comparison of cell-autonomous and ubiquitous *dLipin* knockdown

To further analyze the cell growth defects observed after *dLipin* knockdown, I measured the cell and nuclear area of fat body cells (Fig. 11). Whereas a strong statistical difference between the size of control cells and cells with cell-autonomous expression of *dLipinRNAi* was observed, no statistically significant difference was found between cell size of control cells and cells after systemic *dLipinRNAi* expression. However, the standard deviation value for the system-wide knockdown was extremely high, reflecting the extreme variability in cell size. Conducting the F-test to compare the variance in fat body cell size from control animals to the variance in fat body cell size from animals with systemic *dLipin* knockdown revealed a significant difference between the variances of the two samples ($p < 0.0001$). Thus, systemic knockdown of *dLipin* causes significant cell size variability, which indicates that cell growth was altered upon systemic *dLipin* knockdown. Cell-autonomous loss of dLipin activity resulted in a reduction of nuclear area. This points to a decrease in the number of endoreplication cycles, which would suggest that cell-autonomous *dLipin* knockdown induces an overall growth phenotype that affects cytoplasmic cell growth as well as genome replication. Following systemic *dLipin* knockdown, nuclear area is not reduced, but increased. Hence, genome replication does not seem to be negatively affected by systemic *dLipin* knockdown. Looking at the nucleocytoplasmic ratio, I further characterized the nature of growth defects observed after *dLipin* knockdown (Fig. 12).

A)

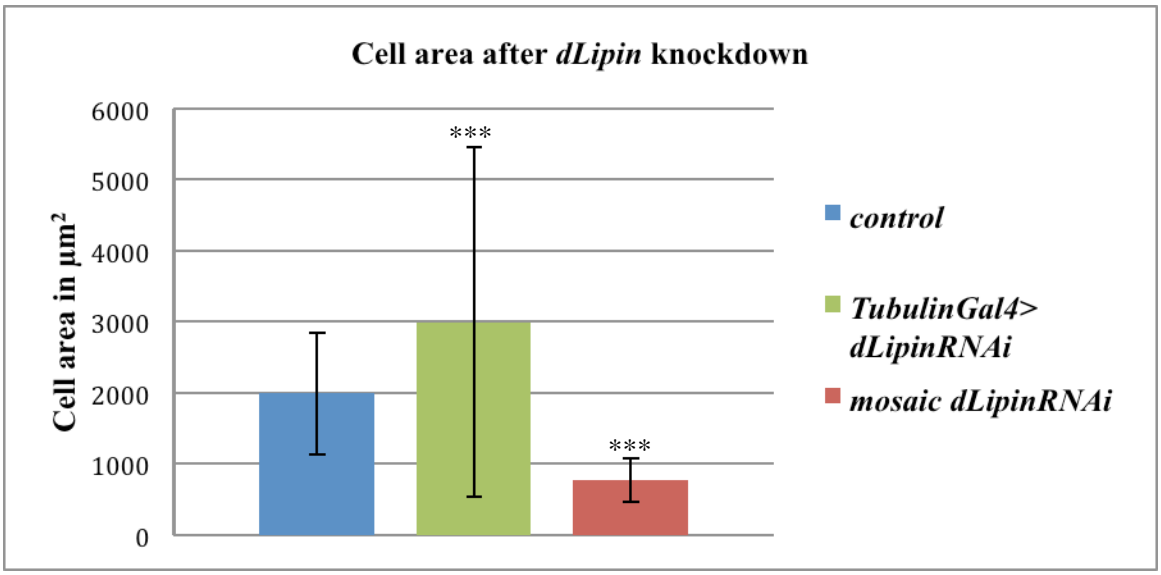

B)

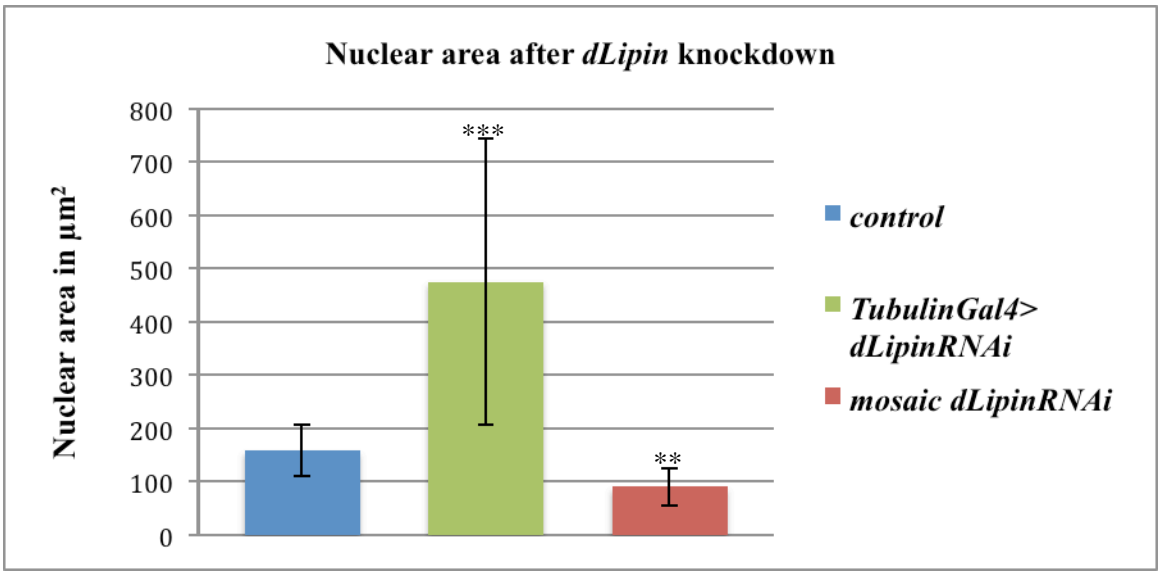

Fig. 11: Knockdown of *dLipin* affected cell and nuclear area. A) Systemic knockdown of *dLipin* (*TubGal4>dLipinRNAi*) led to extreme variability of cell size, hence the big standard deviation. In contrast, cell autonomous loss of *dLipin* resulted in cell size reduction. Cell area in fat bodies was measured from feeding third instar larvae. As a control, cells from mosaic animals without *dLipinRNAi* expression were measured. Cell area was measured using the Axioware software package. Unpaired t –Test, *** $p < 0.0001$. B) The mosaic *dLipin* deficient fat body cells displayed a reduction in nuclear area, which indicates that endoreplication was negatively affected in these cells. After systemic knockdown of *dLipin*, fat body cells displayed larger nuclei when compared to control cells. Nuclei of feeding third instar larvae were measured. Nuclear area was determined using the Axioware software package. Unpaired t-Test, *** $p < 0.0001$; ** $p = 0.0002$. Error bars indicate standard deviation (SD).

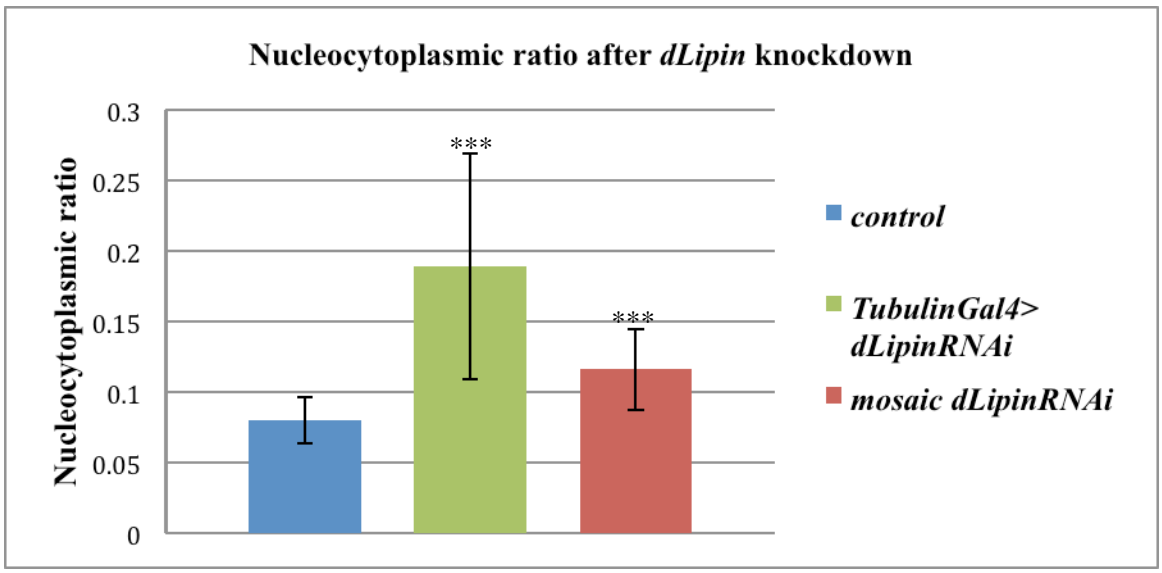

Fig. 12: Cytoplasmic growth was negatively affected in cells following knockdown of *dLipin*. The nucleocytoplasmic ratio was elevated in cells with, either cell-autonomous or systemic *dLipin* knockdown, indicating that cytoplasmic growth was affected, and affected to a stronger extent than endoreplicative growth. Fat body cells of feeding third instar larvae were measured. Unpaired t-Test, *** $p < 0.0001$. Error bars indicate SD.

Both cell-autonomous loss of dLipin activity as well as systemic reduction of dLipin activity resulted in an increase in the nucleocytoplasmic ratio (Fig. 12). This implicates that overall cytoplasmic cell growth was more severely affected by reduced *dLipin* expression than genome replication. This effect was even more pronounced in fat body cells from animals with systemic *dLipin* knockdown.

These data support the conclusion that dLipin is required for proper cell growth, as both cell-autonomous as well as systemic *dLipin* knockdown lead to cell size defects. Cell-autonomous dLipin loss caused a decrease in overall cell growth indicating that dLipin activity is required in single cells for proper cell growth. It appears that systemic *dLipin* knockdown elicits a secondary compensatory mechanism that compensates the reduced fat body mass after *dLipin*

knockdown by cell overgrowth. A very similar phenotype was observed in transheterozygous *dLipin* mutants (Ugrankar et al., 2011).

Having established a connection between *dLipin* and cell growth, it was of interest to see whether insulin signaling was affected by dLipin activity.

2. dLipin activity is necessary to ensure proper insulin signaling pathway activity in the fat body

Figure 5 illustrates all the important steps involved in the signal transduction cascade of the canonical insulin pathway. One critical step is the synthesis of PIP3 from PIP2, which is catalyzed by PI3K at the plasma membrane. PIP3 recruits the pleckstrin homology domain (PH) of AKT and PDK1 to the plasma membrane, thus allowing PDK1 to phosphorylate AKT. AKT is then further phosphorylated by TORC2 and thereby gains full activation. Activated AKT dissociates from the cell membrane and targets downstream effectors of the pathway. Thus, one way to measure activity of the insulin pathway in the cell is by examining PIP3 levels at the cell membrane.

2.1. PIP3 synthesis is dependent on dLipin

The laboratory of Bruce Edgar generated a transgene that encodes a pleckstrin homology domain-green fluorescent protein fusion, PH-GFP (*tGPH*), which serves as an indicator for PIP3 synthesis (Britton et al., 2002). The PH domain of the fusion protein is recruited to the plasma membrane upon PIP3 synthesis. Green fluorescence from the PH-GFP fusion protein thus reflects PIP3 levels and spatial distribution in the cell. I compared PIP3 levels/localization in fat body cells from animals with fat body-specific *dLipin* knockdown and control animals (Fig. 13A). It was also important to determine whether knockdown of *dLipin* in the fat body alone would be enough to alter insulin pathway activity in other tissues, or whether the effect would be

restricted to the fat body. Thus, I looked at PIP3 localization in the salivary glands of animals with fat body-specific *dLipin* knockdown (Fig. 13B). Additionally I wanted to ensure that potential differences in PIP3 levels/localization were not due to decreased availability of its precursor PIP2. To this end, I used a transgene that encodes a PIP2 specific PH-GFP fusion protein (*ubi-PLC*) (Gervais et al., 2008). This would, as in the case for PIP3, give me information on PIP2 levels and distribution within the cell (Fig. 13C).

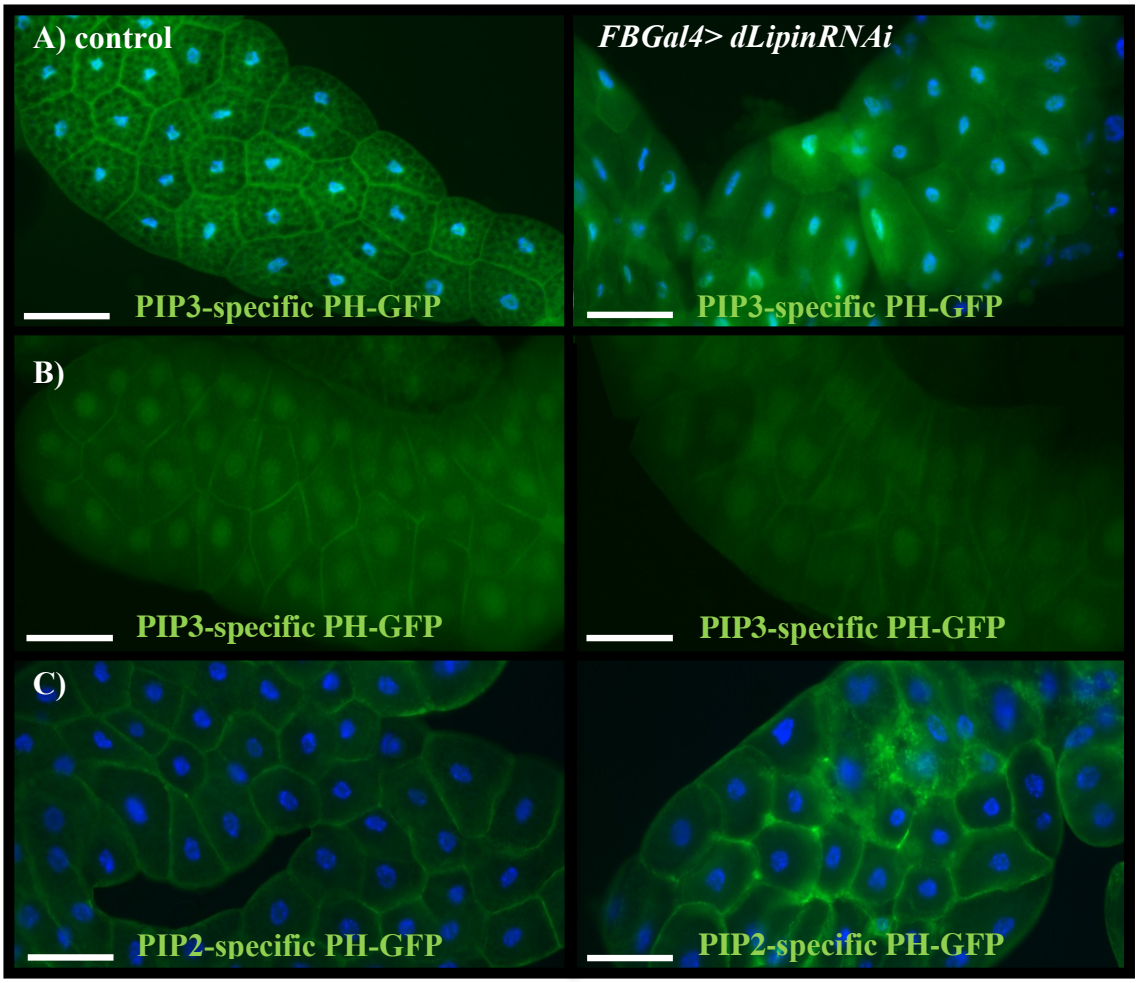

Fig. 13: The second messenger PIP3, but not PIP2, was reduced at the cell membranes of fat body cells that lack dLipin. (A) *dLipin* was knocked down in the fat body of animals expressing the PIP3 reporter *tGPH* (green), and feeding third instar larvae were dissected (*FBGal4> dLipinRNAi*). Membrane association of PH-GFP was strongly reduced in fat body lacking dLipin, but not in fat body of control animals (*FBGal4; tGPH*). (B) In tissues not targeted for *dLipin* knockdown (salivary glands), PIP3 showed normal association with the cell membrane. (C) Fat body cells of animals that express the PIP2 reporter *ubi-PLC* showed no change in the association of PH-GFP with the cell membrane (green) compared to control animals (*FBGal4; ubiPLC*). Nuclei stained with DAPI. Scale bar: 100µm.

dLipin knockdown in the fat body had a clear negative effect on insulin pathway activity, as demonstrated by the complete lack of PIP3 at the cell membrane (Fig. 13A). In control cells, strong PIP3-GFP signals coincided with the cell membrane. This pattern was lost following

dLipin knockdown. All PIP3 seemed to be lost from the cell membrane, which suggests a severe disruption of the insulin pathway. There was no observable effect on PIP3 localization in tissues outside of the fat body, as salivary gland cells exhibited unchanged membrane association of PIP3. Therefore, the consequences of *dLipin* knockdown in the fat body seemed to be tissue limited. The level and membrane association of PIP2 did not appear to be negatively affected in the fat body indicating that it was indeed the conversion of PIP2 into PIP3 that was disturbed. To further validate this result, I looked at PIP3 and PIP2 in *dLipin* transheterozygous mutants (*dLipin*^{e00680}*/Df(3R)Exel7095*).

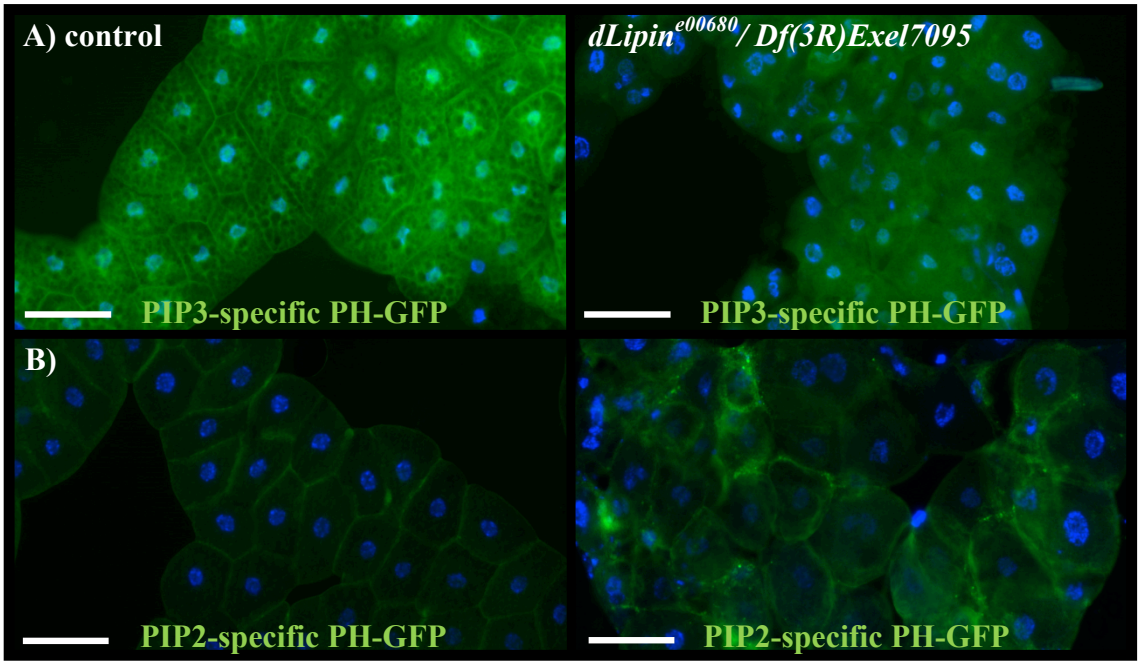

Fig. 14: PIP3 association with the cell membrane was lost in *dLipin* mutants (*dLipin*^{e00680}*/Df(3R)Exel7095*). A) PIP3 was no longer localized at the cell membrane in *dLipin* mutants, which confirmed the results obtained by the *dLipinRNAi* experiment. B) PIP2 appeared to be located at the cell membrane, indicating no change in PIP2 availability in these cells. PH-GFP: green, nuclei stained with DAPI. Scale bar: 100µm.

I confirmed the earlier results with this second set of experiments. Membrane association of PIP3 was no longer detectable, whereas PIP2 localization remained unchanged.

The results from the PIP3/PIP2 visualization experiments clearly indicate that pathway activity is disrupted after loss of dLipin, pointing to dLipin as a contributor to insulin pathway activity in the fat body.

2.2. *dLipin* knockdown in the fat body does not result in cell growth defects

As mentioned earlier, diminished insulin signaling pathway activity often results in a reduction of cell size. Cell size should therefore be negatively affected in the fat body cells after fat body-specific *dLipin* knockdown (*FBGal4>dLipinRNAi*) as these cells clearly showed a loss of PIP3 membrane association (Fig. 13).

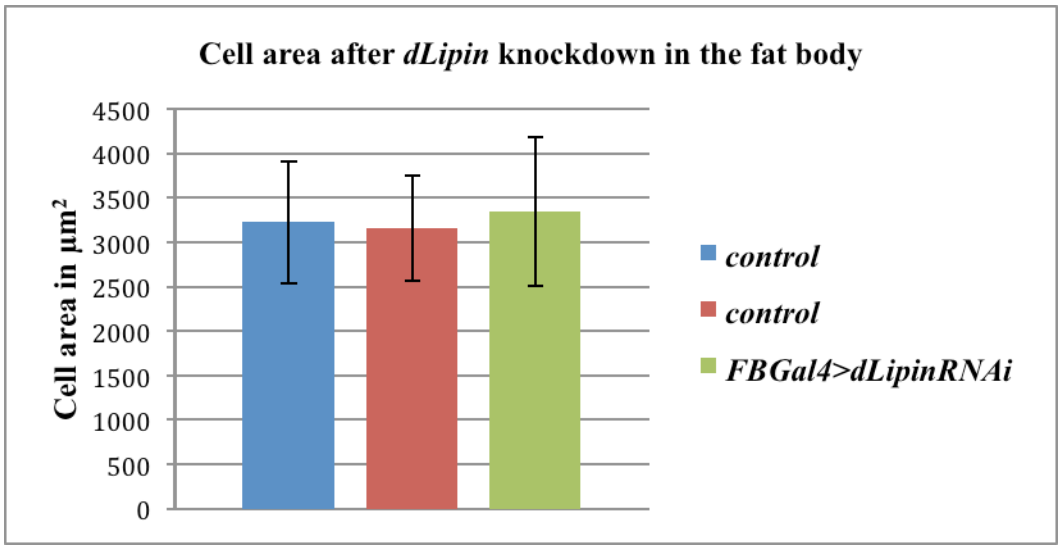

Fig. 15: Knockdown of *dLipin* via RNAi in the fat body did not result in a growth defect. Cellular area of fat body cells after *dLipin* knockdown (green: *FBGal4>dLipinRNAi*) was measured and compared to control fat body cell area (red: fat body of animals carrying only the *Gal4* transgene; blue: fat body of animals carrying only the *dLipinRNAi* transgene). No significant difference in cell area was detected for either genotype. Fat body cells were from wandering third instar larvae. Error bars indicate SD.

The measurement of cell area showed no significant difference in cell size between the fat body cells following fat body-specific *dLipin* knockdown (*FBGal4>dLipinRNAi*) and control

cells. This was a surprising result considering the fact that PIP3 membrane association was lost in these cells and therefore insulin pathway activity should have been strongly decreased.

In addition, development and size of larvae and pupae did not seem to be affected by fat body-specific knockdown of *dLipin*.

To further elucidate the relationship between dLipin and the insulin signaling cascade I concentrated on genetic interaction experiments among members of the canonical insulin signaling cascade and dLipin.

3. *dLipin* genetically interacts with the insulin signaling pathway

To screen for potential interactions between dLipin and members of the insulin signaling cascade I set up numerous crosses.

3.1. *dLipin* and *insulin receptor* act in concert in fat body development and cell growth

To assess possible genetic interactions between *dLipin* and genes of the insulin pathway, I examined animals expressing *dLipinRNAi* and a dominant negative form of the insulin receptor (InRDN). The single knockdown of *dLipin* resulted in fat body cells with small fat droplets, and *InRDN* expression led to fat body cells of smaller size, but seemingly normal fat content. Combining both transgenes in the fat body changed the morphology of the cells dramatically, and reduced fat body mass. Fat body cells displayed a rounded morphology, with an increase in cell size. This phenotype strongly resembled the *dLipin* mutant phenotype described in Ugrankar *et al*. 2011, as well as the phenotype after *TubulinGal4>dLipinRNAi* systemic knockdown (Fig. 10).

To visualize fat body mass in experimental and control larvae, I used the fat body marker *Dcg-GFP* (Suh et al., 2007). Fat body tissue of animals carrying this marker exhibits green fluorescence when irradiated with light of the appropriate wavelength. To characterize the cell growth defect following loss of InR activity, I measured the cell area of cells expressing *InRDN*.

A)

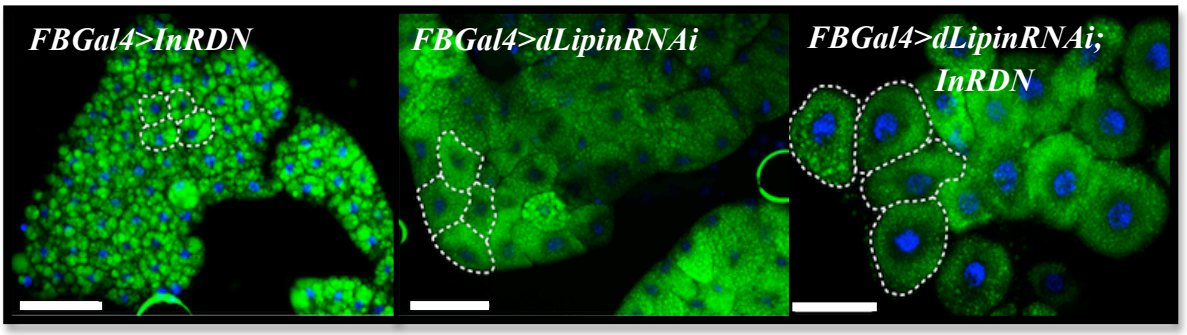

B)

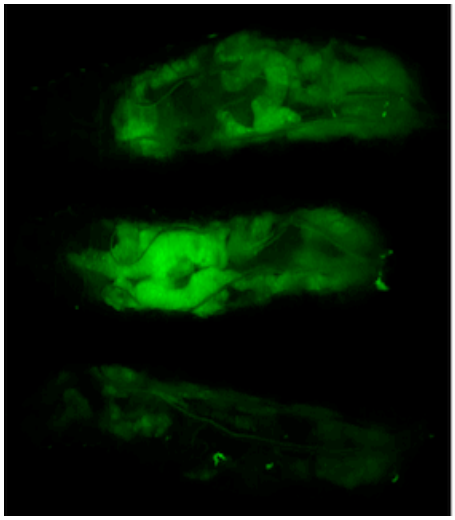

C)

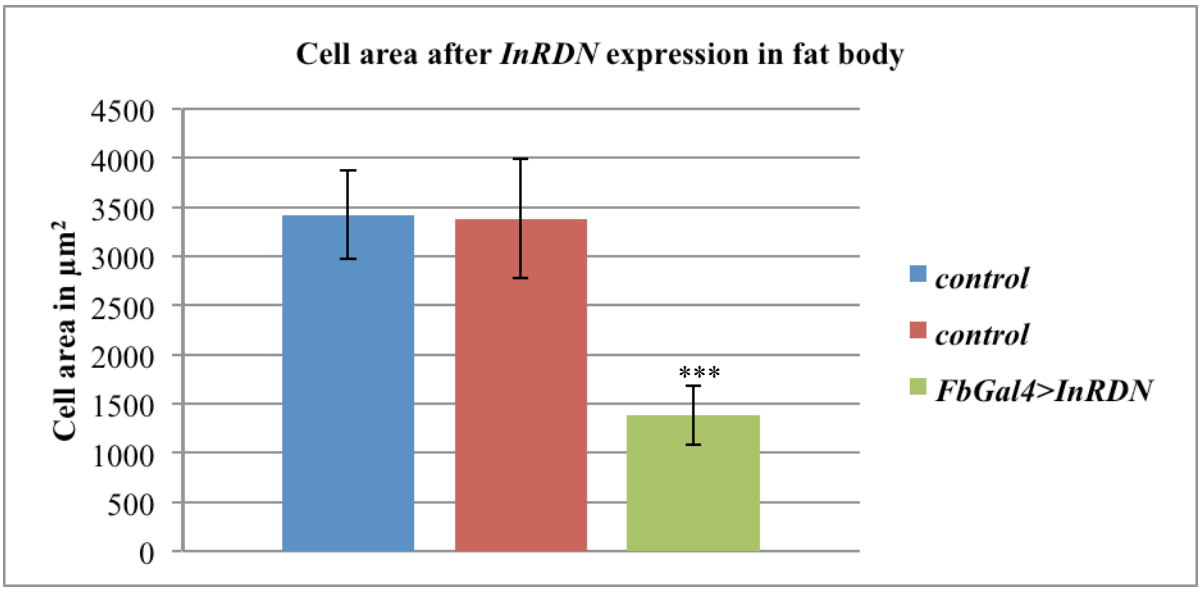

Fig. 16: dLipin and insulin signaling act in concert in fat body development and cell growth. (A) Feeding third instar larvae expressing a *dLipinRNAi* transgene and a transgene encoding a dominant negative form of the insulin receptor (*InRDN*) exhibited a severe fat body defect with increased cell size variability and small fat droplets; a phenotype that strongly resembles the *dLipin* mutant phenotype. Fat droplets were visualized by Bodipy staining (green) and nuclei with DAPI (blue). Scale bar: 100µm (B) Larvae carrying both transgenes had less fat body mass compared to larvae expressing either one of the transgenes. Fat body tissue was labelled with *Dcg-GFP* (green). C) Area of fat body cells was reduced in animals expressing *InRDN*. Cells of wandering third instar larvae were measured and compared to cells of control animals (red: animals carrying only the Gal4 transgene; blue: animals only carrying the *InRDN* transgene). Unpaired t-Test, *** $p < 0.0001$. Error bars indicate SD.

I tried to rescue the defects in fat body development observed in animals with fat body specific dLipin deficiency and *InRDN* expression by knocking down Dullard activity (*FBGal4> dLipinRNAi; DullardRNAi/InRDN*). Dullard is a phosphatase that targets an insulin-sensitive phosphorylation site within Lipin1 (Wu et al., 2011). If Dullard has the same function in *Drosophila*, reducing Dullard in the cell would increase insulin pathway input on dLipin and thus, possibly counteract the effect of *InRDN* expression on dLipin. However, RNAi knockdown

of *Dullard* in concert with *dLipin* knockdown and *InRDN* expression did not rescue phenotypes and did not have an obvious phenotypic affect when carried out alone (data not shown).

Through genetic interaction experiments I was able to further weave dLipin within the fabric of the insulin network. It became clear that both dLipin as well as the insulin receptor are required for normal fat body development, and that loss of dLipin in a *InRDN* genetic background led to a cell overgrowth phenotype resembling the transheterozygous *dLipin* mutant phenotype (Ugrankar et al., 2011). This suggests that dLipin activity during adipogenesis and in fat synthesis is dependent on the insulin pathway.

3.1.1. Reduced dLipin activity with simultaneous *InRDN* expression does not cause an organismal growth defect

To further address the possibility of an interaction between *dLipin* and *InRDN* in cell growth control, I tested animals with weak ubiquitous expression of both transgenes for effects on organismal growth (*daGal4>dLipinRNAi; InRDN*). I was not able to detect any organismal growth defect in these animals when compared to control animals. To score for growth defects, I measured the size of pupae (data not shown).

3.1.2. Viability is reduced after *dLipin* knockdown with concomitant *InRDN* knockdown

While studying the effects of *InRDN* expression and *dLipin* knockdown on fat body development and morphology, I noticed that the viability of animals carrying both transgenes appeared to be reduced. To document this phenotype I counted pupae formed for lines carrying either or both transgene/s and compared them to a control fly line. All four genotypes compared emerged from one single cross. Thus, I could compare the number of pupae formed by animals with experimental genotypes (*FBGal4>dLipinRNAi; FBGal4>InRDN;*

FBGal4>dLipinRNAi;InRDN) to the number of pupae formed by animals with control genotype (*FBGal4*). I set the number of pupae formed by animals with control genotype to 100%. I compared each experimental genotype with the control phenotype using a Chi-Square test, as the expected frequency for each genotype was known. A very significant rise in larval lethality after knockdown of *dLipin* in an *InRDN* background was detected, whereas neither the control line nor single transgene carrying lines displayed any difference in pupation capacity (Fig. 17). This increased larval lethality was reflected by a decrease in the number of pupae formed, as most animals perished during larval development.

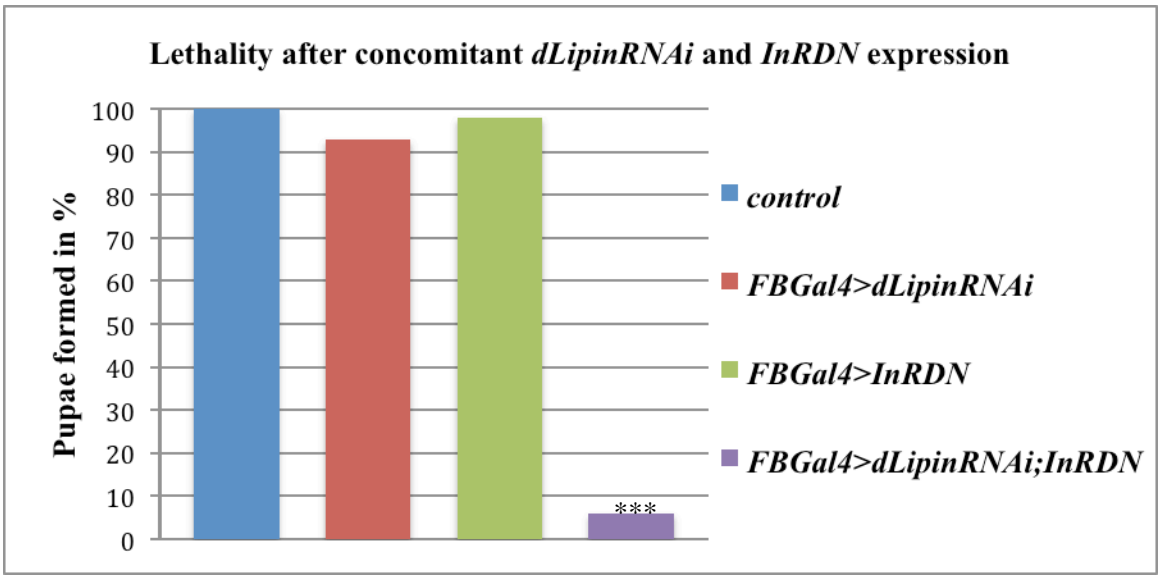

Fig. 17: Viability is decreased following *InRDN* expression with simultaneous *dLipin* knockdown. *dLipinRNAi* was expressed concomitant with *InRDN* (dominant negative form of InR). Animals carrying both transgenes exhibited a decrease of viability, with very few individuals reaching the pupal stage. Two tailed Chi-Square Test, *** P< 0.0001. No statistically significant difference was found between either the single transgenes or between the single transgenes and the control (only *FBGal4* driver). Animals carrying the driver transgene only were used as the control animals.

At this point, I had firmly established that a change in dLipin activity elicits changes in insulin pathway activity, as PIP3 synthesis was reduced. It also became apparent that dLipin and

the insulin pathway interact in fat body development. The defect in fat body development appeared to be caused by a further decrease of dLipin activity upon *InRDN* expression, which indicates that dLipin activity is dependent on input from the insulin pathway.

3.2. Interaction studies between *dLipin* and genes of the insulin pathway

In addition to the genetic interaction between *dLipin* and *InR*, I investigated possible interactions between *dLipin* and numerous other genes of the insulin pathway

All these interaction studies failed to show phenotypes or caused lethality but should be mentioned here for the sake of completeness.

dLipinRNAi/InR$^{const.active}$;FB(r4): Overexpression of a constitutively active form of Insulin Receptor in the fat body with concomitant *dLipin* knockdown. No interaction detected, as overexpression of *InR$^{const.active}$* alone did not lead to an insulin overactivation phenotype in the fat body.

dLipinRNAi/InR$^{cont.active}$; DJ761: Ubiquitous expression of a constitutively active form of Insulin Receptor in concert with *dLipin* knockdown. No interaction detected, as overexpression of *InR$^{const.active}$* did not lead to an insulin overactivation phenotype in the fat body.

dLipinRNAi/PI3K21BHA; FB(r4): Simultaneous knockdown of dLipin and PI3K21B activity in the fat body. Neither flies of genotype *dLipinRNAi; FB(r4)* nor flies of genotype *PI3K21BHA; FB(r4)* could be established due to lethality.

dLipinRNAi/PI3K21BHA; DJ761: Ubiquitous simultaneous knockdown of dLipin and PI3K21B activity. Neither flies of genotype *dLipinRNAi; DJ761* nor flies of genotype *PI3K21BHA; DJ761* could be established due to lethality.

PI3K21BHA; LipinWT6M/FB(r4): Overexpression of *dLipin* in fat body tissue with loss of PI3K21B activity. No rescue of the loss-of-function phenotype observed in *PI3K21BHA* by overexpression of *dLipin*.

dLipinRNAi/FB(cg); PI3K92E$^{dom.neg.}$: Simultaneous *dLipin* knockdown and loss of PI3K92E activity. No interaction detected, as *PI3K92E$^{dom.neg.}$* animals not display an insulin signaling knockdown phenotype.

dLipin^{e00680}/ dLipin^{e00680}; AKT^{myr}/ FB(r4): Expression of constitutively active AKT in *dLipin* hypomorphic mutant. No interaction detected, as *AKT^{myr}* animals did not display an insulin signaling overactivation phenotype.

dLipin^{e00680}/Df(3R)Exel7095; AKT^{myrlacZ}/FB(r4): Overexpression of AKT in *dLipin* transheterozygous mutant. No interaction detected, as *AKT^{myrlacZ}* did not display an insulin signaling overactivation phenotype.

To confirm that insulin pathway activity was indeed interrupted downstream of PIP3 synthesis, I examined AKT activity in fat body tissue upon *dLipin* knockdown.

4. *dLipin* knockdown reduces insulin pathway activity downstream of InR and PIP3

PIP3 at the cell membrane serves as an anchor for AKT. AKT migrates to the membrane and is activated by phosphorylation of 2 amino acid residues. One phosphorylation is carried out by PDK1 and the other by TORC2 at serine505 (S505). The AKT phosphorylation at S505 corresponds to AKT serine473 (S473) phosphorylation in mammals. Mammalian AKT S473 phosphorylation is required for full activation of AKT (Hemmings and Restuccia, 2012).

To address possible changes in AKT activity upon reduced dLipin activity I examined S505 phosphorylation levels of AKT. dLipin deficiency resulted in a reduction of PIP3 synthesis, which suggests that the insulin pathway is interrupted. To test this, western blot analysis was carried out with antibodies against panAKT and S473 phosphoAKT and fat body samples from third instar larvae with fat body-specific *dLipin* knockdown (*FBGal4>dLipinRNAi*) (Fig. 18A). The S473 phosphoAKT antibody is known to react with *Drosophila* S505 phosphoAKT. By measuring levels of overall AKT (panAKT) as well as phosphoAKT levels, it is possible to deduce whether not only AKT phosphorylation but also general AKT levels are modified within the cell. To verify the results collected with tissue from animals expressing *dLipinRNAi*, I repeated the western blot with fat body tissue from *dLipin* mutants ($dLipin^{e00680}/Df(3R)Exel7095$) (Fig. 18B).

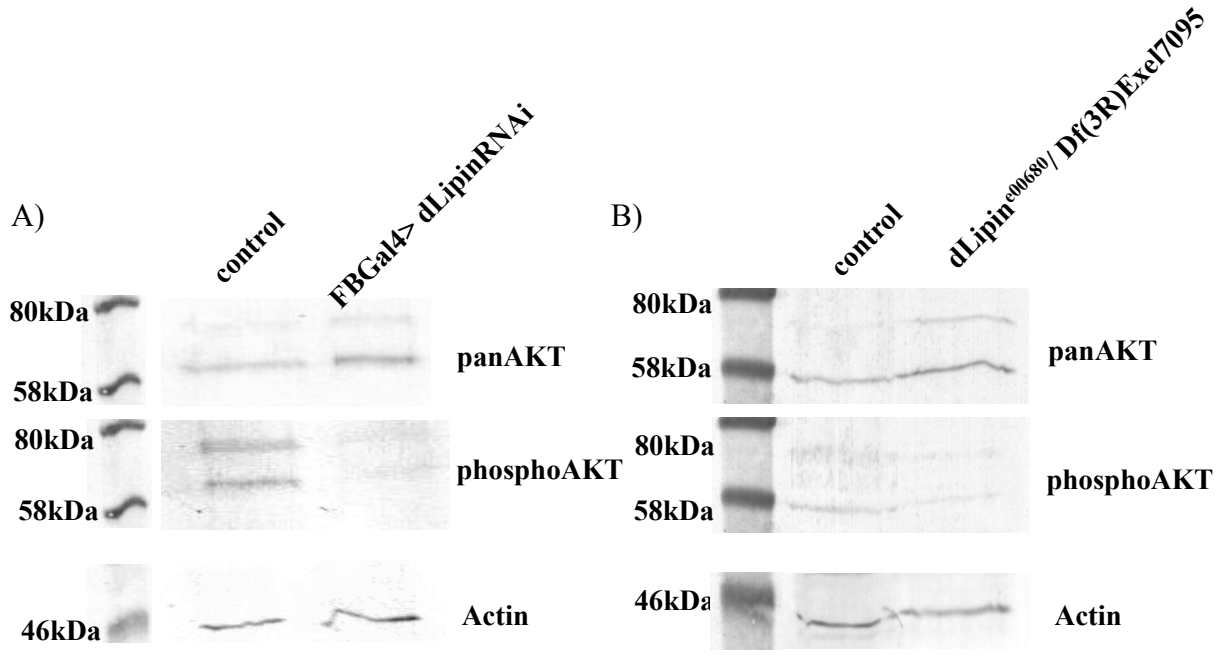

Fig. 18: Insulin pathway activity is interrupted downstream of PIP3. A) Western Blots show that levels of AKT^{phospho} were greatly reduced in fat body tissue from feeding third instar larvae expressing a *dLipinRNAi* transgene, while the overall AKT (panAKT) levels remained unchanged. Fat bodies from *w1118* animals were used as control tissue. B) PhosphoAKT levels were also reduced in fat body tissue from *dLipin* mutant feeding third instar larvae (*dLipin*^{e00680}/ *Df(3R)Exel7095*). Fat body tissue from heterozygous (either *dLipin*^{e00680} or *Df(3R)Exel7095*) animals was used as control tissue. The lower band corresponds to the AKT protein. Actin served as a loading control.

Western blot analysis shows that phosphoAKT levels in the fat body are reduced upon *dLipin* knockdown (*FBGal4>dLipinRNAi*) and in *dLipin* mutants (*dLipin*^{e00680}/ *Df(3R)Exel7095*). Overall AKT levels remained unchanged, indicating that TORC2 mediated phosphorylation is inhibited. These data confirm that insulin pathway activity downstream of PIP3 is reduced in fat body cells after a reduction of dLipin activity. The next question asked was whether dLipin acts downstream or upstream of PI3K or whether it affects PI3K activity itself to interrupt the signaling cascade. To this end I tested whether loss of dLipin is sufficient to counteract the effects of PI3K overactivation.

5. dLipin affects insulin pathway activity by either affecting PI3K or PTEN activity

Overexpression of *Dp110*, the catalytic subunit of PI3K, in the fat body induces strong overgrowth of cells. This is due to an overactivation of the insulin pathway. If dLipin acts on, or downstream of *PI3K*, loss of dLipin activity should reduce or reverse the cell overgrowth observed after *Dp110* overexpression.

5.1. *dLipin* knockdown counteracts *Dp110* overactivation-induced cell overgrowth

I combined a transgene encoding a constitutively active form of Dp110 (*Dp110CAAX*) and *dLipinRNAi* with a fat body-specific driver and examined possible cell growth effects (Fig. 19). The CAAX signal added to the C-terminus of Dp110 is a farnesylation signal that promotes protein-membrane interaction, and thus directs Dp110 directly to the cell membrane where it then generates PIP3. This increase in PIP3 synthesis induces cell growth.

A)

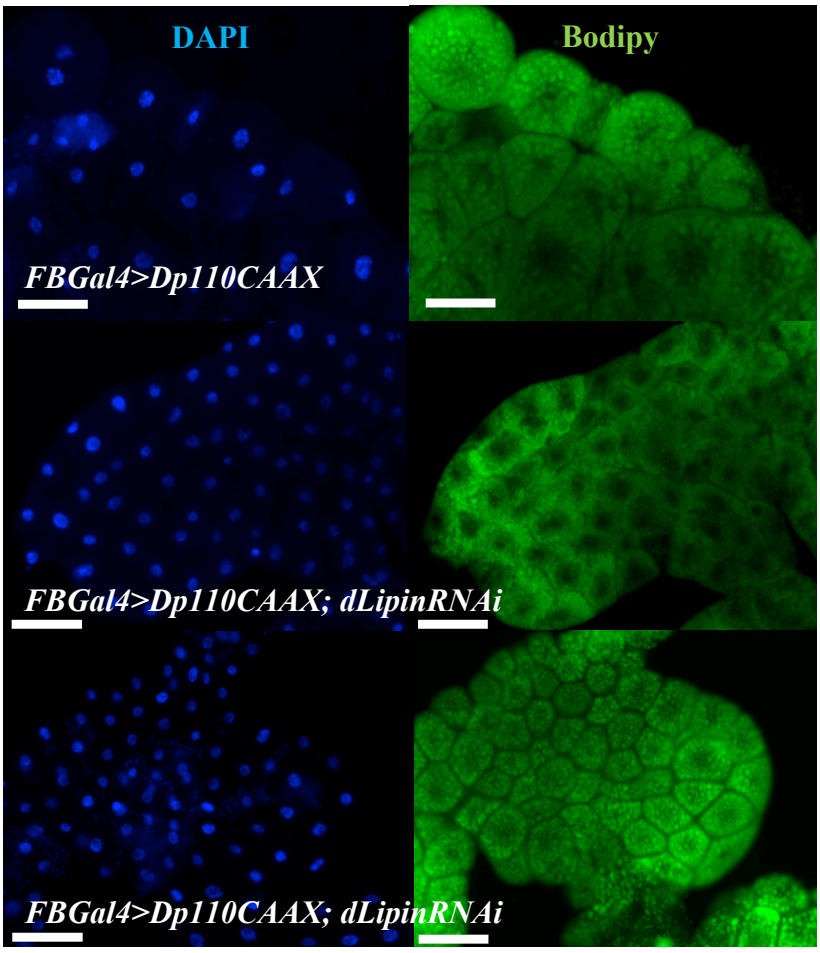
DAPI
Bodipy
FBGal4>Dp110CAAX
FBGal4>Dp110CAAX; dLipinRNAi
FBGal4>Dp110CAAX; dLipinRNAi

B)

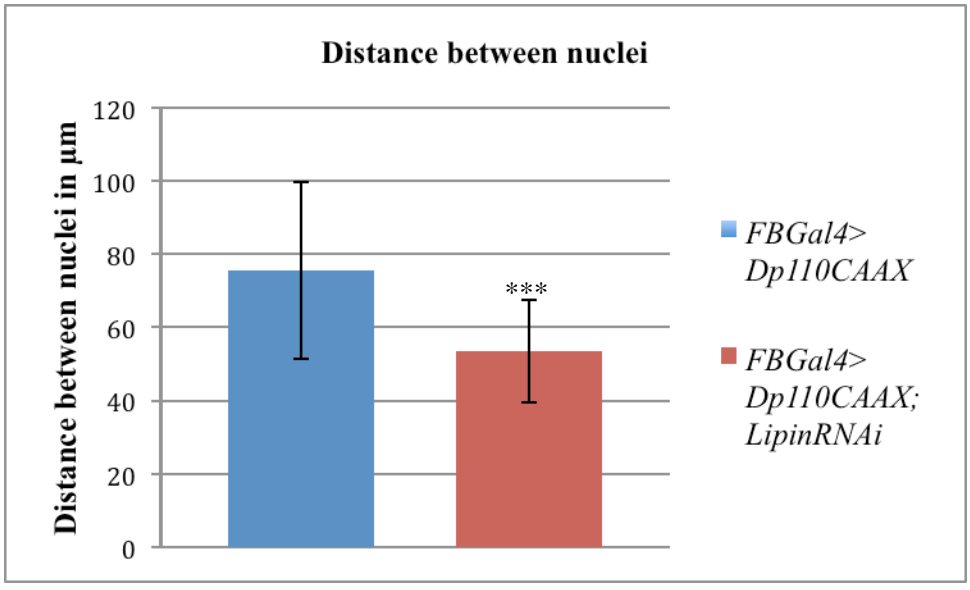
Distance between nuclei
Distance between nuclei in µm
120
100
80
60
40
20
0
***
FBGal4> Dp110CAAX
FBGal4> Dp110CAAX; LipinRNAi

Fig. 19: *dLipinRNAi* knockdown can suppress the overgrowth phenotype observed after Dp110 overactiviation. A) Fat body-specific expression of a constitutively active version of Dp110 (catalytic subunit of PI3K), *Dp110CAAX*, resulted in overgrowth of fat body cells. When *Dp110CAAX* expression was combined with *dLipin* knockdown, this growth effect was reversed, with cells appearing normal in size. There was a variability of phenotypes observed after *dLipin* knockdown. Some tissue samples displayed the typical *dLipinRNAi* phenotype with small fat droplets, while other samples showed no difference in fat droplet morphology. Fat droplets were stained with Bodipy (green) and nuclei visualized with DAPI (blue). Tissue was collected from feeding third instar larvae. Scale bar: 100µm. B) Distance between neighboring nuclei was measured as a means to determine cell size. The distance between nuclei in fat body tissue from animals expressing *Dp110CAAX* was significantly larger when compared to fat body tissue from animals expressing both, *Dp110CAAX* and *dLipinRNAi*. Unpaired t-Test, *** $P < 0.0001$. Error bars indicate SD.

The cell overgrowth observed after *Dp110CAAX* expression in the fat body was reversed after reduction of *dLipin* transcripts via RNAi. Depending on the extent of the RNAi-induced knockdown of *dLipin*, two different manifestations of the phenotype existed. After strong *dLipin* knockdown, cell overgrowth was reduced, and fat droplets were small in size. If RNAi-mediated knockdown of *dLipin* was not as pronounced, cell overgrowth was reversed as well but fat droplet size was unchanged. It is apparent from both phenotypes that the overgrowth induced by *Dp110CAAX* expression was successfully repressed by *dLipin* knockdown.

Paradoxically, some animals with *Dp110CAAX* expression in the fat body showed extreme hypotrophy of fat tissue (data not shown).

5.2. *dLipin* knockdown suppresses Dp110-induced activation of the insulin pathway

As *Dp110CAAX* expression leads to an overactivation of insulin pathway downstream of PI3K, I investigated whether this overactivation can be reversed by loss of dLipin activity. I looked at PIP3 localization in fat body cells from larvae that carry the *Dp110CAAX* transgene and from larvae with both the *Dp110CAAX* and the *dLipinRNAi* transgene (Fig. 20).

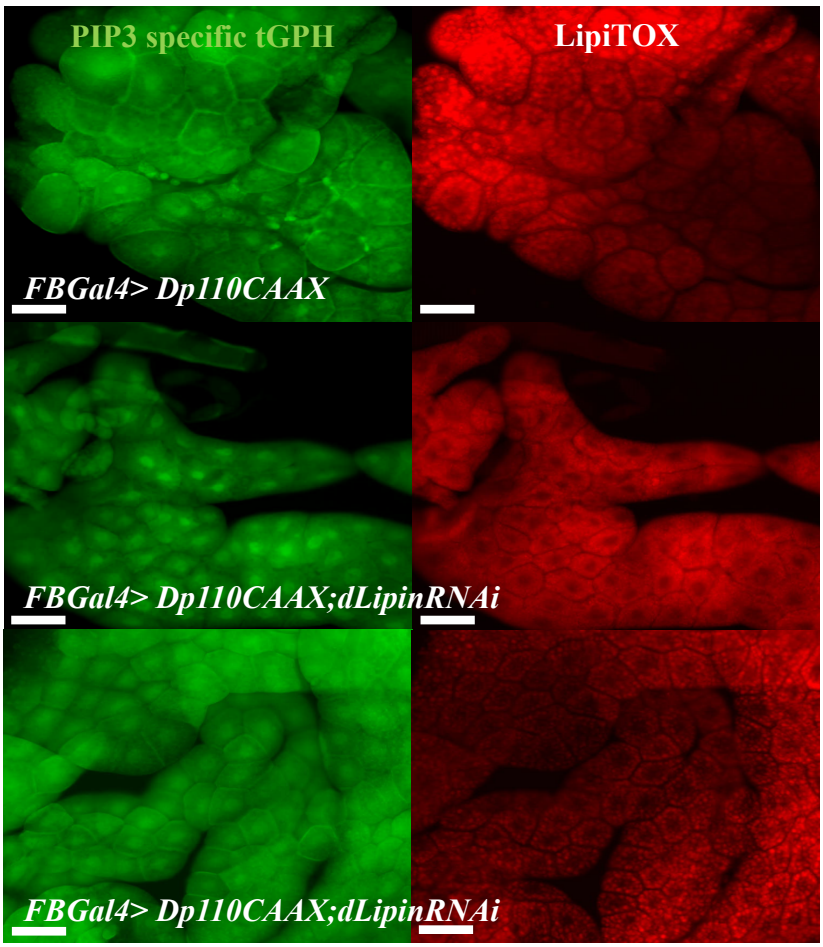

Fig. 20: Loss of dLipin is sufficient to downregulate insulin pathway activity in fat body cells with constitutively active PI3K. The PIP3 reporter PH-GPH was membrane associated in cells expressing *Dp110CAAX*. When *dLipin* was knocked down strongly in the fat body cells of these animals (*FBGal4> Dp110CAAX; dLipinRNAi*) the membrane association was no longer detectable (middle picture). In cases of weaker *dLipin* knockdown, PIP3 remained at the cell membrane (bottom picture). To have another measure of the severity of the *dLipin* knockdown, I stained fat droplets with LipiTOX (red). A strong *dLipin* knockdown corresponded to smaller fat droplets. Feeding third instar larvae were dissected. Scale bar: 100µm.

PIP3 localization at the plasma membrane in animals with *Dp110CAAX* expression was intact in cases of weak *dLipin* knockdown but lost in animals with stronger *dLipin* knockdown (Fig. 20). This indicates, that a reduction in dLipin activity is sufficient to prohibit PIP3 synthesis even in the presence of PI3K overactivation and it also suggests that dLipin affects PIP3 synthesis itself.

In addition to the PIP3 experiment, I also performed a western blot analysis to examine AKT phosphorylation levels.

5.2.1. Dp110-induced AKT phosphorylation is suppressed by a knockdown of *dLipin* activity

Overactivation of Dp110 should increase AKT phosphorylation, and RNAi-induced knockdown of *dLipin* should suppress this. To test this hypothesis, I performed a western blot analysis with fat body tissue from third instar feeding larvae expressing *Dp110CAAX* and compared this sample with fat body tissue from animals with *dLipin* knockdown and concomitant *Dp110CAAX* expression.

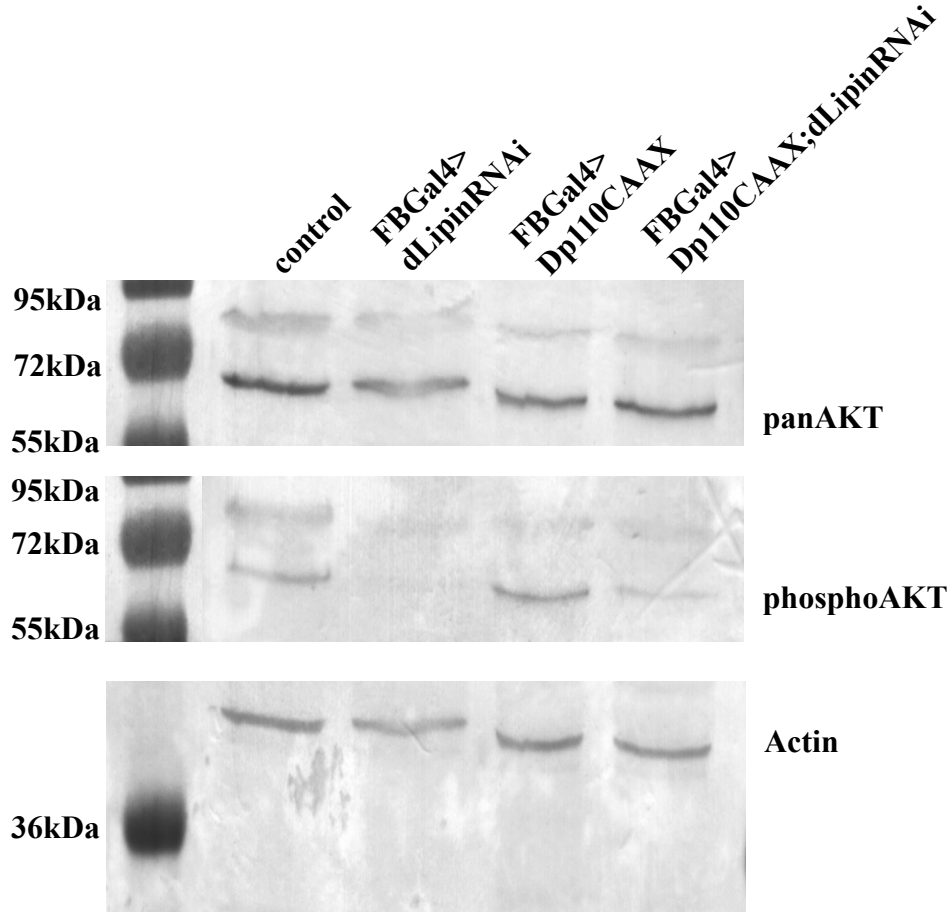

Fig. 21: Reducing dLipin levels in Dp110 overactivation background reduces phosphoAKT levels. Overactivation of Dp110 (*FBGal4>Dp110CAAX*) resulted in increased phosphoAKT levels. When *dLipinRNAi* was introduced into this genetic background (*FBGal4>Dp110CAAX; dLipinRNAi*), levels of phosphoAKT were greatly reduced, although more phosphoAKT was present in these samples compared to *dLipin* knockdown alone (*FBGal4>dLipinRNAi*). Tissue samples from animals expressing only the *Gal4* transgene were used as control. Fat body tissue was dissected from feeding third instar larvae. Actin served as a loading control.

Increased AKT phosphorylation after PI3K overactivation was reduced in animals with concomitant *dLipin* knockdown. Loss of dLipin activity overrode the effect that PI3K activation had on AKT phosphorylation.

This experiment showed that even in cells expressing a constitutively active PI3K it is sufficient to knockdown *dLipin* in order to downregulate insulin pathway activity. Reduced dLipin activity was able to override the PI3K input on the insulin pathway downstream of PI3K.

At this point of my work I was able to place dLipin as a contributor to insulin pathway activity, most likely acting at the level of PIP3 synthesis.

5.3. Can reduced dLipin activity be compensated for by inducing expression of insulin signaling effectors upstream or downstream of PI3K?

To determine whether dLipin deficiency can be compensated for by expression of insulin signaling cascade members downstream of PI3K, I overexpressed a constitutively active form of AKT in the fat body in concert with *dLipinRNAi*. However when performing the crosses I observed that AKT overexpression itself did not cause a phenotype, even when strongly expressed with *TubulinGal4* (data not shown). I used two different AKT fly lines with the same result. I also tried to rescue the PIP3 phenotype by expression of *chico* (the *Drosophila* homolog of the insulin receptor substrate) in cells with *dLipin* knockdown, but expression of *chico* alone

and in concert with *dLipinRNAi* appeared to have no effect. Also, expression of *InR* concomitant with *dLipinRNAi* in the fat body did not elicit an obvious effect. I furthermore tried to determine whether dLipin has a direct influence on PI3K activity by investigating PI3K transition to the cell membrane. To this end, I used an antibody that recognizes human p110 protein and that was predicted to cross react with *Drosophila* p110. Unfortunately this antibody did not show a specific reaction with *Drosophila* p110.

In conclusion, I was not able to determine whether expression of insulin signaling cascade effectors downstream or upstream of PI3K can compensate for a reduction of dLipin activity. To obtain additional evidence that dLipin interferes with insulin sensitivity in the fat body I asked whether the reduction of PI3K and AKT activity observed after a decrease of *dLipin* expression caused an increase in circulating sugars.

6. Circulating blood sugar levels are elevated in *dLipin* mutant animals

A hallmark of diabetes is the development of insulin resistance, which results in an increase in circulating blood sugar in the presence of insulin. With the major metabolic tissue of the developing larvae displaying signs of insulin insensitivity (Fig. 13 and 14), it seemed reasonable to assume, that a disruption of fat body insulin sensitivity alone might be sufficient to raise hemolymph sugar levels.

I measured hemolymph sugar levels of feeding third instar larvae with a transheterozygous *dLipin* mutant background (*dLipin*^{e00680}*/Df(3R)Exel7095*). The major circulating sugar of *Drosophila melanogaster* is trehalose, a sugar that can be converted to glucose by the enzyme trehalase. Hemolymph of feeding larvae was treated with trehalase and total glucose levels measured (Fig. 22).

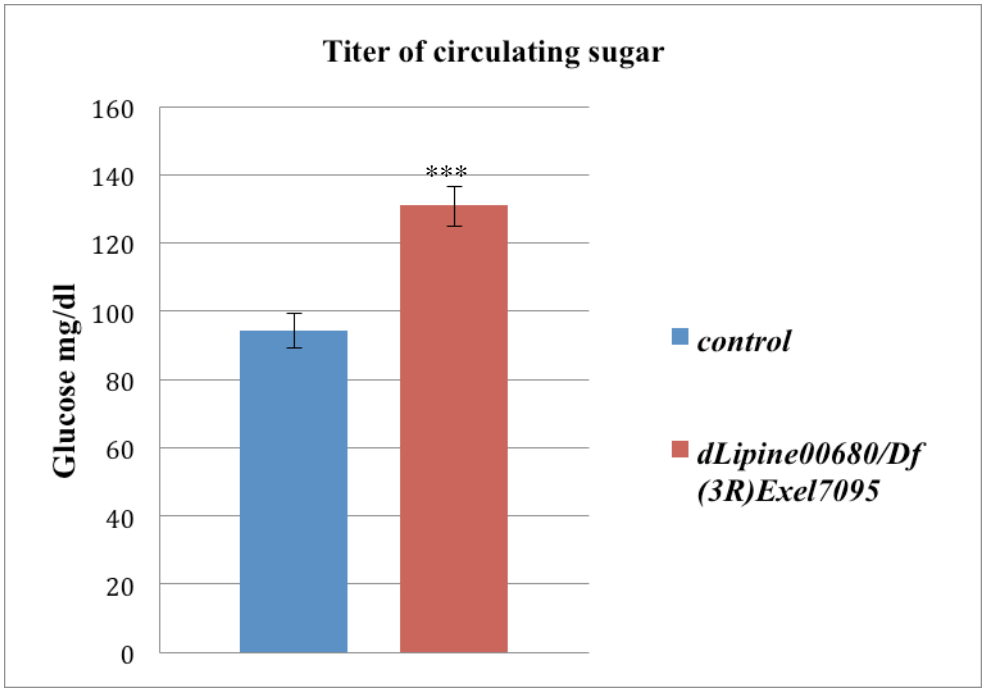

Fig. 22: Titers of circulating sugars are elevated in animals lacking dLipin. Hemolymph samples were obtained from feeding third-instar larvae heterozygous for *dLipin*^{e00680} or *Df(3R)Exel7095* (control) or transheterozygous *dLipin*^{e00680}*/ Df(3R)Exel7095*. Trehalose was enzymatically converted to glucose and total glucose measured. Unpaired t-Test, *** $p < 0.01$; error bars indicate standard error of the mean.

Measuring the levels of sugar in the hemolymph of mutant *dLipin* larvae established that a reduction of dLipin activity leads to insulin resistance, as hemolymph sugar levels were significantly increased (Fig. 22).

In summary, these data show that dLipin is necessary for proper insulin sensitivity in the fat body, and that insulin resistance induced by a lack of dLipin activity in the fat body results in elevated hemolymph sugar levels.

The next question(s) addressed was how dLipin activity itself was affected by insulin signaling.

7. dLipin levels are regulated by insulin signaling

Studies in adipocyte cell lines suggest an influence of insulin signaling on Lipin1's subcellular localization (Harris et. al. 2007, Peterfy et. al. 2009). It was demonstrated that Lipin1 phosphorylation following activation of insulin signaling leads to an accumulation of Lipin1 in the cytoplasm. To test whether this was also the case for dLipin, I investigated the localization of dLipin in the fat body of wandering third instar larvae after knockdown of insulin signaling.

7.1. dLipin levels, but not dLipin localization, are affected by a reduction in insulin signaling

I either expressed a dominant negative form of the regulatory subunit of PI3K (*PI3K21BHA*) or a dominant negative form of the insulin receptor (*InRDN*) exclusively in the fat body to reduce insulin pathway activity. Animals expressing the *InRDN* transgene displayed reduced fat body cell size, but were otherwise viable and appeared to develop normally. In contrast, animals expressing *PI3K21BHA* not only showed reduced cell size, but also suffered from larval lethality; and the few larvae that reached the pupal stage died during metamorphosis. This is consistent with a moderate reduction of insulin pathway activity with *InRDN* expression and a stronger reduction of insulin pathway activity with the expression of *PI3K21BHA*. To determine how expression of the transgenes affected dLipin expression and distribution, fat body was stained with dLipin antibodies (Fig. 23).

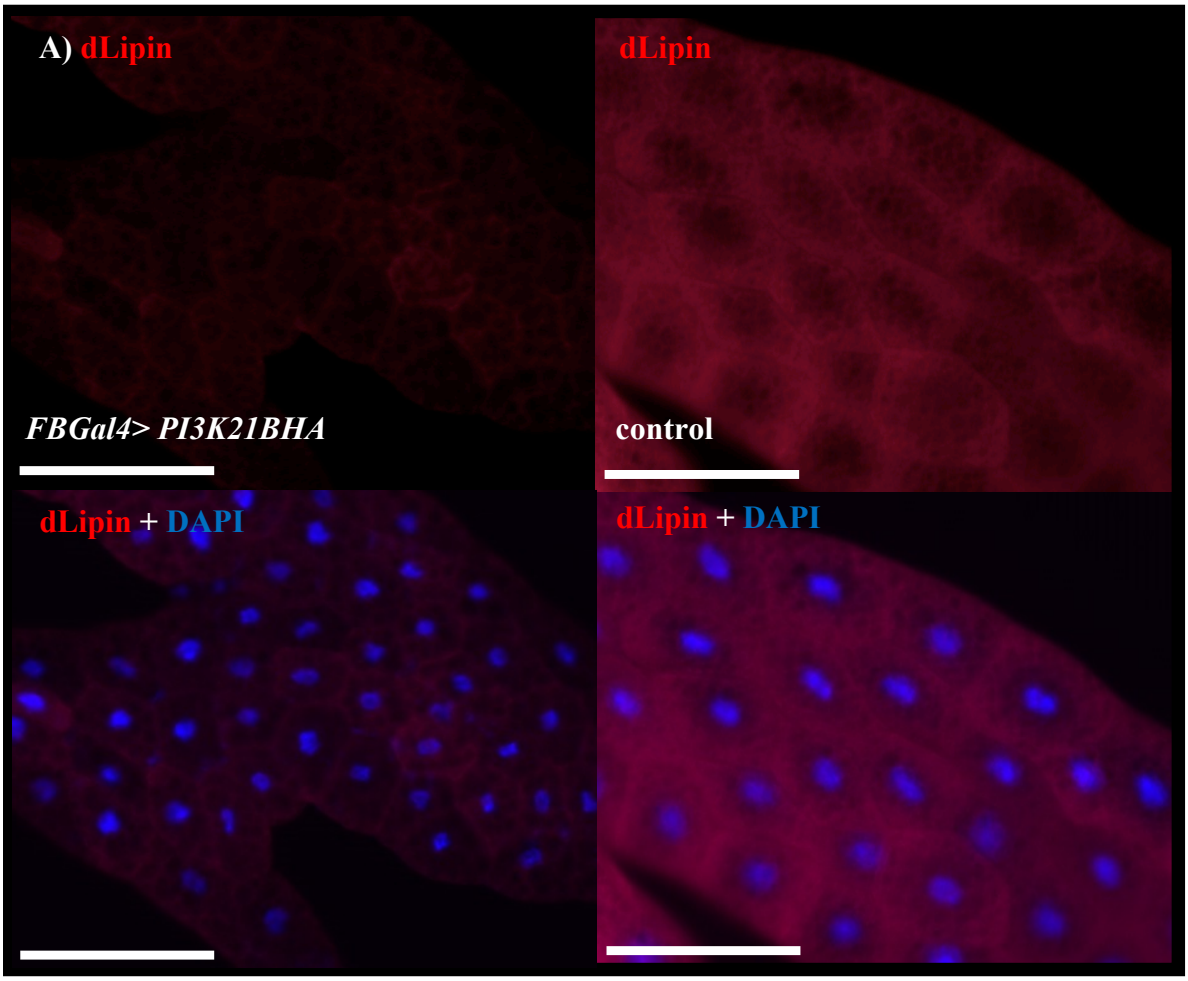
A) dLipin
FBGal4> PI3K21BHA
dLipin
control
dLipin + DAPI
dLipin + DAPI

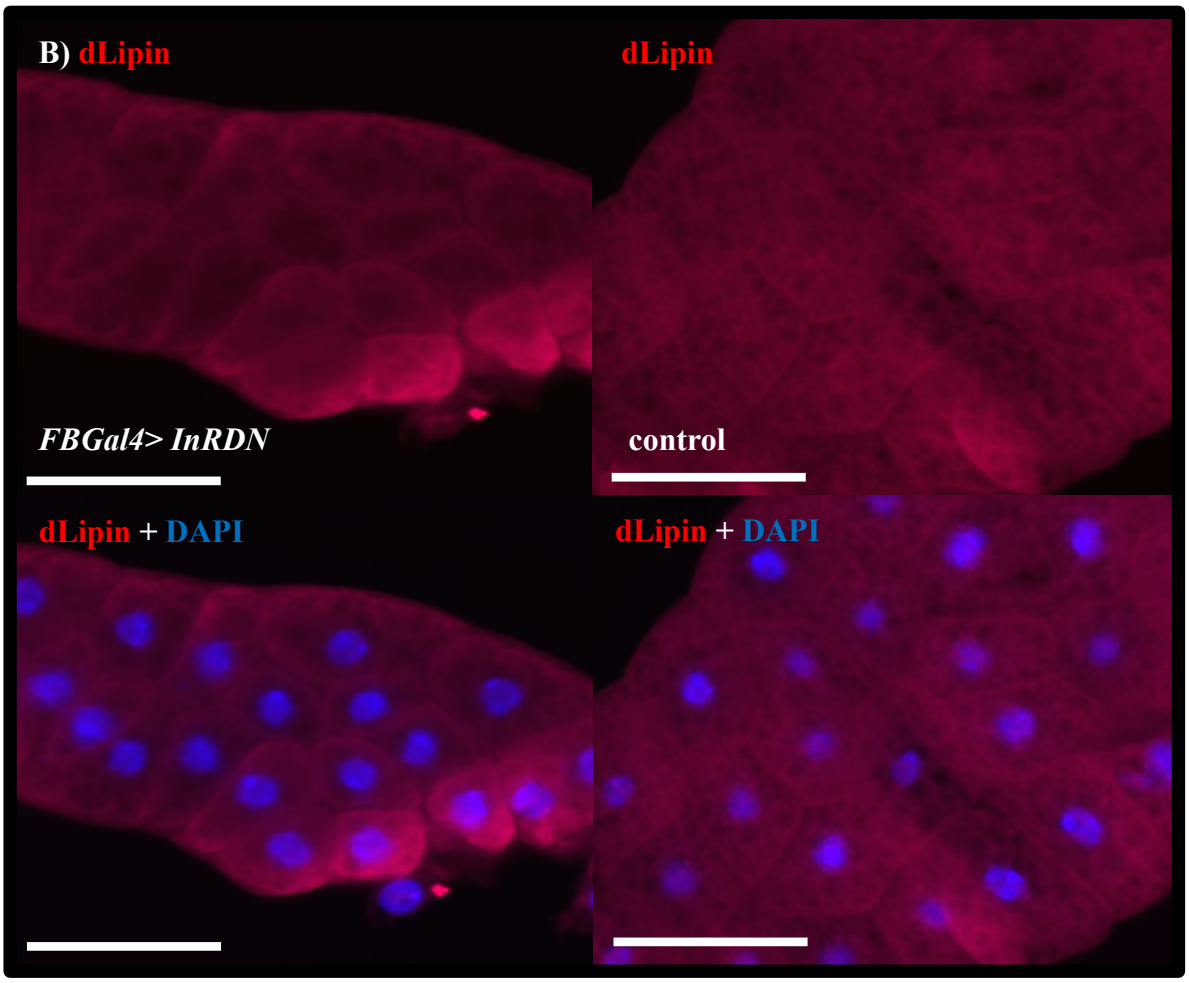

Fig. 23: dLipin levels, but not localization, are altered after knockdown of insulin pathway activity. A) A dominant negative form of the regulatory subunit of PI3K (*PI3K21BHA*) was expressed in the fat body (*FBGal4>PI3K21BHA*). Fat body tissue from third instar wandering larvae was dissected and stained with dLipin antibody (red). Nuclei were visualized with DAPI (blue). The same exposure time was used for all images. B) A dominant negative form of insulin receptor (*InRDN*) was expressed in the fat body, and the tissue stained with dLipin antibody (red). Nuclei were visualized with DAPI (blue). The same exposure time was used for all images. Scale bar: 100µm.

Fig. 23 shows that dLipin localization was not affected by a reduction of insulin pathway activity. It does appear, however, that overall levels of dLipin were reduced in fat body tissue from animals with a strong knockdown of insulin pathway activity (*FBGal4>PI3K21BHA*). This

experiment was also conducted with animals expressing *InRDN* (*FBGal4>InRDN*). The fat body showed no difference in dLipin levels.

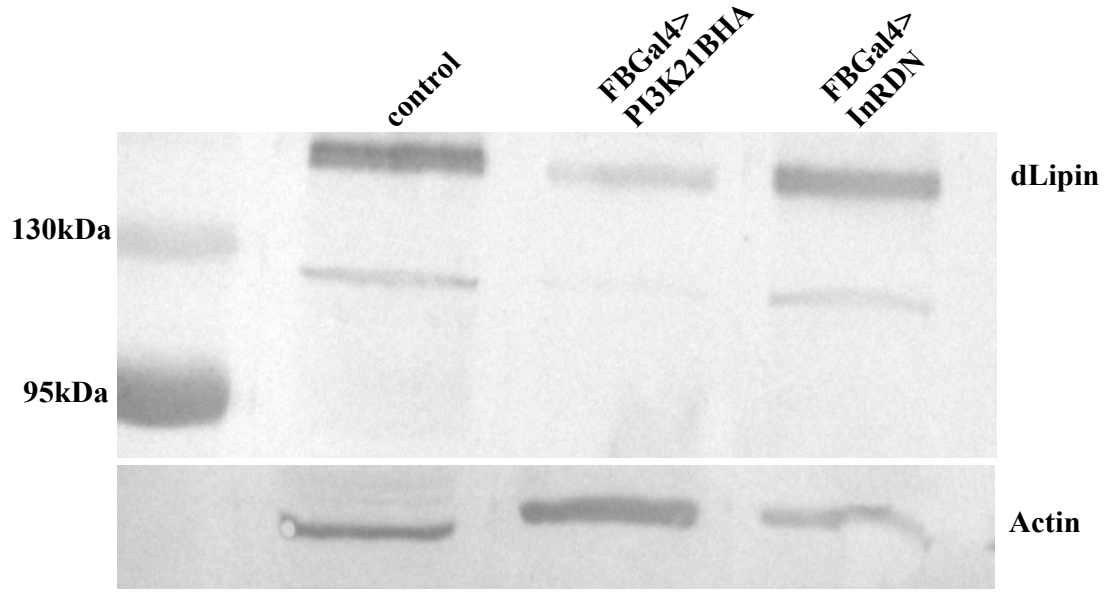

Fig. 24: dLipin levels are reduced upon strong downregulation of insulin pathway activity. Western analysis with dLipin antibody confirmed that dLipin levels are lowered in fat body tissue after strong knockdown of insulin signaling (*FBGal4>PI3K21BHA*). The weaker insulin phenotype of *FBGal4; InRDN* did not cause a decrease in dLipin levels. Fat body tissue from w^{1118} animals served as a control. Wandering third instar larvae were dissected. Actin served as a loading control.

The immunostaining results were corroborated by western analysis. dLipin antibody was used to detect dLipin in fat body tissue from animals expressing either *PI3K21BHA* or *InRDN* in the fat body. A clear reduction of dLipin was detectable after expression of *PI3K21BHA*, whereas expression of *InRDN* appeared to have no effect on the amount of dLipin. Thus, insulin pathway activity can influence dLipin protein levels, but does not appear to have an obvious effect on subcellular localization of the protein.

7.2. dLipin levels are not affected in cells with an overactivation of the insulin pathway

I was previously able to show that downregulation of insulin pathway activity leads to a decrease in dLipin levels in fat body cells. Thus, it is plausible that an activation of insulin signaling may have the opposite effect, namely an increase in dLipin levels. I conducted a western blot analysis to test whether expression of *Dp110CAAX* has an effect on dLipin levels (Fig. 25). Expression of *Dp110CAAX* overstimulates the insulin pathway.

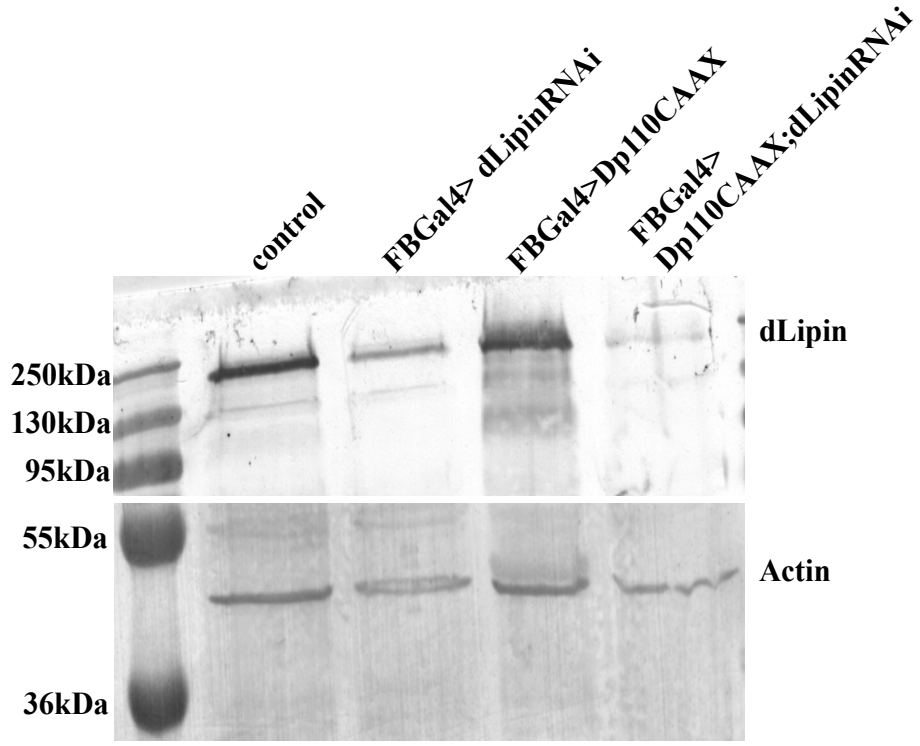

Fig. 25: PI3K overactivation has no effect on dLipin levels. Western blot analysis with fat body tissue from control animals (only FBGal4 transgene), *FBGal4>dLipinRNAi* animals, *FBGal4>Dp110CAAX* animals and *FBGal4>Dp110CAAX; dLipinRNAi* animals showed that overactivation of PI3K had no effect on dLipin levels, and that *dLipinRNAi* knockdown is effective in *FBGal4> Dp110CAAX; dLipinRNAi* animals. Actin served as a loading control.

Western analysis revealed that overactivating the insulin pathway via *Dp110CAAX* expression has no discernible effect on dLipin levels in fat body cells.

8. Summary of part A Results

I was able to establish that dLipin influences insulin pathway activity in the larval fat body. Cell-autonomous loss of dLipin activity resulted in a growth defect. PIP3 synthesis by PI3K and, thus, PI3K activity was disrupted in cells lacking dLipin. The TORC2 mediated phosphorylation of AKT was consequently negatively affected in fat body from animals with fat body-specific *dLipin* knockdown and in fat body from transheterozygous *dLipin* mutants, which indicates that insulin pathway activity downstream of PI3K was indeed downregulated. Furthermore, it appeared that *dLipin* and *InR* act in concert in fat body development. Hemolymph sugar levels were significantly increased in *dLipin* mutants, consistent with the conclusion that loss of *dLipin* causes insulin resistance in the fat body. dLipin activity itself was also influenced by a disruption of insulin signaling resulting in a reduction in dLipin abundance. Upregulation of the insulin pathway on the other hand, did not alter dLipin levels. With regard to narrowing down the target of dLipin in the canonical insulin pathway, I was able to show that dLipin activity influences insulin pathway activity at the PIP3 synthesis step.

I was then interested in pinpointing possible mechanisms by which dLipin is able to enact its effect on the insulin cascade.

B. To elucidate the mechanism that underlies insulin resistance caused by reduced dLipin activity

An unphysiological reduction of adipose tissue is called lipodystrophy; it is a condition known to result in insulin resistance (Huang-Doran et. al, 2010). Lipodystrophy in mice can be caused by a mutation in the *lipin1* gene (Reue et al., 2000). Therefore, one possible explanation for how dLipin influences insulin sensitivity in the fat body is through its PAP activity. A loss of dLipin activity results in a reduction of PAP activity in the cell, which leads to an increase in PA and a reduction in DAG, and hence lowered TAG content. Therefore it is possible that either elevated PA levels or lowered DAG/TAG levels negatively affect insulin sensitivity of the cell.

1. Knockdown of *GPAT4* or *AGPAT3* mirrors *dLipin* knockdown with regard to PIP3 synthesis

To test whether insulin resistance caused by the lack of dLipin is a result of the ensuing lipodystrophy, I examined PIP3 synthesis in fat body tissue from animals with RNAi-induced knockdown of fat synthesis enzymes, GPAT4, AGPAT3 and DGAT2. These enzymes are essential for TAG production. RNAi-induced knockdown was limited to the fat body, and feeding third instar larvae were dissected. I observed a reduction of fat droplet size after knockdown of *GPAT4*, knockdown of *AGPAT3*, but not with *DGAT2* knockdown (Fig. 26, *DGAT2* knockdown data is not shown). These phenotypes mirrored the fat body-specific effects of *dLipin* knockdown. This result then led me to look at PIP3 synthesis in fat body cells from animals expressing *GPAT4RNAi* and *AGPAT3RNAi* (Fig. 26). In concert with a decrease in fat droplet size I observed a loss of PIP3 membrane association upon *GPAT4* or *AGPAT3* knockdown. This phenotype strongly resembled the phenotype upon *dLipin* knockdown.

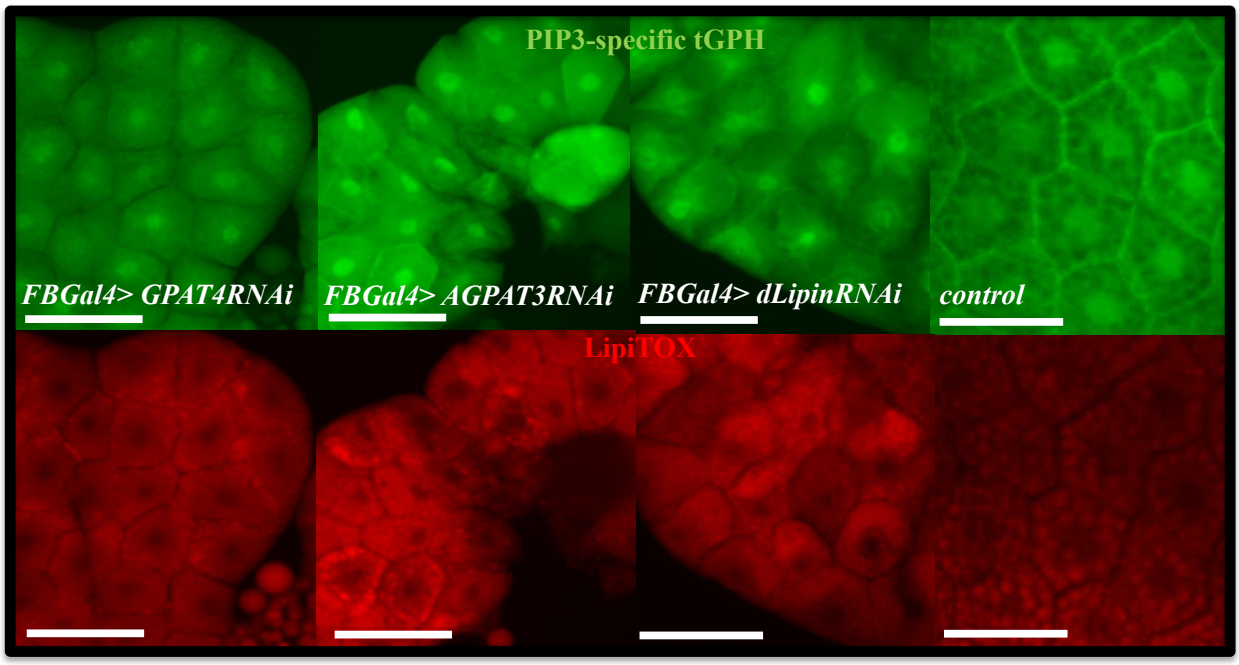

Fig. 26: Knockdown of TAG synthesis enzymes leads to loss of PIP3 membrane association. PIP3 was membrane associated in cells expressing the *FBGal4* driver only (control). In fat body cells from animals with *GPAT4* and *AGPAT3* knockdown (*FBGal4>GPAT4RNAi* and *FBGal4>AGPAT3RNAi*), PIP3 was no longer detectable at the membrane, and fat droplet size was strongly reduced. This mirrored the *dLipin* RNAi phenotype (*FBGal4>dLipinRNAi*). PIP3 was detected by tGPH (green) and fat droplets by LipiTOX (red). Feeding third instar larvae were dissected. Scale bar: 100µm.

Results from this experiment point to TAG synthesis or fat content as the parameter that influences insulin responsiveness, as PIP3 synthesis was disrupted in fat body cells upon RNAi-induced knockdown of not only dLipin, but two other enzymes of the glycerol-3-phosphate pathway.

2. PAP activity of dLipin is critical for insulin pathway activity

To examine whether indeed the PAP activity of dLipin and not its transcriptional co-regulator activity is required for normal insulin sensitivity of fat body cells, I generated two mutant forms of dLipin. In one form, the amino acid residue within the PAP motif at position 812 was altered from aspartate to glutamate (D812E) (*ΔPAPdLipin*). In the other form, the

putative nuclear localization signal (*ΔNLSdLipin*) at position 276-281 was deleted. Thus, ΔPAPdLipin should not exhibit PAP activity, and ΔNLSdLipin should not translocate to the nucleus and hence should not be able to function as a transcriptional co-regulator. I conducted co-expression experiments with these *dLipin* contructs and the *dLipinRNAi* transgene in the fat body. If indeed the PAP activity of dLipin is responsible for modulating insulin pathway activity, then expression of *ΔPAPdLipin* should not rescue the loss of PIP3 synthesis in animals with *RNAi*-induced *dLipin* knockdown. On the other hand, if the co-regulator activity of dLipin is responsible, then expression of *ΔNLSdLipin* should not rescue. As a positive control I expressed a *WTdLipin* construct. Before I started the PIP3 rescue experiments, I had to establish the fact that ΔNLSdLipin does not enter the nucleus and that ΔPAPdLipin exhibits no PAP activity.

2.1. Characterization of ΔNLSdLipin and ΔPAPdLipin

ΔNLSdLipin was expressed concomitantly with *TORRNAi* in the fat body, and subsequent changes in subcellular localization examined. Knockdown of TOR activity in a wildtype genetic background results in a translocation of dLipin from the cytoplasm into the nucleus (Fig. 27 upper right panel, Fig. 34). This important finding will be further documented in Part C.

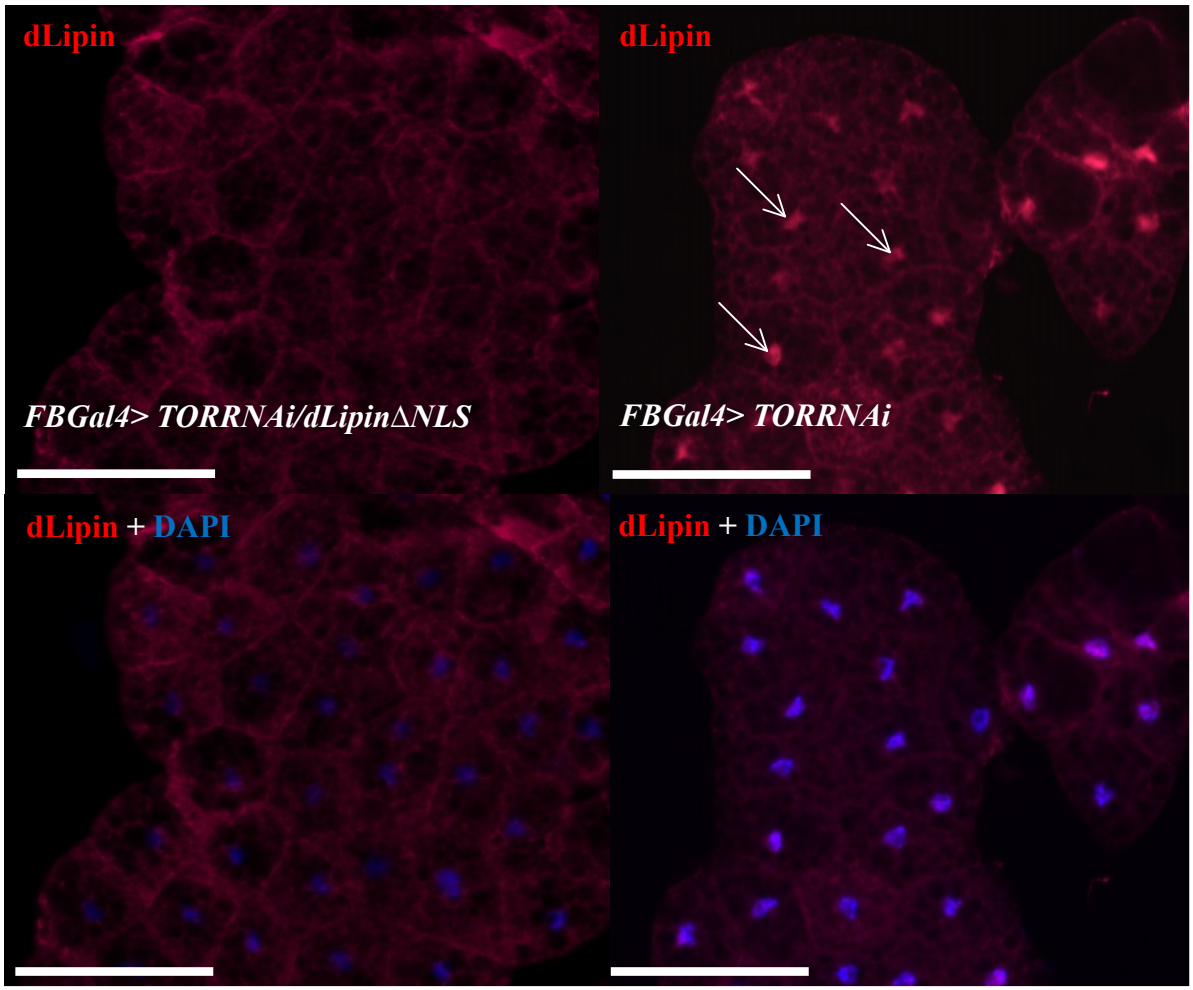

Fig. 27: ΔNLSdLipin does not enter the nucleus and prevents endogenous dLipin from entering the nucleus. Δ*NLSdLipin* was expressed in the fat body concomitantly with *TORRNAi*. Knocking down *TOR* leads to a translocation of dLipin (red) into the nucleus (arrows) as confirmed by double-staining with DAPI (blue). When co-expressing *TORRNAi* and Δ*NLSdLipin* this translocation was no longer observed, indicating that ΔNLSdLipin not only cannot enter the nucleus, but also inhibits the endogenous dLipin from entering the nucleus. Scale bar: 100µm.

The results of this experiment confirmed that the ΔNLSdLipin was not able to translocate to the nucleus. Furthermore, it caused a dominant negative phenotype by prohibiting endogenous dLipin from entering the nucleus.

To verify that ΔNLSdLipin retains PAP activity, and that ΔPAPdLipin lost PAP activity, I set up rescue experiments wherein I expressed *WTdLipin*, *ΔNLSdLipin* and *ΔPAPdLipin* in the

fat body of tranheterozygous *dLipin* mutant animals (*dLipin*^{e00680}*/ Df(3R)Exel7095*) and looked for improvements in fat body morphology.

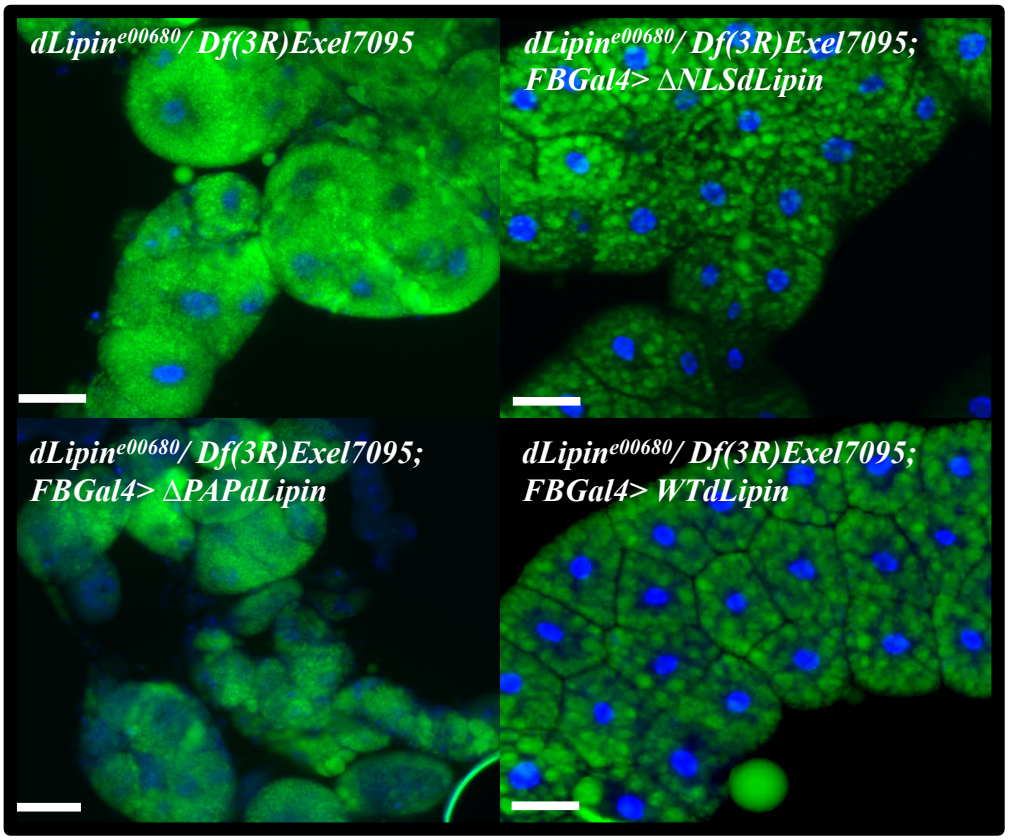

Fig. 28: Expression of mutant and wildtype *dLipin* constructs in *dLipin* mutant background rescues defects in fat body morphology. *WTdLipin*, *ΔNLSdLipin* and *ΔPAPdLipin* were expressed in transheterozygous *dLipin* mutant (*dLipin*^{e00680}*/ Df(3R)Exel7095*) animals. Expression was limited to the fat body. Fat body defects visible in the *dLipin* mutant are rescued by expression of *WTdLipin*, and *ΔNLSdLipin* but not *ΔPAPdLipin*. Fat droplet morphology is visualized by Bodipy staining (green) and nuclei are stained with DAPI (blue). Scale bar: 100µm.

Expression of *WTdLipin* and *ΔNLSdLipin* rescued the fat body defects observed in dLipin mutants. This indicates that, like WTdLipin, ΔNLSdLipin possesses normal PAP function. Fat droplet size was increased and cell shape polygonal after expression of these two constructs. ΔPAPdLipin on the other hand was not able to compensate for loss of PAP activity in *dLipin*

mutants. The fat body defects observed in *dLipin* mutants were still present after expression of *ΔPAPdLipin*. These data are consistenet with a lack of PAP activity in the ΔPAPdLipin construct. .

2.1.1. Expression of any *dLipin* construct in the fat body alone does not rescue developmental defects

While performing rescue experiments, I noted that expression of any of the *dLipin* constructs in the fat body alone was not able to rescue lethality and developmental delay of *dLipin* mutant animals. To examine rescue effects, I set up crosses and compared the formation of pupae by transheterozygous *dLipin* mutants and transheterozygous *dLipin* mutants with concomitant expression of either *WTdlipin* or *ΔNLSdLipin* or *ΔPAPdLipin* in the fat body. I set up an individual rescue cross for each single *dLipin* construct (*WTdlipin* or *ΔNLSdLipin* or *ΔPAPdLipin*). As both genotypes (control: *Df/Rb; Gal4*; experimental genotype: *Df/Rb; Gal4/ WTdlipin* or *Df/Rb; Gal4/ ΔNLSdLipin* or *Df/Rb; Gal4/ ΔPAPdLipin*) emerge from the same cross, I knew the expected genotype frequency for each genotype. I compared the number of pupae with control genotype (*dLipin* mutant: *Df/Rb; WTdlipin or ΔNLSdLipin or ΔPAPdLipin*) to the number of pupae with experimental genotype (*Df/Rb; Gal4/ WTdlipin* or *Df/Rb; Gal4/ ΔNLSdLipin* or *Df/Rb; Gal4/ ΔPAPdLipin*). I was thus able to use pairwise Chi-square analyses to score for significant differences between control and experimental genotype. *dLipin* transheterozygous animals served as a control, thus I set the number of pupae formed by these animals as 100%. For a more detailed explanation please refer to Materials and Methods section.

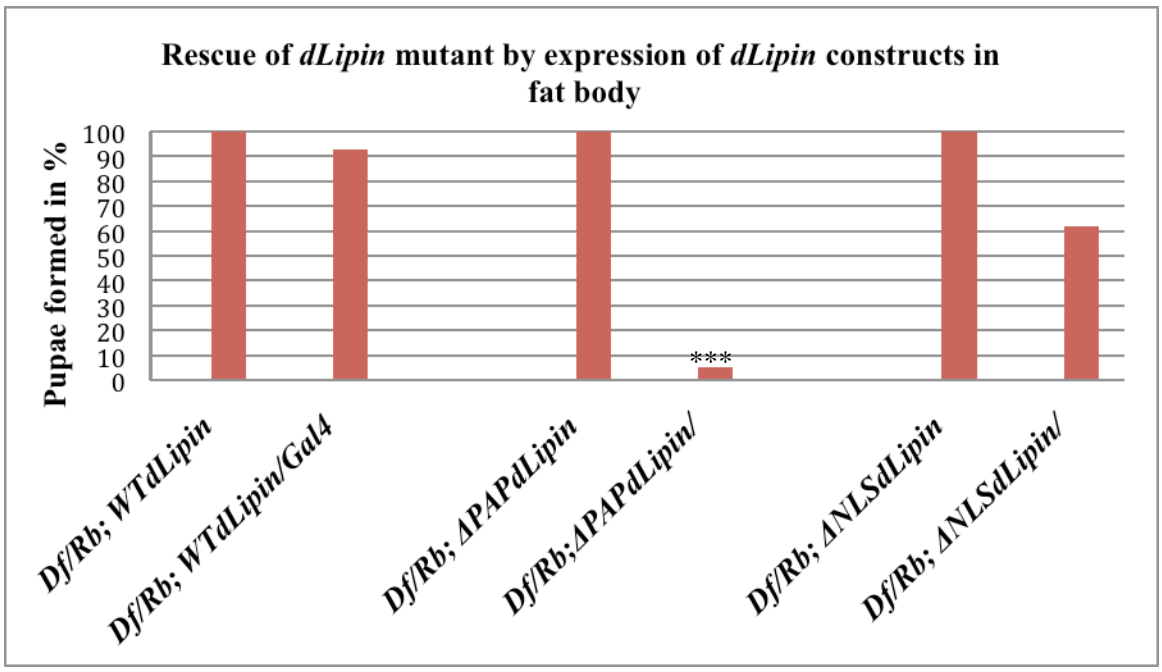

Fig. 29: Expression of *WTdLipin*, *ΔNLSdLipin* and *ΔPAPdLipin* in the fat body of *dLipin* mutant animals (*dLipin*^{e00680}/ *Df(3R)Exel7095, Df/Rb*) does not rescue larval lethality. To screen for larval lethality, I scored pupation rates of *dLipin* mutant animals and *dLipin* mutant animals expressing one of three dLipin constructs *(dLipin*^{e00680}*/ Df(3R)Exel7095; FBGal4/ WTdLipin, dLipin*^{e00680}*/ Df(3R)Exel7095; FBGal4/ ΔNLSdLipin, dLipin*^{e00680}*/ Df(3R)Exel7095; FBGal4/ ΔPAPdLipin)*. Expression of the *dLipin* constructs was restricted to the fat body. No rescue effects on survival were present for either *dLipin* construct, in fact, expression of *ΔPAPdLipin* lowered pupation rates significantly. The transheterozygous *dLipin* mutant genotype (*dLipin*^{e00680}*/ Df(3R)Exel7095)* is abbreviated to *Df/Rb* in the graph. Two tailed Chi-Square Test, *** $p < 0.0001$.

Expression of *dLipin* rescue constructs in the fat body of *dLipin* mutants alone did not rescue larval lethality of *dLipin* mutants. No significant increase in the number of pupae formed was observed for either *dLipin* construct. To the contrary, expression of *ΔPAPdLipin* seemed to have a dominant negative effect, as pupation rates of these animals were even lower than those of *dLipin* mutant control animals. Furthermore, the dominant-negative effect observed after *ΔPAPdLipin* expression is a positive indicator that the transgene is indeed expressed. I also set up a rescue experiment with the *daGal4* driver, but no rescue effects were observed.

2.1.2. Expression of *ΔPAPdLipin* results in a dominant negative phenotype

To further investigate the possibility that expression *ΔPAPdLipin* results in a dominant negative effect, I expressed this construct with a strong ubiquitous driver, *TubulinGal4* (TubGal4), in a *dLipin* mutant background and in a wild-type genetic background. No difference in lethality was observed after ubiquitous *ΔPAPdLipin* expression in a wild-type genetic background (data not shown), but ubiquitous expression of *ΔPAPdLipin* in a *dLipin* mutant background significantly reduced viability (Fig. 30). Both genotypes resulted from the same cross with known genotype frequencies, hence I was able to use Chi-Square analyses to score for statistical significance.

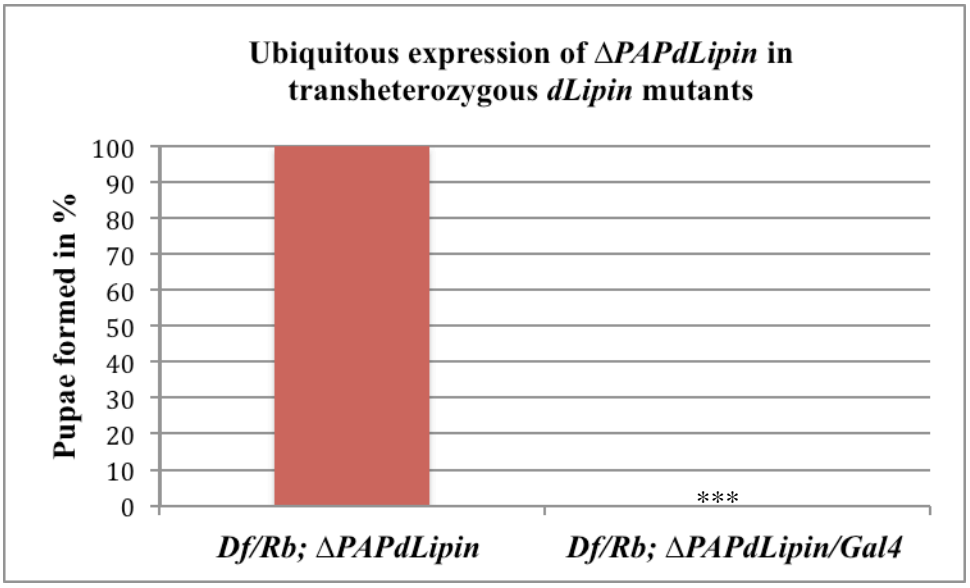

Fig. 30: Ubiquitous expression of *ΔPAPdLipin* in *dLipin* mutant background causes dominant negative effect. Expression of *ΔPAPdLipin* driven by *TubulinGal4* in a *dLipin* mutant genetic background (*dLipin*^{e00680}*/ Df(3R)Exel7095; ΔPAPdLipin/TubGal4*) resulted in reduced viability. The number of larvae reaching the pupal stage was significantly reduced in animals expressing *ΔPAPdLipin*, compared to *dLipin* mutants (*dLipin*^{e00680}*/ Df(3R)Exel7095, Df/Rb*). The transheterozygous *dLipin* mutant genotype (*dLipin*^{e00680}*/ Df(3R)Exel7095)* is abbreviated as *Df/Rb* in the graph. Two tailed Chi-Square Test, *** p= 0.0009.

Expression of a *dLipin* construct with a mutation in the motif responsible for its PAP activity resulted in a dominant negative phenotype with regard to viability only when expressed in a *dLipin* mutant genetic background, but not when expressed in a wild-type genetic background.

2.2.2. PIP3 synthesis depends on PAP activity

To determine whether the impact dLipin has on PI3K activity requires its transcriptional co-regulator activity or its PAP activity and to further explore whether it is indeed fat synthesis that is key to insulin sensitivity of the fat body, I set up crosses in which I expressed *WTdLipin*, *ΔNLSdLipin* and *ΔPAPdLipin* in a background of fat body-specific *dLipin* knockdown (*FBGal4> dLipinRNAi;* tGPH/*WTdLipin; FBGal4>dLipinRNAi; tGPH/ΔNLSdLipin; FBGal4>dLipinRNAi; tGPH/ΔPAPdLipin*). To monitor PIP3 synthesis I expressed the PIP3 marker *tGPH*. I had already shown that *dLipin* knockdown interferes with PIP3 synthesis (Fig. 13, Fig. 14). Expression of *WTdLipin* in a *dLipin* knockdown background should rescue the loss of PIP3 from the cell membrane. Expression of this construct therefore served as a positive control. *ΔNLSdLipin* and *ΔPAPdLipin* expression may, or may not reconstitute PIP3 synthesis in animals with loss of dLipin activity. Results of this experiment are depicted in Fig. 31.

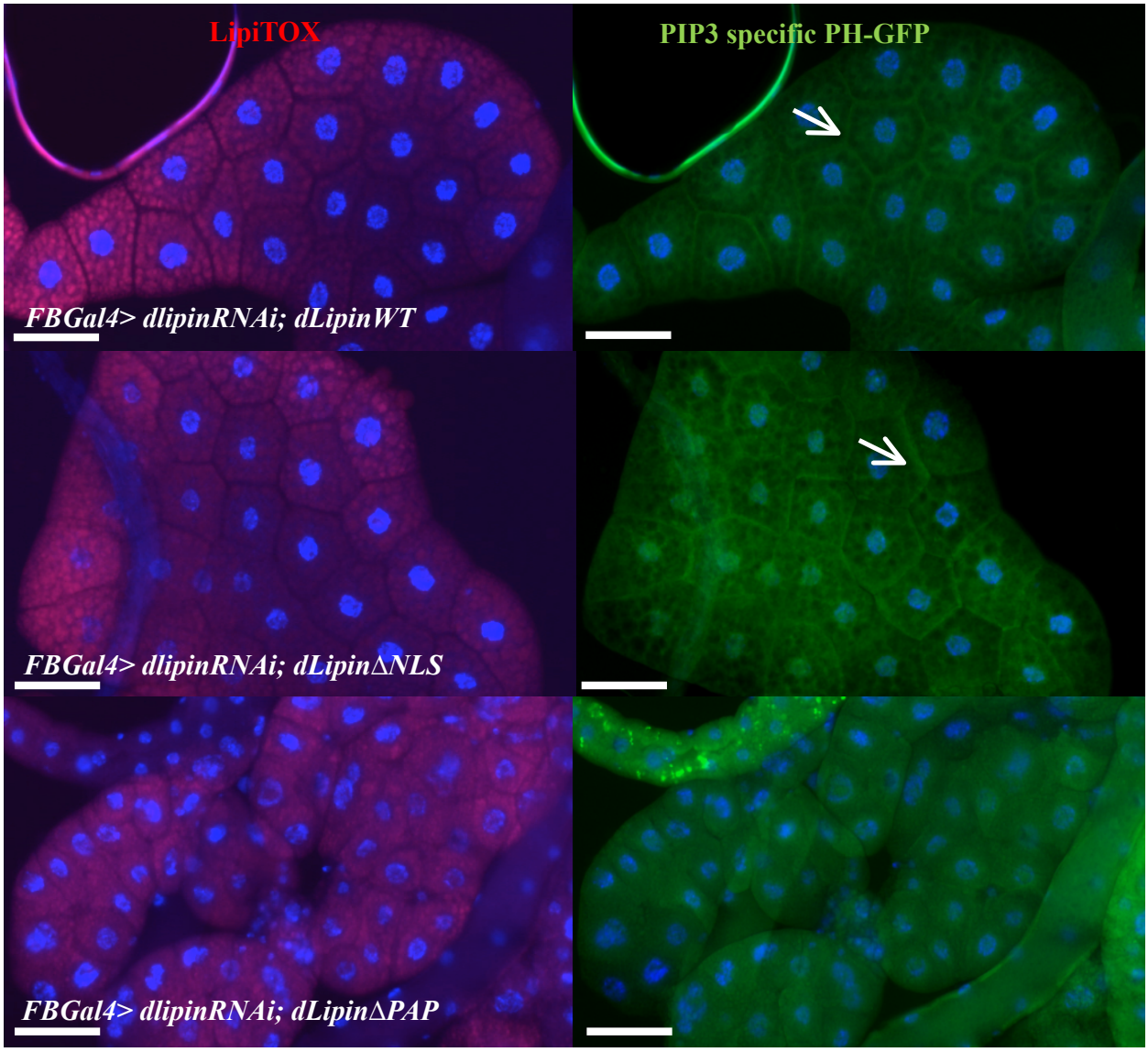

Fig. 31: PAP activity of dLipin is required for PIP3 synthesis. Expression of both *WTdLipin* and *ΔNLSdLipin* is sufficient to restore PIP3 synthesis after *dLipin* knockdown (*FBGal4>dLipinRNAi; WTdLipin* and *FBGal4>dLipinRNAi; ΔNLSdLipin*). PIP3 was again located at the cell membrane (arrows). In contrast, expression of *ΔPAPdLipin* could not rescue the loss of PIP3 synthesis in animals with a loss of dLipin activity (*FBGal4>dLipinRNAi; ΔPAPdLipin*). PIP3 was not located at the cell membrane. PIP3 was visualized by expression of PIP3 marker *tGPH* (green). Furthermore, fat droplet size was increased in fat body tissue from animals with *WTdLipin* and *ΔNLSdLipin* expression but not in animals with of *ΔPAPdLipin* expression. Fat droplet morphology was visualized by LipiTOX staining (red). Nuclei were stained with DAPI (blue). Scale Bar: 100 µm.

The results show that PAP activity is required for PIP3 synthesis in the fat body. Expression of *WTdLipin* and *ΔNLSdLipin* was able to reconstitute PIP3 synthesis in fat body cells in concert with rescuing the reduction of fat droplet size. Expression of *ΔPAPdLipin* on the other hand, could not reestablish PIP3 synthesis or increase the size of fat droplets. Therefore it is likely that fat content and PIP3 synthesis are linked and that dLipin's transcriptional co-regulatory function is not responsible for the effects on the insulin pathway.

2.2.3. Expression of *AtPAH1* in animals with fat body-specific *dLipin* knockdown

To validate the results described in the previous section, I attempted to rescue PIP3 synthesis by expressing one of the *Arabidopsis thaliana* lipin homologs, *AtPAH1*. The encoded *Arabidopsis* Lipin protein does not seem to function as transcriptional co-regulators, only as phosphatidate phosphatase enzymes as sequence alignments show that *Arabidopsis* Lipins lack a co-regulator motif (Peterfy et al., 2001). Using the *AtPAH1* lipin homolog one can thus investigate whether PAP activity alone is enough to restore insulin sensitivity in *dLipin* deficient animals. Fat body-specific expression of *AtPAH1* from a UAS construct did not rescue fat body defects following *dLipin* knockdown (Fig. 32). This might have been due to either failed construct expression or due to the fact that *dLipin* and *AtPAH1* have diverged to a point where functions are no longer conserved between the two encoded proteins. Further experimentation is required to distinguish between these possibilities.

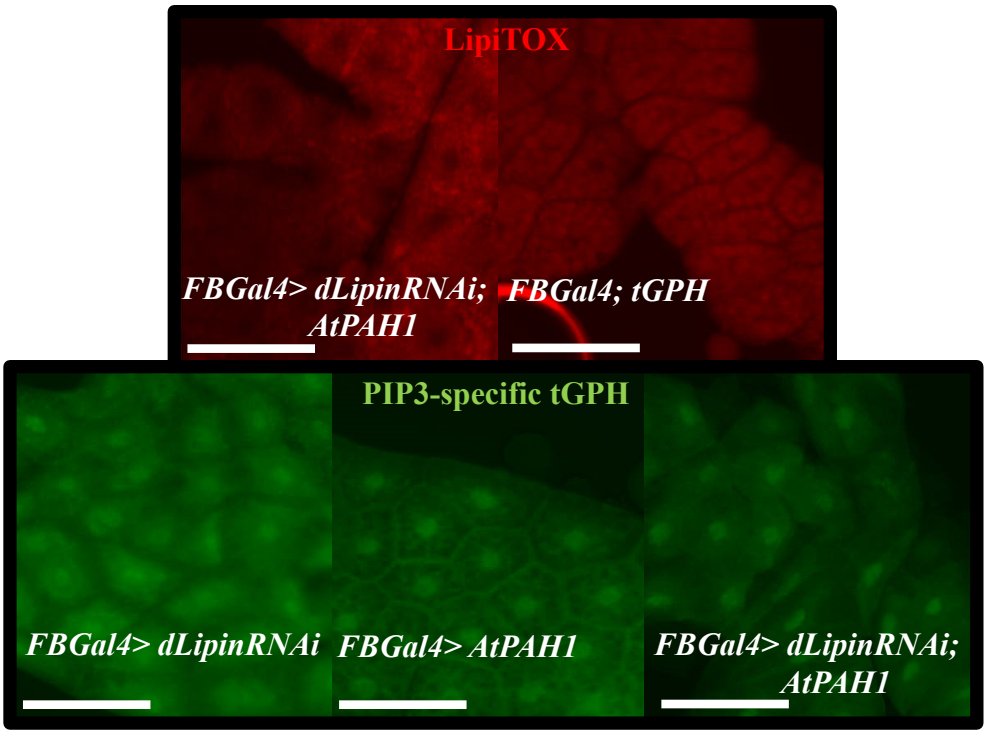

Fig. 32: The *Arabidopsis thaliana* homolog of *dLipin* cannot rescue the loss of PIP3 membrane association after *dLipin* knockdown. The *Arabidopsis* homolog of *Lipin* was expressed to rescue the loss of PIP3 from the cell membrane. No rescue of the *dLipinRNAi* phenotype was observed. The *Arabidopsis* homolog of *Lipin* was not able to rescue either the reduced fat droplet size (red) or the loss of PIP3 from the cell membrane (green). Scale bar 100μm.

3. *Dp110* transcript levels are reduced following *dLipin* knockdown

dLipin in its function as a transcriptional co-regulator could manipulate expression levels of genes involved in the insulin signaling cascade, and thus influence insulin pathway activity. Previously I had established that dLipin is able to attenuate Dp110 function in the fat body (5.2.1.). I therefore investigated whether *Dp110* expression levels were reduced in animals with knockdown of *dLipin* in the fat body (*FBGal4>dLipinRNAi*). qRT-PCR was conducted and transcript levels of *Dp110* quantified (Fig. 33).

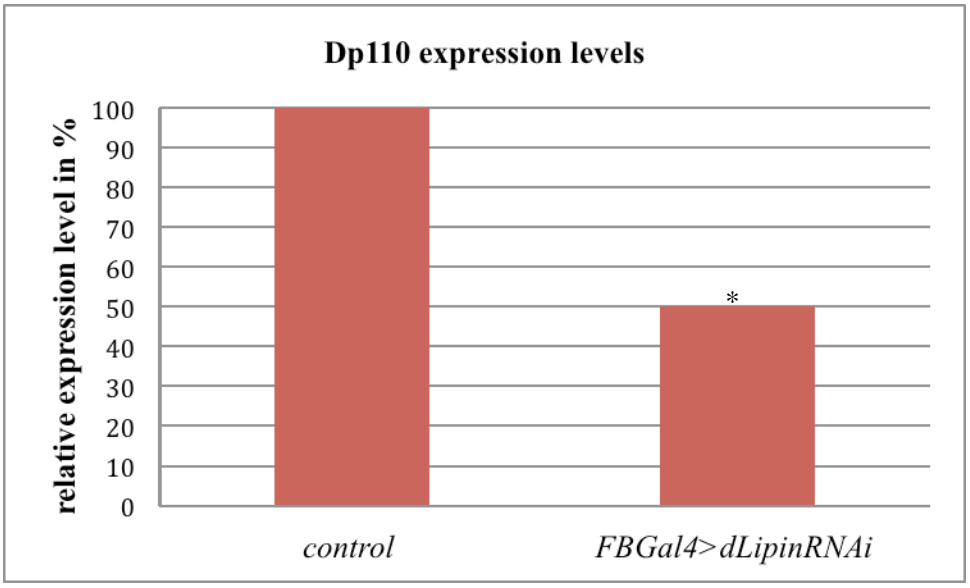

Fig. 33: Levels of *Dp110* RNA are reduced following *dLipin* knockdown. Levels of mRNA encoding the PI3K subunit Dp110 were reduced 2-fold in fat body of larvae expressing a *dLipinRNAi* transgene. *Dp110* RNA was quantified by qRT-PCR; *rp49* RNA served as the normalizer. The difference between control (w^{1118}) and knockdown animals was statistically significant. RNA was extracted from fat body tissue. * $p < 0.05$.

Knockdown of *dLipin* in the fat body led to a moderate reduction of *Dp110* transcript levels, suggesting that dLipin participtes directly or indirectly in the transcriptional regulation of the *Dp110* gene.

4. Summary part B Results

I was able to establish a link between TAG synthesis and insulin pathway activity. Loss of dLipin's PAP activity was responsible for reduced PIP3 synthesis following *dLipin* knockdown. Nuclear dLipin activity might play a contributory role, but did not appear to have a major influence on insulin pathway activity.

C. To elucidate the relationship between dLipin and TOR in *D. melanogaster*

One of the downstream targets of insulin signaling is the TOR kinase, more specifically TOR Complex 1 (TORC1). Having shown that dLipin is an important contributor to insulin pathway activity in the fat body of developing larvae, I proceeded to illuminate dLipin's potential interaction with the TOR signaling pathway.

In mammals, mTOR signaling is implicated in lipid biosynthesis (Laplante and Sabatini, 2009) and is responsible for Lipin1 phosphorylation (Huffman et al., 2002). So far, no interaction studies have been conducted for dLipin and TOR interaction(s) in *Drosophila melanogaster.* As was the case with insulin signaling, I focused my research on the major metabolic organ of the developing larvae, the fat body.

1. dLipin levels and subcellular localization are dependent on TORC1 activity

In mammals Lipin1 was shown to be posttranslationally modified in a TOR-dependent manner (Huffman et al., 2002). Numerous rapamycin-sensitive phosphorylation sites within Lipin1 were identified. Rapamycin acts as a TOR antagonist. Posttranslational modifications of Lipin1 in response to TOR signaling are connected to changes in Lipin1's subcellular localization (Peterson et al., 2011). Therefore, I investigated the spatial distribution of dLipin after *TOR* knockdown (*FBGal4>TORRNAi*).

I looked at dLipin in fat body cells from third instar wandering larvae (Fig. 34). While investigating subcellular localization, I noticed that overall dLipin levels appeared to be lowered after *TOR* knockdown. To measure overall dLipin levels, I conducted a western analysis with fat body tissue from animals expressing *TORRNAi* in the fat body (*FBGal4>TORRNAi*) probed with dLipin antibodies (Fig. 34).

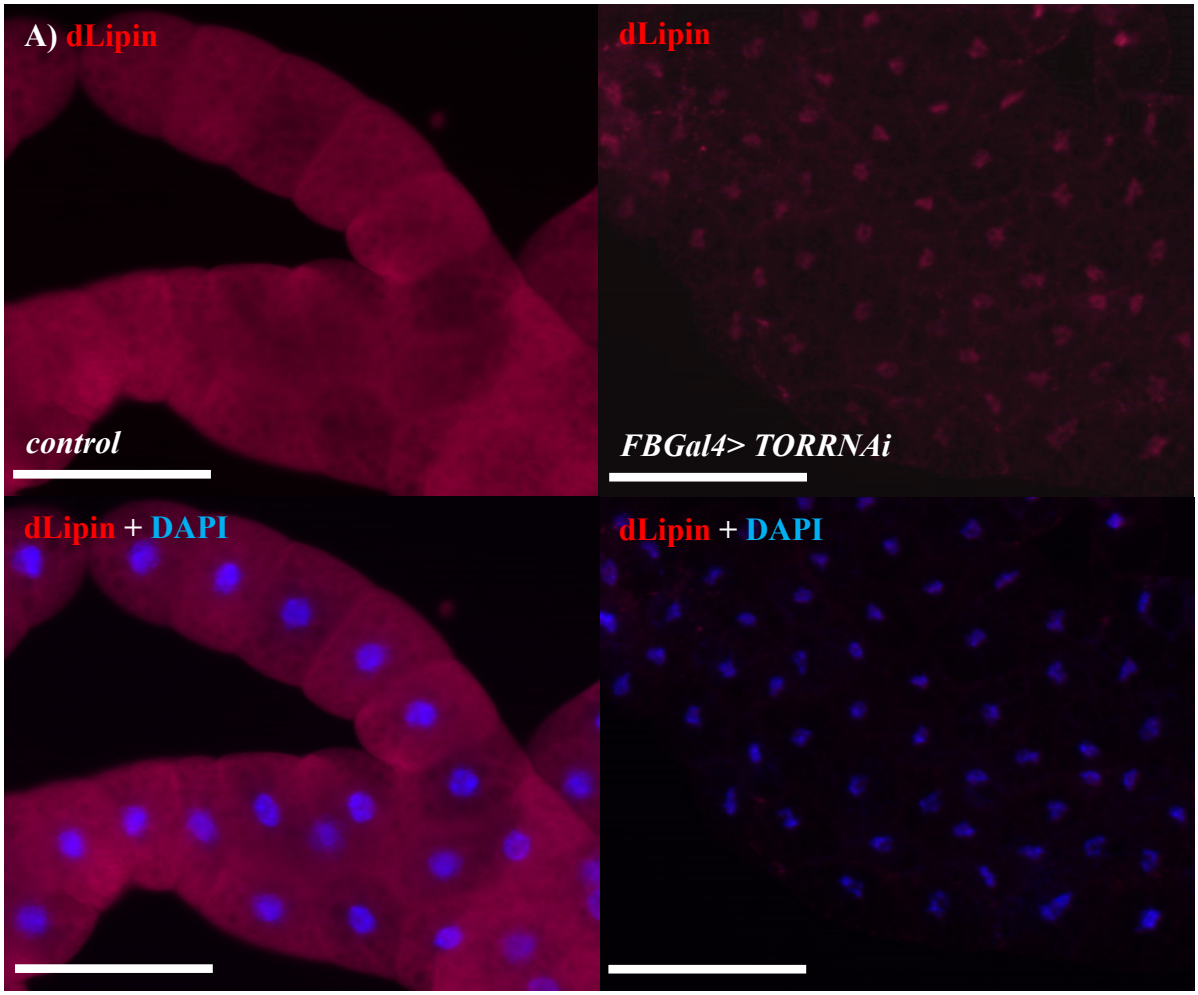
A) dLipin
dLipin
control
FBGal4> TORRNAi
dLipin + DAPI
dLipin + DAPI

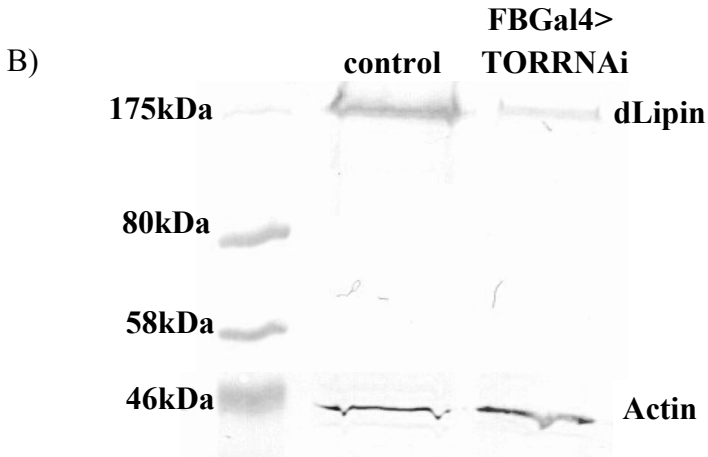
B)
control
FBGal4>
TORRNAi
175kDa
dLipin
80kDa
58kDa
46kDa
Actin

Fig. 34: *TOR* knockdown results in diminished levels of dLipin and translocation of dLipin into the nucleus in fat body tissue of third instar larvae. A) *TORRNAi* was expressed in the fat body (*FBGal4>TORRNAi*) and dLipin detected using dLipin antibody (red). Cells were counterstained with DAPI to visualize the nuclei. dLipin is noticeably more concentrated in the nuclei compared to the cytoplasm. Furthermore, dLipin levels seemed to be decreased compared to the control (w^{1118}). Scale Bar 100μm. B) Reduction of dLipin levels was also observed when western blot analysis was conducted with fat body tissue samples from control (w^{1118}) and experimental animals (*FBGal4>TORRNAi*). The blot was treated with dLipin antibody and Actin was used as a loading control.

Subcellular localization and total dLipin levels are indeed influenced by TOR activity. A reduction of TOR resulted in lowered dLipin levels and the residual dLipin translocated into the nucleus, leaving little dLipin in the cytoplasm. It is interesting to note that although dLipin levels were strongly reduced, fat droplet size appeared normal (data not shown). Cell size of fat body cells after *TOR* knockdown was smaller compared to cells from control animals, a known effect of TOR deficiency (Oldham et al., 2000).

A knockdown of TOR not only affects TORC1 but also TORC2, as TOR is an integral member of both complexes. To determine whether the effects observed were due to a loss of TORC1 or TORC2 activity, I studied the interaction of dLipin with *raptor* and *rictor*. Raptor is a member of TORC1 only, and Rictor only associates with TORC2 (Loewith and Hall, 2011). *raptor* and *rictor* were specifically downregulated using RNAi in the larval fat body, and fat body cells examined for dLipin levels and localization. I did not observe any altered phenotype after *rictor* knockdown. To determine if *rictorRNAi* was effective, I analyzed at S505 phosphoAKT levels in fat body cells expressing *rictorRNAi* and control cells. S505 phosphorylation is catalyzed by TORC2, which means that if *rictor* knockdown is efficient, AKT phosphorylation should be lowered. I was not able to detect an effect on AKT phosphorylation (data not shown). Thus, RNAi-mediated knockdown of *rictor* seemed to be inefficient. However,

raptor knockdown was effective as fat body cell size of animals expressing *raptorRNAi* was smaller. Next I examined the amount and distribution of dLipin protein in fat body tissue after *raptorRNAi* expression (Fig. 35).

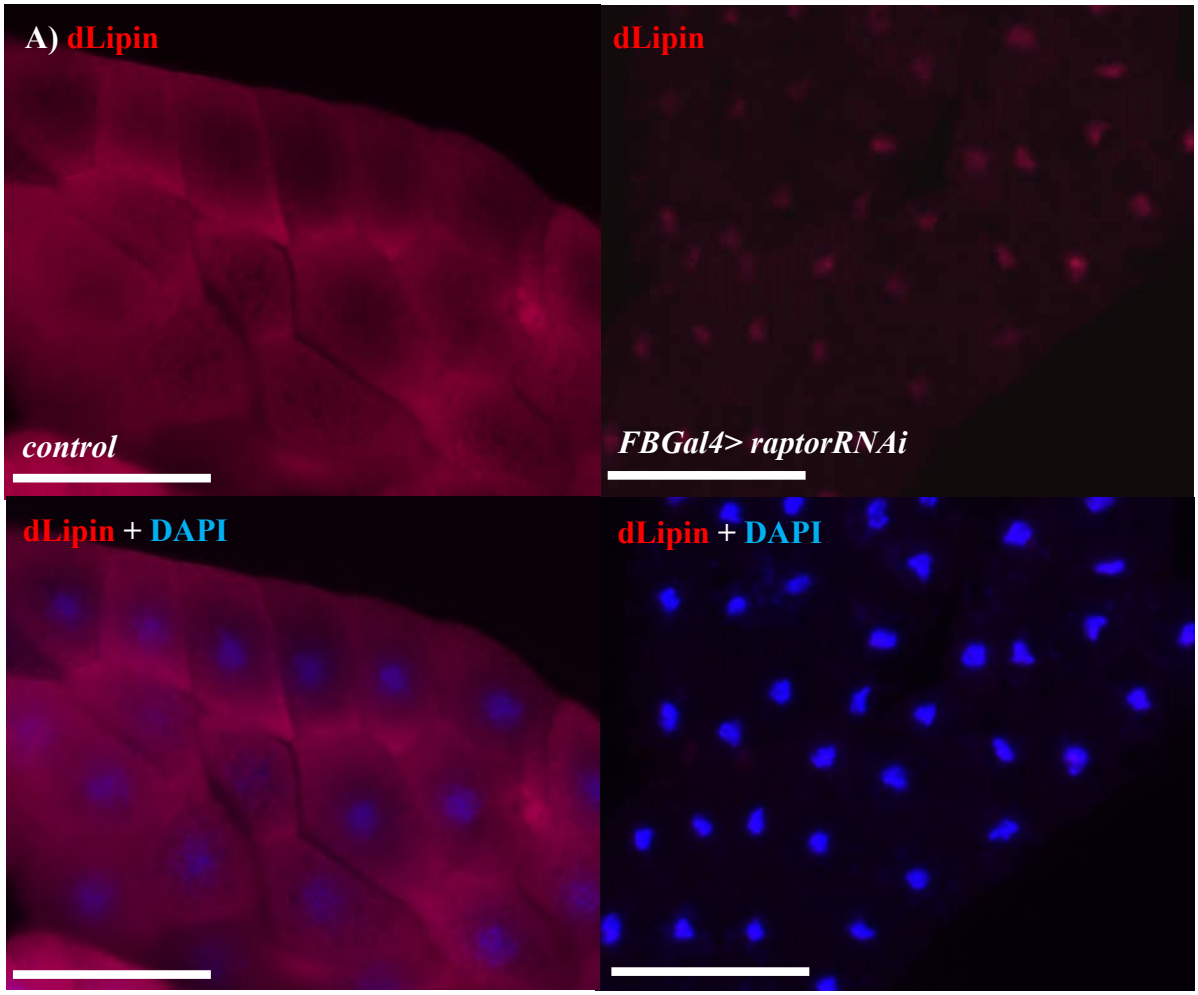

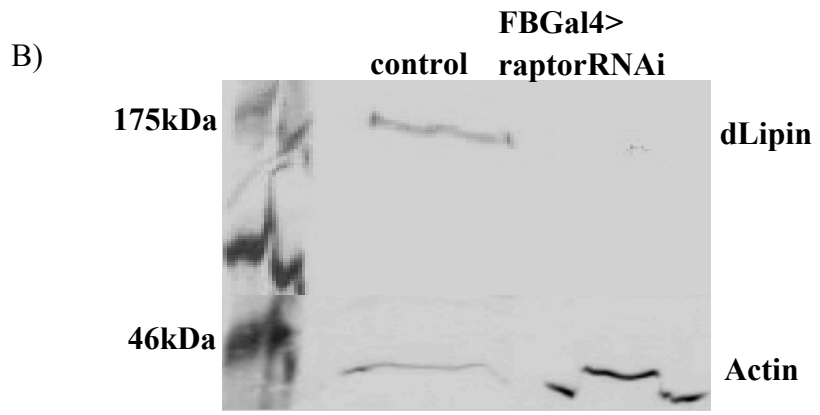

Fig. 35: *raptor* knockdown results in diminished levels of dLipin and translocation of dLipin into the nucleus of fat body cells of third instar larvae. A) *raptorRNAi* was expressed in the fat body (*FBGal4>raptorRNAi*) and dLipin detected using dLipin antibody (red). Cells were counterstained with DAPI to visualize the nuclei. dLipin was noticeably more concentrated in the nuclei compared to the cytoplasm. Furthermore, dLipin levels seemed to be decreased compared to control (w^{1118}). Scale Bar 100μm. B) Reduction of dLipin levels was also observed when western blot analysis was conducted with fat body tissue samples from control (w^{1118}) and experimental animals (*FBGal4>raptorRNAi*). The blot was incubated with dLipin antibody and actin was used as a loading control.

Comparing Fig. 34 and Fig. 35, it is clear that the effects of *raptor* and *TOR* knockdown were identical. It therefore appears that the phenotype observed after *TOR* knockdown is most likely caused by a decrease in TORC1 activity. This experiment thus linked dLipin activity and TORC1 signaling. Nuclear translocation of dLipin indicates an increased need for dLipin's nuclear function under conditions when TORC1 activity is low. In mammalian and yeast systems, it has been shown that Lipin acts as a transcriptional co-regulator (Donkor et al., 2009; Finck et al., 2006; Koh et al., 2008; Santos-Rosa et al., 2005). However, so far no nuclear function has been demonstrated for dLipin.

1.1. Binding of dLipin to polytene chomosomes

One way to determine whether dLipin is likely to affect transcriptional activity is by looking at the binding of dLipin to chromosomes. Therefore, I stained chromosomes of fat body and salivary gland cells with dLipin antibody. As salivary gland chromosomes go through more cycles of endoreplications, they contain a higher DNA content and are bigger and easier to stain than fat body chromosomes. Hence, I expressed *dLipin* in the salivary gland and tried to detect target loci of dLipin binding. To express dLipin in the salivary gland, I used a ubiquitous heat shock driver. I looked at chromosomes at different time points after heat shock induction to analyze binding at different titers of dLipin protein (Fig. 36).

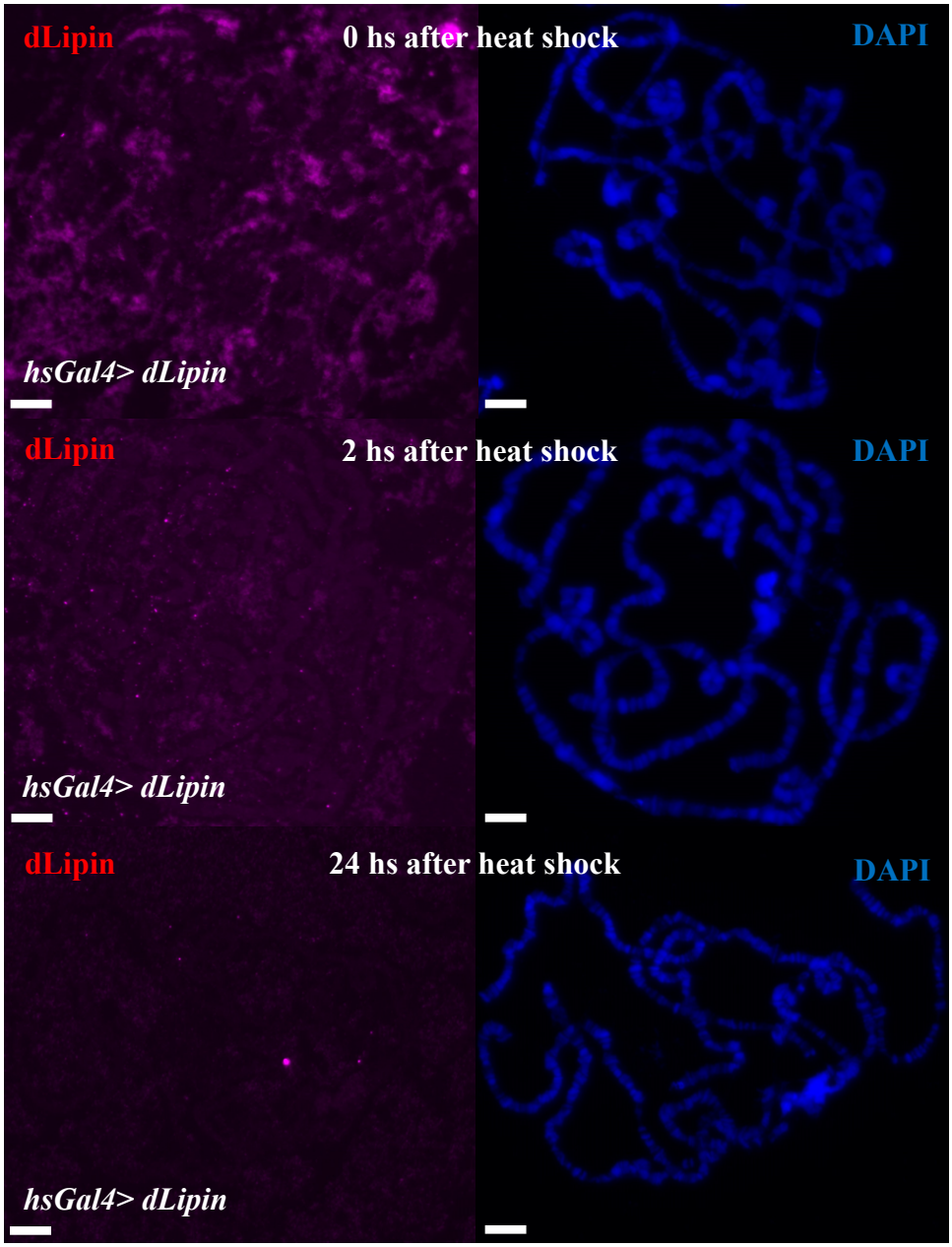

Fig. 36: Chromosome staining of salivary gland chromosomes does not reveal specific binding loci for dLipin. *dLipin* expression was induced by heat shock (*hsGal4>dLipin*), and salivary gland chromosomes were stained with dLipin antibody (purple). dLipin antibody staining was conducted immediately after heat shock treatment, 2 hours after heat shock and 24 hours after heat shock. DNA was stained with DAPI. No binding sites for dLipin were detected. Scale Bar 50μm.

I was not able to detect any specific signals on chromosomes for dLipin. Only background staining of the dLipin antibody was detected. As dLipin did not appear to bind to

salivary gland chromosomes, I proceeded with fat body chromosome staining. I prepared chromosome squashes with wild-type fat body chromosomes, and with fat body chromosomes from animals expressing *TORRNAi* (*FBGal4>TORRNAi*). I was not able to detect any specific loci of dLipin binding for any of the genotypes (data not shown).

To further elucidate the relationship between dLipin and TORC1, I conducted genetic interaction studies.

2. *dLipin* and *raptor* interact in larval development

I focused on *raptor* to test for a possible genetic interaction between TORC1 and dLipin. Raptor functions as an integral part of TORC1. Thus *raptor* knockdown will diminish TORC1 activity. I concomitantly expressed *dLipinRNAi* and *raptorRNAi* with *FBGal4,* thereby achieving a fat body-specific knockdown of both RNAi targets. I examined fat body morphology, PIP3 localization and larval development of both single and double-knockdown animals.

2.1. *raptor* and *dLipin* together regulate larval development

I noticed a strong decrease of larval size after *dLipin* and *raptor* double knockdown. *dLipin* knockdown animals behaved and looked like wild-type animals. Animals with only *raptor* knockdown showed a minor delay and slightly decreased larval size. Larvae pupariate 1-2 days later compared to *dLipin* knockdown animals. Raptor knockdown larvae develop into pupae that die before adult flies can eclose. Thus, knockdown of *raptor* leads to a developmental delay.

This developmental delay was further enhanced in animals with combined *dLipin* and *raptor* knockdown as they never entered the wandering stage and perished in the food between 8-12 days after egg deposition (AED) (Fig. 37). Larvae were translucent, which suggests that fat

body tissue was underdeveloped. Figure 37 documents the developmentof larvae of the different genotypes (Fig. 37).

Fig. 37: Fat body specific knockdown of *dLipin* and *raptor* together results in a developmental delay and larval lethality. Animals expressing *dLipinRNAi* develop normally (*FBGal4>dlipinRNAi*); animals with *raptorRNAi* are delayed by 1-2 days (*FBGal4> raptorRNAi*). This delay is further enhanced in animals with concomitant dLipin knockdown (*FBGal4>dLipinRNAi; raptorRNAi*). Animals displayed a slow growth rate, hence their diminutive body size. They never entered the wandering stage and never formed pupae. Animals were photographed 5 days AED.

Knockdown of *dLipin* in a *raptor* deficient background enhanced the developmental delay observed after *raptor* knockdown. A possible explanation for this is that dLipin activity is further reduced in animals with concomitant *dLipin*/*raptor* knockdown, leading to a severe fat body underdevelopment. As *dLipin* knockdown also results in a down regulation of insulin pathway activity, the developmental delay could alternatively be explained by reduced insulin pathway activity in *dLipin*/*raptor* knockdown animals. Another possibility is that further reduced TORC1 activity in animals with concomitant *raptor* and *dLipin* knockdown could have elicited the enhancement in developmental delay.

2.2. *dLipin* and *raptor* interaction affects fat body morphology

raptor knockdown led to a cellular growth defect that resulted in smaller fat body cells. Fat body cells continued to be smaller until pupariation, an indication that the smaller cell size resulted from a true growth defect rather than developmental delay. Insulin pathway activity following *raptor* knockdown appeared to be unaffected, as PIP3 membrane association was conserved. When combined with *dLipin* knockdown, fat body cell size was further reduced and PIP3 membrane association was no longer detectable (Fig. 38). The fat body seemed to be substantially underdeveloped. The fact that PIP3 synthesis was not reconstituted in animals with dLipin knockdown by concomitant *raptor* knockdown indicates that insulin resistance in animals with *dLipin* knockdown is not caused by TORC1 overactivation, as is the case in type2 diabetes.

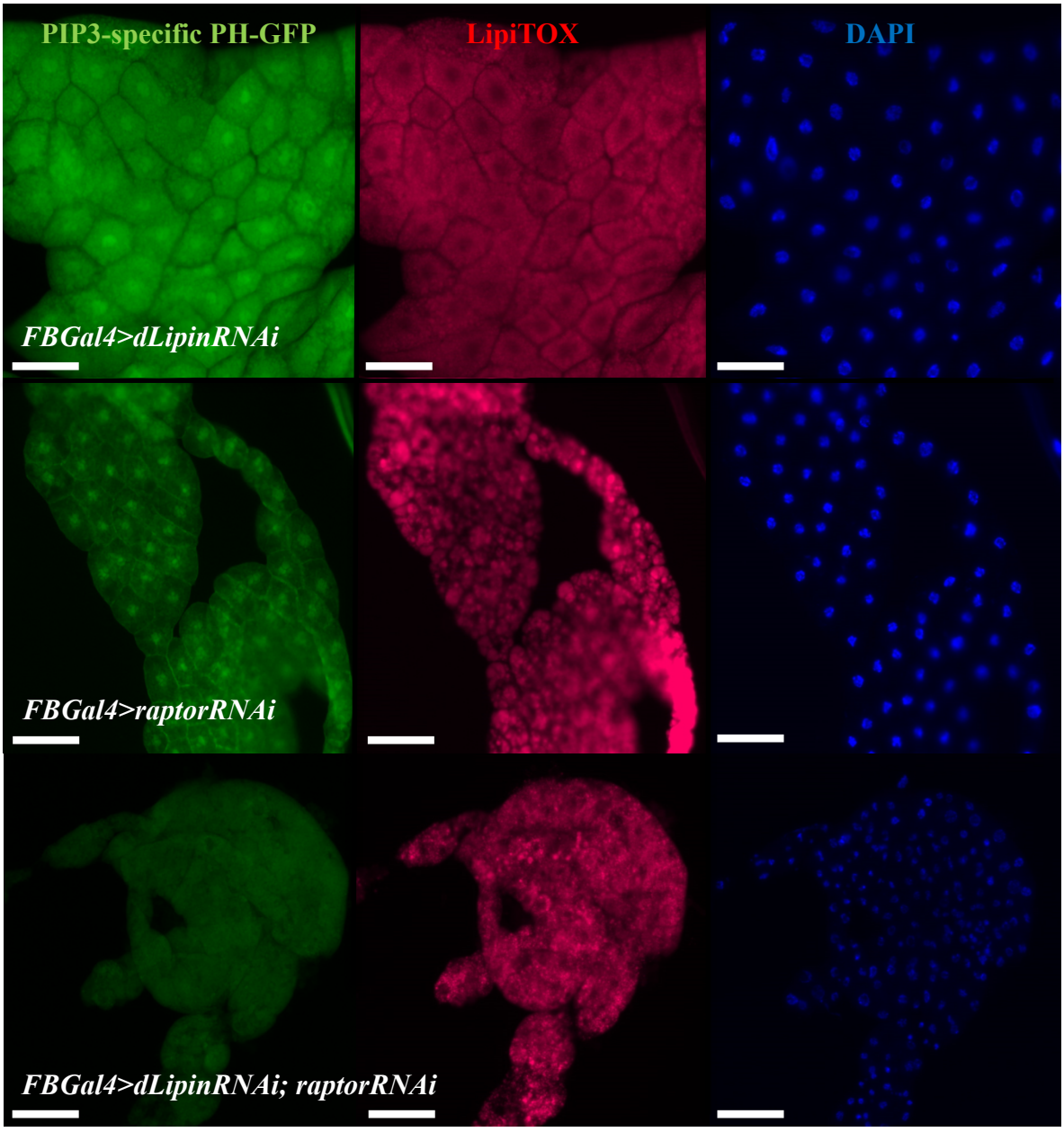

Fig. 38: Simultaneous *dLipin* and *raptor* knockdown affects fat body development. Fat body of larvae (5 days AED) was dissected and fat droplet morphology visualized by LipiTOX staining (red). PIP3 localization was determined by expression of the PIP3 reporter *tGPH* (green). DAPI was used to stain cell nuclei. The size of fat body cells from animals expressing *raptorRNAi* (*FBGal4>raptorRNAi*) is reduced when compared to *dLipin* knockdown alone (*FBGal4>dLipinRNAi*). This phenotype is strongly enhanced by concomitant loss of dLipin (*FBGal4>dLipinRNAi; raptorRNAi*). PIP3 localization is not altered after *raptor* knockdown, but *dLipin* knockdown as well as *dLipin* knockdown with concomitant *raptor* knockdown, showed a loss of PIP3 membrane association. Scale Bars: 100 μm.

To further document the decrease in cell size observed after *dLipin* knockdown with concomitant *raptor* knockdown, I measured cell area, nuclear area and nucleocytoplasmic ratio (Fig. 39).

A)

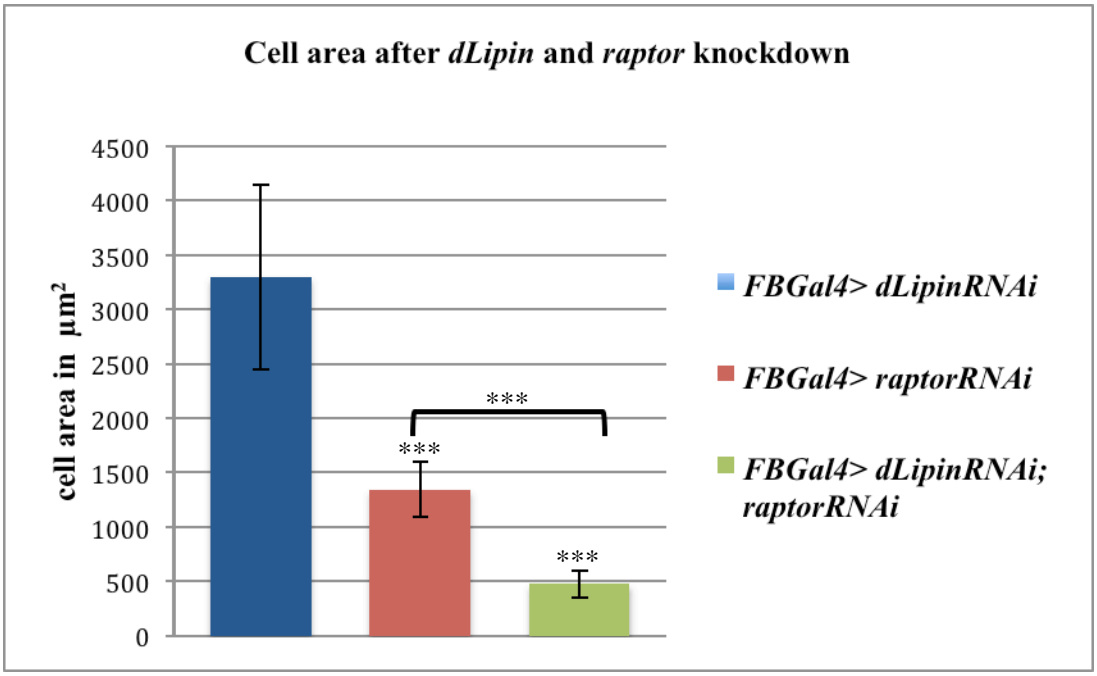

B)

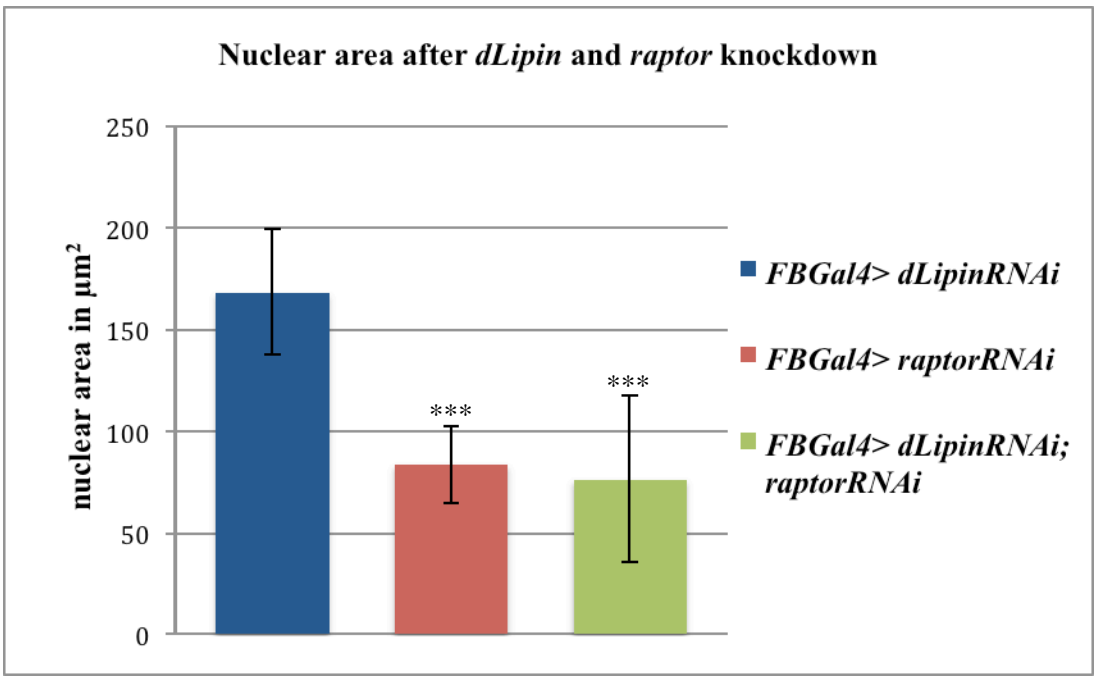

C)

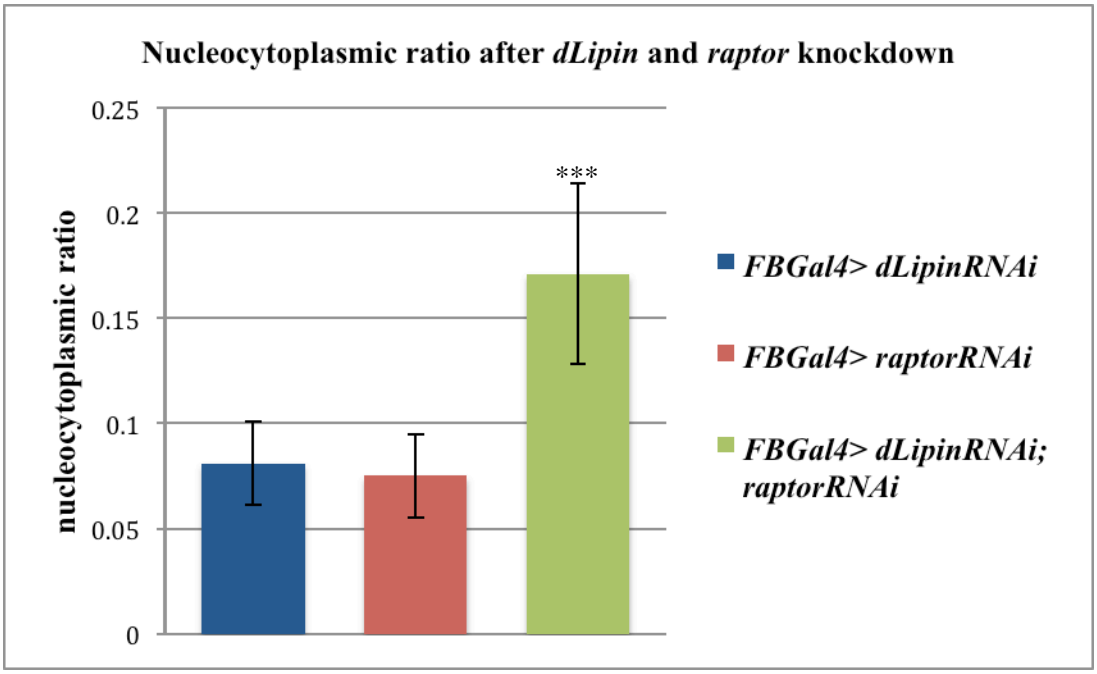

Fig. 39: Concomitant knockdown of *dLipin* and *raptor* in the fat body leads to diminished cell area and increased nucleocytoplasmic ratio. A) Cell area was measured in animals with *dLipin* knockdown (*FBGal4>dLipinRNAi*), animals with *raptor* knockdown (*FBGal4>raptorRNAi*) and animals carrying both knockdown transgenes (*FBGal4>dLipinRNAi; raptorRNAi*). Cell area of timed larvae was measured (5 days AED). Cell area after *raptor* knockdown is significantly reduced compared to *dLipin* knockdown cell area. When *dLipinRNAi* is introduced into *raptorRNAi* the growth deficit is significantly enhanced compared to *dLipinRNAi* as well as to *raptorRNAi* knockdown. This significance between *raptorRNAi* cell

size and *dLipinRNAi/raptorRNAi* cell size is indicated by the *** above the bracket. B) Nuclear area measured in animals with *dLipin* knockdown (*FBGal4> dLipinRNAi*), animals with *raptor* knockdown (*FBGal4> raptorRNAi*) and animals carrying both knockdown transgenes (*FBGal4> dLipinRNAi; raptorRNAi*). Nuclear area of timed larvae was measured (5 days AED). Nuclear area after *raptor* knockdown is significantly reduced compared to *dLipin* knockdown. This reduction in nuclear size is only slightly more pronounced after combining both *raptor* and *dLipin* knockdown, but no statistical difference was found. C) Nucleocytoplasmic ratio of timed larvae (5 days AED) was measured. The ratio was significantly increased after knockdown of *dLipin* in concert with *raptor*, whereas no significant difference could be found between the single knockdowns. Error bars indicate standard deviation. Unpaired t –Test, ∗∗∗P < 0.0001.

Fat body cell size of larvae (5 days AED) was reduced in animals with *raptor* knockdown; a phenotype further enhanced in animals with concomitant *dLipin* knockdown. Nuclear area of larvae with *raptor* knockdown in the fat body was also significantly smaller when compared to *dLipin* knockdown nuclei. Knocking down both *dLipin* and *raptor* did not significantly decrease nuclear size any further, but had a strong effect on cytoplasmic growth. This resulted in a strongly increased nucleocytoplasmic ratio of cells after concomitant *dLipin* and *raptor* knockdown. *raptor* knockdown, which affected cytoplasmic growth and DNA replication to the same extent, led to a proportional growth defect.

The data presented suggests that a concomitant reduction of dLipin and TORC1 activity strongly reduces cytoplasmic growth of cells, but not DNA replication. This effect might be caused by the reduced insulin pathway activity after *dLipin* knockdown in cells with concomitant *raptor* knockdown.

2.3. Interaction between *raptor* and *dLipin* is dependent on the PAP activity of dLipin, but not the co-regulator activity

As mentioned before, dLipin has the ability to act in two different ways, as a PAP enzyme and a co-regulator of transcription. To determine whether it was indeed the loss of dLipin's PAP activity or its co-regulator activity that resulted in enhanced developmental delay and reduced cytoplasmic growth in animals with concomitant *dLipin* and *raptor* knockdown, I co-expressed *WTdLipin*, *ΔNLSdLipin* or *ΔPAPdLipin* with *dLipinRNAi* and *raptorRNAi* in the fat body and examined developmental delay and fat body cell size.

2.3.1. dLipin is no longer detectable in the nucleus after concomitant *raptor*/*dLipin* knockdown

As shown before (Fig. 35), dLipin migrates into the nucleus upon *raptor* knockdown. Thus, a loss of nuclear activity of dLipin in *dLipin*/*raptor* double knockdown animals might explain the enhanced phenotype. To test this, I first determined that indeed no dLipin is present in nuclei of animals with simultaneous *dLipin/raptor* knockdown. Nuclear localization of dLipin was greatly reduced in animals with concomitant reduction of dLipin and Raptor activity (Fig. 40).

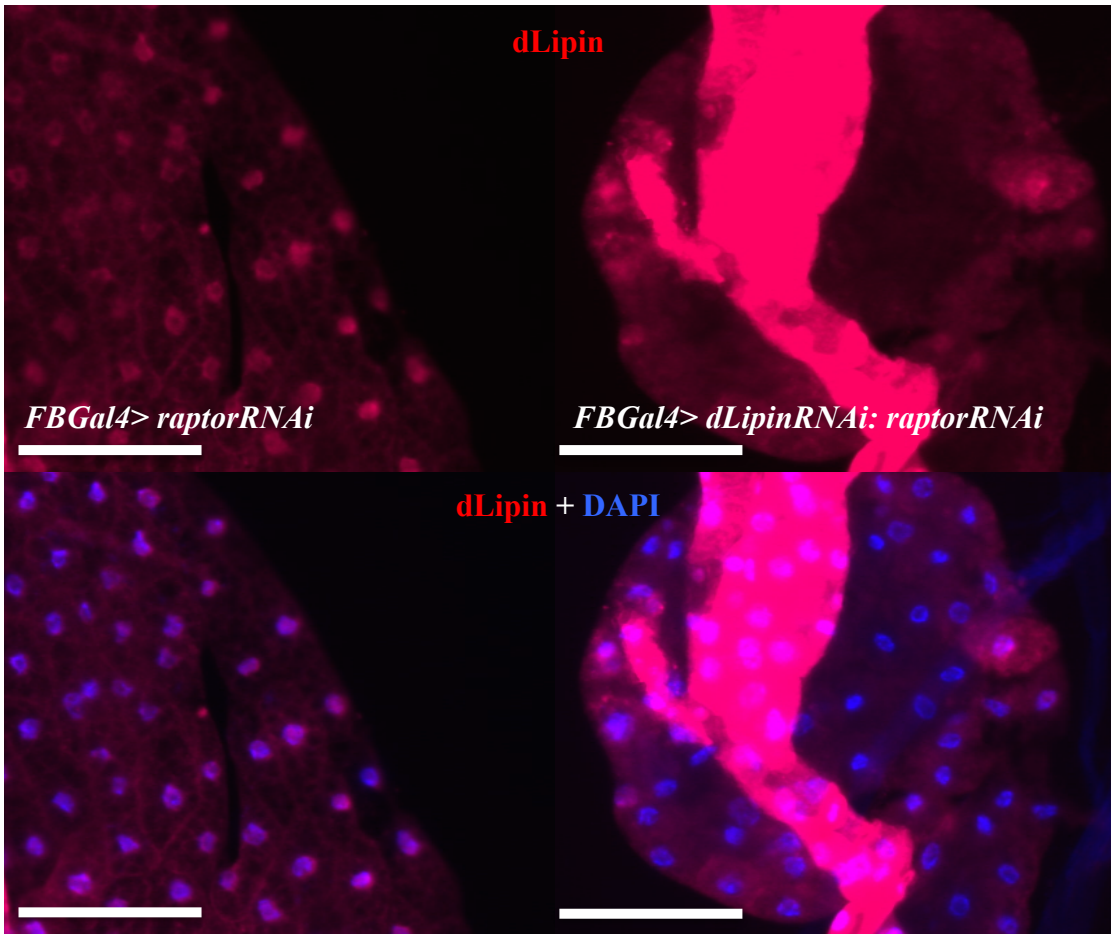

Fig. 40: dLipin is reduced in the nucleus after concomitant knockdown of *dLipin* and *raptor*. *dLipin* was detected using dLipin antibody in fat body of feeding third instar larvae. Larvae either expressed only *raptorRNAi* (*FBGal4>raptorRNAi*), or only *raptorRNAi* as well as *dLipinRNAi* (*FBGal4>dLipinRNAi; raptorRNAi*) in the fat body. After *raptor* knockdown, dLipin was concentrated in the nucleus. This nuclear concentration of dLipin was no longer present in most cells after simultaneous knockdown of *dLipin* and *raptor*. dLipin appears red and nuclei are stained with DAPI and appear blue. Scale Bar: 100μm.

2.3.2. PAP activity mediates the *raptor*/*dLipin* interaction in larval development

To test whether the deficit in nuclear activity of dLipin is responsible for the growth rate defect observed after simultaneous *dLipin*/*raptor* knockdown or whether a reduction in PAP activity causes the developmental delay, I tried to rescue larvae with *dLipin*/*raptor* knockdown by individually expressing *WTdLipin*, *ΔNLSdLipin* and *ΔPAPdLipin* in the fat body of these animals. I timed the larvae and looked at the morphology of whole larvae 5 days AED.

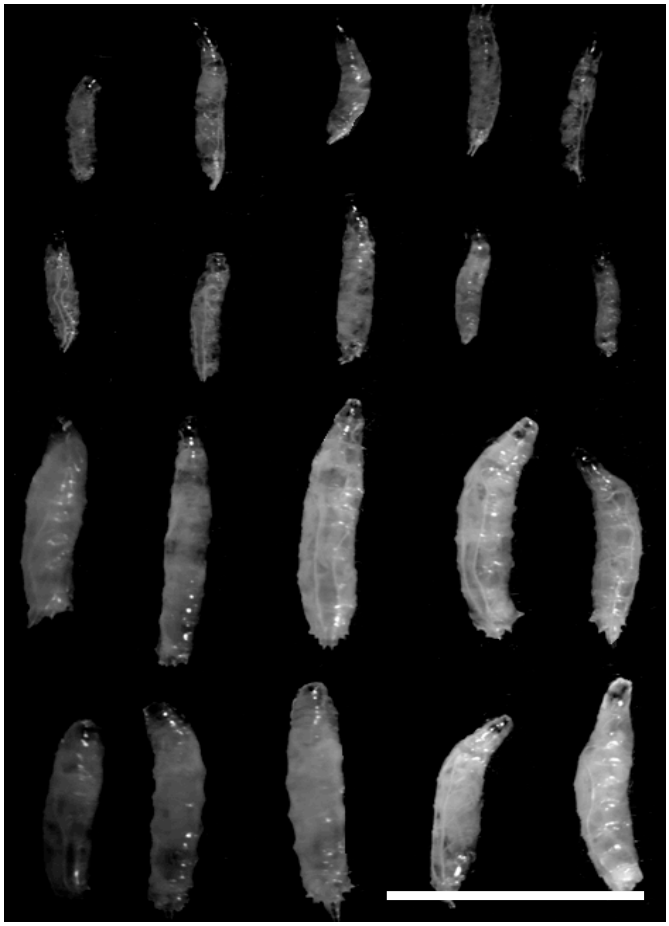

Fig. 41: Developmental delay caused by simultaneous *raptor*/*dLipin* knockdown can be rescued by expression of *WTdLipin* and *ΔNLSdLipin*, but not *ΔPAPdLipin*. Concomitant knockdown of *dLipin* and *raptor* in the fat body resulted in a severe developmental delay. This delay can be reversed by expression of *WTdLipin* and *ΔNLSdLipin*. Larval size was significantly bigger when compared to *dLipin/raptor* double knockdown animals. Expression of dLipin lacking PAP activity, *ΔPAPdLipin,* was not able to reverse the developmental delay. Larvae were timed and pictures taken 5 days AED.

The enhanced developmental delay observed after simultaneous knockdown of *dLipin* and *raptor* in the fat body was reversed after expression of *WTdLipin* and *ΔNLSdLipin*. Larval size was significantly increased in these animals and animals underwent pupariation. However, expression of *ΔPAPdLipin* did not rescue the enhanced developmental delay. Larval size was the same as after the *dLipin*/*raptor* knockdown. This suggests that loss of PAP activity was responsible for the severe developmental delay observed after *dLipin/raptor* double knockdown.

2.3.3. PAP activity mediates the *raptor*/*dLipin* interaction with regard to fat body development

To verify that loss of PAP activity is responsible for the enhanced cell growth defect after concomitant *dLipin*/*raptor* knockdown, I expressed *WTdLipin*, *ΔNLSdLipin* and *ΔPAPdLipin* in *raptor/dLipin* double knockdown animals. Furthermore, distance between neighboring nuclei was measured as an estimate for cell size. It was not possible to measure cellular area directly, as cell boundaries were not visible in animals with *FBGal4>dLipinRNAi; raptorRNAi* and *FBGal4>dLipinRNAi; raptorRNAi*/*ΔPAPdLipin* genotypes.

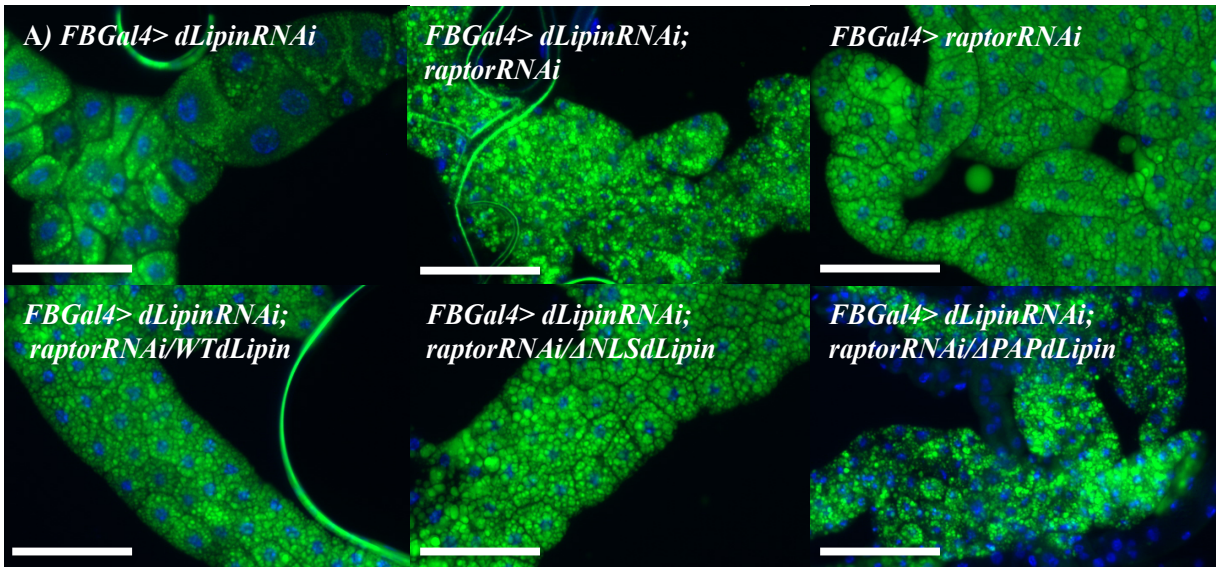

B)

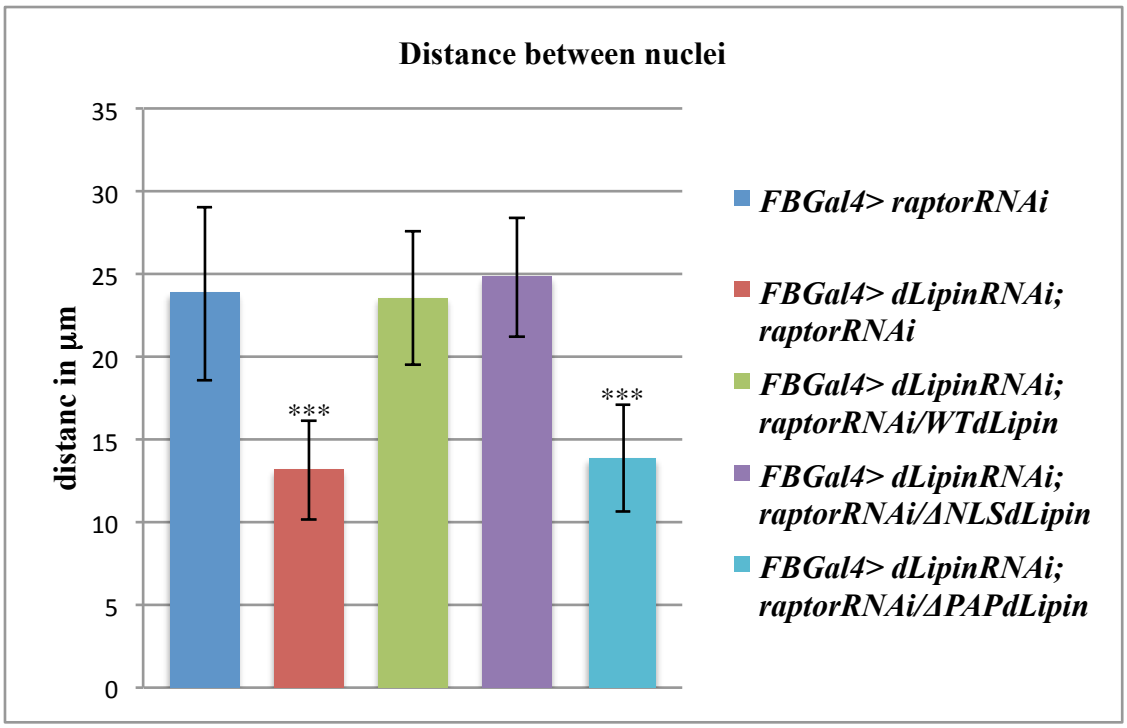

Fig. 42: Fat body cell size of larvae with *dLipin* and *raptor* knockdown is rescued by expression of *WTdLipin* and *ΔNLSdLipin*, but not *ΔPAPdLipin*. A) Expression of *raptorRNAi* in the fat body resulted in a growth defect reflected by smaller cell size. *dLipin* knockdown in the fat body did not cause growth defects. When combining *dLipin* and *raptor* knockdown in the fat body, cell size was further decreased. Expression of *WTdLipin* and *ΔNLSdLipin*, but not *ΔPAPdLipin* increased cell size significantly. Larvae were timed (5 days AED) and fat body tissue stained with Bodipy (green) to visualize fat droplets, and DAPI (blue) to visualize cell nuclei. Scale Bar: 100µm. B) When expressing *WTdLipin* or *ΔNLSdLipin* in *dLipin*/*raptor* knockdown fat body cells, the reduction in cell size after double knockdown was no longer present. Instead, cells were the same size as *raptor* knockdown cells. Expression of *ΔPAPdLipin* did not rescue the growth defect. Error bars reflect SD. Unpaired t –Test, *** $p < 0.0001$.

Reduced size of fat body cells observed after *raptor* knockdown was enhanced by concomitant *dLipin* knockdown. This was no longer the case when either *WTdLipin* or *ΔNLSdLipin* were expressed in the knockdown animals. Thus, WTdLipin and ΔNLSdLipin were capable of rescuing the enhancement. However, they were not able to compensate for the loss of *raptor* activity, as cell size after *WTdLipin* and *ΔNLSdLipin* expression was not significantly increased compared to cell size after *raptor* knockdown alone.

The observation that expression of *WTdLipin* and *ΔNLSdLipin*, but not *ΔPAPdLipin*, can abolish the enhancement of fat body defects strongly suggests that loss of PAP activity, but not of the transcriptional co-regulator activity of dLipin caused a cytoplasmic growth defect in animals with concomitant *raptor* knockdown.

3. Overactivation of TOR activity in the fat body

I pursued two approaches to determine whether elevated TOR activity can rescue phenotypes observed after *dLipin* knockdown. First, I tried to activate TOR in the larval fat body of animals with *dLipin* knockdown by simultaneously knocking down both *Tsc1* and *Tsc2*. Both Tsc1 and Tsc2 function as inhibitors of TORC1 activity. Thus, downregulation of *Tsc1* and *Tsc2* should activate TORC1 signaling. Unfortunately, I was not able to observe any effect of *Tsc1* and *Tsc2* knockdown alone on cell morphology. TORC1 overactivation should result in cell overgrowth. Hence, efficient *Tsc1* or *Tsc2* knockdown should have resulted in cell overgrowth. However, I was not able to detect any growth effects. Second, I tried to activate TOR by overexpressing the TORC1 activator *Rheb* in animals of the genotype *FBGal4/dLipinRNAi; Rheb/InR*$^{dom.neg}$. Expression of *Rheb* alone did not lead to any discernible growth effect in fat body tissue. Hence, expression of *Rheb* was not able to activate TORC1.

I was not able to achieve TORC1 activation either by knocking down its inhibitors or activating its activators.

4. dLipin deficiency does not affect TORC1 activity

At this point I had established that a strong interaction exists between dLipin and TORC1 (Raptor). I was able to show that dLipin protein level and dLipin's subcellular localization

depend on TORC1 activity and that a reduction of dLipin's PAP activity in a *raptor*-deficient background strongly enhances developmental delay and cell growth defects.

The enhancement of the *raptor* phenotype could result from a further decrease of TORC1 activity following *dLipin* knockdown. To measure TORC1 activity, I assayed phosphorylation levels of the TOR target 4EBP1 an inhibitor of translation (Hara et. al., 1997). 4EBP1 phosphorylation deactivates 4EBP1 and thereby promotes translational activity. 4EBP1 phosphorylation levels of fat body cells were examined after knockdown of *dLipin* and compared to control sample. Antibodies for pan4EBP1 and phospho4EBP1 were used in this western blot.

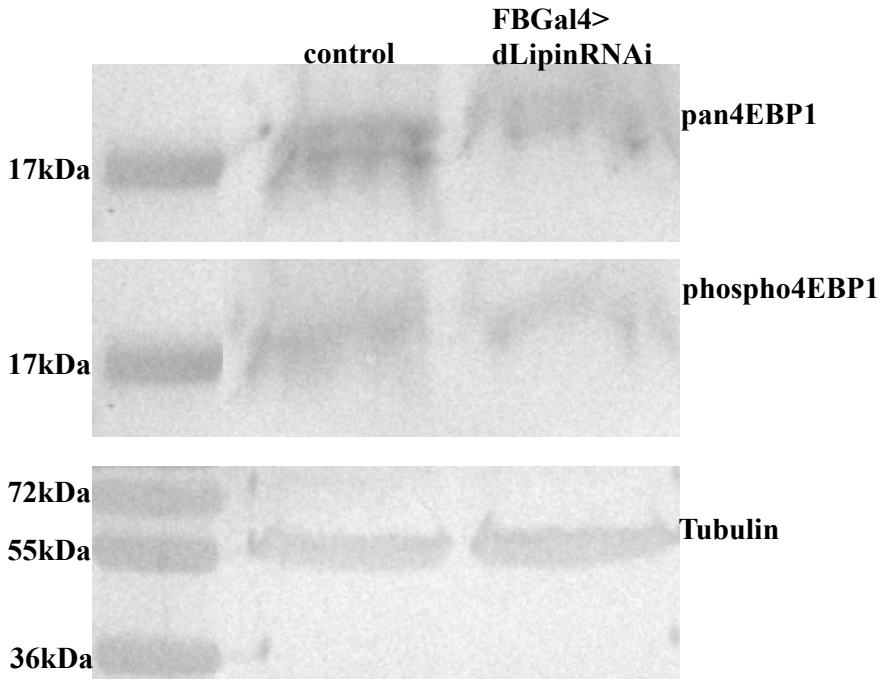

Fig. 43: *dLipin* knockdown does not reduce 4EBP1 phosphorylation levels. Western blot analysis was performed with fat body samples from feeding third instar larvae. The membranes were probed either with antibodies for phospho4EBP1 or pan4EBP1. Samples from animals with dLipin knockdown in the fat body (*FBGal4>dLipinRNAi*) were compared to samples from control animals carrying only the Gal4 transgene (*FBGal4*). Tubulin was used as a loading control.

Western analysis revealed that *dLipinRNAi* expression did not reduce TORC1 activity. 4EBP phosphorylation levels in the fat body of experimental and control animals were similar. *raptor* knockdown alone led to a complete loss of 4EBP1 phosphorylation (data not shown). This made it impossible to look into a possible enhancement of the effect of reduced Raptor activity on 4EBP1 phosphorylation by concomitant knockdown of *dLipin*.

Thus, the enhancement of cell growth defects and organismal developmental delay observed after *dLipin* knockdown in *raptor*-deficient background may not be due to a further decrease of TORC1 activity in these animals.

5. Summary of part C Results

I discovered a strong genetic interaction between *dLipin* and *raptor* during larval and fat body development. This interaction appeared to influence fat body cell size and larval growth and it required the PAP activity of dLipin. I furthermore showed that Raptor, and therefore TORC1, regulates not only dLipin abundance, but also its subcellular localization. This indicates that dLipin activity is regulated by TORC1 and therefore, is subject to control by nutrient signaling.

D. Experiments not directly linked to insulin or TOR signaling

1. dLipin's subcellular localization is not influenced by intracellular dLipin levels

When looking at dLipin distribution within fat body cells, I discovered that knockdown of insulin pathway activity via expression of *PI3K21BHA*, and knockdown of TORC1 pathway activity via expression of *raptorRNAi* each resulted in a reduction of dLipin levels. At the same time, reducing TORC1 activity led to translocation of dLipin into the nucleus whereas reducing insulin pathway activity did not affect dLipin localization. One possible explanation for this

difference could be that intracellular dLipin levels influence its distribution. it could be that dLipin only navigates into the nucleus after knockdown of TORC1 activity because dLipin levels are lower in these cells than in cells with a reduction in PI3K21B activity.

To address this possibility, I determined the amount of dLipin protein in samples from fat body of feeding third instar larvae expressing either *PI3K21BHA* (dominant negative form of PI3K21B) or *raptorRNAi* by western blot analysis.

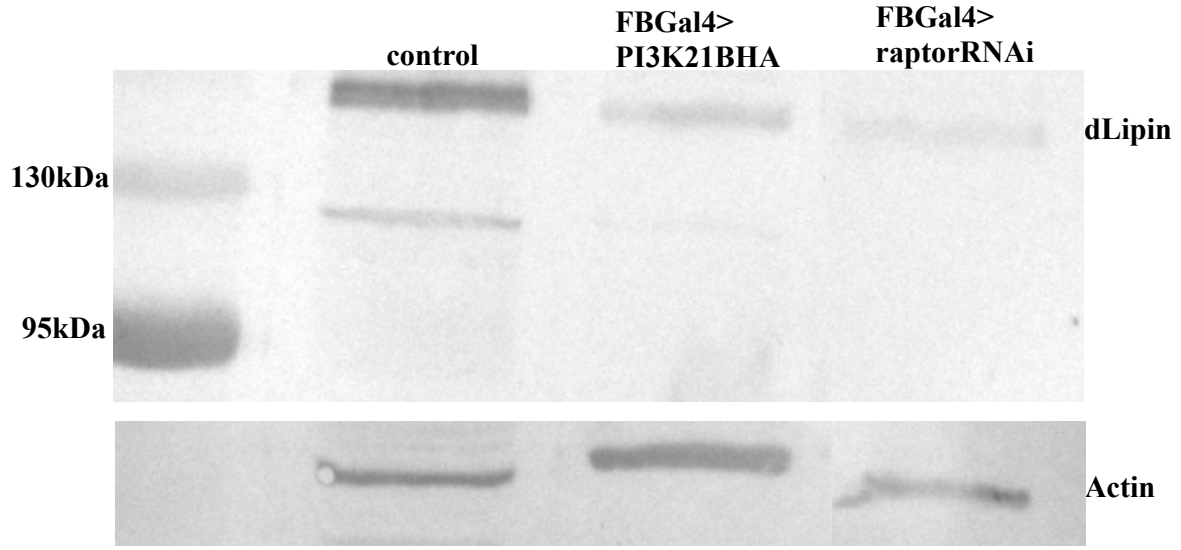

Fig. 44: dLipin levels are similar after knockdown of *raptor* and expression of *PI3K21BHA*. To determine whether more dLipin is present after *PI3K21BHA* (*FBGal4>PI3K21BHA*) expression compared to *raptorRNAi* (*FBGal4>raptorRNAi*) expression, I conducted a western blot analysis with dLipin antibodies. Control sample was from w^{1118} animals. Fat body was from wandering third instar larvae. Actin served as a loading control.

The western analysis showed that dLipin levels were comparably low after *PI3K21BHA* expression and *raptor* knockdown. This indicates that differences in subcellular localization following *PI3K21BHA* expression and *raptor* knockdown were not caused by differences in intracellular dLipin levels.

2. Generation of donor fly lines for ends-in-targeting gene replacement

In order to study the two different dLipin functions, PAP activity and transcriptional co-regulator activity, I attempted to create fly lines in which the endogenous *dLipin* gene was replaced by a *dLipin* gene with a mutation that either interferes with PAP activity or co-regulator activity. In theory, this would allow us to determine the direct effects of loss of either dLipin activity on metabolism and development. A fly strain carrying the *dLipin* gene with a mutation in the PAP motif was successfully generated. This fly line proved to be homozygous lethal, which showed that the PAP function of dLipin is essential for survival. Characterization of this fly line was performd by Qiuyu Chen and is described elsewhere (Qiuyu Chen, Investigation of Nuclear and Cytoplasmic Functions of the dLipin Protein of Drosophila Melanogaster, Masters Thesis, 2014).

The ends-in-targeting gene replacement method (Rong and Golic; 2000) was chosen to generate flies with a replacement of endogenous *dLipin* with either *ΔPAPdLipin* or *ΔNLSdLipin*. This method employs a two-step approach. First, a mutated copy of the targeted gene is introduced in the genome, and second, part of the endogenous gene is replaced with the mutated copy, which leaves only one (mutated) copy of the gene in the genome.

I participated in the mutagenesis experiment by creating transgenic donor fly lines that carry both the endogenous *dLipin* gene and the donor construct with the mutant copy of *dLipin*. *dLipinΔPAP* and *dLipinΔNLS* donor constructs were inserted into the genome by P-element transformation. Each construct contained two flanking FRT sites, an I-CreI-recognition site as well as an I-SceI recognition site. The fly lines carrying either of these constructs within their genomes are called donor stocks.

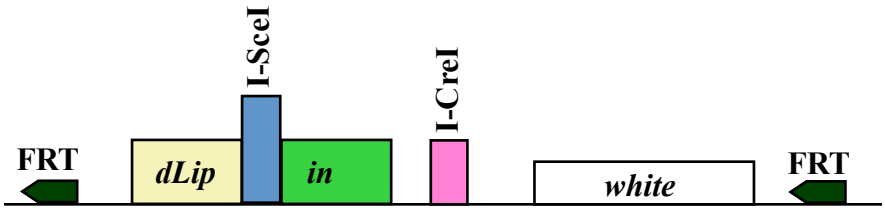

Fig. 45: Depiction of donor constructs. FRT sites are flanking the construct. The mutated *dLipin* gene carried either the NLS deletion or nucleotide change in the PAP motif. The I-SceI site is located in the middle of the *dLipin* gene. The construct further contains the I-CreI recognition site and the *white* marker gene.

After I had created the two donor stocks, I handed them over to fellow graduate student Qiuyu Chen. She continued the mutagenesis experiment that was meant to provide *dLipin* mutants for both of our projects. For the sake of completeness, I will shortly explain the steps she took to obtain the mutants. First, the donor line was crossed with flies expressing FLP recombinase and I-SceI endonuclease. This leads to the excision of the construct at the FRT sites and induces a double strand break at the I-SceI site. The double strand break triggers homologous recombination between the endogenous *dLipin* gene and the mutated version. Homologous recombination results in a duplication of the *dLipin* gene, with the mutated and the endogenous copy lying next to each other, separated by the *white* gene and I-CreI site. To remove one copy of the *dLipin* gene, flies were crossed with flies expressing the I-CreI recombinase. This resulted in another homologous recombination step that left only one copy of the *dLipin* gene in the genome. Flies were then examined to see if they contain the mutated *dLipin* gene or the wild-type *dLipi*n gene by PCR. Qiuyu Chen was able to generate a fly line in which *dLipin* carried the mutation in its PAP active site. She did not obtain a fly line in which the endogenous *dLipin* was replaced by *dLipin* lacking its NLS.

3. Ecdysone treatment rescues the dominant negative effect of *ΔNLSdLipin* expression on larval development and lethality

While carrying out experiments with the *ΔNLSdLipin* construct, I observed that strong ubiquitous overexpression of *ΔNLSdLipin* with the Tubulin driver (*TubGal4>dLipinΔNLS*) resulted in developmental delay and larval lethality. As fat body morphology of these animals looked normal (data not shown), developmental delay and larval lethality were likely caused by a defect in another tissue. As already shown (Fig. 27), like *dLipinΔPAP* overexpression, *dLipinΔNLS* overexpression had a dominant negative effect leading to the exclusion of endogenous dLipin from the nucleus. A potential tissue in which a complete loss of dLipin's nuclear activity could cause developmental effects is the ring gland. Ugrankar *et al*. (2011) showed that dLipin is abundantly present in ring gland tissue of third instar larvae. The prothoracic gland, which is part of the ring gland, is the primary location of ecdysone synthesis and release. Ecdysone is then converted into the steroid hormone 20-hydroxyecdysone (20HE) in peripheral tissues. This steroid hormone controls developmental progression from embryogenesis to adult development. 20-HE binds to the Ecdysone Receptor (EcR), which is a nuclear receptor that regulates expression of ecdysone-responsive genes as part of a heterodimeric complex with Ultraspiracle (Usp) (Yamanaka et al., 2013).

To test whether expression of *ΔNLSdLipin* affects ecdysone synthesis or release, I fed larvae that ubiquitously expressed *ΔNLSdLipin* with food containing 20-HE. I let animals develop on food with or without 20-HE and compared larval development and lethality. I examined animals with expression of *dLipinΔNLS* (*TubGal4>dLipinΔNLS*) as well as animals only carrying the *dLipinΔNLS* transgene but no driver (control). Both genotypes arose from the

same cross. Therefore, I was able to directly compare the number of pupae formed and developmental delay of these two genotypes.

A)

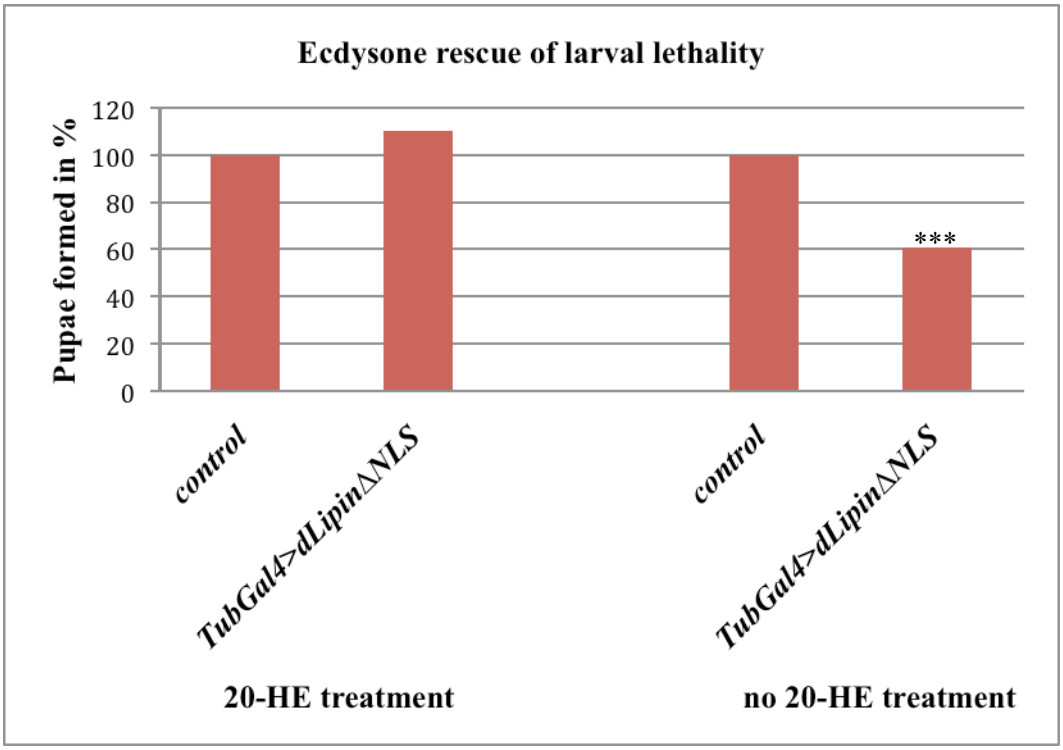

B)

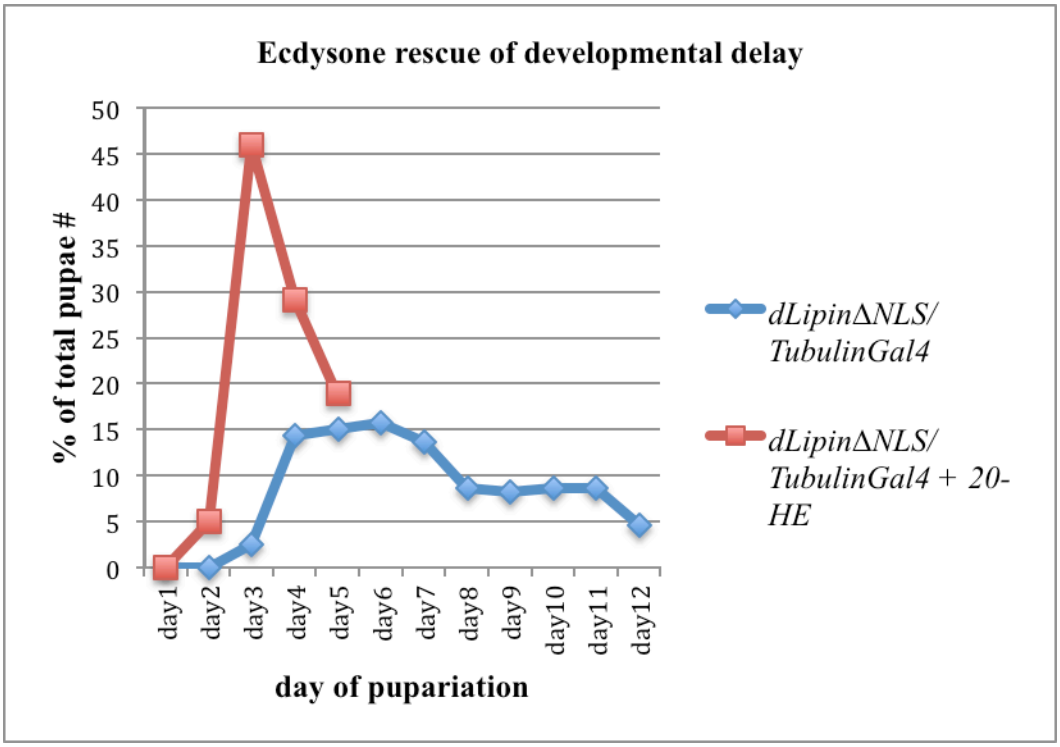

Fig. 46: 20-HE treatment can rescue larval lethality and developmental delay caused by a *dLipinΔNLS* overexpression. A) Feeding 20-HE to larvae expressing *dLipinΔNLS* driven by TubGal4 strongly reduced the larval lethality normally observed in animals with *dLipinΔNLS* overexpression. No statistically significant difference between numbers of pupae was found when experimental animals (*TubGal4>dLipinΔNLS*) were compared to control animals (only *dLipinΔNLS,* no driver transgene). Without 20-HE treatment significantly fewer experimental animals reached the pupal stage compared to control animals. Two tailed Chi-Square Test, *** p= 0.0001. B) Developmental delay of animals that overexpress *dLipinΔNLS* was rescued by 20HE treatment. The majority of larvae reached the pupal stage earlier when fed 20-HE. Newly formed pupae/prepupae were counted and plotted as percent of total number of pupae formed. Day 1 represents the day of first puparium formation.

20-HE treatment rescued the developmental delay and larval lethality observed after *ΔNLSdLipin* overexpression. This points to a defect in either ecdysone synthesis or ecdysone release in larvae with *ΔNLSdLipin* overexpression. To further confirm this result, I tried to rescue developmental delay and larval lethality of transheterozygous *dLipin* mutants (*dLipin*^{e00680}/ *Df(3R)Exel7095*) (Ugrankar et. al., 2011) by feeding 20-HE to these animals. However, 20-HE

treatment had no rescue effect on *dLipin*^{e00680}*/Df(3R)Exel7095* mutants (data not shown). This indicates that providing 20-HE alone cannot overcome the severe developmental delay in transheterozygous *dLipin* mutant animals. The may be due to the severe underdevelopment of the fat body that characterizes these animals, in contrast to animals that overexpress *ΔNLSdLipin,* which have a fat body that appears normal.

4. Expression of human *lipin* homologs can rescue larval lethality of transheterozygous *dLipin* mutants

dLipin has 3 homologous genes in *Homo sapiens*, *lipin1*, *lipin2* and *lipin3*. The three paralogs have diverged over time and display different spatial expression patterns (Donkor et al., 2007). To test whether the three human lipin genes can compensate for loss of *dLipin* in *Drosophila*, or whether one or more of these genes diverged to where they have lost this ability, I expressed *lipin1*, *lipin2* and *lipin3* in transheterozygous *dLipin* mutants (*dLipin*^{e00680}*/Df(3R)Exel7095*).

An important aspect of this experiment is the assessment to what degree results attained in *Drosophila* can be translated to mammalian systems. If *lipin1*, *lipin2* and *lipin3* retained known *dLipin* functions, it is more likely that they will affect fat metabolism and diabetes in a way similar to *dLipin*, and results gathered in *Drosophila* can be extrapolated, at least to a certain degree, to lipin function(s) in mammals.

As described in Ugrankar et al. (2011) many *dLipin* transheterozygous mutant animals die during larval development, with only 23 % reaching the wandering stage, and only very few of these successfully pupariate. Therefore, to assess the rescue effects of *lipin1*, *lipin2* and *lipin3* expression, I examined the number of pupae formed. Both control genotype

(*dLipin*^{e00680}*/Df(3R)Exel7095*; either lipin transgene alone) and either experimental genotype (*dLipin*^{e00680}*/Df(3R)Exel7095; Gal4/lipin1, dLipin*^{e00680}*/Df(3R)Exel7095; Gal4/lipin2, dLipin*^{e00680}*/Df(3R)Exel7095; Gal4/lipin3)* arose from the same cross, which allowed me to directly compare genotypes with regard to the number of pupae formed.

A)

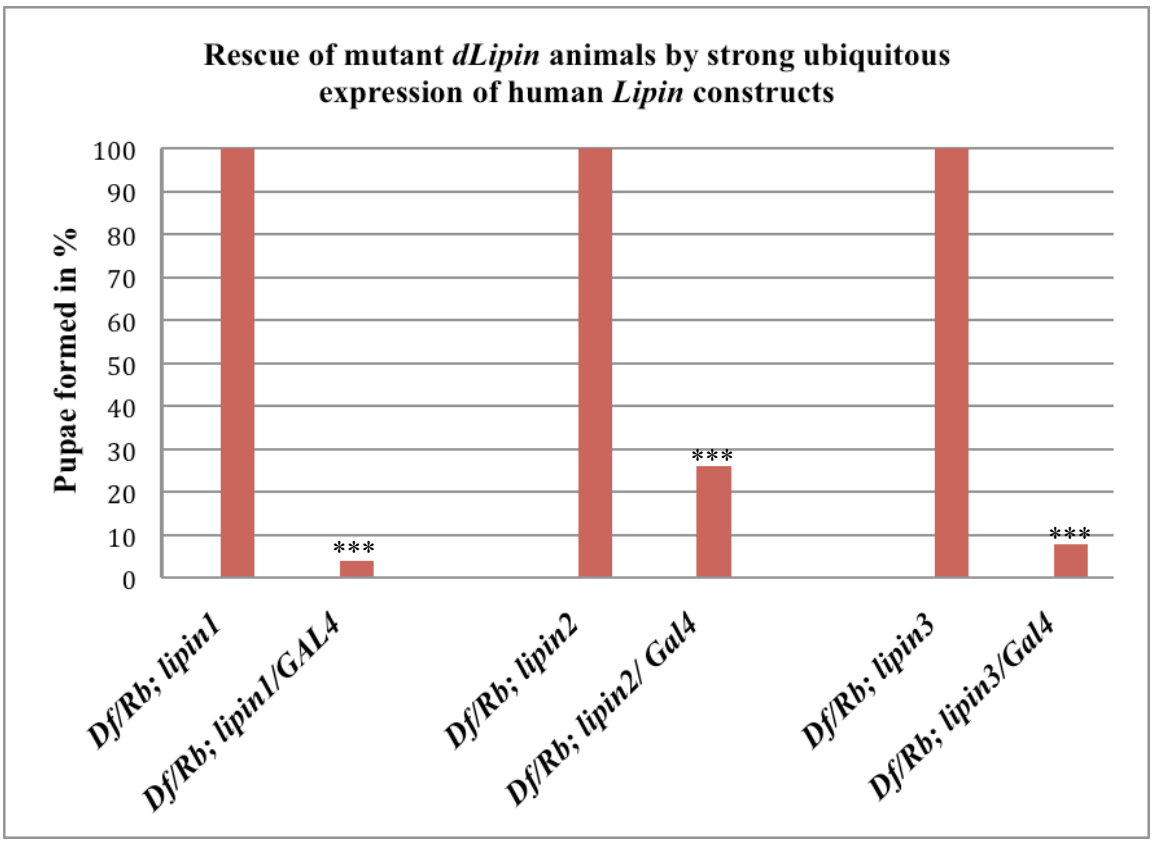

B)

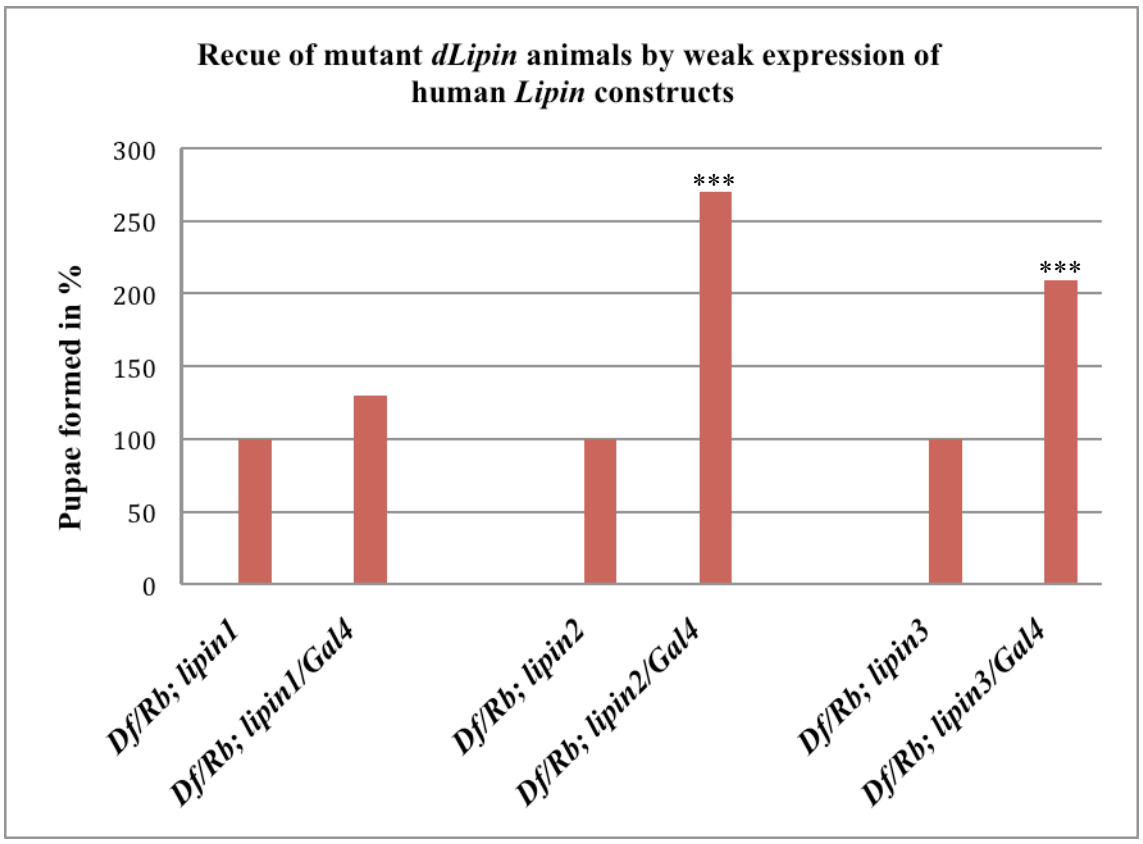
Recue of mutant dLipin animals by weak expression of human Lipin constructs
Pupae formed in %
300
250
200
150
100
50
0
***
***
Df/Rb; lipin1
Df/Rb; lipin1/Gal4
Df/Rb; lipin2
Df/Rb; lipin2/Gal4
Df/Rb; lipin3
Df/Rb; lipin3/Gal4

C)

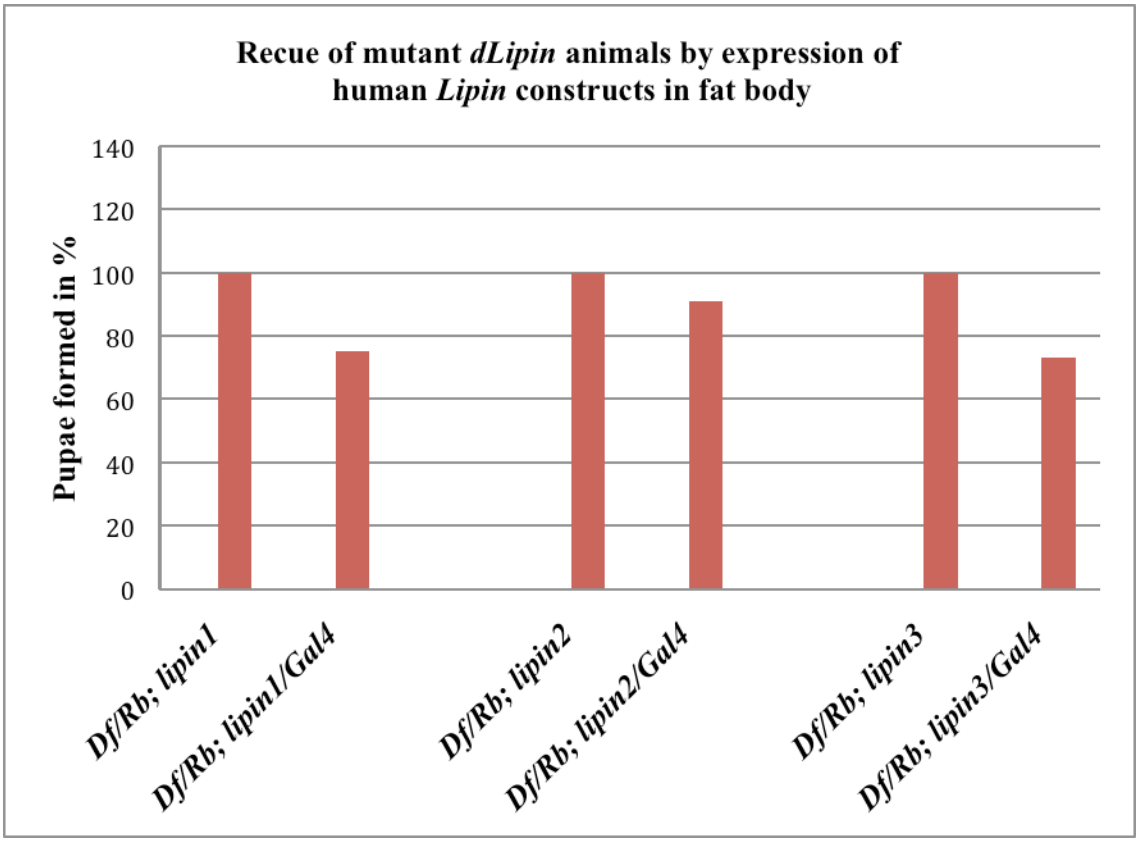

Fig. 47: Rescue of transheterozygous *dLipin* mutants (*dLipin*^{e00680}/ *Df(3R)Exel7095*) by expression of human *dLipin* homologs (*lipin1, lipin2, lipin3*). Using three different driver lines, I examined the rescue potential of the human *lipin* genes. To score for rescue effects I examined the number of pupae formed. A) Weak, nearly ubiquitous expression using the *DJ761* driver results in a significant rescue effect for *lipin2* and *lipin3*, and a clear trend for *lipin1*. *DJ761Gal4* is expressed in all larval tissues except CNS and imaginal discs (M. Lehmann personal communication) B) Strong ubiquitous expression with *TubGal4* of *lipin1*, *lipin2* and *lipin3* significantly lowered the ability of *dLipin* mutants to pupariate. C) Fat body-specific expression driven by *FBGal4* of *lipin1*, *lipin2* and *lipin3* did not affect the number of pupae formed. The transheterozygous *dLipin* mutant genotype (*dLipin*^{e00680}/ *Df(3R)Exel7095)* is abbreviated to *Df/Rb* in the graph. Two tailed Chi-Square Test, $*** p < 0.0001$.

Nearly ubiquitous but weak expression of *lipin2* and *lipin3* significantly reduced lethality of *dLipin* mutants. *lipin1* expression also seemed to have an effect on the number if pupae formed, but the difference to the control was not statistically significant.

Strong ubiquitous expression of any of the human lipin paralogs seemed to further decrease viability of *dLipin* mutants. Specific expression of human lipin paralogs in the fat body had no rescue effect. On the contrary, similar to the strong ubiquitous expression data, these data revealed that fat-body specific expression of the human lipin genes may have a negative effect as well.

Weak ubiquitous expression of human *lipin* genes in *dLipin* mutant animals was able to significantly increase the pupariation rate and improve fat body morphology. Hence, one can infer that human *lipin* genes posses functions of *dLipin* with regard to fat body development.

IV. Discussion

Mammalian *dLipin* homologs have long been implicated in mediating insulin sensitivity (Reue et al., 2000; Ryu et al., 2009; Suviolathi et al., 2006) and insulin signaling itself has been shown to influence Lipin1 activity (Harris et al., 2007, Huffman et al., 2002; Peterfy et al., 2010) and *lipin* expression (Manmontri et al., 2008). It is known that TOR signaling has an effect on Lipin1's subcellular localization and posttranslational modification (Eaton et al., 2013; Huffman et al., 2002; Peterson et al., 2011) and it has been demonstrated that TORC1 and Lipin1 interact in the control of lipid metabolism (Peterson et al., 2011). dLipin, the *Drosophila* counterpart of the mammalian Lipin proteins, has been shown to be a regulator of larval metabolism by contributing to fat body development and fat synthesis (Ugrankar et al., 2011). Goal of my research was to address the question of whether dLipin is, as its mammalian homologs, a mediator of insulin sensitivity, and whether the association between Lipin and TORC1 is evolutionarily conserved. An additional aim was to elucidate the link between Lipin's dual molecular functions, PAP activity and co-regulator activity, and the insulin and TORC1 pathways.

1. Background

Cell growth defects often result from a deregulation of insulin signaling or TORC1 signaling. Cells show overgrowth phenotypes under conditions with insulin pathway overactivation, whereas down regulation of the insulin pathway leads to a decrease in cell size (Britton et al., 2002).

It is widely assumed that growth defects brought about by changes in the insulin signaling pathway are in part caused by subsequent modifications of TORC1 activity (Saucedo et al.,

2003). To date, it has not been shown that this pathway exists as proposed in the fly under physiological conditions (Dong and Pan, 2004; Oldham et al., 2000; Pallares-Cartes et al., 2012; Schleich and Teleman, 2009). It is therefore not clear to what extent the TORC1 and insulin signaling pathways act in concert or independently in cell growth and metabolic control in *Drosophila melanogaster*.

2. dLipin and insulin pathway interact in fat body of *D. melanogaster*

To characterize the relationship between dLipin and the insulin pathway I conducted experiments to investigate the effects of dLipin on insulin pathway activity. I also examined the effects of insulin pathway signaling on dLipin activity.

2.1. dLipin is required for cell growth and TAG production cell-autonomously

Knocking down dLipin activity in a cell-autonomous fashion in the larval fat body reduced cell size. This reduction in cell size was accompanied by a near absence of fat droplets (Fig. 9). Nuclear area, although also significantly reduced compared to control cell nuclei, was disproportionally big in relation to cell area (Fig. 12). The reduction in nuclear size strongly suggests that cell growth was indeed interrupted, and the decreased amount of fat in cells deprived of dLipin activity did not cause the reduction in cell size.

The increase in the nucleocytoplasmic ratio in fat body cells was also observed after system-wide loss of dLipin activity (Fig. 12). This phenotype can be interpreted as an indication of reduced cytoplasmic growth during endoreplication cycles. Cell growth and DNA replication in endoreplicating tissues are tightly regulated in response to nutritional signals mediated primarily by circulating growth factors (Britton and Edgar, 1998). The increase in the

nucleocytoplasmic ratio could thus result from a deregulation of insulin/TOR activity in cells with cell-autonomous *dLipin* knockdown.

Taken together, the decrease in nuclear area in concert with the reduction of cellular area following cell-autonomous knockdown of *dLipin* strongly suggests that dLipin is required for cell growth in a cell-autonomous fashion. Cells also displayed a severe reduction in fat droplet accumulation. Thus, dLipin is also essential for proper fat synthesis cell-autonomously.

To determine whether cell growth is affected due to a change in the activity of the insulin pathway upon *dLipin* knockdown, I looked at PIP3 localization in fat body tissue from animals with fat body-specific knockdown of dLipin activity and *dLipin* transheterozygous mutants.

2.2. dLipin is required for fat body insulin sensitivity

PIP3 synthesis was disrupted in fat body cells upon knockdown of dLipin activity (Fig. 13 and 14). PIP3 is a second messenger generated by PI3K at the cell membrane under conditions of active insulin signaling. The deficiency in PIP3 was not caused by scarcity of its precursor PIP2, as PIP2 membrane levels appeared unaffected (Fig. 13 and 14). When dissecting fat body tissue from *dLipin* mutants and *dLipin* knockdown animals, it was apparent that membrane integrity was negatively affected. Cells tended to easily dissociate from each other resulting in an increased fragility of the tissue. DAG synthesis is catalyzed by the activity of Lipin proteins. DAG serves as a precursor for membrane phospholipids (Bishop and Bell, 1988). Therefore, loss of dLipin activity may have mediated changes in cell membrane composition. Furthermore, PAH1, a yeast homolog of dLipin, participates in the transcriptional control of phospholipid synthesis (Santos-Rosa et al., 2005). Thus, changes in phospholipid content of the cell membrane might have prohibited proper PIP3 synthesis at the cell membrane. However, as

PIP2 membrane localization seemed to be unaffected it seems likely. It is more likely that the absence of PIP3 from the plasma membrane after *dLipin* knockdown was caused by a defect in its synthesis and not by alterations in membrane structure.

Another parameter required for insulin pathway activity is phosphorylation of AKT. Under normal insulin signaling conditions, AKT is recruited to the cell membrane by PIP3 and subsequently phosphorylated at two specific residues in order to attain full activity (Liao and Hung, 2010). Measuring AKT phosphorylation in fat body from animals with fat body-specific *dLipin* knockdown and *dLipin* transheterozygous mutants showed a clear reduction of AKT phosphorylation (Fig. 18). I specifically examined phosphorylation at residue 505 (S505), which is catalyzed by TORC2. The reduction of phosphorylation after loss of dLipin activity points to a reduction in TORC2 and subsequently, AKT activity.

The reduction in PIP3 synthesis taken together with decreased phosphoAKT levels shows that reduced dLipin activity leads to reduced insulin pathway activity in the fat body.

2.3. dLipin affects PI3K activity

I was able to place dLipin at the level of PIP3 synthesis in the insulin signaling cascade by showing that a decrease in dLipin activity ameliorates the effects of PI3K over activation (Fig. 19) and that dLipin is required for PI3K activity (Fig. 20, Fig. 21). I expressed *Dp110CAAX*, a constitutively active Dp110, and observed a strong increase in cell size. When dLipin activity was down regulated in fat body cells with Dp110 overactivation, the overgrowth phenotype was reversed (Fig. 19). Furthermore, PIP3 synthesis (Fig. 20) and AKT phosphorylation levels (Fig. 21) were strongly reduced in cells with concomitant *Dp110AAX* expression and *dLipin* knockdown compared to cells with *Dp110CAAX* expression only. Because

PIP3 synthesis is negatively affected, even in the presence of PI3K overactivation, it seems likely that dLipin affects insulin pathway activity by either modulating PI3K or PTEN activity.

Another possible explanation for the loss of PI3K activity after *dLipin* knockdown is that dLipin's effect on AKT S505 phosphorylation is enough to blunt overexpression effects of PI3K. As mentioned before, phosphorylation of AKT at residue 505 was reduced upon a decrease of dLipin activity (Fig. 18). This phosphorylation step is catalyzed by TORC2. It has been shown that reduction of AKT phosphorylation by TORC2 is sufficient to attenuate hyperactivation of PI3K (Hietakangas and Cohen, 2007). However, this would not explain why PIP3 synthesis, and thus PI3K activity itself, was reduced.

Taken together, these data strongly suggest that dLipin is necessary for insulin pathway activity in the fat body at PI3K or PTEN level, and that loss of dLipin activity is sufficient to weaken PI3K signaling.

Further experiments will have to be conducted in order to be able to pinpoint where exactly dLipin influences the signaling cascade. Examining PTEN activity in cells with reduced *dLipin* expression may elucidate which step in PIP3 synthesis is affected by diminished dLipin activity.

It deserves to be noted that in addition to fat body hypertrophy, I observed animals with severe hypotrophy of the fat body after *Dp110CAAX* expression. It would be interesting to examine the expression levels of genes involved in fat synthesis, adipogenesis and lipolysis in these animals using RNASeq to further investigate whether fat synthesis is inhibited or whether lipolysis is increased.

I was not able to conduct experiments in which *dLipin* knockdown or knockdown of the insulin signaling pathway was combined with overactivation of TORC1. This would have been helpful to better understand the crosstalk between TORC1 and insulin pathway in vivo. I was not able to overactivate TORC1, neither by knocking down its repressors (*Tsc1* and *Tsc2*) nor by overexpression of an activator (*Rheb*). Future experiments should concentrate on finding alternative ways to activate TORC1, possibly by feeding flies a diet high in amino acid content or by overexpression of amino acid transporters. This would help to examine possible rescue effects of TORC1 on insulin resistance caused by a lack of dLipin.

2.4. Disrupting dLipin activity in the fat body results in fat body insulin resistance but has no apparent systemic effect

Transheterozygous *dLipin* mutants displayed a significant increase in circulating sugar levels (Fig. 22), but no overall systemic growth defect. Two sugars circulate in *Drosophila* hemolymph, glucose and trehalose, with trehalose being the major circulating sugar (Wyatt and Kale, 1957). Trehalose is a disaccharide synthesized in the fat body. The rise in circulating hemolymph sugars may indicate that glycogen breakdown in the fat body is increased in *dLipin* mutant larvae. This rise in circulating sugar suggests that the fat body is insulin resistent. The fact that transheterozygous *dLipin* mutants showed no defect in systemic growth implies that the influence of dLipin on insulin pathway activity is largely or exclusively restricted to the fat body. Disrupted insulin pathway activity in combination with normal growth was also present on the cellular level, as fat body cells of animals with fat body-specific *dLipin* knockdown were not reduced in size, although PIP3 synthesis was strongly reduced. This result implies that the disruption in insulin pathway activity observed in fat body cells with fat body-specific *dLipin* knockdown is not strong enough to induce obvious growth defects. Consistent with this

interpretation was the finding that overall 4EBP1 abundance was not increased in animals with fat body-specific *dLipin* knockdown (Fig. 43). 4EBP transcription is positively regulated by FOXO and FOXO activity is elevated upon insulin resistance (Teleman et al., 2005). Thus, 4EBP levels should have been elevated in cells after *dLipin* knockdown. Furthermore, data exists that indicates that AKT activity, although possibly reduced, is not abolished under conditions of reduced S505 phosphorylation. It was shown that under these conditions enough residual AKT activity is present to ensure downstream insulin pathway activity. Hence, investigation of S505 phosphorylation alone might not be a reliable indicator for AKT activity or overall insulin pathway activity (Hietakangas and Cohen, 2007).

These data all lead to the speculation that RNAi-induced knockdown of *dLipin* in fat body cells might only result in a weak reduction of insulin pathway activity, and that residual AKT activity was sufficient to trigger downstream signaling events. This suggests that the PIP3 reporter tGPH might not be a very sensitive measure of PIP3 levels. To further assess this interpretation it would be informative to test FOXO activity in cells after *dLipin* knockdown, for instance, by directly visualizing its nuclear translocation.

In addition, this result also points to a parallel pathway, that contributes to growth on a cellular level, and which functions independently of insulin input and promotes cell growth even in the presence of moderate or weak insulin resistance as caused by *dLipin* knockdown. Larvae with *dLipin* knockdown in the fat body seem to feed normally and therefore consume nutrients like amino acids. Amino acids activate the main nutrient-sensing pathway, the TORC1 pathway (Li et al, 2010). One can speculate that TORC1 activity alone may be enough to promote cell growth under conditions of weak or moderate insulin resistance in fat body cells. TORC1 signaling promotes translation and other cellular growth processes, and thus in turn promotes cell

growth. It has been proposed that under physiological conditions TORC1 and insulin signaling are not necessarily interconnected, but rather act in parallel pathways (Dong and Pan, 2004; Oldham et al., 2000; Pallares-Cartes et al., 2012; Schleich and Teleman, 2009). Indeed, TORC1 activity was not reduced in animals with fat body specific *dLipin* knockdown, as 4EBP1 phosphorylation remained unchanged (Fig. 43). Thus, moderate or weak insulin resistance in animals with fat body-specific *dLipin* knockdown might be compensated for on a cellular level by TORC1 activity.

Thus, the absence of any growth defect in fat body cells with RNAi-mediated *dLipin* knockdown may simply be due to the fact that this *dLipin* knockdown only elicits a very weak reduction in insulin pathway activity.

As mentioned previously, unlike tissue-wide *dLipin* knockdown, cell-autonomous loss of dLipin activity has a clear negative effect on cell growth. This seems to be caused by a more severe loss of dLipin activity in these cells as compared to the fat body-specific knockdown of *dLipin*. Cells after cell-autonomous loss of dLipin contained few, if any, fat droplets; an indication that in these cells fat synthesis, and therefore dLipin activity was most severely affected (Fig. 9). This is also reflected in cells seen in system-wide RNAi knockdown, as cells that did not contain any fat droplets appeared to be the smallest cells (Fig. 10). A stronger reduction of dLipin activity after cell-autonomous reduction of *dLipin* might thus be responsible for a more pronounced loss of insulin pathway activity and consequently, a reduction in cell size. Whether this reduction in cell size could also be caused by a subsequent downregulation of TORC1 activity due to a stronger decrease of insulin activity is not clear at this point. If TORC1 activity remained unchanged, this could possibly indicate the existence of a threshold measure for insulin pathway activity below which effects in cell growth become apparent.

The fat body represents the major metabolic organ of the developing larvae. Transheterozygous *dLipin* mutants displayed elevated circulating sugar levels, most likely caused by insulin resistance in the fat body. It would be interesting to explore whether systemic insulin signaling is subsequently modified to counteract the rise of hemolymph sugar levels in animals with reduced insulin sensitivity of the fat body. In mammalian systems, insulin resistance elicits increased insulin production in order to sensitize tissues for sugar uptake (Cavaghan et al., 2000). dILPs (Drosophila insulin-like peptides) represent signaling peptides secreted from the brain and other tissues, and act in neuroendocrine signaling and control carbohydrate and lipid metabolism as well as growth and reproduction (Brogiolo et al., 2001; Groenke et al., 2010; Colombani et al., 2012; Garelli et al., 2012). Although the exact mechanism that controls dILP release is not completely understood, it is known that a humoral signal originating from the fat body triggers dILP release from the neurosecretory cells in the brain (Geminard et al., 2009). This signal is most likely fat body produced dIPL6, which represses release of dILP2 and 5 from the brain (Bai et al., 2012). It has been previously documented that insulin resistance in the fat body can be accompanied by an increase in brain *dILP* expression, as seen for *miR-278* mutant flies (Teleman et al., 2006). Thus, the possibility exists that a reduction of dILP6 release from the fat body triggers dILP2 and dILP5 release from the brain to increase dILP levels in response to insulin resistance in the fat body. This increase in dILP hemolymph levels could represent a systemic response to insulin resistance in the fat body, mirroring increased insulin production in individuals with type2 diabetes. Measuring expression levels of *Dilps* in transheterozygous *dLipin* mutants and animals with fat body-specific *dLipin* knockdown could help determine whether dILP production is influenced by reduced insulin sensitivity of the fat body caused by decreased dLipin activity.

Overall, these data allow for the speculation that RNAi-induced fat body-specific *dLipin* knockdown only elicits weak to moderate insulin resistance in the fat body. TORC1 activity in these cells remains unchanged and allows for normal cell growth. In cells with severely compromised dLipin activity on the other hand, insulin signaling pathway activity appears to be strongly downregulated and, hence, cell growth is reduced.

2.5. Insulin pathway activity and dLipin activity are mutually dependent

Genetic interaction experiments between *dLipin* and the *Insulin receptor* (*InR*) revealed a strong connection between *dLipin* and *InR* in the development of fat body tissue. Using a GFP marker for fat body tissue, I observed that loss of InR activity concomitant with *dLipin* knockdown results in a severe underdevelopment of the fat body in developing larvae (Fig. 16). It is known that Lipin1 is required for proper adipogenesis (Kim et al., 2013; Phan et al., 2004; Zhang et al., 2012). Zhang et al. (2012) showed that Lipin1 affects adipogenic gene expression by influencing phosphatidic acid (PA) levels. Elevated levels of PA inhibit expression of adipogenic genes, amongst them the key regulator *peroxisome proliferator-activated receptor γ* (*Pparγ*). It is also known that Lipin1 physically interacts with PPARγ, and thereby regulates PPARγ activity in adipogenic gene expression. This activity of Lipin1 is independent of its PAP activity, and relies on Lipin1's nuclear activity (Kim et al., 2013). Insulin signaling is also a positive regulator of adipogenesis, as AKT activation alone can promote differentiation of 3T3-L1 cells into adipocytes by inducing *Pparγ* expression (Kohn et al., 1996; Xu and Liao, 2004). If the effects on adipogenesis in *Drosophila* are also mediated via PPARγ, or by a different adipogenic factor cannot be answered at this point. So far, no fly homolog for PPARγ has been identified (Hong et al., 2010).

It is possible that a reduction of insulin pathway activity further lowered dLipin activity in cells with *dLipinRNAi* and *InRDN* expression. Insulin pathway activity has been identified as a regulator of Lipin1 activity. Insulin influences phosphorylation and subcellular localization of Lipin1 (Harris et al., 2007; Peterfy et al., 2010). Reduction of InR activity in cells with *dLipin* knockdown could thus further lower PAP activity, and consequently increase PA levels. Increased PA levels might inhibit proper adipogenic gene expression. A disruption in adipogenesis would result in a decrease of fat body cell number and subsequently a reduction of larval fat body mass. This reduction of fat body mass concomitant with diminished TAG synthesis during larval development could explain the severe underdevelopment of the fat body in larvae with *dLipinRNAi* and *InRDN* expression. A loss of dLipin activity might also enhance insulin resistance in developing larvae expressing *InRDN* by further lowering AKT activity, and thus prohibiting adipocyte differentiation. This defect in adipogenic gene expression would also result in reduced fat body cell mass.

It is most likely that a combination of reduced dLipin activity due to decreased insulin pathway activity in concert with reduced insulin pathway activity due to decreased dLipin activity led to the severe defects in adipogenesis. This would point to an interdependent relationship between dLipin and insulin pathway activity during adipogenesis.

In addition to fat body mass, cell growth was altered in cells with concomitant expression of *dLipinRNAi* and *InRDN* in the fat body. Expression of *InRDN* alone significantly reduces cell area (Fig. 16), whereas *dLipinRNAi* expression has no effect on cell size (Fig. 15). When both transgenes were combined, cell size increased, cell shape became rounded and cell adherence decreased (Fig. 16). As this phenotype closely resembled the fat body phenotype of transheterozygous *dLipin* mutants (Ugrankar et al., 2011), one can speculate that the concomitant

dLipinRNAi and *InRDN* expression mimics the effect of a strong dLipin deficiency with regard to cell growth. As in the *dLipin* mutant, significant loss of fat body mass is being compensated by a secondary mechanism, which leads to the overgrowth of cells. The overgrowth is most likely induced to achieve critical weight required for larval maturation (Ugrankar et al., 2011). The strong reduction of fat body mass and TAG content may also be the cause of increased larval lethality observed after concomitant *dLipinRNAi* and *InRDN* expression. It would be interesting to address the question whether the overgrowth of fat body cells observed in *dLipin* mutants and in larvae with concomitant *dLipinRNAi*/*InRDN* expression represents a phenotype that is specific for *dLipin*, or is the result of a general reduction in fat body mass. Investigation of strong mutants for other enzymes involved in glycerolipid synthesis (e.g. AGPAT3, GPAT4, DGAT2) could shed light on this question.

I was able to show that strongly reduced insulin pathway activity in the fat body led to a reduction in dLipin protein levels (Fig. 24). However, subcellular localization appeared to be unaffected (Fig. 23). Insulin signaling positively regulates cytoplasmic retention of mammalian Lipin1, either by phosphorylation or by mediating an interaction between Lipin1 and 14-3-3 proteins (Harris et al., 2007; Peterfy et al, 2010). Thus, a decrease in insulin pathway activity should have caused a decrease in cytoplasmic dLipin localization and a translocation of dLipin to the nucleus or perinuclear region (ER). To further elucidate the effects of insulin pathway activity on dLipin activity, it would be interesting to measure PAP activity after insulin pathway overactivation and insulin pathway knockdown. In addition, dLipin phosphorylation status upon insulin pathway modifications should be investigated using native gel electrophoresis and mass spectrometry. These experiments would help elucidate whether PAP activity itself is modulated by insulin pathway activity and whether different stages of phosphorylation correlate with

differential PAP activity of dLipin. It would also be worthwhile to elucidate whether dLipin's microsomal association is affected, using confocal microscopy. Furthermore, it would be interesting to investigate whether AKT is the kinase responsible for insulin-mediated Lipin phosphorylation.

Thus, it appears that dLipin protein levels are regulated by insulin pathway activity. Subcellular distribution of dLipin on the other hand appears unaffected by insulin pathway activity. Whether the phosphorylation status of dLipin is modified by insulin pathway activity remains to be elucidated. It furthermore seems that dLipin activity during adipogenesis and in TAG synthesis is dependent on insulin pathway activity. These data also suggest that dLipin may regulate insulin pathway activity during adipogenesis.

2.6. dLipin's PAP activity is required for normal insulin sensitivity of the fat body

Animals with a reduction in GPAT4 or AGPAT3 activity in the fat body displayed a reduction in fat droplet size and PIP3 synthesis, mirroring the phenotype caused by *dLipin* knockdown (Fig. 26). GPAT4 and AGPAT3 are enzymes of the canonical TAG synthesis pathway and act directly upstream of dLipin, producing lysophosphatidic acid (LPA) and phosphatidic acid (PA), respectively. The fact that a reduction in the activity of these glycerolipid synthesis enzymes caused a reduction in PIP3 synthesis suggests that the process of TAG synthesis itself represents a mechanism that controls insulin sensitivity in the fat body. This hypothesis was further validated by experiments that showed that dLipin with intact nuclear function, but no PAP activity, was capable of reconstituting insulin sensitivity in the fat body of animals with *dLipin* knockdown (Fig. 31). The reconstitution of insulin sensitivity went hand in hand with an increase in fat droplet size in the fat body. Insulin pathway activity and fat body

morphology in animals expressing *dLipin* lacking PAP activity concomitant with *dLipin* knockdown remained disturbed (Fig. 31). Thus, it appears that dLipin can influence the insulin pathway through its role as a PAP enzyme.

TAG synthesis intermediates have been implicated as second messengers affecting insulin signaling. Elevated phosphatidic acid (PA) levels reduce activity of mTORC2 and increase mTORC1 activity (Blaskovich et al., 2013; Zhang et al., 2012). Preliminary data links PA to phospho kinase C (PKC) activation (Limatola et al., 1994; Stasek et al., 1993). PA levels are increased upon a reduction in Lipin activity (Han et al., 2006). Increased Lysophosphatidic acid (LPA) levels can lead to insulin resistance (Neschen et al., 2005; Rancoule et al., 2014). LPA levels might be elevated following AGPAT3 knockdown, as LPA is the substrate of AGPAT3. Elevated levels of diacylglycerol (DAG) result in insulin resistance through activation of phospho kinase C (PKC) and a subsequent reduction of PI3K activity (Erion and Shulman, 2010). DAG accumulation would be expected after downregulation of DGAT activity. I was not able to detect changes in PIP3 synthesis after DGAT knockdown. This was most likely due to the fact that DGAT knockdown was not strong enough, as fat content of cells appeared nearly normal. As of now, no involvement of G-3-P in insulin sensitivity has been detected, but as all other lipid intermediates contribute to insulin sensitivity it appears plausible that the same might be true for glycerol-3-phosphate.

Insulin resistance following *GPAT4*, *AGPAT3* and *dLipin* knockdown in the fat body could hence be due to an unphysiological accumulation of lipid intermediates, which in turn negatively affects insulin sensitivity of the tissue. Consistent with the effect of AGPAT3 knockdown in *Drosophila*, insulin resistance has been observed after a reduction of AGPAT activity in adipocyte cell culture (Subauste et al., 2012). PA levels should be elevated in cells

with reduced dLipin activity, as PA is the substrate for dLipin. As previously mentioned, in mammalian systems an elevation in PA levls is associated with increased TORC1 activity (Blaskovich et al., 2013). I did not observe an increase in TORC1 activity in fat body cells, as 4EBP1 phosphorylation was not elevated (Fig. 43). This discrepancy might be due to the fact that results stem from research done in 2 different systems, namely *Drosophila* and mouse, or that the conditions under which results were obtained differed too much. Reduced TORC2 activity caused by PA accumulation cannot explain the reduction in PI3K activity observed in fat body cells with reduced dLipin activity, as it would only affect AKT activity. Thus, it appears that PKC activity is increased upon PA accumulation due to *dLipin* knockdown and subsequently, PI3K activity diminished. This hypothesis should be tested further by conducting genetic interaction experiments between *dLipin* and the different PKC isoforms.

Individuals with lipodystrophy display elevated levels of free fatty acids (Meiniger et al., 2002). Therefore, it is possibile that a total reduction of TAG synthesis following *GPAT*, *AGPAT* or *dLipin* knockdown elicits insulin resistance through an increase in free fatty acids. An increase in free fatty acids has a negative impact on insulin sensitivity by inhibiting glucose uptake (Boden, 2003). Furthermore, SREBP activity is controlled by Lipin1, suggesting that under conditions of Lipin deficiency, SREBP activity, and therefore de-novo fatty acid synthesis, is deregulated (Peterson et al., 2011). Increased insulin levels positively control *SREBP1* expression even in the presence of insulin resistance (Shimomura et al., 2000). As *dLipin* knockdown results in insulin resistance, a possible increase in dILP levels could further raise SREBP activity, which would perpetuate the insulin resistant condition.

Another effect of insulin resistance is a rise in FOXO activity that goes hand in hand with an upregulation of Fatty Acid Synthase (FAS) (Luong et al., 2006). It would be worthwhile to

measure free fatty acid levels following *dLipin*, *AGPAT* and *GPAT* knockdown to test whether fatty acid levels are indeed elevated. Also, SREBP and FAS mRNA or protein levels should be investigated. In addition, the lipid profile of animals after a reduction of dLipin activity should be analyzed via chromatography.

qRT-PCR measuring *Dp110* transcript levels of fat body tissue from animals with fat body-specific *dLipin* knockdown showed that upon reduced dLipin activity, PI3K activity appears to be reduced as reflected in decreased *Dp110* mRNA levels (Fig. 33). Whether this moderate reduction in *Dp110* mRNA is a direct effect of dLipin deficiency, or a secondary effect of reduced insulin pathway activity caused by dLipin deficiency remains elusive at this point. As insulin sensitivity of the fat body appeared to be mainly dependent on dLipin's PAP activity and not dLipin's nuclear activity, the observed decrease of *Dp110* transcript appears to have no major impact on insulin sensitivity.

Overall, my data indicate that disrupted TAG synthesis is a cause for reduced fat body insulin sensitivity. A reduction in dLipin-mediated PAP activity thereby affected either PI3K or PTEN activity. Reduced insulin pathway activity upon dLipin knockdown manifested in cell growth defects and increased hemolymph sugar levels. Furthermore, dLipin's activity during adipogenesis and in TAG synthesis appeared to be dependent on insulin pathway activity. Thus, TAG biosynthesis and insulin pathway activity are closely interconnected, and dLipin appears to be an important link between the two pathways. My data furthermore provides a novel insight into how lipodystrophy induces insulin resistance in *Drosophila*. Previous data linked HIV-related lipodystrophy in humans with a disruption of the insulin cascade downstream of AKT activity (Haugaard et al., 2005). My data suggests that lipodystrophy-induced insulin resistance might develop via different mechanisms in *Drosophila* and humans.

3. Characterization of the relationship between dLipin and TOR signaling

To elucidate the relationship between dLipin and TOR signaling in *D. melanogaster*, I evaluated the effects of TOR activity on dLipin function. Furthermore, I examined the combined effects of TORC1 and *dLipin* knockdown on cell growth and larval development.

3.1. dLipin is a target of TORC1 signaling in the fat body

I established that TORC1 signaling acts as a regulator of dLipin activity in vivo. dLipin's subcellular localization as well as cellular abundance was clearly affected by a loss in TORC1 activity (Fig. 35). Following a knockdown of TORC1 activity via *raptor* knockdown, dLipin migrated into the nucleus and overall dLipin levels were greatly reduced. The same nuclear redistribution was observed for Lipin1 after loss of TORC1 activity (Peterson et al., 2011). Thus, dLipin cytoplasmic retention is positively controlled by TORC1 and this interaction is evolutionary conserved.

Several phosphorylation sites of Lipin1 in mammals are known to be rapamycin-sensitive, which indicates that TOR activity is involved in phosphorylation at these sites (Harris et al., 2007). Peterson et al. (2011) found that mTORC1 directly phosphorylates Lipin1 and thereby positively regulates cytoplasmic retention of Lipin1 protein. Once located in the nucleus, Lipin1 interferes with SREBP activity and thus prohibits lipid biosynthetic gene expression (Peterson et al., 2011). Furthermore, Lipin1 has been identified as a transcriptional co-regulator of beta-oxidation genes and also influences adipogenic gene expression (Chen et al., 2012; Kim et al., 2013). To affect gene expression and SREBP activity, Lipin1 translocates to the nucleus. Thus, TORC1 negatively controls these specific nuclear functions of Lipin1.

In response to low TORC1 activity, dLipin showed nuclear translocation comparable to Lipin1. This suggests that dLipin's cellular localization and hence its function is controlled by TORC1 activity and this furthermore implicates that dLipin's role in lipid metabolism is similarly dependent on TORC1 activity.

Upon nuclear entry, dLipin might like its mammalian counterpart participate in the transcriptional control of beta-oxidation and adipogenesis genes and other genes involved in starvation resistance. dLipin might also negatively affect SREBP activity, and thus lipogenesis (Finck et al., 2006; Zhang et al., 2008; Peterson et al., 2011). RNASeq using fat body tissue from animals with a reduction in TORC1 signaling in the presence or absence of a concomitant *dLipin* knockdown could help identify targets genes of dLipin.

In addition to TOR, insulin signaling pathway activity appears to influence the phosphorylation status of Lipin1 (Harris et al., 2007; Peterfy et al., 2010). Similar to TOR, insulin appears to promote Lipin1's cytoplasmic retention and opposes membrane association. It also appears that insulin and TOR regulate Lipin1 phosphorylation in concert (Huffman et al., 2002).

My data show that in contrast to reduced TORC1 activity, a reduction in PI3K activity did not lead to the nuclear concentration of dLipin (Fig. 23). It therefore appears that the posttranslational modifications of dLipin that are brought about by TOR, which promote cytoplasmic retention of dLipin, are not insulin-dependent. In accordance with this finding are results by Peterson et al. (2011) that show that nuclear translocation of Lipin1 cannot be reversed by activation of the insulin pathway. Therefore, my data points to the possibility that multiple phosphorylation states of dLipin exist, depending on TORC1 and/or insulin signaling pathway

activity. Some phosphorylation sites might thereby be controlled in concert by both pathways, and others independently.

As intracellular dLipin levels could potentially influence subcellular dLipin localization, I measured dLipin protein levels in cells with TORC1 knockdown and PI3K knockdown. I found that dLipin levels were comparably low after both knockdowns. Thus, the translocation of dLipin into the nucleus is not affected by intracellular levels of dLipin (Fig. 44) but rather appears to be controlled by posttranslational modifications depending on TORC1 activity. I did not observe dLipin binding to chromosomes (Fig. 36). This may be due to the fact that dLipin functions as a transcriptional co-regulator and does not directly bind to DNA. During the experiment, the physical interaction between dLipin and its regulatory interaction partners might have been interrupted, which could have resulted in dLipin dissociating from the chromosome.

My data suggest that dLipin activity in lipid metabolism is regulated by TORC1 independently of the insulin pathway. Subcellular localization of dLipin is determined by TORC1, as under conditions of reduced TORC1 signaling dLipin is found in the nucleus. This indicates that under conditions of reduced nutrient signaling, the requirement for dLipin's nuclear function is increased, possibly in order to prohibit de-novo lipogenesis by SREBP and to activate genes involved in beta-oxidation and starvation responses.

3.2. dLipin and TORC1 control larval growth in concert

Larval growth appeared to be negatively affected by concomitant reduction of dLipin and TORC1 activity. Larval size 5 days after egg deposition was significantly reduced in animals with concomitant *dLipin* and *raptor* knockdown compared to *dLipin* and *raptor* single knockdowns (Fig. 37). Furthermore, larval development was terminally halted at the feeding

third larval instar stage. *raptor* knockdown itself resulted in a moderate developmental delay and a reduction of fat body cell size. As larvae with fat body-specific *raptor* knockdown did not appear to be bigger in size despite a prolonged larval feeding phase, one can speculate that larval growth rate during development was reduced. Fat body cell size reduction was not accompanied by a reduction in PI3K activity, as PIP3 synthesis remained intact (Fig. 38). *dLipin* knockdown did not result in a developmental delay or a reduction of cell size but, as mentioned before, interfered with PIP3 synthesis and AKT S505 phosphorylation.

Rescue experiments with dLipin lacking either its co-regulator or PAP activity showed that the enhanced reduced larval growth in *dLipin*/*raptor* knockdown larvae was caused by a reduction of dLipin-mediated PAP activity (Fig. 41). *raptor* knockdown itself most likely does not elicit a strong reduction in PAP activity, as fat droplet size remained unchanged in the presence of a reduction in Raptor activity. dLipin was nearly absent from the cytoplasm and concentrated in the nucleus following *raptor* knockdown, suggesting that only small amounts of cytoplasmic dLipin are enough to provide cells with sufficient PAP activity.

A combination of reduced TORC1 signaling via *raptor* knockdown in concert with decreased PIP3 synthesis via *dLipin* knockdown might be responsible for reduced larval growth and increased larval lethality. Both TOR activity and insulin pathway activity influence larval growth (Colombani et al., 2003; Gupta et al., 2013; Rulifson et al., 2002; Walkiewicz and Stern, 2009). As TORC1 activity does not appear to be affected by dLipin input, a further reduction of TORC1 in animals with concomitant *raptor*/*dLipin* knockdown is likely not the cause of the growth defect (Fig. 43). Thus, these data support a model in which growth is controlled, at least in part, by the independent action of the TORC1 and insulin pathways.

One possible explanation for this result is that TORC1 and insulin pathway signaling in the fat body both influence a mechanism that integrates the overall energy status of the animal. Geminard et al. (2009) found that the fat body relays the nutritional status of the animals to the neurosecretory cell of the brain and thus the nutritional status of the fat body has a direct effect on dILP release. Increased dILP release then triggers larval growth (Geminard et al., 2009). *raptor* knockdown in the fat body alone slows down larval development, possibly due to reduced larval growth rate, suggesting that nutritional signals from the fat body affect growth. Thus, in larvae with reduced dLipin activity, and hence reduced insulin pathway activity and concomittantly reduced TORC1 activity via *raptor* knockdown, nutritional signaling from the fat body could have been significantly altered, decreasing larval growth even further.

Taken together, these data indicate that larval growth is regulated in concert by the insulin pathway and TORC1 and that lack of dLipin can interfere with this interaction by reducing PIP3 synthesis and thus decreasing insulin pathway activity.

3.3. dLipin and TORC1 control cytoplasmic growth

Nucleocytoplasmic ratio was increased in fat body cells from animals with concomitant reduction in dLipin and TORC1 activity (Fig. 39). Likewise, severe loss of dLipin activity, either cell-autonomously or system-wide, also affected this tight connection between DNA replication and cytoplasmic growth (Fig. 12). As *raptor* knockdown alone did not result in an increase in the nucleocytoplasmic ratio, the rise in nucleocytoplasmic ratio observed after concomitant *dLipin* and *raptor* knockdown does not appear to result from an enhancement of the growth phenotype caused by *raptor* knockdown. This is also consistent with the fact that I did not observe a reduction in TORC1 activity after RNAi-mediated *dLipin* knockdown (Fig. 43). Hence, this

growth defect is most likely caused by a reduction in insulin pathway activity in concert with reduced TORC1 activity in animals with concomitant *dLipin*/*raptor* knockdown as opposed to further reduced TORC1 activity.

This increase in nucleocytoplasmic ratio may be due to a decoupling of endoreplicative genome replication from cytoplasmic growth. The larval fat body is an endocreplicative tissue, undergoing multiple rounds of G1/S phase transitions without cell division. Endoreplication uses much of the same machinery as standard mitotic G1/S transition, and it is usually assumed that genome replication and cytoplasmic growth are tightly coupled (Edgar and Orr-Weaver, 2001). Endoreplication is a process closely controlled by nutritional and growth factor signals (Britton and Edgar, 1998). A severe deficiency in dLipin, and thus insulin pathway activity, or a reduction in TOR activity could result in changes in growth factor and nutrient signaling and consequently influence cytoplasmic growth. The double fat body-specific *dLipin* and *raptor* knockdown might mirror this defect, and likewise inhibit cytoplasmic growth.

Alternatively, autophagic activity may be increased in fat body cells upon strong cell-autonomous *dLipin* knockdown and concomitant knockdown of *dLipin* and *raptor*. Autophagy is a catabolic process in which cytoplasmic component are degraded in autolysosomes to provide energy for the cell. Autophagy is usually triggered as a response to starvation (Codogno and Meijer, 2005). A reduction in TORC1 activity is known to induce autophagy (Castets et al., 2013), and recently Lipin1 has been identified as a contributor to autophagic flux in muscle tissue (Zhang et al., 2014). Furthermore, insulin pathway activity controls autophagic activity, with a reduction in insulin signaling resulting in increased autophagy (Codogno and Meijer, 2005). Autophagy can result in reduced cytoplasmic volume, as cells consume cytoplasmic components to provide energy (Neufeld, 2012). It is possible that in cells with concomitant

dLipin and *raptor* knockdown the decrease in TORC1 activity together with reduced insulin pathway activity due to *dLipin* knockdown upregulates autophagy and, hence, decreases cytoplasmic volume. Strong cell-autonomous knockdown of *dLipin* alone might also be enough to increase autophagic activity in fat body cells.

Further experiments will need to be conducted to address the exact mechanism causing the increased nucleocytoplasmic ratio upon severe *dLipin* knockdown and concomitant *dLipin*/*raptor* knockdown. Investigating autophagic activity in animals with *dLipin/raptor* knockdown and in animals with cell-autonomous *dLipin* knockdown may be a first step in answering this question.

4. Expression of *dLipin* with a mutation in the PAP active site or deletion of NLS motif has a dominant negative phenotype

Expression of dLipin lacking an intact PAP active site or NLS motif resulted in dominant negative phenotypes (Fig. 27, Fig. 30). When *ΔNLSdLipin* was expressed in the fat body, it not only did not enter the nucleus, but it also prevented endogenous dLipin from entering the nucleus (Fig. 27). Expression of *ΔPAPdLipin* in *dLipin* transheterozygous mutants resulted in a decrease of larval viability (Fig. 30). Lipin1, 2 and 3 proteins are known to form hetero- and homo-oligomers in adipocyte cell culture (Liu et al., 2010). dLipin might therefore form oligomers as well. Dominant-negative effects seen after expression of both *ΔNLSdLipin* and *ΔPAPdLipin* suggest that both functions of dLipin, PAP and co-regulator activity, require proper oligomerization. GST-pulldown experiments would help elucidate whether dLipin proteins can form oligomers in vitro, and co-immunoprecipitation experiments with animals expressing

tagged dLipin and endogenous dLipin may elucidate whether dLipin proteins oligomerize in vivo.

5. dLipin might regulate ecdysone release or synthesis in larval ring gland

Strong ubiquitous expression of *ΔNLSdLipin* resulted in larval lethality and developmental delay; a phenotype that could be rescued by adding 20-HE to the fly food (Fig. 46). *dLipin* is abundantly expressed in the larval ring gland, the place of synthesis and release of the 20-HE precursor ecdysone (Ugrankar et al., 2011). Fat body tissue from these animals was well developed, which excludes fat body underdevelopment as a cause for the developmental delay. Another possibility is that dLipin may be involved in ecdysone synthesis in the ring gland itself, possibly through its role as a transcriptional co-regulator. 20-HE supplementation was not sufficient to compensate for *dLipin* deficiency in transheterozygous *dLipin* mutants. This may be because of the severe fat body underdevelopment in these animals that may prevent normal developmental progression despite supplementation with 20-HE.

The fact that expression of *WTdLipin* in fat body of transheterozygous *dLipin* mutants cannot rescue developmental delay and larval lethality corroborates the hypothesis that dLipin function in tissues other than fat body is essential for larval survival and development.

Specifically knocking down *dLipin* in the ring gland should help elucidate the role of dLipin in ecdysteroidogenesis. RNAseq experiments could be conducted to further investigate the involvement of dLipin in ecdysteroidogenesis. This would help identify genes controlled by dLipin in the ring gland, and clarify whether dLipin is indeed a critical regulator of ecdysone synthesis and release.

6. dLipin functions are conserved in *Homo sapiens* Lipin proteins

Rescue experiments with the human *dLipin* paralogs revealed that they possess at least some *dLipin* function by partially compensating for loss of *dLipin* activity (Fig. 47). Lipin1 did not show a significant rescue effect, but a clear trend was seen and it is likely, a larger sample size would have resulted in statistical significance. It is interesting to note that stronger expression of either of the *Homo sapiens lipin* homologs in fat body or ubiquitous expression had a negative effect on the number of pupae formed. This indicates that strong expression of *Homo sapiens lipin* genes induces lethality. The reason for this effect may be that human *lipin* genes carry out some functions that *dLipin* does not have and that are detrimental to fly viability.

In summary, I was able shed light on the effects of lipodystrophy elicited by a lack of dLipin activity on insulin pathway activity in the fly. I was also able to link insulin pathway acitivity and dLipin activity during adipogenesis and TAG synthesis. Additionally I further elucidated an interaction between TORC1 and dLipin in *Drosophila melanogaster*.

In larvae with reduced dLipin activity the insulin pathway was disrupted, as evidenced by a lack of PIP3 synthesis and increased circulating sugar levels. Cell-autonomous reduction of dLipin resulted in cell growth defects, likely caused by reduced insulin pathway activity in these cells. Insulin resistance in the fat body of lipodystrophic larvae with *dLipin* knockdown was possibly caused either by an unphysiological accumulation of lipid intermediates, an overall reduction in cellular TAG stores or a combination of both. Additionally, dLipin activity during adipogenesis and in TAG synthesis appeared to be controlled by the insulin pathway. Furthermore, functions of the insulin pathway during adipogenesis appeared to be negatively

affected by reduced dLipin activity. Thus, the functions of the insulin pathway and of dLipin in lipid metabolism are in part mutually dependent.

dLipin localization and abundance was controlled by TORC1, and therefore nutrient signaling. Reduced TORC1 activity promoted nuclear concentration of dLipin, which in turn may affect lipid metabolism by facilitating dLipin-mediated expression of beta-oxidation genes and by inducing dLipin-mediated SREBP inhibition. These data indicate that dLipin's role in lipid metabolism might be strongly dependent on TORC1 activity.

It further appeared that the insulin and TORC1 pathways are decoupled pathways in fat body of developing larvae. I was also able to attribute a possible novel function in ecdysteriodigenesis to dLipin and, thus help guide future dLipin research into a new and interesting direction.

Taken together, my data revealed that TAG synthesis and the insulin and TOR signaling pathways are tightly interconnected in the fat body of *Drosophila* and that dLipin may represent an important link between anabolic lipid metabolism, catabolic lipid metabolism and insulin and TOR pathway activity.

V. Summary

I was able to further our understanding of underlying mechanisms that cause insulin resistance in lipodystrophic individuals by investigating the relationship between dLipin, the *Drosophila* homolog of mammalian Lipins, and insulin pathway activity. Lipin proteins are known to act as PAP enzymes and a disruption of mammalian Lipin1 function results in metabolic disturbances, including insulin resistance and lipodystrophy (Langner et al., 1991; Reue et al., 2000). Ugrankar et al. (2011) previously established that a loss of dLipin activity similarly results in lipodystrophy (Ugrankar et al., 2011). I was able to show that dLipin activity is also crucial for fat body insulin sensitivity in *Drosophila*. Reduced dLipin activity in the fat body interfered with PI3K-mediated PIP3 synthesis and reduced insulin pathway activity downstream of PI3K. Genetic interaction experiments shed light on the epistatic relationship between dLipin and the insulin pathway. These experiments revealed that dLipin affects insulin pathway activity by modifying activity of either PI3K or PTEN. Levels of circulating sugars were significantly elevated in transheterozygous *dLipin* mutants, an indication that a loss of dLipin activity elicits insulin resistance.

Strong cell-autonomous knockdown of dLipin activity significantly reduced fat body cell size. This is consistent with my findings that implicate dLipin in PI3K activity; as insulin pathway activity is a major driving force of cell growth. Thus, dLipin might affect cell growth by influencing insulin pathway activity. Additionally, fat synthesis was dependent on dLipin activity in a cell-autonomous fashion.

Rescue experiment carried out with dLipin lacking PAP activity and dLipin lacking nuclear activity demonstrated that PIP3 synthesis was dependent on dLipin-mediated PAP

activity, and that loss of nuclear dLipin activity had no discernible effect on fat body insulin sensitivity. This indicates that dLipin affects insulin pathway activity via its role as a PAP enzyme, and not by regulating gene transcription as a putative transcriptional co-regulator.

In addition, dLipin activity itself appeared to be regulated by the insulin pathway. Cellular abundance of dLipin was significantly reduced upon downregulation of insulin pathway activity. Subcellular localization of dLipin, however, appeared to be unaffected. Furthermore, insulin pathway activity appeared to regulate dLipin activity during adipogenesis and in TAG synthesis. My data also implicate dLipin as a possible contributor to insulin pathway activity during adipogenesis.

To further investigate the relationship between Lipin and TOR activity, I examined dLipin's subcellular localization upon reduction of TORC1 activity. Upon loss of TORC1 activity, dLipin translocates into the nucleus. Thus, cytoplasmic retention of dLipin is positively regulated by TORC1 activity. The fact that dLipin translocates into the nucleus upon reduced TORC1 activity suggests that TORC1 influences dLipin activity in lipid metabolism. Nuclear Lipin1 is known to participate in the expression of beta-oxidation and adipogenesis genes and to inhibit SREBP-mediated lipogenesis (Finck et al., 2006; Zhang et al., 2008; Peterson et al., 2011). Consequently, dLipin's role in lipid metabolism seems to depend on TORC1 activity.

Genetic interaction experiments between *dLipin* and TORC1 (*raptor*) revealed that dLipin and TORC1 influence larval growth rate and cell growth in concert, but not through the same pathway. It appeared that growth is controlled, at least in part, by the independent actions of the TORC1 and insulin pathways and that dLipin can interfere with this interaction by reducing insulin pathway activity.

TORC1 activity itself, as measured by 4EBP1 phosphorylation, remained unchanged upon *dLipin* knockdown suggesting that insulin resistance and growth defects in cells with reduced dLipin activity are not caused by changes in TORC1 activity. This result furthermore suggests that TORC1 signaling and the insulin pathway are parallel pathways in the larval fat body.

Additionally, I was able to uncover a potential new function of dLipin in ecdysone synthesis or release in the *Drosophila* ring gland. Strong ubiquitous expression of *dLipin* lacking nuclear function resulted in developmental delay and larval lethality, a phenotype that was rescued by 20-hydroxyecdysone supplementation.

Investigation of dLipin lacking PAP activity and dLipin lacking nuclear activity pointed to the possibility that both functions of dLipin demand oligomerization, but further validation is required. Finally, rescue experiments with mammalian *lipin* homologs revealed that mammalian Lipins execute some of dLipin functions in vivo.

VI. Bibliography

Adeyo O, Horn PJ, Lee S, Binns DD, Chandrahas A, Chapman KD, Goodman JM. The yeast lipin orthologue Pah1p is important for biogenesis of lipid droplets. J Cell Biol. 2011 Mar 21;192(6):1043-55.

Arrese EL, Soulages JL. Insect fat body: energy, metabolism, and regulation. Annu Rev Entomol. 2010;55:207-25.

Assimacopoulos-Jeannet F, Brichard S, Rencurel F, Cusin I, Jeanrenaud B. In vivo effects of hyperinsulinemia on lipogenic enzymes and glucose transporter expression in rat liver and adipose tissues. Metabolism. 1995 Feb;44(2):228-33.

Aulchenko YS, Pullen J, Kloosterman WP, Yazdanpanah M, Hofman A, Vaessen N, Snijders PJ, Zubakov D, Mackay I, Olavesen M, Sidhu B, Smith VE, Carey A, Berezikov E, Uitterlinden AG, Plasterk RH, Oostra BA, van Duijn CM. LPIN2 is associated with type 2 diabetes, glucose metabolism, and body composition. Diabetes. 2007 Dec;56(12):3020-6.

Bai H, Kang P, Tatar M. Drosophila insulin-like peptide-6 (dilp6) expression from fat body extends lifespan and represses secretion of Drosophila insulin-like peptide-2 from the brain. Aging Cell. 2012 Dec;11(6):978-85.

Baker KD, Thummel CS. Diabetic larvae and obese flies-emerging studies of metabolism in Drosophila. Cell Metab. 2007 Oct;6(4):257-66.

Ben-Sahra I, Howell JJ, Asara JM, Manning BD. Stimulation of de novo pyrimidine synthesis by growth signaling through mTOR and S6K1. Science. 2013 Mar 15;339(6125):1323-8.

Berggreen C, Gormand A, Omar B, Degerman E, Göransson O. Protein kinase B activity is required for the effects of insulin on lipid metabolism in adipocytes. Am J Physiol Endocrinol Metab. 2009 Apr;296(4):E635-46.

Betz C, Hall MN. Where is mTOR and what is it doing there? J Cell Biol. 2013 Nov 25;203(4):563-74.

Bishop WR, Bell RM. Assembly of phospholipids into cellular membranes: biosynthesis, transmembrane movement and intracellular translocation. Annu Rev Cell Biol. 1988;4:579-610.

Birse RT, Choi J, Reardon K, Rodriguez J, Graham S, Diop S, Ocorr K, Bodmer R, Oldham S. High-fat-diet-induced obesity and heart dysfunction are regulated by the TOR pathway in Drosophila. Cell Metab. 2010 Nov 3;12(5):533-44.

Blair SS. Genetic mosaic techniques for studying Drosophila development. Development. 2003 Nov;130(21):5065-72.

Boden G. Effects of free fatty acids (FFA) on glucose metabolism: significance for insulin resistance and type 2 diabetes. Exp Clin Endocrinol Diabetes. 2003 May;111(3):121-4.

Britton JS, Edgar BA. Environmental control of the cell cycle in Drosophila: nutrition activates mitotic and endoreplicative cells by distinct mechanisms. Development. 1998 Jun;125(11):2149-58.

Britton JS, Lockwood WK, Li L, Cohen SM, Edgar BA. Drosophila's insulin/PI3-kinase pathway coordinates cellular metabolism with nutritional conditions. Dev Cell. 2002 Feb;2(2):239-49.

Brogiolo W, Stocker H, Ikeya T, Rintelen F, Fernandez R, Hafen E. An evolutionarily conserved function of the Drosophila insulin receptor and insulin-like peptides in growth control. Curr Biol. 2001 Feb 20;11(4):213-21.

Broughton SJ, Piper MD, Ikeya T, Bass TM, Jacobson J, Driege Y, Martinez P, Hafen E, Withers DJ, Leevers SJ, Partridge L. Longer lifespan, altered metabolism, and stress resistance in Drosophila from ablation of cells making insulin-like ligands. Proc Natl Acad Sci U S A. 2005 Feb 22;102(8):3105-10.

Blaskovich MA, Yendluri V, Lawrence HR, Lawrence NJ, Sebti SM, Springett GM. Lysophosphatidic acid acyltransferase beta regulates mTOR signaling. PLoS One. 2013 Oct 31;8(10):e78632.

Burgering BM, Kops GJ. Cell cycle and death control: long live Forkheads. Trends Biochem Sci. 2002 Jul;27(7):352-60.

Canavoso LE, Jouni ZE, Karnas KJ, Pennington JE, Wells MA. Fat metabolism in insects. Annu Rev Nutr. 2001;21:23-46.

Carnevalli LS, Masuda K, Frigerio F, Le Bacquer O, Um SH, Gandin V, Topisirovic I, Sonenberg N, Thomas G, Kozma SC. S6K1 plays a critical role in early adipocyte differentiation. Dev Cell. 2010 May 18;18(5):763-74.

Cavaghan MK, Ehrmann DA, Polonsky KS. Interactions between insulin resistance and insulin secretion in the development of glucose intolerance. J Clin Invest. 2000 Aug;106(3):329-33.

Centers for Disease Control and Prevention. National Diabetes Statistics Report: Estimates of Diabetes and Its Burden in the United States, 2014. Atlanta, GA: U.S. Department of Health and Human Services; 2014.

Chakrabarti P, English T, Shi J, Smas CM, Kandror KV. Mammalian target of rapamycin complex 1 suppresses lipolysis, stimulates lipogenesis, and promotes fat storage. Diabetes. 2010 Apr;59(4):775-81.

Chang YC, Chang LY, Chang TJ, Jiang YD, Lee KC, Kuo SS, Lee WJ, Chuang LM. The associations of LPIN1 gene expression in adipose tissue with metabolic phenotypes in the Chinese population. Obesity (Silver Spring). 2010 Jan;18(1):7-12.

Chen Z, Gropler MC, Mitra MS, Finck BN. Complex interplay between the lipin 1 and the hepatocyte nuclear factor 4 α (HNF4α) pathways to regulate liver lipid metabolism. PLoS One. 2012;7(12):e51320.

Codogno P, Meijer AJ. Autophagy and signaling: their role in cell survival and cell death. Cell Death Differ. 2005 Nov;12 Suppl 2:1509-18.

Colombani J, Raisin S, Pantalacci S, Radimerski T, Montagne J, Léopold P. A nutrient sensor mechanism controls Drosophila growth. Cell. 2003 Sep 19;114(6):739-49.

Cong LN, Chen H, Li Y, Zhou L, McGibbon MA, Taylor SI, Quon MJ. Physiological role of Akt in insulin-stimulated translocation of GLUT4 in transfected rat adipose cells. Mol Endocrinol. 1997 Dec;11(13):1881-90.

Csaki LS, Dwyer JR, Fong LG, Tontonoz P, Young SG, Reue K. Lipins, lipinopathies, and the modulation of cellular lipid storage and signaling. Prog Lipid Res. 2013 Jul;52(3):305-16.

Czech MP, Tencerova M, Pedersen DJ, Aouadi M. Insulin signalling mechanisms for triacylglycerol storage. Diabetologia. 2013 May;56(5):949-64.

Dann SG, Thomas G. The amino acid sensitive TOR pathway from yeast to mammals. FEBS Lett. 2006 May 22;580(12):2821-9.

Deckelbaum RJ, Williams CL. Childhood obesity: the health issue. Obes Res. 2001 Nov;9 Suppl 4:239S-243S.

DiAngelo JR, Birnbaum MJ. Regulation of fat cell mass by insulin in Drosophila melanogaster. Mol Cell Biol. 2009 Dec;29(24):6341-52.

Dibble CC, Manning BD. Signal integration by mTORC1 coordinates nutrient input with biosynthetic output. Nat Cell Biol. 2013 Jun;15(6):555-64.

Dong J, Pan D. Tsc2 is not a critical target of Akt during normal Drosophila development. Genes Dev. 2004 Oct 15;18(20):2479-84.

Donkor J, Sariahmetoglu M, Dewald J, Brindley DN, Reue K. Three mammalian lipins act as phosphatidate phosphatases with distinct tissue expression patterns. J Biol Chem. 2007 Feb 9;282(6):3450-7.

Donkor J, Sparks LM, Xie H, Smith SR, Reue K. Adipose tissue lipin-1 expression is correlated with peroxisome proliferator-activated receptor alpha gene expression and insulin sensitivity in healthy young men. J Clin Endocrinol Metab. 2008 Jan;93(1):233-9.

Donkor J, Zhang P, Wong S, O'Loughlin L, Dewald J, Kok BP, Brindley DN, Reue K. A conserved serine residue is required for the phosphatidate phosphatase activity but not the transcriptional coactivator functions of lipin-1 and lipin-2. J Biol Chem. 2009 Oct 23;284(43):29968-78.

Dubots E, Cottier S, Péli-Gulli MP, Jaquenoud M, Bontron S, Schneiter R, De Virgilio C. TORC1 regulates Pah1 phosphatidate phosphatase activity via the Nem1/Spo7 protein phosphatase complex. PLoS One. 2014 Aug 12;9(8):e104194.

Duevel K, Yecies JL, Menon S, Raman P, Lipovsky AI, Souza AL, Triantafellow E, Ma Q, Gorski R, Cleaver S, Vander Heiden MG, MacKeigan JP, Finan PM, Clish CB, Murphy LO, Manning BD. Activation of a metabolic gene regulatory network downstream of mTOR complex 1. Mol Cell. 2010 Jul 30;39(2):171-83.

Eaton JM, Mullins GR, Brindley DN, Harris TE. Phosphorylation of lipin 1 and charge on the phosphatidic acid head group control its phosphatidic acid phosphatase activity and membrane association. J Biol Chem. 2013 Apr 5;288(14):9933-45.

Edgar BA, Orr-Weaver TL. Endoreplication cell cycles: more for less. Cell. 2001 May 4;105(3):297-306.

Erion DM, Shulman GI. Diacylglycerol-mediated insulin resistance. Nat Med. 2010 Apr;16(4):400-2.

Farmer SR. Transcriptional control of adipocyte formation. Cell Metab. 2006 Oct;4(4):263-73.

Ferguson PJ, Chen S, Tayeh MK, Ochoa L, Leal SM, Pelet A, Munnich A, Lyonnet S, Majeed HA, El-Shanti H. Homozygous mutations in LPIN2 are responsible for the syndrome of chronic recurrent multifocal osteomyelitis and congenital dyserythropoietic anaemia (Majeed syndrome). J Med Genet. 2005 Jul;42(7):551-7.

Ferré P, Foufelle F. SREBP-1c transcription factor and lipid homeostasis: clinical perspective. Horm Res. 2007;68(2):72-82.

Finck BN, Gropler MC, Chen Z, Leone TC, Croce MA, Harris TE, Lawrence JC Jr, Kelly DP. Lipin 1 is an inducible amplifier of the hepatic PGC-1alpha/PPARalpha regulatory pathway. Cell Metab. 2006 Sep;4(3):199-210.

Frayn KN. Adipose tissue and the insulin resistance syndrome. Proc Nutr Soc. 2001 Aug;60(3):375-80.

García-Martínez JM, Alessi DR. mTOR complex 2 (mTORC2) controls hydrophobic motif phosphorylation and activation of serum- and glucocorticoid-induced protein kinase 1 (SGK1). Biochem J. 2008 Dec 15;416(3):375-85.

Garelli A, Gontijo AM, Miguela V, Caparros E, Dominguez M. Imaginal discs secrete insulin-like peptide 8 to mediate plasticity of growth and maturation. Science. 2012 May 4;336(6081):579-82.

Géminard C, Rulifson EJ, Léopold P. Remote control of insulin secretion by fat cells in Drosophila. Cell Metab. 2009 Sep;10(3):199-207.

Gervais L, Claret S, Januschke J, Roth S, Guichet A. PIP5K-dependent production of PIP2 sustains microtubule organization to establish polarized transport in the Drosophila oocyte. Development. 2008 Dec;135(23):3829-38.

Gingras AC, Gygi SP, Raught B, Polakiewicz RD, Abraham RT, Hoekstra MF, Aebersold R, Sonenberg N. Regulation of 4E-BP1 phosphorylation: a novel two-step mechanism. Genes Dev. 1999 Jun 1;13(11):1422-37.

Go AS, Mozaffarian D, Roger VL, Benjamin EJ, Berry JD, Borden WB, Bravata DM, Dai S, Ford ES, Fox CS, Franco S, Fullerton HJ, Gillespie C, Hailpern SM, Heit JA, Howard VJ, Huffman MD, Kissela BM, Kittner SJ, Lackland DT, Lichtman JH, Lisabeth LD, Magid D, Marcus GM, Marelli A, Matchar DB, McGuire DK, Mohler ER, Moy CS, Mussolino ME, Nichol G, Paynter NP, Schreiner PJ, Sorlie PD, Stein J, Turan TN, Virani SS, Wong ND, Woo D, Turner MB; American Heart Association Statistics Committee and Stroke Statistics Subcommittee. Heart disease and stroke statistics--2013 update: a report from the American Heart Association. Circulation. 2013 Jan 1;127(1):e6-e245.

Golden A, Liu J, Cohen-Fix O. Inactivation of the C. elegans lipin homolog leads to ER disorganization and to defects in the breakdown and reassembly of the nuclear envelope. J Cell Sci. 2009 Jun 15;122(Pt 12):1970-8.

Gomez-Muñoz A, Hatch GM, Martin A, Jamal Z, Vance DE, Brindley DN. Effects of okadaic acid on the activities of two distinct phosphatidate phosphohydrolases in rat hepatocytes. FEBS Lett. 1992 Apr 13;301(1):103-6.

Gorjánácz M, Mattaj IW. Lipin is required for efficient breakdown of the nuclear envelope in Caenorhabditis elegans. J Cell Sci. 2009 Jun 15;122(Pt 12):1963-9.

Gowri PM, Sengupta S, Bertera S, Katzenellenbogen BS. Lipin1 regulation by estrogen in uterus and liver: implications for diabetes and fertility. Endocrinology. 2007 Aug;148(8):3685-93.

Grewal SS. Insulin/TOR signaling in growth and homeostasis: a view from the fly world. Int J Biochem Cell Biol. 2009 May;41(5):1006-10.

Grimsey N, Han GS, O'Hara L, Rochford JJ, Carman GM, Siniossoglou S. Temporal and spatial regulation of the phosphatidate phosphatases lipin 1 and 2. J Biol Chem. 2008 Oct 24;283(43):29166-74.

Groenke S, Mildner A, Fellert S, Tennagels N, Petry S, Müller G, Jäckle H, Kühnlein RP. Brummer lipase is an evolutionary conserved fat storage regulator in Drosophila. Cell Metab. 2005 May;1(5):323-30.

Gupta A, Toscano S, Trivedi D, Jones DR, Mathre S, Clarke JH, Divecha N, Raghu P. Phosphatidylinositol 5-phosphate 4-kinase (PIP4K) regulates TOR signaling and cell growth during Drosophila development. Proc Natl Acad Sci U S A. 2013 Apr 9;110(15):5963-8.

Gutierrez E, Wiggins D, Fielding B, Gould AP. Specialized hepatocyte-like cells regulate Drosophila lipid metabolism. Nature. 2007 Jan 18;445(7125):275-80.

Han GS, Siniossoglou S, Carman GM. The cellular functions of the yeast lipin homolog PAH1p are dependent on its phosphatidate phosphatase activity. J Biol Chem. 2007 Dec 21;282(51):37026-35.

Han GS, Wu WI, Carman GM. The Saccharomyces cerevisiae Lipin homolog is a Mg2+-dependent phosphatidate phosphatase enzyme. J Biol Chem. 2006 Apr 7;281(14):9210-8.

Hara K, Yonezawa K, Kozlowski MT, Sugimoto T, Andrabi K, Weng QP, Kasuga M, Nishimoto I, Avruch J. Regulation of eIF-4E BP1 phosphorylation by mTOR. J Biol Chem. 1997 Oct 17;272(42):26457-63.

Harris TE, Huffman TA, Chi A, Shabanowitz J, Hunt DF, Kumar A, Lawrence JC Jr. Insulin controls subcellular localization and multisite phosphorylation of the phosphatidic acid phosphatase, lipin 1. J Biol Chem. 2007 Jan 5;282(1):277-86.

Haugaard SB, Andersen O, Madsbad S, Frøsig C, Iversen J, Nielsen JO, Wojtaszewski JF. Skeletal muscle insulin signaling defects downstream of phosphatidylinositol 3-kinase at the level of Akt are associated with impaired nonoxidative glucose disposal in HIV lipodystrophy. Diabetes. 2005 Dec;54(12):3474-83.

Hemmings BA, Restuccia DF. PI3K-PKB/Akt pathway. Cold Spring Harb Perspect Biol. 2012 Sep 1;4(9):a011189.

Hennig KM, Colombani J, Neufeld TP. TOR coordinates bulk and targeted endocytosis in the Drosophila melanogaster fat body to regulate cell growth. J Cell Biol. 2006 Jun 19;173(6):963-74.

Hietakangas V, Cohen SM. Re-evaluating AKT regulation: role of TOR complex 2 in tissue growth. Genes Dev. 2007 Mar 15;21(6):632-7.

Hietakangas V, Cohen SM. Regulation of tissue growth through nutrient sensing. Annu Rev Genet. 2009;43:389-410.

Hong JW, Park KW. Further understanding of fat biology: lessons from a fat fly. Exp Mol Med. 2010 Jan 31;42(1):12-20.

Huang-Doran I, Sleigh A, Rochford JJ, O'Rahilly S, Savage DB. Lipodystrophy: metabolic insights from a rare disorder. J Endocrinol. 2010 Dec;207(3):245-55.

Huffman TA, Mothe-Satney I, Lawrence JC Jr. Insulin-stimulated phosphorylation of lipin mediated by the mammalian target of rapamycin. Proc Natl Acad Sci U S A. 2002 Jan 22;99(2):1047-52.

Iadevaia V, Liu R, Proud CG. mTORC1 signaling controls multiple steps in ribosome biogenesis. Semin Cell Dev Biol. 2014 Dec;36:113-20.

Ishimoto K, Nakamura H, Tachibana K, Yamasaki D, Ota A, Hirano K, Tanaka T, Hamakubo T, Sakai J, Kodama T, Doi T. Sterol-mediated regulation of human lipin 1 gene expression in hepatoblastoma cells. J Biol Chem. 2009 Aug 14;284(33):22195-205.

Johnston LA, Gallant P. Control of growth and organ size in Drosophila. Bioessays. 2002 Jan;24(1):54-64.

Kannan K, Fridell YW. Functional implications of Drosophila insulin-like peptides in metabolism, aging, and dietary restriction. Front Physiol. 2013 Oct 16;4:288.

Kim HE, Bae E, Jeong DY, Kim MJ, Jin WJ, Park SW, Han GS, Carman GM, Koh E, Kim KS. Lipin1 regulates PPARγ transcriptional activity. Biochem J. 2013 Jul 1;453(1):49-60.

Kim J, Guan KL. Amino acid signaling in TOR activation. Annu Rev Biochem. 2011;80:1001-32.

Kim HB, Kumar A, Wang L, Liu GH, Keller SR, Lawrence JC Jr, Finck BN, Harris TE. Lipin 1 represses NFATc4 transcriptional activity in adipocytes to inhibit secretion of inflammatory factors. Mol Cell Biol. 2010 Jun;30(12):3126-39.

Kim J, Kundu M, Viollet B, Guan KL. AMPK and mTOR regulate autophagy through direct phosphorylation of Ulk1. Nat Cell Biol. 2011 Feb;13(2):132-41.

Kishimoto H, Hamada K, Saunders M, Backman S, Sasaki T, Nakano T, Mak TW, Suzuki A. Physiological functions of Pten in mouse tissues. Cell Struct Funct. 2003 Feb;28(1):11-21.

Koh YK, Lee MY, Kim JW, Kim M, Moon JS, Lee YJ, Ahn YH, Kim KS. Lipin1 is a key factor for the maturation and maintenance of adipocytes in the regulatory network with CCAAT/enhancer-binding protein alpha and peroxisome proliferator-activated receptor gamma 2. J Biol Chem. 2008 Dec 12;283(50):34896-906.

Kohn AD, Summers SA, Birnbaum MJ, Roth RA. Expression of a constitutively active Akt Ser/Thr kinase in 3T3-L1 adipocytes stimulates glucose uptake and glucose transporter 4 translocation. J Biol Chem. 1996 Dec 6;271(49):31372-8.

Kopelman P. Health risks associated with overweight and obesity. Obes Rev. 2007 Mar;8 Suppl 1:13-7.

Koren I, Reem E, Kimchi A. DAP1, a novel substrate of mTOR, negatively regulates autophagy. Curr Biol. 2010 Jun 22;20(12):1093-8.

Khalil M, Sundaram M, Zhang HY, Links PH, Raven JF, Manmontri B, Sariahmetoglu M, Tran K, Reue K, Brindley DN, Yao Z. The level and compartmentalization of phosphatidate phosphatase-1 (lipin-1) control the assembly and secretion of hepatic VLDL. J Lipid Res. 2009 Jan;50(1):47-58.

Kramer JM, Davidge JT, Lockyer JM, Staveley BE. Expression of Drosophila FOXO regulates growth and can phenocopy starvation. BMC Dev Biol. 2003 Jul 5;3:5.

Kumar A, Lawrence JC Jr, Jung DY, Ko HJ, Keller SR, Kim JK, Magnuson MA, Harris TE. Fat cell-specific ablation of rictor in mice impairs insulin-regulated fat cell and whole-body glucose and lipid metabolism. Diabetes. 2010 Jun;59(6):1397-406.

Lang F, Böhmer C, Palmada M, Seebohm G, Strutz-Seebohm N, Vallon V. (Patho)physiological significance of the serum- and glucocorticoid-inducible kinase isoforms. Physiol Rev. 2006 Oct;86(4):1151-78.

Langner CA, Birkenmeier EH, Ben-Zeev O, Schotz MC, Sweet HO, Davisson MT, Gordon JI. The fatty liver dystrophy (fld) mutation. A new mutant mouse with a developmental abnormality in triglyceride metabolism and associated tissue-specific defects in lipoprotein lipase and hepatic lipase activities. J Biol Chem. 1989 May 15;264(14):7994-8003.

Langner CA, Birkenmeier EH, Roth KA, Bronson RT, Gordon JI. Characterization of the peripheral neuropathy in neonatal and adult mice that are homozygous for the fatty liver dystrophy (fld) mutation. J Biol Chem. 1991 Jun 25;266(18):11955-64.

Laplante M, Sabatini DM. An emerging role of mTOR in lipid biosynthesis. Curr Biol. 2009 Dec 1;19(22):R1046-52.

Laplante M, Sabatini DM. mTOR signaling in growth control and disease. Cell. 2012 Apr 13;149(2):274-93.

Lehner CF. The beauty of small flies. Nat Cell Biol. 1999 Sep;1(5):E129-30.

Li X, Gao T. mTORC2 phosphorylates protein kinase Cζ to regulate its stability and activity. EMBO Rep. 2014 Feb;15(2):191-8.

Liao Y, Hung MC. Physiological regulation of Akt activity and stability. Am J Transl Res. 2010 Jan 1;2(1):19-42.

Limatola C, Schaap D, Moolenaar WH, van Blitterswijk WJ. Phosphatidic acid activation of protein kinase C-zeta overexpressed in COS cells: comparison with other protein kinase C isotypes and other acidic lipids. Biochem J. 1994 Dec 15;304 (Pt 3):1001-8.

Liu GH, Gerace L. Sumoylation regulates nuclear localization of lipin-1alpha in neuronal cells. PLoS One. 2009 Sep 15;4(9):e7031.

Liu GH, Qu J, Carmack AE, Kim HB, Chen C, Ren H, Morris AJ, Finck BN, Harris TE. Lipin proteins form homo- and hetero-oligomers. Biochem J. 2010 Nov 15;432(1):65-76.

Loewith R, Hall MN. Target of rapamycin (TOR) in nutrient signaling and growth control. Genetics. 2011 Dec;189(4):1177-201.

Luong N, Davies CR, Wessells RJ, Graham SM, King MT, Veech R, Bodmer R, Oldham SM. Activated FOXO-mediated insulin resistance is blocked by reduction of TOR activity. Cell Metab. 2006 Aug;4(2):133-42.

Magnuson B, Ekim B, Fingar DC. Regulation and function of ribosomal protein S6 kinase (S6K) within mTOR signalling networks. Biochem J. 2012 Jan 1;441(1):1-21.

Manmontri B, Sariahmetoglu M, Donkor J, Bou Khalil M, Sundaram M, Yao Z, Reue K, Lehner R, Brindley DN. Glucocorticoids and cyclic AMP selectively increase hepatic lipin-1 expression, and insulin acts antagonistically. J Lipid Res. 2008 May;49(5):1056-67.

Manning BD, Cantley LC. Rheb fills a GAP between TSC and TOR. Trends Biochem Sci. 2003 Nov;28(11):573-6.

Manning BD, Cantley LC. AKT/PKB signaling: navigating downstream. Cell. 2007 Jun 29;129(7):1261-74.

Meininger G, Hadigan C, Laposata M, Brown J, Rabe J, Louca J, Aliabadi N, Grinspoon S. Elevated concentrations of free fatty acids are associated with increased insulin response to standard glucose challenge in human immunodeficiency virus-infected subjects with fat redistribution. Metabolism. 2002 Feb;51(2):260-6.

Milhavet F, Cuisset L, Hoffman HM, Slim R, El-Shanti H, Aksentijevich I, Lesage S, Waterham H, Wise C, Sarrauste de Menthiere C, Touitou I. The infevers autoinflammatory mutation online registry: update with new genes and functions. Hum Mutat. 2008 Jun;29(6):803-8.

Miranda M, Chacón MR, Gómez J, Megía A, Ceperuelo-Mallafré V, Veloso S, Saumoy M, Gallart L, Richart C, Fernández-Real JM, Vendrell J; Adipocyte Differentiation Study Group. Human subcutaneous adipose tissue LPIN1 expression in obesity, type 2 diabetes mellitus, and human immunodeficiency virus--associated lipodystrophy syndrome. Metabolism. 2007 Nov;56(11):1518-26.

Miyoshi H, Perfield JW 2nd, Souza SC, Shen WJ, Zhang HH, Stancheva ZS, Kraemer FB, Obin MS, Greenberg AS. Control of adipose triglyceride lipase action by serine 517 of perilipin A globally regulates protein kinase A-stimulated lipolysis in adipocytes. J Biol Chem. 2007 Jan 12;282(2):996-1002.

Mlinar B, Pfeifer M, Vrtacnik-Bokal E, Jensterle M, Marc J. Decreased lipin 1 beta expression in visceral adipose tissue is associated with insulin resistance in polycystic ovary syndrome. Eur J Endocrinol. 2008 Dec;159(6):833-9.

Nakamura Y, Koizumi R, Shui G, Shimojima M, Wenk MR, Ito T, Ohta H. Arabidopsis lipins mediate eukaryotic pathway of lipid metabolism and cope critically with phosphate starvation. Proc Natl Acad Sci U S A. 2009 Dec 8;106(49):20978-83.

Neschen S, Morino K, Hammond LE, Zhang D, Liu ZX, Romanelli AJ, Cline GW, Pongratz RL, Zhang XM, Choi CS, Coleman RA, Shulman GI. Prevention of hepatic steatosis and hepatic insulin resistance in mitochondrial acyl-CoA:glycerol-sn-3-phosphate acyltransferase 1 knockout mice. Cell Metab. 2005 Jul;2(1):55-65.

Neufeld TP. Autophagy and cell growth--the yin and yang of nutrient responses. J Cell Sci. 2012 May 15;125(Pt 10):2359-68.

Oldham S, Montagne J, Radimerski T, Thomas G, Hafen E. Genetic and biochemical characterization of dTOR, the Drosophila homolog of the target of rapamycin. Genes Dev. 2000 Nov 1;14(21):2689-94.

Palanker L, Tennessen JM, Lam G, Thummel CS. Drosophila HNF4 regulates lipid mobilization and beta-oxidation. Cell Metab. 2009 Mar;9(3):228-39.

Pallares-Cartes C, Cakan-Akdogan G, Teleman AA. Tissue-specific coupling between insulin/IGF and TORC1 signaling via PRAS40 in Drosophila. Dev Cell. 2012 Jan 17;22(1):172-82.

Park KW, Waki H, Choi SP, Park KM, Tontonoz P. The small molecule phenamil is a modulator of adipocyte differentiation and PPARgamma expression. J Lipid Res. 2010 Sep;51(9):2775-84.

Patel PH, Thapar N, Guo L, Martinez M, Maris J, Gau CL, Lengyel JA, Tamanoi F. Drosophila Rheb GTPase is required for cell cycle progression and cell growth. J Cell Sci. 2003 Sep 1;116(Pt 17):3601-10.

Pelletier M, Frainier AS, Munini DN, Wiemer JM, Karpie AR, Sattora JJ. Identification of a novel lipin homologue from the parasitic protozoan Trypanosoma brucei. BMC Microbiol. 2013 May 8;13:101.

Péterfy M, Harris TE, Fujita N, Reue K. Insulin-stimulated interaction with 14-3-3 promotes cytoplasmic localization of lipin-1 in adipocytes. J Biol Chem. 2010 Feb 5;285(6):3857-64.

Péterfy M, Phan J, Reue K. Alternatively spliced lipin isoforms exhibit distinct expression pattern, subcellular localization, and role in adipogenesis. J Biol Chem. 2005 Sep 23;280(38):32883-9.

Péterfy M, Phan J, Xu P, Reue K. Lipodystrophy in the fld mouse results from mutation of a new gene encoding a nuclear protein, lipin. Nat Genet. 2001 Jan;27(1):121-4.

Peterson TR, Sengupta SS, Harris TE, Carmack AE, Kang SA, Balderas E, Guertin DA, Madden KL, Carpenter AE, Finck BN, Sabatini DM. mTOR complex 1 regulates lipin 1 localization to control the SREBP pathway. Cell. 2011 Aug 5;146(3):408-20.

Phan J, Péterfy M, Reue K. Lipin expression preceding peroxisome proliferator-activated receptor-gamma is critical for adipogenesis in vivo and in vitro. J Biol Chem. 2004 Jul 9;279(28):29558-64.

Phan J, Reue K. Lipin, a lipodystrophy and obesity gene. Cell Metab. 2005 Jan;1(1):73-83.

Porstmann T, Santos CR, Griffiths B, Cully M, Wu M, Leevers S, Griffiths JR, Chung YL, Schulze A. SREBP activity is regulated by mTORC1 and contributes to Akt-dependent cell growth. Cell Metab. 2008 Sep;8(3):224-36.

Puig O, Marr MT, Ruhf ML, Tjian R. Control of cell number by Drosophila FOXO: downstream and feedback regulation of the insulin receptor pathway. Genes Dev. 2003 Aug 15;17(16):2006-20.

Rancoule C, Dusaulcy R, Tréguer K, Grès S, Attané C, Saulnier-Blache JS. Involvement of autotaxin/lysophosphatidic acid signaling in obesity and impaired glucose homeostasis. Biochimie. 2014 Jan;96:140-3.

Reue K, Brindley DN. Thematic Review Series: Glycerolipids. Multiple roles for lipins/phosphatidate phosphatase enzymes in lipid metabolism. J Lipid Res. 2008 Dec;49(12):2493-503.

Reue K, Xu P, Wang XP, Slavin BG. Adipose tissue deficiency, glucose intolerance, and increased atherosclerosis result from mutation in the mouse fatty liver dystrophy (fld) gene. J Lipid Res. 2000 Jul;41(7):1067-76.

Reue K, Zhang P. The lipin protein family: dual roles in lipid biosynthesis and gene expression. FEBS Lett. 2008 Jan 9;582(1):90-6.

Rong YS, Golic KG. Gene targeting by homologous recombination in Drosophila. Science. 2000 Jun 16;288(5473):2013-8.

Rulifson EJ, Kim SK, Nusse R. Ablation of insulin-producing neurons in flies: growth and diabetic phenotypes. Science. 2002 May 10;296(5570):1118-20.

Ryu D, Oh KJ, Jo HY, Hedrick S, Kim YN, Hwang YJ, Park TS, Han JS, Choi CS, Montminy M, Koo SH. TORC2 regulates hepatic insulin signaling via a mammalian phosphatidic acid phosphatase, LIPIN1. Cell Metab. 2009 Mar;9(3):240-51.

Sancak Y, Bar-Peled L, Zoncu R, Markhard AL, Nada S, Sabatini DM. Ragulator-Rag complex targets mTORC1 to the lysosomal surface and is necessary for its activation by amino acids. Cell. 2010 Apr 16;141(2):290-303.

Sancak Y, Thoreen CC, Peterson TR, Lindquist RA, Kang SA, Spooner E, Carr SA, Sabatini DM. PRAS40 is an insulin-regulated inhibitor of the mTORC1 protein kinase. Mol Cell. 2007 Mar 23;25(6):903-15.

Santos-Rosa H, Leung J, Grimsey N, Peak-Chew S, Siniossoglou S. The yeast lipin Smp2 couples phospholipid biosynthesis to nuclear membrane growth. EMBO J. 2005 Jun 1;24(11):1931-41.

Sarbassov DD, Guertin DA, Ali SM, Sabatini DM. Phosphorylation and regulation of Akt/PKB by the rictor-mTOR complex. Science. 2005 Feb 18;307(5712):1098-101.

Saucedo LJ, Gao X, Chiarelli DA, Li L, Pan D, Edgar BA. Rheb promotes cell growth as a component of the insulin/TOR signalling network. Nat Cell Biol. 2003 Jun;5(6):566-71.

Schleich S, Teleman AA. Akt phosphorylates both Tsc1 and Tsc2 in Drosophila, but neither phosphorylation is required for normal animal growth. PLoS One. 2009 Jul 17;4(7):e6305.

Scott RC, Schuldiner O, Neufeld TP. Role and regulation of starvation-induced autophagy in the Drosophila fat body. Dev Cell. 2004 Aug;7(2):167-78.

Sengenes C, Bouloumie A, Hauner H, Berlan M, Busse R, Lafontan M, Galitzky J. Involvement of a cGMP-dependent pathway in the natriuretic peptide-mediated hormone-sensitive lipase phosphorylation in human adipocytes. J Biol Chem. 2003 Dec 5;278(49):48617-26.

Shimomura I, Matsuda M, Hammer RE, Bashmakov Y, Brown MS, Goldstein JL. Decreased IRS-2 and increased SREBP-1c lead to mixed insulin resistance and sensitivity in livers of lipodystrophic and ob/ob mice. Mol Cell. 2000 Jul;6(1):77-86.

Shimomura I, Shimano H, Korn BS, Bashmakov Y, Horton JD. Nuclear sterol regulatory element-binding proteins activate genes responsible for the entire program of unsaturated fatty acid biosynthesis in transgenic mouse liver. J Biol Chem. 1998 Dec 25;273(52):35299-306.

Siddle K. Molecular basis of signaling specificity of insulin and IGF receptors: neglected corners and recent advances. Front Endocrinol (Lausanne). 2012 Feb 28;3:34.

Siniossoglou S. Lipins, lipids and nuclear envelope structure. Traffic. 2009 Sep;10(9):1181-7.

Stahl A, Evans JG, Pattel S, Hirsch D, Lodish HF. Insulin causes fatty acid transport protein translocation and enhanced fatty acid uptake in adipocytes. Dev Cell. 2002 Apr;2(4):477-88.

Stasek JE Jr, Natarajan V, Garcia JG. Phosphatidic acid directly activates endothelial cell protein kinase C. Biochem Biophys Res Commun. 1993 Feb 26;191(1):134-41.

Subauste AR, Das AK, Li X, Elliott BG, Evans C, El Azzouny M, Treutelaar M, Oral E, Leff T, Burant CF. Alterations in lipid signaling underlie lipodystrophy secondary to AGPAT2 mutations. Diabetes. 2012 Nov;61(11):2922-31.

Suh JM, Zeve D, McKay R, Seo J, Salo Z, Li R, Wang M, Graff JM. Adipose is a conserved dosage-sensitive antiobesity gene. Cell Metab. 2007 Sep;6(3):195-207.

Sul HS, Latasa MJ, Moon Y, Kim KH. Regulation of the fatty acid synthase promoter by insulin. J Nutr. 2000 Feb;130(2S Suppl):315S-320S.

Suviolahti E, Reue K, Cantor RM, Phan J, Gentile M, Naukkarinen J, Soro-Paavonen A, Oksanen L, Kaprio J, Rissanen A, Salomaa V, Kontula K, Taskinen MR, Pajukanta P, Peltonen L. Cross-species analyses implicate Lipin 1 involvement in human glucose metabolism. Hum Mol Genet. 2006 Feb 1;15(3):377-86.

Taguchi A, White MF. Insulin-like signaling, nutrient homeostasis, and life span. Annu Rev Physiol. 2008;70:191-212.

Tange Y, Hirata A, Niwa O. An evolutionarily conserved fission yeast protein, Ned1, implicated in normal nuclear morphology and chromosome stability, interacts with Dis3, Pim1/RCC1 and an essential nucleoporin. J Cell Sci. 2002 Nov 15;115(Pt 22):4375-85.

Teleman AA. Molecular mechanisms of metabolic regulation by insulin in Drosophila. Biochem J. 2009 Dec 14;425(1):13-26.

Teleman AA, Chen YW, Cohen SM. Drosophila Melted modulates FOXO and TOR activity. Dev Cell. 2005 Aug;9(2):271-81.

Teleman AA, Maitra S, Cohen SM. Drosophila lacking microRNA miR-278 are defective in energy homeostasis. Genes Dev. 2006 Feb 15;20(4):417-22. Erratum in: Genes Dev. 2006 Apr 1;20(7):913.

Thiele C, Spandl J. Cell biology of lipid droplets. Curr Opin Cell Biol. 2008 Aug; 20(4):378-85.

Thompson, N, Trehalose – The Insect 'Blood' Sugar, Advances in Insect Physiology, Academic Press, 2003, Volume 31, Pages 205-285.

Treins C, Warne PH, Magnuson MA, Pende M, Downward J. Rictor is a novel target of p70 S6 kinase-1. Oncogene. 2010 Feb 18;29(7):1003-16.

Ugrankar R, Liu Y, Provaznik J, Schmitt S, Lehmann M. Lipin is a central regulator of adipose tissue development and function in Drosophila melanogaster. Mol Cell Biol. 2011 Apr;31(8):1646-56.

Valente V, Maia RM, Vianna MC, Paçó-Larson ML. Drosophila melanogaster lipins are tissue-regulated and developmentally regulated and present specific subcellular distributions. FEBS J. 2010 Nov;277(22):4775-88.

van Harmelen V, Rydén M, Sjölin E, Hoffstedt J. A role of lipin in human obesity and insulin resistance: relation to adipocyte glucose transport and GLUT4 expression. J Lipid Res. 2007 Jan;48(1):201-6.

Vogt PK, Hart JR, Gymnopoulos M, Jiang H, Kang S, Bader AG, Zhao L, Denley A. Phosphatidylinositol 3-kinase: the oncoprotein. Curr Top Microbiol Immunol. 2010;347:79-104.

Walkiewicz MA, Stern M. Increased insulin/insulin growth factor signaling advances the onset of metamorphosis in Drosophila. PLoS One. 2009;4(4):e5072.

Wilfling F, Wang H, Haas JT, Krahmer N, Gould TJ, Uchida A, Cheng JX, Graham M, Christiano R, Fröhlich F, Liu X, Buhman KK, Coleman RA, Bewersdorf J, Farese RV Jr, Walther TC. Triacylglycerol synthesis enzymes mediate lipid droplet growth by relocalizing from the ER to lipid droplets. Dev Cell. 2013 Feb 25;24(4):384-99.

Wu R, Garland M, Dunaway-Mariano D, Allen KN. Homo sapiens dullard protein phosphatase shows a preference for the insulin-dependent phosphorylation site of lipin1. Biochemistry. 2011 Apr 19;50(15):3045-7.

Wullschleger S, Loewith R, Hall MN. TOR signaling in growth and metabolism. Cell. 2006 Feb 10;124(3):471-84.

Wyatt GR, Kale GF. The chemistry of insect hemolymph. II. Trehalose and other carbohydrates. J Gen Physiol. 1957 Jul 20;40(6):833-47.

Xu J, Liao K. Protein kinase B/AKT 1 plays a pivotal role in insulin-like growth factor-1 receptor signaling induced 3T3-L1 adipocyte differentiation. J Biol Chem. 2004 Aug 20;279(34):35914-22.

Yamanaka N, Rewitz KF, O'Connor MB. Ecdysone control of developmental transitions: lessons from Drosophila research. Annu Rev Entomol. 2013;58:497-516.

Yao Y, Suraokar M, Darnay BG, Hollier BG, Shaiken TE, Asano T, Chen CH, Chang BH, Lu Y, Mills GB, Sarbassov D, Mani SA, Abbruzzese JL, Reddy SA. BSTA promotes mTORC2-mediated phosphorylation of Akt1 to suppress expression of FoxC2 and stimulate adipocyte differentiation. Sci Signal. 2013 Jan 8;6(257):ra2.

Yao-Borengasser A, Rasouli N, Varma V, Miles LM, Phanavanh B, Starks TN, Phan J, Spencer HJ 3rd, McGehee RE Jr, Reue K, Kern PA. Lipin expression is attenuated in adipose tissue of

insulin-resistant human subjects and increases with peroxisome proliferator-activated receptor gamma activation. Diabetes. 2006 Oct;55(10):2811-8.

Yuan M, Pino E, Wu L, Kacergis M, Soukas AA. Identification of Akt-independent regulation of hepatic lipogenesis by mammalian target of rapamycin (mTOR) complex 2. J Biol Chem. 2012 Aug 24;287(35):29579-88.

Zeharia A, Shaag A, Houtkooper RH, Hindi T, de Lonlay P, Erez G, Hubert L, Saada A, de Keyzer Y, Eshel G, Vaz FM, Pines O, Elpeleg O. Mutations in LPIN1 cause recurrent acute myoglobinuria in childhood. Am J Hum Genet. 2008 Oct;83(4):489-94.

Zhang C, Wendel AA, Keogh MR, Harris TE, Chen J, Coleman RA. Glycerolipid signals alter mTOR complex 2 (mTORC2) to diminish insulin signaling. Proc Natl Acad Sci U S A. 2012 Jan 31;109(5):1667-72.

Zhang HH, Huang J, Düvel K, Boback B, Wu S, Squillace RM, Wu CL, Manning BD. Insulin stimulates adipogenesis through the Akt-TSC2-mTORC1 pathway. PLoS One. 2009 Jul 10;4(7):e6189.

Zhang P, O'Loughlin L, Brindley DN, Reue K. Regulation of lipin-1 gene expression by glucocorticoids during adipogenesis. J Lipid Res. 2008 Jul;49(7):1519-28.

Zhang P, Takeuchi K, Csaki LS, Reue K. Lipin-1 phosphatidic phosphatase activity modulates phosphatidate levels to promote peroxisome proliferator-activated receptor γ (PPARγ) gene expression during adipogenesis. J Biol Chem. 2012 Jan 27;287(5):3485-94.

Zhang P, Verity MA, Reue K. Lipin-1 regulates autophagy clearance and intersects with statin drug effects in skeletal muscle. Cell Metab. 2014 Aug 5;20(2):267-79.